UNIVERSITY OF RIJEKA

FACULTY OF BIOTECHNOLOGY AND DRUG
DEVELOPMENT

Beti Zaharija

INVESTIGATING THE AGGREGATION OF DISC1 IN NEUROPSYCHIATRIC DISORDERS

DOCTORAL THESIS

Rijeka, 2025

UNIVERSITY OF RIJEKA

FACULTY OF BIOTECHNOLOGY AND DRUG DEVELOPMENT

Beti Zaharija

INVESTIGATING THE AGGREGATION OF DISC1 IN NEUROPSYCHIATRIC DISORDERS

DOCTORAL THESIS

Mentor: Assoc. Prof. Nicholas J. Bradshaw, PhD

Co-mentor: Assoc. Prof. Rozi Andretić Waldowski, PhD

Rijeka, 2025

SVEUČILIŠTE U RIJECI
FAKULTET BIOTEHNOLOGIJE I RAZVOJA LIJEKOVA

Beti Zaharija

KARAKTERIZACIJA AGREGACIJE DISC1 PROTEINA U NEUROPSIHIJATRIJSKIM POREMEĆAJIMA

DOKTORSKI RAD

Mentor: Izv. prof. dr. sc. Nicholas J. Bradshaw
Komentor: Izv. prof. dr. sc. Rozi Andretić Waldowski

Rijeka, 2025.

Mentor: Assoc. Prof. Nicholas J. Bradshaw

Co-mentor: Assoc. Prof. Rozi Andretić Waldowski

Doctoral thesis was defended on XX/XX/XXXX at the University of Rijeka, Faculty of Biotechnology and Drug Development, in front of the Evaluation Committee:

1. _____

2. _____

3. _____

Acknowledgements

There are many, many people to whom I owe thanks for their support throughout this academic journey. First and foremost, I want to express my sincere thanks to my mentor, Nicholas J. Bradshaw, for his continuous support and guidance. Nick, thank you for giving me an opportunity to join your lab when it was just a bit more than a half-empty room, and to watch it grow to what it is today! You have been there for every question and every concern that I have had (and I have had quite a lot!). Your dedication and care for my academic growth has helped me become a scientist that I am now. I will always be grateful to you for the time I had spent as a member of the Bradshaw group.

During my doctoral research, I have had the great privilege to be a part of another research group, the Fly Lab. I extend my sincere thanks to my co-mentor, Rozi Andretić Waldowski, for offering me a chance to learn a completely new set of skills, and for always pushing me to strive for greatness. Rozi, the knowledge I have gained while working at your lab has been invaluable for me. Thank you for offering me that chance. To the awesome members of the Fly Lab: Franka Rigo, Ana Filošević-Vujnović, Marta Medija and Milan Petrović – thank you. I would not be able to complete this part of my thesis without your help.

My academic journey would not be complete without my wonderful, awesome lab mates – both past and present. To the girlboss team – Bobana Samardžija, Maja Juković and Matea Kršanac – you were the greatest lab mates I could have wished for. Bobana, you have stood by me through the best and the worst of it. Thank you for always being there to help, for your company during the long and stressful hours, and for your continuous mental support. But most importantly, sorry for all the stress I have caused you by never (ever) checking my phone! I could not have asked for a better PhD half. Maja, thank you for being the best student I've ever had, and for the wonderful colleague you have become to me. I am so happy that I had a chance to work side by side with you, and to have your help, support and friendship. Matea, we haven't known each other for a long time, but I am so glad that you have joined us. Your humour is incomparable, and your Kimi memes keep us all afloat. Thank you!

To my awesome colleagues – Martina Mušković, Nikolina Mohović, Patrizia Janković Bevandić and Robert Kolman – the time I've spent at work would have never been as fun as it was without our coffee breaks and gatherings. You are the greatest, most fun and caring group of colleagues there is. Muškić, I don't know what I'd do without your support and friendship. I could (literally) count on you day and night. You are the best. Nikolina, thank you for all the talks and help whenever I needed it. You are amazing, and I'll never be able to listen to In Corpore Sano without laughing again. Robi & Pat, you are a force to be reckoned with! Thank you for all the laughs and great office shenanigans. I was lucky to be surrounded by such wonderful people during my academic journey.

A very special thanks goes to my friends, Haja and Tina. Haja, my colleague by the full moon, even though you live in a different country, I could always count on you and your support. Thank you for always offering a shoulder I could lean on. Tina, as a clone, you already know everything I want to say to you. You are the best.

I would be amiss not to thank Mr Stephen "Steven" "Shawn" McSomething for his glorious effort of proof-reading. This thesis would otherwise be riddled with as many mistakes as there are misspellings of your name.

And last but not least, I want to thank my family and my partner. Words cannot describe what your love and endless support mean to me.

To my partner, Krešimir, you are my pillar of strength. Thank you for always holding me up when things were the hardest, and for loving me throughout all the chapters of this journey. Love you.

Mama, nona, volin vas. Hvala ča ste vavik bile uz mene i ča ste verovale va me. Ne bin bila tu kadi san bez vas.

Za Vikota, Ivana

i Profesora.

U predvečerje, iznenada,

Ni od kog iz dubine gledan,

Pojavio se ponad grada

Oblak jedan.

Vjetar visine ga je njiho,

I on je stao da se žari,

Al oči sviju ljudi bijehu

Uprte u zemne stvari.

I svak je išo svojim putem:

Za vlašću, slavom il za hljebom,

A on – krvareći ljepotu – svojim nebom.

I plovio je sve to više,

Ko da se kani dić do Boga;

Vjetar visine ga je njiho,

Vjetar visine raznio ga.

∼*∼

Abstract

To date, the pathophysiology of psychiatric disorders remains poorly understood. While traditionally investigated using genetics, disrupted protein homeostasis has been suggested as a biological basis for these diseases in at least a subset of patients. Several proteins previously implicated by genetic studies have been shown to form insoluble aggregates in such illnesses, including Disrupted in Schizophrenia 1 (DISC1). DISC1 is a cytosolic, multi-functional scaffolding protein involved in numerous disease-related neuronal pathways. Due to its large interaction network, it has many reported roles, including, but not limited to, brain development, maturation, migration and proliferation of neuronal cells, synapse regulation and mitochondrial trafficking. However, delineation of the domain structure of DISC1 has only recently been attempted, using high-throughput analysis in *Escherichia coli*. This approach identified four distinct stable regions, named D, I, S and C. Here, we used both empirical and theoretical data to confirm and refine the domain structure of DISC1 when expressed in mammalian cells, as well as test the functionality of each region through protein-protein interactions. We then utilised this knowledge to identify the exact part of DISC1 responsible for its aggregation. Moreover, we created *Drosophila* lines expressing human DISC1, to assess behavioural phenotypes corresponding to symptoms often linked with psychiatric disorders.

First, we attempted to refine the borders of DISC1 by combining previously published bioinformatics data on DISC1 domains with the recent empirical data. Constructs encoding variants of D, I and C regions were cloned, with borders modified based on theoretical predictions. These were transfected into HEK293 cells and tested for stability via proteasome inhibition assay. Results obtained by immunoblotting implicated that modified versions of D and C regions have improved stability over their empirical counterparts, with evidence that the I region may not represent a stable folded region by itself. The D, S and C domains were further shown to be functional in isolation, although only the C region was capable of forming interactions with known protein binding partners.

In order to investigate which structural region(s) might be responsible for its aggregation, fragments of DISC1 were expressed in SH-SY5Y neuroblastoma cells and their localization patterns viewed by fluorescent microscopy. Single regions exhibited clear

cytoplasmic localization with no aggregate formation. In contrast, the combination of D and I region showed clear signs of aggregation, with full length DISC1 used as a positive control. Based on this, we hypothesized that the unstructured region between these two regions, D and I, is responsible for DISC1 aggregation propensity, which was verified using further truncation constructs.

Finally, we created transgenic *Drosophila* lines expressing human DISC1 on both the second and third chromosome by using the *Gal4*-UAS system, which allows selective activation of any cloned gene in a variety of neuronal clusters. We assessed flies' abilities to climb vertical surfaces, as well as locomotor activity and sleep patterns, which are often prone to disturbances in neuropsychiatric disorders. Our results signified that locomotor activity and sleep in *Drosophila* are affected by both the *DISC1* insertion and protein expression, in correlation to symptoms reported by psychiatric patients.

With this thesis, we confirmed and refined the domain structure of DISC1, a known risk factor for mental disorders. Additionally, our results provided an insight into its aggregation as an important emerging aspect of DISC1 pathology, as well as the direct effect of *DISC1* expression on the behavioural phenotypes seen in *Drosophila* animal models. Together, our data will aid in elucidation of pathogenic mechanisms underlying psychiatric disorders, and generation of new, high-quality animal models to study behavioural consequences and relevance of DISC1 aggregation for major psychiatric disorders.

Key words: DISC1, psychiatric disorders, domain structure, protein aggregation, *Drosophila*

Sažetak

Unatoč velikim znanstvenim napretcima postignutim tijekom posljednjih desetljeća, patofiziologija psihijatrijskih poremećaja još uvijek nije u potpunosti razjašnjena. Dok se tradicionalni pristup istraživanja primarno fokusirao na genetske aspekte bolesti, nova saznanja ukazuju na poremećaje u homeostazi proteina kao biološku bazu ovih bolesti. Štoviše, nekolicina proteina prethodno impliciranih u genetskim studijama neuropsihijatrijskih poremećaja također imaju sposobnost stvaranja toksičnih, netopljivih proteina u mozgovima pacijenata, uključujući i Disrupted in Schizophrenia 1 (DISC1) protein.

DISC1 je citosolični, multifunkcionalni protein uključen u velik broj neuralnih procesa kritičnih za normalno obnašanje kognitivnih i tjelesnih funkcija. Zahvaljujući širokoj mreži interakcijskih proteina, DISC1 ima ulogu u razvoju mozga, maturaciji, migraciji i proliferaciji neuronalnih stanica, regulaciji sinapsi te mitohondrijskom transportu. No unatoč važnosti ovog proteina, tek je nedavno, uz pomoć visokopropusnih tehnologija, razotkrivena njegova strukturalna organizacija. Ovim su pristupom identificirane četiri stabilne regije proteina, nazvane D, I, S i C. U ovome radu koristili smo kombinaciju empirijskih i teorijskih podataka kako bismo potvrdili i usavršili strukturu domene DISC1 proteina u stanicama sisavaca te testirali funkcionalnost svake regije kroz interakciju sa drugim proteinima. Nadalje, identificirali smo točnu regiju DISC1 proteina odgovornu za njegovu agregaciju te proizveli linije vinskih mušica koje eksprimiraju ljudski DISC1 kako bismo evaluirali fenotipe ponašanja koji su u skladu sa čestim simptomima viđenim u psihijatrijskim poremećajima.

Za potrebe optimizacije granica DISC1 regija kombinirali smo prethodno publicirana bioinformatička saznanja sa nedavnim eksperimentalnim otkrićima. Klonirali smo modificirane konstrukte koji kodiraju varijante D, I i C regija na temelju teorijskih predviđanja te ih transficirali u HEK293 stanice. Potom smo testirali stabilnost istih inhibicijom funkcije proteasoma. Dobiveni rezultati ukazali su na to da modificirane verzije D i C regije imaju povećanu stabilnost u usporedbi sa eksperimentalno dobivenim konstruktima, kao i da I regija eksprimirana u izolaciji ne predstavlja stabilnu regiju. Nadalje, demonstrirali smo da su D, S i C regije funkcionalne u izolaciji, iako je samo potonja demonstrirala sposobnost interakcije sa poznatim veznim partnerima.

Kako bismo istražili koje strukturalne regije imaju sposobnost agregacije eksprimirali smo fragmente DISC1 proteina u SH-SY5Y stanicama neuroblastoma te pratili njihovu lokalizaciju koristeći fluorescentnu mikroskopiju. Izolirane regije demonstrirale su citoplazmatsku lokalizaciju s izostankom agregacije. Suprotno tome, kombinacija D i I regije demonstrirala je jasne znakove agregacije, u korespondenciji sa agregacijom vidljivom pri ekspresiji nefragmentiranog DISC1 proteina korištenog kao pozitivna kontrola. Temeljem ovih rezultata, pretpostavili smo kako je nestrukturirani dio između D i I regije zaslužan za sklonost DISC1 proteina ka formaciji agregata, što smo potvrdili daljnom ekspresijom fragmentiranih konstrukata te regije.

Naposlijetku, proizveli smo transgenične linije vinskih mušica koje eksprimiraju ljudski DISC1 protein na drugom i trećem kromosomu, koristeći *Gal4*-UAS sistem koji omogućava selektivnu aktivaciju bilo kojeg kloniranog gena u različitim skupinama neurona. Testirali smo sposobnost transgeničnih linija pri uspinjanju vertikalnih površina te lokomotornu aktivnost i obrasce spavanja, čiji su poremećaji česta pojava u neuropsihijatrijskim bolestima. Dobiveni rezultati ukazali su na to kako insercija *DISC1* gena i ekspresija proteina obje utječu na lokomotornu aktivnost i spavanje u vinskih mušica, u korelaciji sa simptomima zabilježenim u psihijatrijskih pacijenata.

Ovim doktorskim radom potvrdili smo i optimizirali strukturu domene DISC1 proteina, važnog rizičnog faktora za razvoj mentalnih poremećaja. Nadalje, naši rezultati pružaju uvid u agregaciju ovog proteina kao potencijalnog patofiziološkog mehanizma bolesti, kao i izravan utjecaj ekspresije *DISC1* gena na bihevioralne fenotipove viđene u modelu vinske mušice. Naši će podaci pridonijeti razjašnjenju patogenih mehanizama koji su temeljni uzrok psihijatrijskih poremećaja, kao i generaciji novih životinjskih modela visoke kvalitete koji će omogućiti proučavanje bihevioralnih posljedica DISC1 ekspresije, kao i važnost DISC1 agregacije, u psihijatrijskim poremećajima.

Ključne riječi: DISC1, psihijatrijski poremećaji, struktura domene, agregacija proteina, vinska mušica

Abbreviations

<u>#</u>

βTrCP - beta transducin repeat-containing protein

<u>A</u>

AA – amino acid

ANOVA – Analysis of variance

APP – amyloid precursor protein

APS – ammonium persulfate

ATF4 – Activating Transcription Factor 4

ATPase – Adenosine 5'-Triphosphatase

<u>B</u>

BACE1 – β-site amyloid precursor protein cleaving enzyme 1

bp – base pairs

bZIP – basic-domain leucine zipper

<u>C</u>

cAMP – 3', 5' cyclic-adenosine monophosphate

cGMP – 3', 5' cyclic-guanidine monophosphate

CMI – chronic mental illness

CO_2 – carbon dioxide

CRE – cAMP-response element

CREB – cAMP-response element-binding

CRMP1 – Collapsin Response Mediator Protein 1

CS – *Canton S*

<u>D</u>

DA - dopamine

DAMS – *Drosophila* Activity Monitoring System

DAPI – 4', 6' diamidino-2-phenylindole

DISC1 – Disrupted in Schizophrenia 1

DMEM – Dublecco's Modified Eagle Medium

DMSO – dimethyl sulfoxide

DNA – deoxyribonucleic acid

dNTPs – deoxyribonucleotide thriposphates

DTT – dithiothreitol

E

E. coli – Escherichia coli

EB – elution buffer

EDTA – ethylenediaminetetraacetic acid

EGFP – enhanced green fluorescent protein

ER – endoplasmic reticulum

ERK – extracellular signal-regulated kinase

ESPRIT – Expression of Soluble Proteins by Random Incremental Truncation

F

FBS – foetal bovine serum

FEZ1 – Fasciculation and Elongation Protein Zeta-1

FTLD – frontotemporal lobar degeneration

G

GABA – gamma-aminobutyric acid

GFP – green fluorescent protein

Grb2 – Growth Factor Receptor-Bound Protein 2

GSK3β – Glycogen Synthase Kinase-3 Beta

GWA – Genome-Wide Association

H

H_2O - water

HCl – hydrochloric acid

HD – Huntington's disease

h*DISC1* – human *DISC1*

HEPES – N-2-hydroxyethilpiperazine-N-2-ethane sulfonic acid

HMM – heavy meromyosin

HTT – huntingtin

<u>I</u>

ICC - immunocytochemistry

IPTG – isopropyl beta-D-1-thiogalactopyranoside

<u>K</u>

Kal7 – Kalirin 7

kb – kilobase

kDa – kilodalton

<u>L</u>

L/D – light/dark

L607F – leucine 607 phenylalanine

LB – Lysogeny Broth

LIS1 – Lissencephaly 1

LOD – logarithm of the odds

<u>M</u>

MAP1A – Microtubule-Associated Protein 1A

MRI -magnetic resonance imaging

mRNA – messenger ribonucleic acid

MYO10 – myosin X

<u>N</u>

NanoSPD – NanoScale Pulldown Assay

NMDA – N-methyl-D-aspartate

NDE1/NUDE1 – Nuclear Distribution Element 1

NDEL1/NUDEL1 – Nuclear Distribution Element-Like 1

<u>O</u>

OD – optical density

ODDD – oxygen-dependent degradation domain

ORF – open reading frame

<u>P</u>

PAF – platelet-activating factor

PAFAH1B1 – Platelet-activating Factor Acetylhydrolase 1B regulatory subunit 1

PBS – phosphate-buffered saline

PBS-T – phosphate-bovine serum with Tween 20

PCM1 – Pericentriolar Material 1

PCR – polymerase chain reaction

PDE4 – Phosphodiesterase 4

PHD3 – Prolyl-4-Hydroxylase Domain 3

PI3K – Phosphoinositide 3-kinase

PIPES - 1,4-piperazinediethanesulfonic acid

PKA – Protein Kinase A

PMSF – phenylmethylsulfonyl fluoride

PVDF – polyvinylidene fluoride

<u>Q</u>

Q31L – glutamine 31 leucine

<u>R</u>

RNA – ribonucleic acid

rpm – revolutions per minute

RT – room temperature

<u>S</u>

S704C – serine 704 cysteine

Sarkosyl – N-lauroylsarcosine sodium salt

SDS – sodium dodecyl sulfate

SDS-PAGE – sodium dodecyl sulfate-polyacrylamide electrophoresis

SOB – Super Optimal Broth

SR – serine racemase

<u>T</u>

TAE – Tris/acetic acid/EDTA

TDP-43 – TAR DNA-binding Protein 43

TEMED – tetramethylethylenediamine

tg*DISC1* – transgenic *DISC1*

TNIK – TRAF2 and NCK-interacting Protein Kinase

TRIOBP-1 – TRIO and F-Actin Binding Protein

<u>U</u>

UAS – upstream activating sequence

UCR – upstream conserved region

UP H_2O – ultrapure water

UPS – ubiquitin-proteasome system

UV/VIS – ultraviolet/visible

<u>W</u>

WB – Western blot

WD 40 – tryptophan aspartate 40

wt – wild type

Contents

1. Introduction

1.1 Chronic mental illnesses

Chronic mental illnesses (CMIs) present one of the leading causes of disability worldwide, primarily due to the complexity of their genetic background. The term CMIs refers to highly heritable conditions of unknown aetiology, characterized by clinically significant disturbance in an individual's cognition, emotional regulation or behaviour that reflects a dysfunction in the psychological, biological or developmental processes that underlie mental and behavioural functioning (Park et al., 2008; World Health Organization, 2024). These disturbances are primarily associated with impairment or distress in personal, familial, social, educational, occupational or other important areas of functioning (World Health Organization, 2024). CMIs include highly debilitating conditions such as schizophrenia, major depressive disorder and bipolar disorder.

Statistical data from the Global Burden of Disease study shows that over 970 million people worldwide, or 13% of the population, suffered from some form of mental disorder in the year 2019 (IHME, 2024). Out of these, more than 185 million were affected by major depressive disorder, while 39 million and 23 million people were found suffering from bipolar disorder and schizophrenia, respectively (IHME, 2024). While these diseases possess distinct diagnostic criteria, they share common biological features, such as similar endophenotype characteristics and neuropsychological mechanisms (Clark et al., 2017; Yang et al., 2019).

Although the aetiology of these diseases is yet to be fully understood, research has shown that both biological and environmental factors (Clark et al., 2017) play the role in their development. Biological factors known to have a role in the development of CMIs include genetics (H. Lu et al., 2021; Rodriguez et al., 2023; Smoller et al., 2013), neurotransmitter abnormalities (Pan et al., 2018; Nikolaus et al., 2019; Beeraka et al., 2022), infections (Dickerson et al., 2019; Elpers et al., 2023), as well as brain abnormalities (Kyriakopoulos et al., 2008; Shen et al., 2023). Environmental causes include a high variety of factors, such as stress (Ota et al., 2014; Zhang et al., 2022), substance abuse (Hawken & Beninger, 2014; Voce et al., 2018; Calarco & Lobo, 2021), and early childhood trauma (Van Os et al., 2010; Varese et al., 2012; Yu et al., 2019).

1

Considering their complex nature, CMIs often lead to long-term chronic impairment. However, due to a lack of understanding of the pathophysiology of CMIs, diagnosing major mental illnesses is still primarily based on psychiatric evaluation, through the use of two major diagnostic manuals – the International Classifiaction of Diseases and the Diagnostic and Statistical Manual of Mental Disorders. On the contrary, biological testing is being used only to exclude alternative diagnoses (Bradshaw & Korth, 2019). As such, alternative approaches have been considered as an underlying mechanism behind the pathophysiology of CMIs, including proteostasis disbalance (Bradshaw & Korth, 2019).

1.1.1 Schizophrenia

Derived from the Greek words "schizo" (splitting) and "phren" (mind) (Bleuler, 1911; Kuhn & Cahn, 2004), schizophrenia and other primary psychotic disorders are a part of the group of disorders characterised by significant impairments in the perception of reality, and alterations in behaviour (World Health Organization, 2024). These alterations manifest through multiple psychiatric symptoms, separated into three groups: positive, negative and cognitive symptoms (**Figure 1**). Positive symptoms are thoughts and behaviours that are not normally present, but result in a loss of touch with reality, such as hallucinations, delusions, disorganised behaviour and formal thought disorder, usually manifested as disorganised speech (American Psychiatric Association, 2013; World Health Organisation, 2022). Negative symptoms are characterised by loss of motivation, and incorporate paucity of speech, anhedonia, psychomotor disturbances and reduced display of affection (American Psychiatric Association, 2013; World Health Organisation, 2022), while cognitive symptoms include a broad set of cognitive disfunctions like impaired processing speed, decline in attention, and verbal memory recall (Korth, 2012; Kahn et al., 2015). To be classified as schizophrenia, at least two of these symptoms need to occur with sufficient intensity and frequency to deviate from normal population expectations. However, it is important to note that these symptoms do not occur due to substance abuse or another medical condition under different classification. Other primary psychotic disorders include schizoaffective disorder, schizotypal disorder, acute and transient psychotic disorder, and others (American Psychiatric Association, 2013; World Health Organisation, 2022).

1.1.1.1 Clinical features

The course and onset of schizophrenia are highly variable, with some patients experiencing periodical exacerbations and remissions of symptoms, while others experience gradual exacerbations of symptoms. Unlike negative and cognitive symptoms, positive symptoms tend to decrease naturally and are tied to a better prognosis (American Psychiatric Association, 2013; World Health Organisation, 2022). Phases of schizophrenia include the generally asymptomatic risk phase, the prodromal phase characterised by the appearance of negative and cognitive symptoms, acute psychosis with periodical exacerbations and remissions of symptoms, and chronic debilitating psychosis (American Psychiatric Association, 2013; World Health Organisation, 2022) (**Figure 1**). While the prevalence of schizophrenia is relatively low, more than half of the patients suffering from schizophrenia also have significant comorbid disorders, making it one of the top 25 leading causes of disability worldwide (Chong et al., 2016).
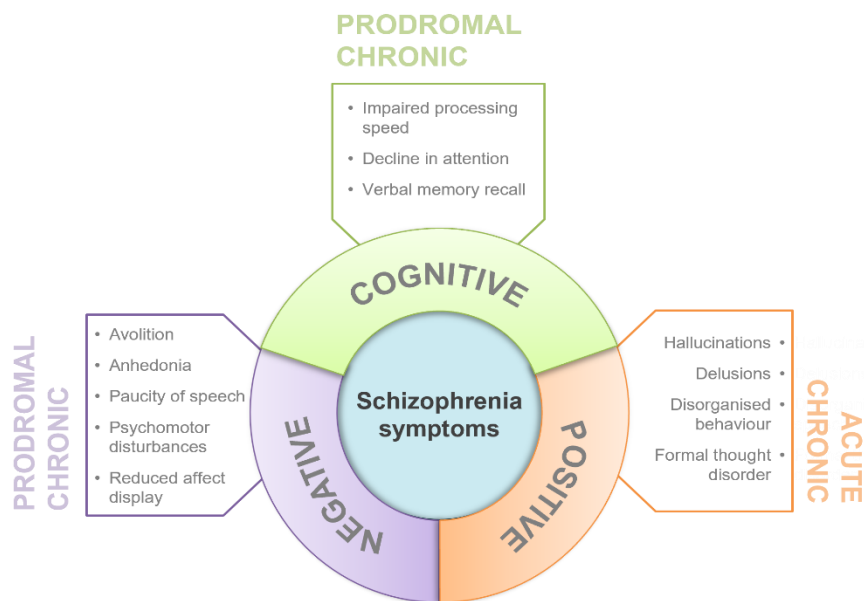
Figure 1. Schematic model of schizophrenia symptoms. Symptoms of schizophrenia can be divided into three groups: positive, negative and cognitive symptoms. The prodromal phase of the disease indicates the onset prior to manifestation of psychotic symptoms, and it includes the appearance of both cognitive and negative symptoms. The prodromal phase is followed by the acute phase in which patients experience periodical exacerbations and remissions of positive symptoms. Final, chronic phase of the disease is marked by chronic debilitating psychosis with a variety of symptoms.

1.1.1.2 Disease onset

The prodromal phase marks the onset of the illness prior to manifestation of psychotic symptoms, which usually appears in early adolescence (Kahn et al., 2015). A prodromal phase can precede the onset of psychotic symptoms by weeks or months, and it is characterised with loss of interest in socialising, neglect of hygiene and personal appearance, anxiety and inversion of the sleep cycle. Acute phases can be interjected by residual phases with similar effect as the prodromal phase (American Psychiatric Association, 2013; World Health Organisation, 2022; World Health Organization, 2024).

Incidence of the disease onset has been found to be higher in men than women. Age of onset of the first psychotic episode also differs by gender, with men experiencing onset above 20 years of age, with peak incidence at 22 years, while women primarily experienced onset at ages 28 and above (Sommer et al., 2020). However, it is important to note that affective and social functioning are more likely to be preserved with later onset of the disease (World Health Organization, 2024).

1.1.1.3 Pathophysiology of schizophrenia

1.1.1.3.1 Genetic evidence

While schizophrenia is considered a multifactorial disorder, it has primarily been investigated through genetic studies. Evidence of heritability of the disease has primarily been investigated through twin and adoption studies. Meta-analysis of twelve twin studies has shown that the estimate of schizophrenia heritability is as high as 81% (Sullivan et al., 2003). A more recent study combining two nationwide registers, the Danish Twin Register and the Danish Psychiatric Research Register, revealed that the concordance of schizophrenia values at 33% in monozygotic and 7% in dizygotic twins, respectively, while the heritability estimate amounted to 79% (Hilker et al., 2018). A population-based study conducted in Sweden showed that first-degree relatives have increased risk of disease, with highest risk seen in full-siblings, albeit half siblings also exhibited significantly increased risk. Interestingly, adopted children with parents suffering from schizophrenia also had an increased risk of being diagnosed with the same disease, as did biological siblings growing up in different families (Lichtenstein et al., 2009).

Throughout the years, many genome-wide linkage and association studies of families with history of schizophrenia were also undertaken. Linkage analyses have the ability

detect strong genetic effects segregating within families, including multiple rare variants within one locus or several weakly associated loci in the same region (Ng et al., 2009). A genome-wide linkage analyses of 12 heritable neurocognitive and neurophysiological endophenotypes collectively identified 12 regions displaying genome-wide significant or suggestive evidence for linkage (Greenwood et al., 2013). Furthermore, genome-wide association (GWA) study from 2008 identified 3 out of 12 loci with strong evidence for association (O'Donovan et al., 2008), while another yielded genome-wide significant association with schizophrenia for seven loci, with three significant loci detected in a joint analysis with a bipolar disorder sample (Ripke et al., 2011). Further investigation identified as many as 128 independent associations spanning 108 conservatively defined loci, with associations at multiple genes involved in glutamatergic neurotransmission (Ripke et al., 2014). The latest iteration of this study reported common variant associations at as many as 287 distinct genomic loci which were concentrated in genes expressed in excitatory and inhibitory neurons of the central nervous system (Trubetskoy et al., 2022).

Most recent study in subjects of European ancestry showed that, while no genome-wide significant locus was identified, single-nucleotide polymorphism-based heritability was estimated to be between 17-21%. Copy-number variants were also found to have a role in the disease, which associated to length and number of deletions (Sada-Fuente et al., 2023).

1.1.1.3.2 Neurochemical abnormalities

The hypothesis pertaining neurochemical abnormalities in the aetiology of schizophrenia has been a long-standing point of research into the disease. Disruption in dopamine (DA) signalling has been of a particular interest, with numerous animal models showing behavioural, cognitive and pharmacological abnormalities consistent with aberrant DA network (Niwa et al., 2010; Eyles et al., 2012; Kesby et al., 2013). Furthermore, positron emission tomographic imaging studies of patients suffering from schizophrenia also heavily implicates abnormalities in DA synthesis, regulation and neurotransmission (Fusar-Poli & Meyer-Lindenberg, 2013; Howes et al., 2011, 2012, 2013).

Considering that DA modulates excitability of both glutamatergic and GABAergic (*gamma*-aminobutyric acid) neurons, which are reciprocally connected, it is not

surprising that abnormalities have been found within these neurotransmitters (Kahn et al., 2015; Marques et al., 2020; Miyazaki et al., 2020; Nakahara et al., 2021), as well as in serotonin and acetylcholine (Scarr et al., 2007; Chuhma et al., 2014; García-Bea et al., 2019). A recent meta-analysis of proton magnetic resonance spectroscopy studies showed that increased glutamatergic and reduced GABA metabolite levels indicate the disruption of excitatory/inhibitory balance in patients with schizophrenia-spectrum disorders (Nakahara et al., 2021). Similarly, previous findings implicate the involvement of serotonin 5-HT$_{2A}$ receptors in the pathophysiology of schizophrenia, with the recent study of post-mortem frontal cortex of patients with schizophrenia indicating supersensitivity of the 5-HT$_{2A}$ receptor (García-Bea et al., 2019). In contrast, a decrease in levels of muscarinic receptors, which are activated by acetylcholine, has been reported in the hippocampus of patients with schizophrenia (Scarr et al., 2007). Taken together, abnormalities in neurotransmitter networks result in a disruption of the fine balance between excitatory and inhibitory signal transmission, which plays an important role in the pathophysiology of schizophrenia and related disorders.

1.1.1.3.3 Neurodevelopmental and structural abnormalities

The neurodevelopmental background of schizophrenia ties into many factors associated with its aetiology. GWA studies implicate deficits in loci with associations to developing cortical neurons and excitatory/inhibitory pathways (Liu et al., 2022; Trubetskoy et al., 2022). Similarly, transcriptome-wide association studies also support the role of altered gene regulation in the prenatal brain associated with schizophrenia (Gusev et al., 2018; Hall et al., 2021). However, it is important to note that environmental factors such as infections during pregnancy (Vlasova et al., 2021), among many others, also play a role in disease development, firmly establishing schizophrenia as a neurodevelopmental, but heterogenous disease.

While neurodevelopmental theory of schizophrenia neatly ties together both genetic and environmental factors, elucidation of cognitive and behavioural changes has been further supported by researching brain anomalies found in schizophrenia patients. A comprehensive meta-analysis from 2016 which analysed brain MRI scans from 2028 patients suffering from schizophrenia and 2540 healthy controls showed that schizophrenia patients have, on average, reduced hippocampus, amygdala, thalamus,

nucleus accumbens and intracranial volumes. Higher volumes of lateral ventricles and pallidum were observed to have association with illness duration, while hippocampal deficits scaled with the proportion of unmedicated patients (Van Erp et al., 2016). A recent multimodal study of treatment-resistant psychosis also reported a reduction in the hippocampal volume, together with superior frontal gyrus, as well as a reduction in antioxidant glutathione levels in the anterior cingulate cortex (Yang et al., 2022). Grey matter loss has been observed in first-episode schizophrenia patients (Torres et al., 2016; Xiao et al., 2015), as well as over the course of the illness (van Haren et al., 2008; Torres et al., 2016), with prefrontal cortex being the most affected region (Xiao et al., 2015). Alongside grey matter decreases in the white matter have been reported (Kelly et al., 2018) across all stages of the disease (Cetin-Karayumak et al., 2019). Abnormalities in the information processing within these regions/structures are closely linked to cognitive, positive and negative symptoms of schizophrenia.

1.1.1.3.4 Disturbance in proteostasis

Through decades of research, many theories regarding pathophysiology of schizophrenia have emerged, with primary focus on genetics, neurotransmitter disbalance and neurodevelopment. However, not all causes of schizophrenia are heritable, which indicates the contribution of non-genetic factors to the neurobiological causes of the disease. The chronic nature and irreversibility of clinical symptoms in a subgroup of patients suffering from schizophrenia and affective disorders prompted a novel approach to researching CMIs, shifting focus from genes to protein homeostasis (proteostasis) disbalance (Leliveld et al., 2008).

Initially, five proteins prone to aggregation were discovered in most cases by isolation of insoluble protein fractions from post-mortem brains of patients suffering from neuropsychiatric disorders (Bradshaw & Korth, 2019).Two of these proteins, Collapsin Response Mediator Protein 1 (CRMP1) (Bader, Ottis, et al., 2012) and TRIO and F-actin binding protein 1 (TRIOBP-1) (Bradshaw et al., 2014), were identified through hypothesis-free proteomics. While these proteins have only recently been associated with CMIs, the remaining three proteins were researched in the context of proteostasis aberration due to being encoded by known CMI risk genes. These proteins include Neuronal PAS domain protein 3 (NPAS3) (Nucifora et al., 2016), Dysbindin-1 (Ottis et

al., 2011) and Disrupted in Schizophrenia 1 (Leliveld et al., 2008), whose corresponding gene is considered to be of a key importance in the pathophysiology of CMIs, as well as in behavioural control (Korth, 2012).

1.2 The *Disrupted in Schizophrenia 1* gene

1.2.1 Discovery of a balanced translocation in a Scottish pedigree

The Disrupted in Schizophrenia 1 (*DISC1*) gene was first discovered in a large Scottish family in which a chromosomal translocation segregates with high incidence of major mental illnesses (Millar et al., 2000). This family was first discovered by Jacobs and colleagues in 1970, who reported a balanced translocation between chromosomes 1 and 11 [t(1;11)(q42.1;q14.3)] in a family member suffering from adolescent conduct disorder. The same translocation was found in the boy's father, paternal grandfather, and in the descendants of the affected grandfather spanning four generations (Jacobs et al., 1970; Blackwood et al., 2001). Follow-up of the family over a twenty-year period revealed an increased incidence of CMIs among relatives with the translocation, including schizophrenia and recurrent major depression. However, no incidence of these disorders was found among the healthy members of the family (Blackwood et al., 2001; St Clair et al., 1990). The family was systematically tracked by researchers and medical professionals for another decade and diagnosed based on DSM-IV, while blinded to the cytogenetic statue of individuals. Subsequently, 87 members of the family were karyotyped, out of which 37 carried the translocation (Blackwood et al., 2001). Diagnoses were made for 29 carriers, with 10 family members suffering from recurrent major depression, 7 diagnosed with schizophrenia, 2 suffering from adolescent conduct disorder, 1 from minor depression, and 1 from bipolar disorder (**Figure 2**). Notably, an offspring (**Figure 2**, V:10) of a translocation carrier with bipolar disorder (**Figure 2**, IV:17) also inherited a translocation and was diagnosed with chronic schizophrenic disorder (**Figure 2**). Additionally, the family member in whom the translocation was originally found and two siblings (**Figure 2**, IV:1, IV:2 and IV:4, respectively) were the only ones diagnosed with adolescent conduct disorder. Considering one of the siblings (**Figure 2**, IV:4) had a normal karyotype, it was concluded that adolescent conduct disorder is most likely unrelated to the translocation. A statistical estimate of likeliness of

genetic loci inheritance (logarithm of the odds score - LOD) for the translocation carriers suffering from any of the major psychiatric disorders was as high as 7.1, while linkage with schizophrenia only, scored a significant 3.6 LOD (Blackwood et al., 2001).
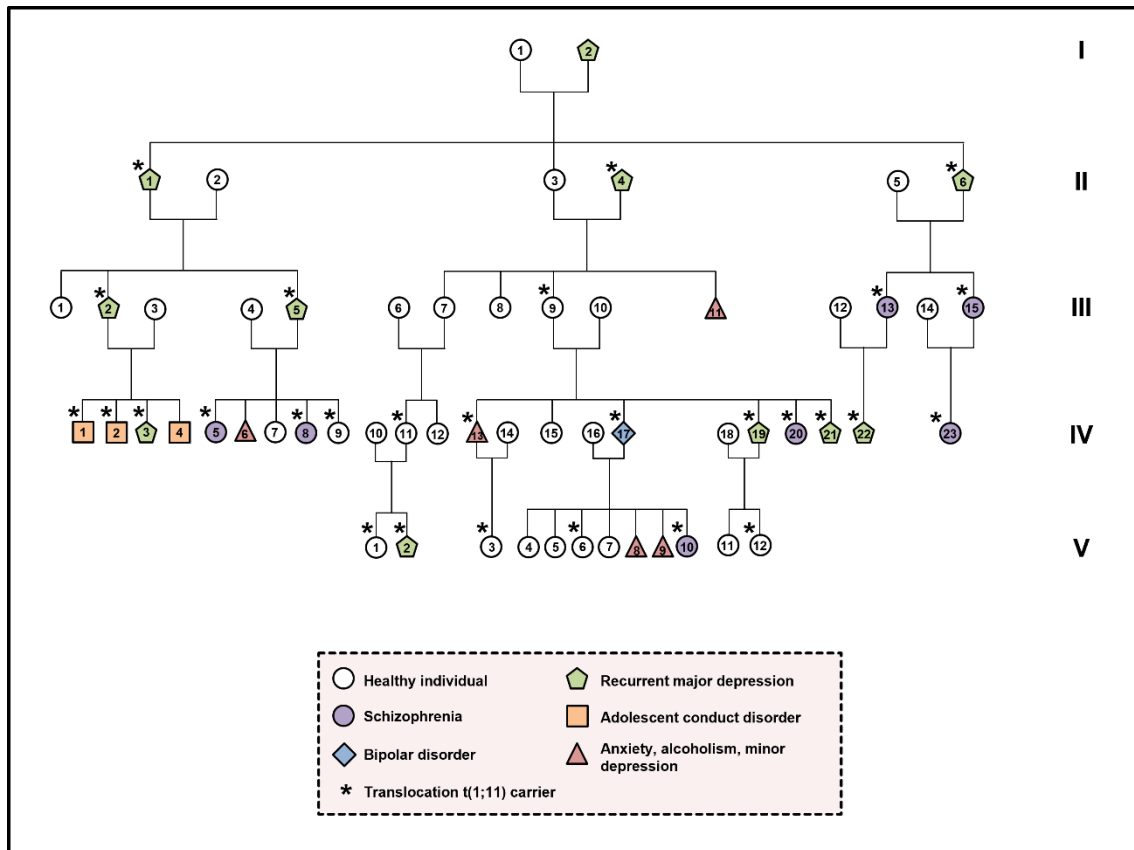
Figure 2. Schematic of a part of the family carrying balanced (1;11) translocation. Family tree depicted shows 58 out of 87 karyotyped family members carrying (1;11) translocation which segregates with schizophrenia and related mental disorders. Shown members are the ones for whom karyotype status was available and psychiatric assessment was possible. Roman numerals on the right are used to annotate generations of family members. Arabic numerals are used to depict the total number of family members within each generation. Legend at the bottom of the figure contains explanations of symbols depicted on the family tree. Adapted from Blackwood et al, 2001.

The genome-wide significance of this translocation to a broad psychiatric phenotype was reaffirmed 15 years later, through the recruitment of additional family members and reassessment of previous findings. New findings emerged as well, linking t(1;11) carriers to reductions in glutamate concentrations in the right dorsolateral prefrontal cortex

(Thomson et al., 2016), which is consistent with the hypothesis of neurotransmitter abnormalities in schizophrenia. The same family was used to study the impact of the translocation on structural connectivity and global white matter structure, where reduced white matter connectivity was found in t(1;11) carriers, thus further confirming the involvement of translocation in the underlying pathophysiology of mental illnesses (Vasistha et al., 2019).

1.2.2 Discovery of the *DISC1* gene

During the 20-year follow-up of the family, major exercises were undertaken to map and clone the t(1;11)(q42.1;q14.3) translocation breakpoints (Chubb et al., 2008), following the hypothesis that the rearrangement between the chromosomes directly disrupts gene function, thus resulting in psychosis. At a protein level, this would result in a loss of all amino acid (AA) residues C-terminal of AA 597 of the full-length protein (854 AA) (Millar et al., 2000). Breakpoint regions were identified on both chromosomes 1 and 11 (Muir et al., 1995), however a long-range restriction map of chromosome 11q14.3 spanning one breakpoint did not yield any genes associated with mental illness (Millar et al., 1998; Blackwood et al., 2001). By contrast, the corresponding breakpoint on chromosome 1 was shown to be gene abundant. Cloning of this region resulted with identification of two novel genes, provisionally named *disrupted in schizophrenia 1* (*DISC1*) and *disrupted in schizophrenia 2* (*DISC2*), due to both genes being disrupted by the translocation. While sequences of both genes overlap each other, *DISC2* seems to act as a non-coding structural RNA gene with a role in regulation *DISC1* expression. As such, alteration of the activity of these two genes has been proposed as a causal link to mental disorders in translocation carriers, either by production of a truncated DISC1 protein, or abnormal expression regulation (Millar et al., 2001). Later report, however, indicates that translocation results in the production of abnormal transcripts due to the fusion of *DISC1* with a disrupted gene on chromosome 11 (*DISC1FP1/Boymaw*), encoding DISC1 amino acids 1-597 plus 1, 60 or 69 amino acids, respectively (Eykelenboom et al., 2012).

1.2.3 *DISC1* locus in schizophrenia: evidence in other populations

The first independent evidence connecting *DISC1* locus to CMIs was found in the Finnish population. The Finnish population originates from a limited number of founders, leading to increased genetic homogeneity, thus enabling easier research into multifactorial

diseases such as schizophrenia (Ekelund et al., 2000). A genome-wide linkage study focusing on identifying genetic loci predisposing to schizophrenia was performed on an isolated Finnish population with a lifetime risk of schizophrenia at 3.2%. Among others, positive results for the schizophrenia predisposition were obtained for q32.2-q41 region of chromosome 1, maximising within the *DISC* locus (Hovatta et al., 1999). Another study of Finnish siblings suffering from schizophrenia or affective disorders also linked the disease to chromosome 1q32.2-q41 (Ekelund et al., 2000). These results were later replicated using a dense set of polymorphic markers, with the strongest markers localizing within *DISC1* locus in both studies (Ekelund et al., 2004).

Another study on the families originating either from the United Kingdom or the Republic of Ireland, affected by either schizophrenia or bipolar disorder, found linkage within the *DISC1* loci on 1q42 with a LOD score of 3.54 (Hamshere et al., 2005). A positive linkage to schizophrenia with 1q41-44 region has also been reported in Taiwanese families with at least two siblings affected by schizophrenia (Hwu et al., 2003). These findings strongly support the influence of *DISC1* on susceptibility to mental disorders.

1.2.4   *DISC1* variation

Additional important *DISC1* mutation was discovered in an American family of three siblings suffering either from schizophrenia or schizoaffective disorder, and their asymptomatic father. All four members of the family were found to be carrying a frameshift mutation within the *DISC1* gene which results in a 4 base pair deletion at the 3' end of exon 12 followed by a premature stop codon, while the same was not observed in any controls nor unrelated probands with schizophrenia or schizoaffective disorder. Interestingly, the mutation was not detected in the sibling suffering from schizotypal disorder nor two siblings suffering from major depression, indicating that, while this mutation implies an association with schizophrenia and similar disorders, it presents an incompletely penetrant risk factor for CMIs (Sachs et al., 2005). However, different polymorphisms within the gene might account for a smaller, but more frequent risk of disease development.

The most notable *DISC1* polymorphisms are S704C (a serine to cysteine substitution at codon 704) and L607P (a leucine to phenyl alanine substitution at codon 607). A common *DISC1* polymorphism S704C and haplotypes containing it were associated with

schizophrenia (Callicott et al., 2005; DeRosse et al., 2007; Di Giorgio et al., 2008). This polymorphism is found within exon 11 (Callicott et al., 2005), which contains an internal splice donor site in human *DISC1* gene (Taylor et al., 2003). Evidence of association between S704C *DISC1* variation and schizophrenia was found within three independent cohorts, in which hippocampal grey matter volume was reduced and function, structure and cognitive engagement of hippocampus was reported (Callicott et al., 2005). In contrast, another study reported hippocampal grey matter volume, which might be explained by haplotypic heterogeneity (Di Giorgio et al., 2008). Similarly, another research group demonstrated that S704C, depending upon the presence or absence of other polymorphisms, can either increase or decrease the risk for schizophrenia (Hennah et al., 2009). Other than hippocampal grey matter variation, reduction of grey matter was found within cingulate cortex as well, together with decreased fractional anisotropy in prefrontal white matter for individuals carrying S704C (Hashimoto et al., 2006). Interestingly, this polymorphism was also correlated with reduced appearance of paranoid delusions, thus influencing lifetime severity of positive symptoms in schizophrenia (DeRosse et al., 2007). Taken together, these findings support clinical relevance of *DISC1* genetic variability in association with schizophrenia, while also correlating to the neurodevelopmental hypothesis of this disease and present structural abnormalities.

In addition, the L607F variant has also been implicated in grey matter reduction. Carriers of this polymorphism suffering from schizophrenia or schizoaffective disorder were found to have lesser cortical grey matter volume in the superior frontal gyrus and anterior cingulate gyrus compared to controls. A significant negative correlation between the severity of hallucinations and superior frontal grey matter volume was also observed in the same cohort (Szeszko et al., 2008). Furthermore, both this variant and S704C were reported to influence cortical thickness and maturation in the developing brain (Raznahan et al., 2011). Both S704C and L607F were also found to have a damaging effect on neurogenesis and neuronal migration via different signalling pathways which can ultimately lead to impaired brain development, correlating to psychiatric phenotypes in schizophrenia (Singh et al., 2011).

1.2.5 Genomic structure of the *DISC1* gene

The human *DISC1* gene consists of thirteen major exons (Millar et al., 2001) spanning across 414.5 kb of genomic DNA (UCSC Genome Browser v466, 2024), with translation

start and stop codons being located within exons 1 and 13, respectively (Millar et al., 2001). Both exons 2 and 9 were found to be unusually large, the latter accounting for approximately one third of the total gene length.

A Northern blot revealed that *DISC1* is present as a major transcript of approximately 7.5 kb in multiple adult human brain tissues (Millar et al., 2000; 2001). Initially, it was shown to produce at least four alternatively spliced isoforms, referred to as Long (L) isoform (EMBL AF222950), Long variant (Lv) isoform (EMBL AB007926), Short (S) isoform (EMBL AJ06177) and Extremely short (Es) isoform (EMBL AJ506178) (Millar et al., 2001; Taylor et al., 2003). The L isoform is encoded by all thirteen exons. In contrast, the Lv form lacks a region of 66 nucleotides while still maintaining the open reading frame (Millar et al., 2000; 2001). This deletion corresponds to a common alternative splicing event (Millar et al., 2000), which arises from utilisation of an internal splice donor site within exon 11 and the corresponding acceptor site of the same exon (Millar et al., 2001). The S isoform splices from exon 9 to an alternate terminal exon and three untranslated regions located within intron 9. Finally, the Es isoform extends the exon 3 open reading frame for two codons, followed by an in-frame stop codon (Taylor et al., 2003; James et al., 2004). To date, more than 50 alternate transcriptional splice variants have been identified (Nakata et al., 2009) within 195 orthologues (Ensembl genome browser 112, 2024), including fish, birds and mammals, as well as invertebrate animals and plants (Taylor et al., 2003; Sanchez-Pulido & Ponting, 2011; Ensembl genome browser 112, 2024).

1.2.6   Expression of the *DISC1* gene

Studies on the expression of human *DISC1* gene have shown it to be present in a wide array of tissues in both adults and foetuses. These include the heart, brain, kidney, pancreas, lung, liver, skeletal muscles and placenta, with gene transcripts being most abundant in placenta, retina, heart and brain (Millar et al., 2000; James et al., 2004; The Human Protein Atlas, 2024). *DISC1* is also widely expressed in multiple brain regions, such as amygdala, caudate nucleus, corpus callosum, substantia nigra, subthalamic nucleus and thalamus (Millar et al., 2000; The Human Protein Atlas, 2024). Moreover, its transcripts were also found to be expressed in hippocampus, cerebellum, medulla, spinal cord, putamen, as well as dorsolateral prefrontal cortex and temporal lobe of the adult brain (Millar et al., 2000; Lipska et al., 2006; The Human Protein Atlas, 2024). Effects

of abnormalities in many of these regions have been well-documented in schizophrenia patients (Mukherjee et al., 2014; Van Erp et al., 2016; Wong et al., 2020; Yang et al., 2022), supporting the involvement of DISC1 in the pathogenesis of the disease. Studies in mice, investigating the role of *DISC1* expression during brain development, show that expression can be seen in primary neurons and interneurons (Austin et al., 2004; Schurov et al., 2004), while being largely absent in astroglial cells (Schurov et al., 2004) during neurogenesis and neuronal migration. Another study showed that the *DISC1* gene expresses in neural progenitors of the mouse embryonic cerebral cortex and hippocampus (Miyoshi et al., 2003; Mao et al., 2009). In human brains, *DISC1* expression was shown to vary across life span. Most prominent expression was detected during the neonatal and infant period, then lowering throughout adolescence and adulthood, thus further confirming the role of *DISC1* in neurodevelopment (Lipska et al., 2006; Wang et al., 2016).

DISC1 was also found to be expressed in peripheral blood, with expression levels being directly connected to cognitive performance, positive and negative symptoms in schizophrenia patients (Rampino et al., 2014; Chen et al., 2022).

1.3 Disrupted in schizophrenia 1 protein

DISC1 is a cytosolic, widely expressed multifunctional scaffold protein. As a scaffold, it lacks enzymatic activity and instead exerts its function by simultaneous interaction with multiple macromolecules (Yerabham et al., 2013; Shao et al., 2017; Teng et al., 2018).

Due to its large interaction network, DISC1 has many reported roles (**Figure 3**). These roles suggest the importance of DISC1 in normal brain development, while the production of aberrant protein, either due to genetic mutations, biological processes or interactions with other proteins, can contribute to aetiology of mental disorders such as schizophrenia (Brandon et al., 2009; Teng et al., 2018). However, the mechanisms by which DISC1 exerts its functions remains largely unknown, in part due to lack of enzymatic activity, as well as the complexity of its vast interaction network and lack of structural information (Soares et al., 2011; Bradshaw & Porteous, 2012).
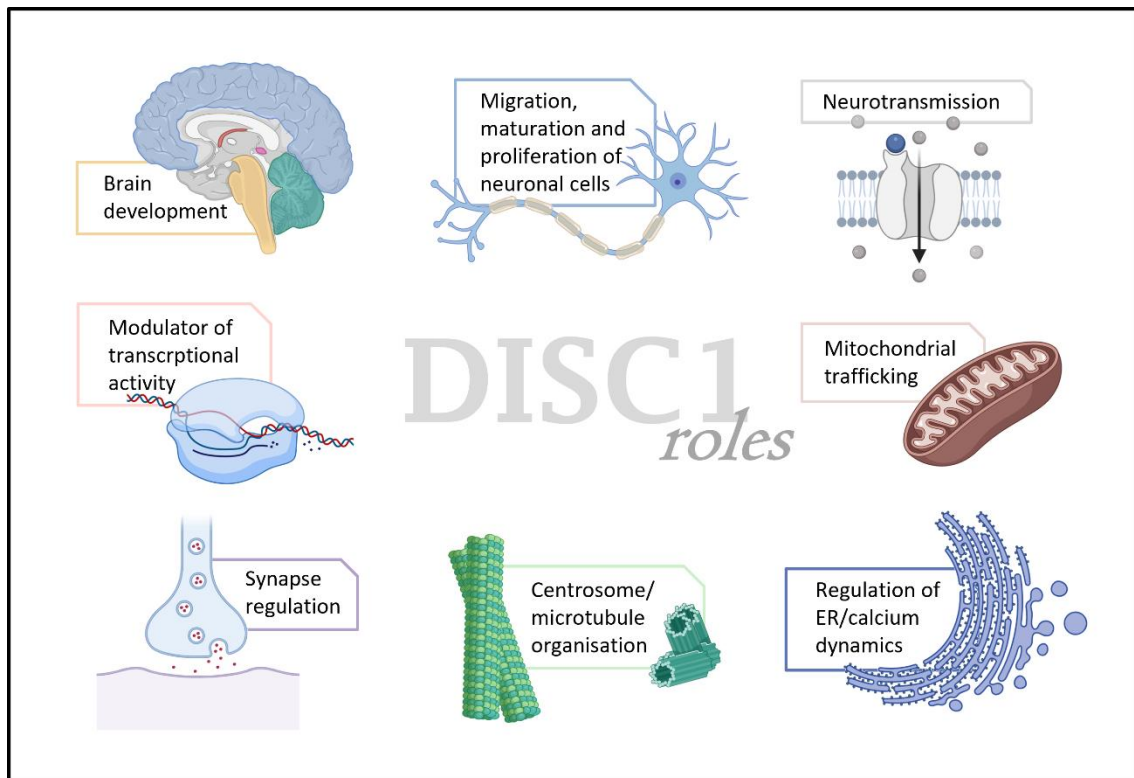
Figure 3. Roles of DISC1. DISC1 has many reported roles, including, but not limited to: brain development, maturation, migration and proliferation of neuronal cells, synapse regulation (Millar et al., 2003; Brandon et al., 2009; Brandon & Sawa, 2011; Singh et al., 2011; Thomson et al., 2013), dopaminergic (Niwa et al., 2010; Jaaro-Peled et al., 2013), glutamatergic (Hayashi-Takagi et al., 2010; Malavasi et al., 2018) and GABA neurotransmission (Kim et al., 2012; Wei et al., 2015), mitochondrial trafficking (Millar et al., 2003; Ogawa et al., 2014; Murphy & Millar, 2017; Norkett et al., 2020), as well as centrosome and microtubule organisation (Millar et al., 2003; Morris et al., 2003; Kamiya et al., 2005; Steinecke et al., 2014). It also acts as a modulator of nuclear localisation and transcriptional activity (Sawamura et al., 2005; Malavasi et al., 2012; Soda et al., 2013; Wang et al., 2021).

While the gene was first linked to CMIs more than twenty years ago, the crystal structure of the full-length DISC1 protein remains unknown to this date. For years, a lack of knowledge about the structure of DISC1 has been impeding further research into its roles and functions within the pathology of mental disorders, partly due to a lack of homology with known proteins and unusually rapid sequence evolution (Sanchez-Pulido & Ponting, 2011; Yerabham et al., 2017). Moreover, the high susceptibility of recombinant DISC1 to aggregation and its low solubility further impended its biophysical characterization

(Leliveld et al., 2009; Yerabham et al., 2017; Bradshaw & Korth, 2019). As such, attempts at defining its structural organization were limited to in silico bioinformatics predictions, while experimental approach was dependent upon shorter constructs and domain delineation of known sequence (Soares et al., 2011).

1.3.1 Structure of DISC1

1.3.1.1 Bioinformatics and biophysical studies

The L isoform of *DISC1* encodes a putative protein of 854 amino acid residues (Millar et al., 2000). Until recently, the full-length DISC1 was proposed to consist of two distinct structural regions (**Figure 4**).
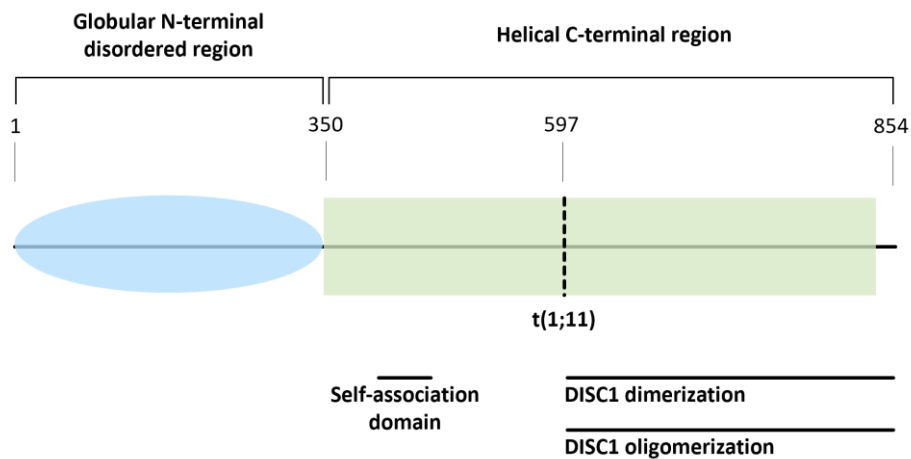
Figure 4. DISC1 structure according to bioinformatics predictions. Schematic of an 854 residue-long DISC1 protein and its initial domain predictions, drawn to scale. The N-terminal globular domain is highlighted in blue, while the helical C-terminal domain is depicted in green. Vertical dashed line annotates the location of the t(1;11) translocation breakpoint at amino acid residue 597 (Millar et al., 2000). Full lines beneath the schematic indicate regions capable of self-association (Leliveld et al., 2009), dimerization and/or oligomerization (Leliveld et al., 2009; Narayanan et al., 2011; Roche & Potoyan, 2019). Adapted from Soares et al, 2011.

The N-terminal domain spanning the first 350 amino acid residues was predicted to be disordered, with no known homology to any folds. It was referred to as the globular head domain, implicating a folded three-dimensional structure in its native state (Millar et al., 2000; Leliveld et al., 2009; Soares et al., 2011). In contrast, the C-terminal domain was

predicted to consist predominately of coiled coils and/or α-helices (Taylor et al., 2003; Leliveld et al., 2009; Soares et al., 2011), with incorporated self-association domain (Leliveld et al., 2009; Soares et al., 2011). The C-terminal region was associated with higher oligomeric states, suggesting formation of dimeric, octameric and multimeric species (Leliveld et al., 2009; Narayanan et al., 2011; Roche & Potoyan, 2019) (**Figure 4**).

Later bioinformatics analysis has also predicted the existence of three UVR-like domains in DISC1 orthologues (Sanchez-Pulido & Ponting, 2011). A UVR domain represents a conserved C-terminal region of the UvrB protein, a part of the *Escherichia coli* endonuclease complex shown to consist of two α-helices connected by a structural loop that adopt an antiparallel hairpin fold (Sohi et al., 2000; Sanchez-Pulido & Ponting, 2011). Two of these structures were identified within the α-helical C-terminal region of DISC1, while, interestingly, one was predicted to exist within the unstructured N-terminal region of the protein. These UVR-like domains were shown to fall within the regions of DISC1 protein whose sequences are among the best conserved across diverse DISC1 orthologues, indicating their role in structural stability of DISC1 (Sanchez-Pulido & Ponting, 2011).

1.3.1.2 Utilisation of ESPRIT and domain delineation of DISC1

Any further characterisation of the DISC1 structure was lacking until the utilisation of a high-throughput ESPRIT (Expression of Soluble Proteins by Random Incremental Truncation) technique (Mas & Hart, 2017; Yerabham et al., 2017; Yumerefendi et al., 2010). The core hypothesis behind the ESPRIT process is that structured (and therefore likely functional) protein domains are more likely to form soluble recombinant proteins when expressed, while incomplete domains are more likely to be insoluble. Therefore, by expressing a vast library of random truncations of the target gene, and selecting those that can produce soluble protein, the likely location of structured regions can be determined (Yerabham et al., 2017). In short, the process (**Figure 5**) includes robotic processing of random DNA libraries with bidirectionally truncated constructs of the target gene. Putative soluble constructs are then purified from small-scale liquid cultures by immobilised metal affinity chromatography, and visualised using SDS-PAGE (sodium dodecyl sulfate-polyacrylamide gel electrophoresis). To determine sequence boundaries,

positive clones are sequenced (Yumerefendi et al., 2010). This library-based screening technique was first implemented for identification of an independently folded C-terminal domain of the of the influenza virus polymerase subunit PB2 (Tarendeau et al., 2007).
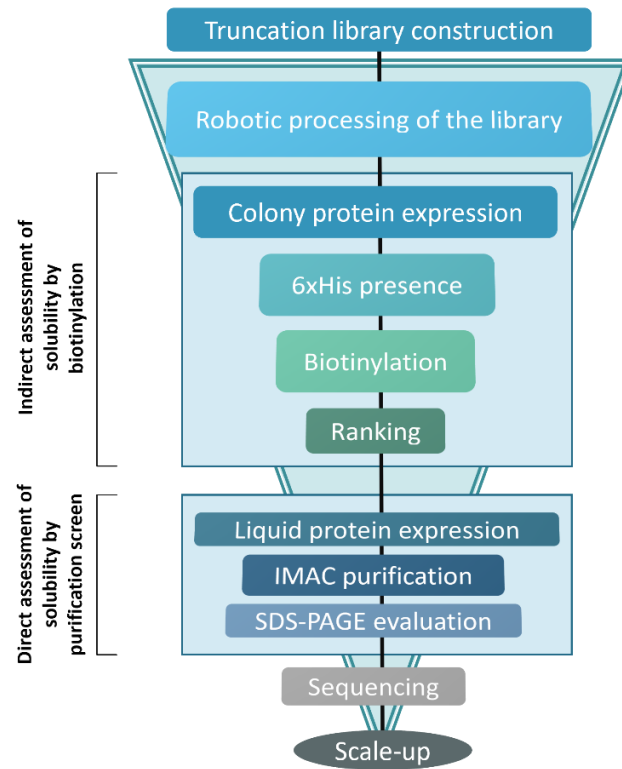
Figure 5. Schematic depiction of ESPRIT construct screening process. Random DNA truncation libraries of the target gene are robotically processed to isolate individual clones from bacterial colonies. Firstly, putative soluble constructs are indirectly assessed for their solubility by measuring in vivo biotinylation. Direct assessment of solubility is performed by testing construct yield and solubility by purification from small-scale bacterial liquid cultures. Positive clones are sequenced to determine construct boundaries compatible for large-scale expression. IMAC – immobilised metal affinity chromatography; SDS-PAGE – sodium dodecyl sulfate-polyacrylamide gel electrophoresis. Adapted from Yumerefendi et al, 2010.

In the case of DISC1, a library of 27, 652 clones was created by random truncation of the *DISC1* gene at one and/or both ends. The most soluble and highly expressed protein fragments were identified, based on the hypothesis that such fragments correspond to stable, distinctly folded domains within the protein. Using this approach, four novel

structural regions of the DISC1 protein were proposed, named "D", "I", "S" and "C", respectively (Yerabham et al., 2017).

1.3.1.2.1 DISC1 D region

The D region was defined based on the two highly similar ESPRIT constructs which corresponded to AA 249-383 and 257-383 of the full-length protein, respectively. These constructs were the only soluble constructs detected within the N-terminal half of DISC1. Further analysis discovered that the D region exists predominately as a dimeric species with a high content of α-helices. These results were in direct contrast with previous bioinformatics studies predicting disorder within the N-terminal part of the protein (Yerabham et al., 2017).

1.3.1.2.2 DISC1 I region

The I region was also discovered to be predominately present as a dimer, based on a single ESPRIT construct encoding AA 539-655. It can be expressed in *Escherichia coli* as a stable, soluble protein in a low-order oligomeric state. However, a purified construct encoding this region exhibited visible aggregation propensity at concentrations higher than 30 μM, making it the least stable out of the four regions. While multiple other ESPRIT constructs overlapping this region were shown to precipitate as well, these constructs do so immediately upon purification, implying that the AA 539-655 construct indeed presents a structured region. Similar to the D region, additional analysis of its content showed the I region to be predominately helical (Yerabham et al., 2017).

Considering the domain architecture of the DISC1 protein, the t(1;11) Scottish translocation at AA 597 would therefore result in a bisected I region. The produced protein would thus have an incorrectly folded I region, as well as the complete lack of the remaining two C-terminal DISC1 regions. Consequently, this translocation-derived version of DISC1 would result in high protein instability, as well as loss of multiple protein-protein interaction sites, further confirming the effect of this translocation on affected carriers (Yerabham et al., 2017).

1.3.1.2.3 DISC1 S region

Unlike other regions, the S region can express in multiple different oligomeric states, at least as a recombinant protein, with the elongated tetrameric state being the most stable

and prominent one. This predominately helical region was defined based on a single ESPRIT construct encoding AA 635-738, thus overlapping both the I and the C region. Curiously, when expressed separately, the recombinant I and S regions exist as stable and soluble proteins with differing oligomeric states. However, the constructs spanning both regions exhibited low solubility and were shown to be highly unstable in regard to their oligomerisation. As such, these regions can be considered distinct from each other, with a potential to represent alternative conformations of the full-length DISC1 protein (Yerabham et al., 2017). Based on these results, the existence of at least two different conformations of DISC1 was proposed, depending on which of the two regions acts as a dominant intermolecular domain (**Figure 6**, A).

In the case of the dominant I region, the ensuing conformation of a full-length protein would represent a dimer (**Figure 6**, B), while a dominant tetrameric S region would result in DISC1 being expressed as higher oligomeric species (**Figure 6**, C) (Yerabham et al., 2017). Both dimeric species and those of higher oligomeric states were previously reported in full-length DISC1 by Narayan and colleagues (Narayanan et al., 2011). The most recent biophysical study of the C-terminal part of the protein, encompassing residues C-terminal of AA 597 (a site of the balanced Scottish translocation), employed transmission electron microscopy to assess DISC1 ability to bind arsenic (Wang et al., 2019). A three-dimensional reconstruction corresponded to the formation of tetrameric complex (Wang et al., 2019), in support of DISC1 ability to form higher oligomers as shown in **Figure 6**, C.
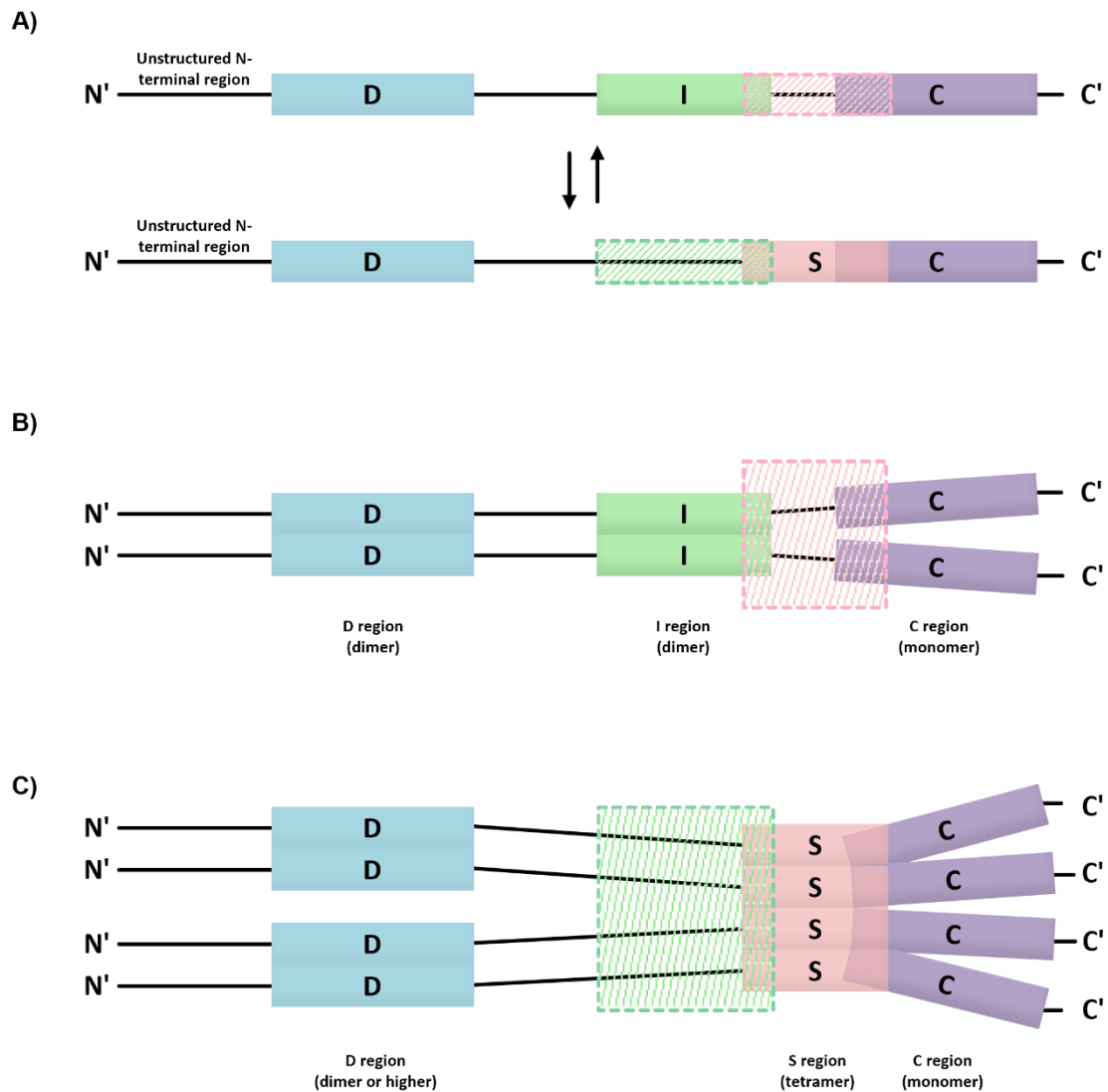
Figure 6. Schematic depiction of DISC1 domain structure and oligomerisation. A) Proposed domain structure of the DISC1 protein with alternative configurations, based on the dominance of either the I or S region. **B)** Schematic representation of the dimeric DISC1 species, with the I region acting as a dominant domain. Both the D and I region form dimers, from which extend the N-terminal region and the monomeric C region. **C)** Schematic representation of the tetrameric DISC1 species, with the S region acting as a dominant domain. In this configuration, the S region exists as a tetramer from which extend the C region monomers, while the D region can form either dimers or a tetramer. Adapted from Yerabham et al, 2017.

1.3.1.2.4 DISC1 C region

The C region of the protein was based on two ESPRIT constructs encoding AA 691-836 and 684-836, however only the lower molecular weight species was shown to be stable. The region exists as an elongated monomer of a primarily helical content, with 25% of the content representing disordered random coils. Another fragment found within the N-terminal part of the C region (AA 718-771) was also predicted to exist as a monomer, although it lacked regular secondary structure (Yerabham et al., 2017). This part of the C region thus appears to account for the random coil content, consistent with previous bioinformatical predictions of this area (Soares et al., 2011).

Elucidation of the DISC1 domain architecture enabled creating region-specific constructs mimicking notable mutations within the gene, such as the previously observed American frameshift mutation (Sachs et al., 2005). At AA 807, this mutation lies within the C region of the DISC1 protein and, as such, could affect the structural integrity of the region. To mimic the truncation of the region as the result of the frameshift mutation, a corresponding construct was created by Yerabham and colleagues. Interestingly, while this construct expressed at 50% the level of the wild-type protein control, its solubility decreased by as much as 90%. It was further shown that the insoluble mutant undergoes aberrant multimerization, ultimately leading to accumulation of protein aggregates that disrupt the structure of the region (Yerabham et al., 2017). The most recent study attempting to characterise the C region of DISC1 uncovered that, apart from helices and coiled coil content, a formation of β-strands can also be found within the region (Cukkemane et al., 2021).

1.3.1.2.4.1 Structural data on DISC1 C region

The functional importance of the C region of DISC1 is highlighted by several factors: within it lies the American frameshift mutation (Sachs et al., 2005), as well as the schizophrenia-associated polymorphism S704C (Callicott et al., 2005). Moreover, a phosphorylation site was found at serine 713 (S713) of DISC1, which coordinates the change of neuronal progenitor cell proliferation to migration during cortical development (Ishizuka et al., 2011). Another construct placed within the C region, encompassing AA 598-785, displayed cell invasiveness and an ability to recruit other proteins into aggresomes, protein degradation structures to which excess or misfolded protein localise (Ottis et al., 2011; Atkin et al., 2012; Bader et al., 2012). C-terminal part of the region

also includes multiple protein interaction sites and plays a role in oligomer assembly (Leliveld et al., 2009). As such, structural information on this part of the DISC1 protein helps in elucidation of its role in normal protein function and its implications in mental illness (Yerabham et al., 2018). For these purposes, Yerabham and colleagues set to create a hypothetical model of the C region of DISC1 by creating a single domain camelid antibody directed against the DISC1 protein. Derived model consisted of three longer α-helices, with the N-terminal helix connecting to the remaining two by a stretch containing three shorter helices. This model also suggested two conformationally significant loops extending within AA 723-737 and 752-771, with S731 being easily accessible for phosphorylation in accordance to its previously described effects on DISC1 (Ishizuka et al., 2011; Yerabham et al., 2018).

During this research, another group successfully solved the high-resolution structure of the short C-terminal fragment of mouse Disc1 in complex with its interactor, Nuclear Distribution Element 1 (NDE1) and Nuclear Distribution Element-Like 1 (NDEL1) protein. The construct used in this study encodes AA 765-835, corresponding to approximately half of the C region (Ye et al., 2017). Mapping data also indicated that this construct produces a stable structural unit independent of the full-length protein (Ye et al., 2017), in correspondence to the ESPRIT data generated by Yerabham et al. DISC1 765-835 was shown to contain two α-helices forming an antiparallel hairpin which, when in complex with the single helix from NDEL1 (AA 238-284), formed the hydrophobic core which pertains to complex formation (Ye et al., 2017).

Following this finding, another group's efforts amounted to generating a high-resolution structure of the same DISC1 construct (AA 765-835) in complex with another interaction partner, Activating Transcription Factor 4 (ATF4). Similar to the results obtained by Ye and colleagues, the DISC1/ATF4 complex formed a structure comprising of three interacting α-helices, with DISC1 forming an antiparallel two-helix structure connected with a loop, while the leucine zipper ATF4 domain (AA 314-349) adopted a single α-helix (Wang et al., 2019). All three helices were shown to adopt a canonical heptad structure containing hydrophobic residues capable of forming interactions between the two proteins. Additionally, several charge-charge interactions were mapped, whose supposed role involves enhancement of binding specificity (Wang et al., 2019).

1.3.2   Interaction network of DISC1

Initially, analysis of the DISC1 amino acid sequence provided matches essentially restricted to structural similarities to structural proteins, myosins and proteins involved in mobility/transport, such as microtubule binding proteins. While providing no clear insight into DISC1 function, many of these proteins are implicated in important cellular processes such as synaptogenesis and intracellular transport along the neurons, indicating that DISC1 could perform a similar role (Millar et al., 2000).

In order to identify proteins in direct interaction with DISC1, yeast two-hybrid assays were utilised by multiple groups (Millar et al., 2003; Miyoshi et al., 2003; Morris et al., 2003; Ozeki et al., 2003; Camargo et al., 2007), resulting in identification of over 200 protein interactors (Camargo et al., 2007; Soares et al., 2011). Among others, these include PDE4B1 (Phosphodiesterase 4B1), ATF4 (Activating Transcription Factor 4), LIS1 (Lissencephaly 1), NDE1 (Nuclear Distribution Element 1) and NDEL1 (Nuclear Distribution Element-Like 1) protein (**Table 1**). Interestingly, many of identified proteins are encoded by genes implicated in schizophrenia, suggesting a convergence in biological processes between multiple risk factors (Camargo et al., 2007; Lipina & Roder, 2014). Due to these multiple interactions, taken together with widespread expression and functions attributed to DISC1, it is customarily referred to as a multifunctional scaffolding protein that 'interacts with and affects the function of different proteins at different locations and developmental times' (Bradshaw & Porteous, 2012).

Table 1. DISC1 interaction partners important for its biological roles[1]

DISC1 interactors	Subcellular localisation	Interaction-dependent role of DISC1	Reference
APP	Centrosome	Regulation of cortical precursor cell migration	(Young-Pearse et al., 2010)
α-tubulin	Microtubule network	Regulation of LIS1/NDE1NDEL1 cytoskeletal binding	(Brandon et al., 2004)

DISC1 interactors	Subcellular localisation	Interaction-dependent role of DISC1	Reference
ATF4	Nucleus	CREB signalling/CRE-mediated gene transcription	(Sawamura et al., 2008)
CRMP1	Aggregates/ aggresome	Proteostasis/recruitment to aggregates	(Bader, Tomppo, et al., 2012)
Dynactin	Centrosome	Regulation of microtubule dynamics	(Kamiya et al., 2005)
Dynein	Centrosome	Regulation of microtubule dynamics	(Kamiya et al., 2005)
Dysbindin	Aggregates/ aggresome	Proteostasis/recruitment to aggregates	(Ottis et al., 2011)
FEZ1	Neuronal growth cones	Neurite outgrowth	(Miyoshi et al., 2003)
Girdin	Distal parts of the axon	Regulation of AKT-mTOR signalling/neurogenesis/neuronal positioning	(Kim et al., 2009)
Grb2	Distal parts of the axon	Regulation of ERK signalling/axon elongation	(Shinoda et al., 2007)
GSK3β	Cytosol	Regulation of Wnt signalling/cell proliferation	(Mao et al., 2009)
Kal-7	Dendritic spines	Regulation of Rac1 signalling/glutamate synaptic spine morphology and function	(Hayashi-Takagi et al., 2010)

DISC1 interactors	Subcellular localisation	Interaction-dependent role of DISC1	Reference
LIS1	Centrosome	Regulation of LIS1/NDE1/NDEL1 complex interaction/function	(Brandon et al., 2004)
MAP1A	Microtubule network	Regulation of microtubule network/protein traffic	(Morris et al., 2003)
NDE1 NDEL1	Centrosome	Regulation of LIS1/NDE1/NDEL1 complex interaction/function	(Kamiya et al., 2006)
PCM1	Centrosome	Cortical development	(Kamiya et al., 2008)
Pericentrin	Centrosome	Regulation of microtubule organisation	(Miyoshi et al., 2004)
PDE4B1/2	Mitochondria	Regulation of cAMP signalling	(Millar et al., 2005)
TNIK	Postsynaptic density	Regulation of synapse composition and function	(Wang et al., 2011)
TRIOBP-1	Aggregates/ aggresome	Proteostasis/recruitment to aggregates	(Samardžija et al., 2023)

[1] *Important DISC1 binding partners tested for protein-protein interactions beyond yeast-two hybrid screening are listed, with corresponding references. Refer to Abbreviations for full names of proteins listed in* **Table 1**.

1.3.2.1 Phosphodiesterase 4B (PDE4B)

1.3.2.1.1 PDE4 family and structure

Phosphodiesterase 4B is a member of a superfamily of enzymes called phosphodiesterases (PDEs) (Houslay & Adams, 2003). These enzymes are a product of eleven different gene families that are grouped according to function, structure and affinity for cAMP (3', 5' cyclic-adenosine monophosphate) and cGMP (3', 5' cyclic-guanidine monophosphate). Out of these, cAMP-specific PDE4s belong to the largest family of four genes (PDE4A-D) with over twenty isoforms (Houslay & Adams, 2003; Fertig & Baillie, 2018). They regulate cAMP by hydrolysing it, which results in inactivation of cAMP signalling, a pathway important in many aspects of central nervous system functions and response, including neuronal maturation (Houslay & Adams, 2003; Thomson et al., 2013). Mammalian orthologues of PDE4s were first discovered thanks to the identification of the *dunce* gene in *Drosophila melanogaster*, one of the *Drosophila* genes involved in conditioned behaviour, cognition and synaptic plasticity (Qiu et al., 1991; Houslay & Adams, 2003). The disruption of this gene leads to impaired memory and learning (Houslay & Adams, 2003). However, the distinction of PDE4 family was first made due to their sensitivity to inhibition by rolipram, a selective PDE inhibitor known for its antidepressant and antipsychotic activity (Bertolino et al., 1988; Houslay & Adams, 2003; Siuciak et al., 2007).

PDE enzymes consist of a C-terminal catalytic core, while the N-terminal domain is unique to each isoform. PDE4 represent long isoforms, whose N-terminal region consists of a subcellular localisation targeting domain and two upstream conserved regions (UCR 1 and 2) connected by two linker regions (**Figure 7**) (Bolger, 1994; Houslay & Adams, 2003; Fertig & Baillie, 2018). UCRs are of special importance due to their effect on phosphorylation of PDE4s by cAMP-dependent Protein Kinase A (PKA), thus affecting the enzyme functionality (MacKenzie et al., 2002).

The PDE4 family members are expressed in abundance within the central nervous system, encompassing many regions of the brain implicated in the pathophysiology of psychiatric disorders. These regions include the prefrontal cortex, hippocampus, nucleus accumbens and substantia nigra. Expression is isoform-specific, indicating a diversity of roles within the brain (Cherry & Davis, 1999; Chubb et al., 2008).
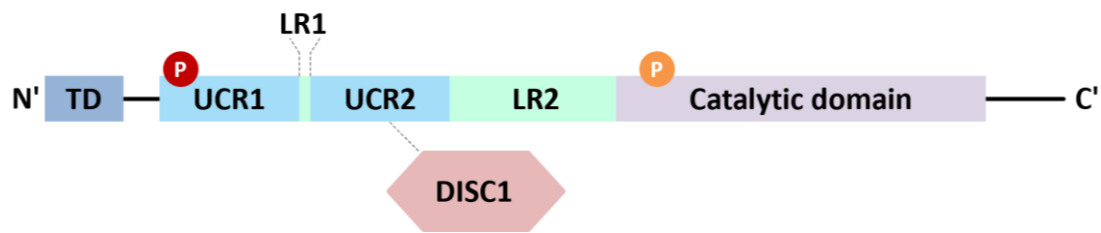
Figure 7. Domain organisation of PDE4B long isoform and its interaction with DISC1. Targeting or transduction domain (TD, shown in dark blue) of PDE4B can be found within the N-terminal region unique to each isoform, and has the role of subcellular localisation. Upstream conserved regions 1 and 2 (UCR 1/2, shown in light blue) serve as regulatory domains. Activation of the enzyme happens upon phosphorylation of UCR1 by Protein Kinase A (red circle – "P" indicates phosphorylation). N-terminal part of DISC1 (depicted in light red) interacts with the UCR2 domain of PDE4B. Linker regions (LR 1/2) are depicted in light green. Catalytic domain of PDE4B (shown in light purple) undergoes phosphorylation by Extracellular Signal-Regulated Kinase (orange circle – "P" indicates phosphorylation). Adapted from Fertig et al, 2018.

1.3.2.1.2   PDE4B and DISC1

PDE4B was first identified as a genetic risk factor in cousins diagnosed with schizophrenia and psychotic disorder who carried a balanced t(1;16)(p31.2;q21) translocation. This translocation breakpoint results in direct disruption of the B1 isoform (*PDE4B1*) of the *PDE4B* gene, which was found to interact with DISC1 in an activity-dependent manner through modulation of cAMP (Millar et al., 2005; Murdoch et al., 2007). Further genetic evidence linking the *PDE4B* gene to the risk of schizophrenia was subsequently found in various populations, including the Scottish (Pickard et al., 2007), Caucasian and African American (Fatemi et al., 2008), Japanese (Numata et al., 2008), and Finnish (Tomppo et al., 2009), among others.

Association of DISC1 and PDE4B happens through the UCR2 domain of PDE4B, in a dynamic manner (**Figure 7**). Their interaction is dependent on phosphorylation of PDE4B, due to DISC1 predominately binding to a dephosphorylated form of PDE4B. Subsequently, elevated cAMP levels lead to PDE4B phosphorylation/activation by PKA, resulting with its dissociation from DISC1 (Millar et al., 2005; Murdoch et al., 2007). Overexpression of DISC1 can also inhibit the induction of PDE4 activity upon elevation of cAMP levels (Carlyle et al., 2011). While the phosphorylation of PDE4 enzymes at the

28

UCR1 domain is catalysed by PKA, phosphorylation of the catalytic domain is exerted by Extracellular Signal-Regulated Kinase (ERK) and serves as a regulator of PDE4 activity (Hill et al., 2005). Interestingly, knockdown of endogenous DISC1 in postnatal rat cortical neurons results in suppression of ERK phosphorylation, further confirming its effect on PDE4 activity (Hashimoto et al., 2006).

Murine studies of DISC1-PDE4B interaction also indicate the involvement of this complex in the pathophysiology of psychiatric disorders. For example, a murine *Disc1* ortholog modelled to represent the effects of the t(1;11) balanced translocation showed elevated cAMP levels as a result of the mutation, leading to altered dendritic growth and axonal targeting within the hippocampus. Consistently, the expression of many PDE4B and PDE4D isoforms has decreased at a protein level (Kvajo et al., 2011; Thomson et al., 2013). Another study with mice models carrying *Disc1* Q31L (a glycine to leucine substitution at codon 31) and L100P (a leucine to phenyl alanine substitution at codon 31) mutation showed significantly reduced binding between PDE4B and DISC1. Moreover, mutant Q31L mice with depressive-like phenotype exhibited a striking 50% reduction in total brain PDE4 activity, while the L100P mutation connected to schizophrenic-like behaviour resulted in greater reduction of DISC1-PDE4B binding (Clapcote et al., 2007). Taken together, these discoveries indicate that DISC1 has a direct role in regulation of PDE4B activation and thus, in cAMP-dependent signal transduction within the developing and adult brain.

1.3.2.2 Activating Transcription Factor 4 (ATF4)

1.3.2.2.1 ATF4 family and structure

Activating Transcription Factor 4 (ATF4) is a member of the activating transcription factor/cAMP-response element binding protein (ATF/CREB) family of transcription factors that bind to the consensus binding sate cAMP responsive element (CRE), which has a role in the transcription of downstream genes (Ameri & Harris, 2008). The ATF family consists of seven proteins, ATF1-7, which all have a role in maintenance of intracellular homeostasis. These proteins are characterized by the presence of a basic-domain leucine zipper (bZIP) region responsible for the formation of multimers with other proteins containing the same region. The bZIP region consists of two elements: a basic domain in a continuous sequence contact with DNA, and a hydrophobic leucine

zipper region. The latter serves as a mediator of homo- and heterodimerisation, which represents a powerful tool for regulation of transcriptional activity and gene expression (Vincent & Struhl, 1992; Chérasse et al., 2007; Chen et al., 2022).

ATF4 is a 351 AA long protein structured into several domains (**Figure 8**) (Pitale et al., 2017; Nwosu et al., 2022). The N-terminal part of the protein has a regulatory role, and consists of a domain required for interaction with P300 acetyltransferase (Lassot 2005, Cherasse 2007), an oxygen-dependent degradation domain (ODDD) responsible for interaction with PHD3 (prolyl-4-hydroxylase domain 3) (Köditz et al., 2007) and a βTrCP (β-transducin repeat-containing protein) domain required for interaction with βTrCP, a component of a E3 ubiquitin ligase complex (Lassot et al., 2001). Functional, C-terminal part of the protein contains the leucine zipper region, along with multiple binding-specific motifs and sites for post-translational modifications, such as phosphorylation (Karpinski et al., 1992; Manni et al., 2012) and ubiquitination (Lassot et al., 2001; Feng et al., 2021). At many sites, phosphorylation of ATF4 leads to its degradation and ubiquitination, for instance through phosphorylation-dependent interaction with βTrCP (Lassot et al., 2001; Pitale et al., 2017).
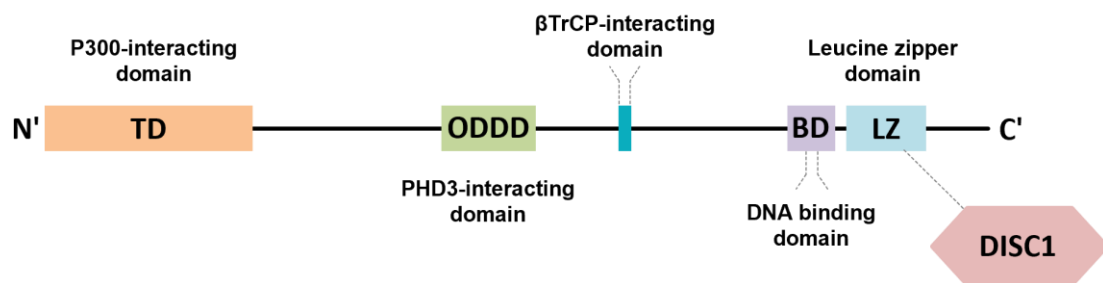
Figure 8. Domain organisation of ATF4 protein and its interaction with DISC1. TD – N-terminal domain; ODDD – oxygen-dependent degradation domain; PHD3 – prolyl-4-hydroxylase domain 3; βTrCP – β-transducin repeat-containing protein; BD – basic domain; LZ – leucine zipper. ATF4 binds to DISC1 (depicted in red) through its LZ domain.

Consistent with its role in gene transcription, *AFT4* mRNA is present in all tissues examined thus far (Hai & Hartman, 2001) and as such, it has multiple physiological roles. It can directly interact with GABA$_B$ (gamma-aminobutyric acid B) receptors (Vernon et

al., 2001), it acts as a mediator of metabolic and oxidative homeostasis, as well as a regulator of the cellular response to ER (endoplasmic reticulum) stress (Han et al., 2013; Chen et al., 2017). It also promotes neuronal cell death and angiogenesis, hence promoting the effects of malignant tumours (Chen et al., 2017). In contrast, it was also proposed that ATF4 can act as a tumour suppressor by promoting autophagy (Abdel-Nour et al., 2019; Dai et al., 2019). In a limited number of studies, *ATF4* gene was also identified as a potential risk factor for schizophrenia (Qu et al., 2008; Tan et al., 2024).

While the studies on the role of ATF4 in mental illness have been limited thus far, it is interesting to note that it has been more extensively researched in the context of neurodegenerative diseases. These include Alzheimer's disease, Parkinson's disease and Huntington's disease, as well as frontotemporal dementia and amyotrophic lateral sclerosis. They are characterised by the loss of neural cells and accumulation of disease-specific misfolded proteins (Lamptey et al., 2022). For many of these diseases, it has been shown that changes in the levels of ATF4 and/or its dysfunction can significantly affect the process of neurodegeneration (Imai et al., 2001; Jankowsky et al., 2004; Jiang et al., 2010; Baleriola et al., 2014).

1.3.2.2.2 ATF4 and DISC1

ATF4 was first discovered as a potential DISC1 interactor in a yeast two-hybrid screen and subsequently confirmed as such by two-hybrid and co-immunoprecipitation in mammalian cells (Morris et al., 2003). It facilitates binding to DISC1 through its leucine zipper domain which is, curiously, also a domain which interacts with $GABA_B$ receptors. Both $GABA_B$ receptors and ATF4 were found to colocalise in the somatodendritic compartment of cultured neurons, and ATF4 localisation into or outside the nucleus was shown to be mediated by $GABA_B$ receptor activation (White et al., 2000; Vernon et al., 2001; Morris et al., 2003). Considering that interaction between ATF4 and truncated DISC1 is lost, this may consequently affect the regulation of $GABA_B$ signalling, a process relevant to schizophrenia (Morris et al., 2003). The recently solved atomic structure of the complex between a C-terminal DISC1 construct and ATF4 enabled further insight into the effects of DISC1 truncation on the DISC1/ATF4 interaction, as well as the role of DISC1/ATF4 complex in synaptic dysregulation (Wang et al., 2019).

Truncated DISC1 (AA 1-597) was also shown to alter subcellular distribution of endogenous ATF4, resulting in inhibition of neurite outgrowth (Pletnikov et al., 2007). Furthermore, transgenic mice with reduced expression of ATF4 exhibit enhanced hippocampal-dependent memory formation and synaptic plasticity (Chen et al., 2003), aspects of which can also be affected by variation in *DISC1* (Callicott et al., 2005). In fact, two *DISC1* variants, S704C and L607F, were shown to disrupt nuclear targeting of DISC1, thus affecting regulatory function of ATF4-mediated gene transcription which can affect cognitive and emotional reactivity (Malavasi et al., 2012).

The role of ATF4 in cAMP signalling is yet another touching point between DISC1 and ATF4. ATF4-dependent gene transcription is mediated by PKA activity, which is cAMP-dependent. Soda and colleagues have shown that DISC1 repression of PDE4D, a member of the PDE4 family, is directly reliant on ATF4. These interactions can consequently affect dopaminergic and noradrenergic signalling through modulation of cAMP levels (Soda et al., 2013).

A study using transgenic *Drosophila* models suggested that nuclear DISC1 acts as a modulator of CRE-mediated gene transcription and sleep homeostasis by interaction with ATF4/CREB2. Given that patients suffering from psychosis have altered levels of nuclear DISC1 (Sawamura et al., 2005), such function may be of significant importance in psychiatric disorders.

1.3.2.3 Lissencephaly 1 (LIS1), Nuclear Distribution Element 1 (NDE1) and Nuclear Distribution Element-Like 1 (NDEL1)

1.3.2.3.1 LIS1

Lissencephaly 1, or PAFAH1B1 (platelet activating factor acetylhydrolase 1B regulatory subunit 1), is a protein encoded by the *LIS1/PAFAH1B1* gene. This gene was the first human neuronal migration gene cloned, and it encodes the non-catalytic α subunit of the 1B isoform of platelet-activating factor acetylhydrolase (Reiner et al., 1993; Hattori et al., 1994; Kato & Dobyns, 2003;). Platelet-activating factor (PAF) is a neuroregulatory molecule involved in many biological and pathological processes, while PAF acetylhydrolase can be found in a variety of tissue cytosols and plasma (Hattori et al., 1994). Haploinsufficiency of this gene in humans results with lissencephaly, a severe developmental malformation in neuronal migration, characterised by a smooth cerebral

surface of the brain (Reiner et al., 1993; Wynshaw-Boris, 2007). In murine models, decreased levels of *Lis1* exhibited defects in neuronal migration and early embryonic lethality (Hirotsune et al., 1998), as well as impairments of cognition and motor coordination (Paylor et al., 1999).

LIS1 protein is highly conserved within species, including the filamentous fungus *Aspergillus nidulans* (Xiang et al., 1995) and *Drosophila* (Swan et al., 1999; Liu et al., 2000). Human LIS1 is nearly identical to its mouse orthologue, and predominately expresses in foetal and adult brain across all ages (Mizuguchi et al., 1995; Reiner et al., 1995).

1.3.2.3.1.1 LIS1 structure and function

The LIS1 protein structure consists of a conserved α-helical LIS1 homology motif found in multiple eukaryotic proteins at the N-terminus, followed by a coiled-coil region and seven WD-40 repeats forming β-propeller structure at the C-terminus (Emes & Ponting, 2001; Mateja et al., 2006). The latter can be found in many signalling proteins of the WD (W- Tryptophan, D - Aspartate) family, which consist of highly conserved repeating units usually ending with Tryptophan-Aspartate amino acids (Neer et al., 1994; Emes & Ponting, 2001; Mateja et al., 2006). The N-terminal part of LIS1 mediates its homodimerization, which is essential for protein interactions and its biological functions (Emes & Ponting, 2001; Mateja et al., 2006).

Many physiological roles of LIS1 are closely related to its interaction partner, dynein, an ATPase (adenosine triphosphate) and microtubule motor protein central to the microtubule-based transport of cytoskeletal components and organelles. This protein is of particular importance for neurons, as it plays a role in axon growth through transportation of small microtubule fragments from the centrosome (Emes & Ponting, 2001; Grabham et al., 2007). Interestingly, LIS1 was shown to regulate dynein localisation and activity through stabilisation of its uninhibited conformation (Marzo et al., 2020). Through its interaction with dynein pathway, LIS1 was implicated in various cellular processes, such as cell and kinetochore mitosis (Faulkner et al., 2000; Tai et al., 2002), neuronal migration and centrosomal positioning (Dujardin et al., 2003; Sasaki et al., 2000), neural progenitor cell morphogenesis/proliferation (Tsai et al., 2005), as well as microtubule organisation (Smith et al., 2000).

1.3.2.3.2   NDE1 and NDEL1

1.3.2.3.2.1   NDE1/NDEL1 structure and function

LIS1 is heavily involved in another pathway connected to dynein. The NUD (nuclear distribution) pathway, first discovered in *Aspergillus nidulans* (Xiang et al., 1995), is a highly conserved signalling pathway that regulates nuclear migration along microtubules by regulation of dynein motor function (Xiang et al., 1995; Wynshaw-Boris, 2007). Mammalian NudE homologues, termed NUDE/NDE1 (Nuclear Distribution Element 1) and NUDEL/NDEL1 (Nuclear Distribution Element-Like 1), were originally identified in yeast two-hybrid screens as LIS1 binding partners (Feng et al., 2000; Kitagawa et al., 2000; Niethammer et al., 2000; Sasaki et al., 2000).

NDE1 and NDEL1 are highly homologous proteins originating from a common ancestral gene, with approximately 60% shared amino acid content (Sasaki et al., 2000). At 335 and 345 residues, respectively, both consist of distinct N- and C-terminal regions (**Figure 9**).
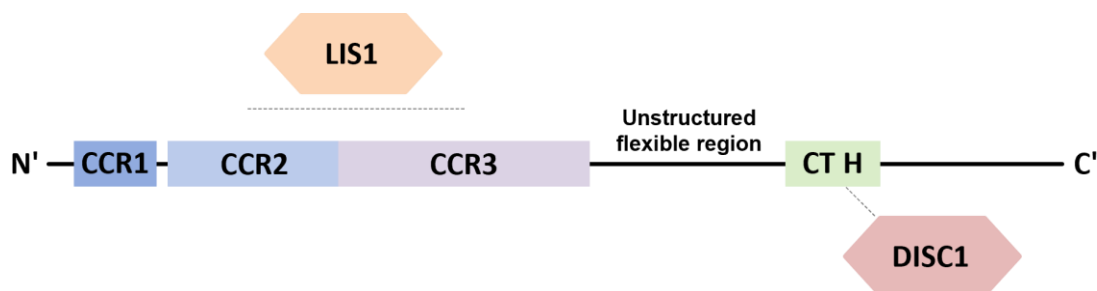
Figure 9. NDE1/NDEL1 domain structure and their interaction with LIS1 and DISC1. The N-terminal part of both proteins predominately consist of coiled coil regions (CCRs), within which lies the LIS1-binding domain (indicated by dashed lines above CCR2/3). The C-terminal (CT) part is predicted to be largely unstructured, excluding a single α-helix (CT H) responsible for binding interaction partners, such as DISC1 (shown in red). Unstructured region linking the N-terminal coils with a C-terminal α-helix exhibits conformational flexibility which facilitates the interaction of N- and C-terminal parts of both proteins. Adapted from Soares et al, 2012.

NDEL1 contains a LIS1 interaction site and is responsible for homodimerization via formation of continuous parallel α-helical coiled coils that account for approximately half of the proteins' length (Derewenda et al., 2007; Soares et al., 2012). In contrast, the C-

terminal parts of both proteins were shown to be flexible, albeit largely unstructured regions, apart from a single well conserved α-helix responsible for protein-protein interactions. These interactions are modulated through numerous phosphorylation sites also found within the C-termini (Bradshaw et al., 2009, 2011; Soares et al., 2012). Due to flexibility of the unstructured region, C-terminal α-helix can also directly interact with its N-terminal coiled-coil domain. Both proteins were shown to be present as both dimeric and tetrameric species, with distinct functions in the brain (Bradshaw et al., 2009, 2013; Soares et al., 2012).

While NDE1 and NDEL1 are highly homologous, they are likely to be functionally distinct (Bradshaw & Hayashi, 2017). Both proteins can be found within the centrosome and are expressed in proliferating neuroblasts and migrating neurons. However, NDE1 expression is most abundant during early embryonic stages, with an essential role in the development of cerebral cortex, while NDEL1 expresses in later stages of development and is important for both cortical and hippocampal developmental functions (Feng et al., 2000; Niethammer et al., 2000; Sasaki et al., 2000, 2005). Complete loss of *Ndel1* in mice results in neuronal migration defects, as well as early embryonic lethality (Sasaki et al., 2005). In contrast, *Nde1* knock-out mice are able to survive to birth, but still exhibit defects in neuronal migration, neurogenesis and mitotic spindle assembly and function (Feng & Walsh, 2004). It is also of note that both proteins have distinct post-translational modification regulation with many phosphorylation sites not conserved between the two, hence further implying functional differentially (Bradshaw et al., 2013).

1.3.2.3.2.2 The role of NDE1/NDEL1 in LIS1 function

NDE1 and NDEL1 both colocalise with LIS1 at the centrosome or microtubule-organising centres, and can bind to multiple centrosomal proteins, including dynein (Feng et al., 2000; Niethammer et al., 2000; Sasaki et al., 2000). While the interaction of LIS1 and NDE1 is less studied, it is known that NDE1 can bind to dynein light chain, through which it exerts its function. Disruption of LIS1/NDE1 interactions in mice models results in the subsequential disruption of neuronal migration, as well as regulation of microtubule organisation and dynamics (Feng et al., 2000). Moreover, recruitment of LIS1 to dynein by NDE1 is known to control the movement of dynein along microtubules, as well as regulation of nuclear movement and microtubule transport (McKenney et al., 2010; Zhao et al., 2022).

35

Unlike NDE1, NDEL1 and LIS1 can directly interact with the heavy chain of cytoplasmic dynein, thus providing a direct link between LIS1 and dynein motors (Niethammer et al., 2000). Moreover, LIS1 overexpression or reduction affects NDEL1 distribution similar to dynein, while NDEL1, but not LIS1, overexpression influences dynein behaviour through redistribution of its intermediate chain (Niethammer et al., 2000). NDEL1 phosphorylation also plays a role in modulation of LIS1/dynein interaction though LIS1 dissociation, which is vital for dynein-driven transport of organelles along the axons (Pandey & Smith, 2011).

The dynein complex, including LIS1, NDE1 and NDEL1, also plays a role in mitosis. LIS1, NDE1 and NDEL1 all localise to kinetochores, while NDE1, but not NDEL1, is also required for kinetochore localisation of dynein. Moreover, cell deficiency in either of these results in mitotic abnormalities (Vergnolle & Taylor, 2007; Bradshaw & Hayashi, 2017).

Taken together, LIS1 interaction with NDE1, NDEL1 and dynein plays a central role in a number of critical pathways, including mitosis, neuronal migration, microtubule maintenance and organisation, as well as cortical development.

1.3.2.3.3 LIS1, NDE1 and NDEL1 in schizophrenia

While LIS1, NDE1 and NDEL1 are known to have a role in neurodevelopmental conditions, such as microcephaly and lissencephaly (Wynshaw-Boris, 2007; Alkuraya et al., 2011), there is also positive evidence of association between their genetic variants and CMIs, such as schizophrenia. Out of the three, the evidence of *NDE1* association is most abundant. Both duplications and deletions in the 16p13.11 locus, which contains *NDE1*, were reported in schizophrenia patients, as well as other psychiatric disorders (Ingason et al., 2011; Johnstone et al., 2015). *NDE1* haplotype has also been associated with schizophrenia in the Finnish and American Caucasian population, amongst the *DISC1* S704C mutation carriers ((Burdick et al., 2008; Hennah et al., 2007). In addition, *NDE1* variations can alter treatment response to specific psychoactive drugs used in patients with psychiatric disorders (Bradshaw et al., 2017), while rare polymorphisms within the locus can contribute to schizophrenia susceptibility (Kimura et al., 2015). *NDEL1* mutations have been observed in Finnish and American families as well, in association to

schizophrenia both together with, and separate from the variation within the *DISC1* gene (Burdick et al., 2008; Tomppo et al., 2009; Nicodemus et al., 2010).

Genetic evidence implicating *LIS1* in psychiatric disorders is still sparse. However, gene variations have been reported within the dorsolateral prefrontal cortex of schizophrenia patients, in association with *DISC1* variation (Lipska et al., 2006). A transgenic rat model of human *DISC1* (tg*DISC1*) gene with inducible expression restricted to forebrain areas also exhibited multiple behavioural abnormalities, associated with decreased expression of endogenous *Disc1* and *Lis1*. Abnormalities included elevated spontaneous hyperactivity, alterations in social interactions, as well as impaired spatial memory. Furthermore, prenatal expression of tg*DISC1* resulted in enlargement of the lateral ventricles and attenuated neurite outgrowth, consistent with the role of LIS1 (Pletnikov et al., 2008). More recently, a deletion in the *Lis1* gene was shown to exert structural and functional changes within the mouse cortex, associated with schizophrenia-like phenotypes (Garcia-Lopez et al., 2021).

1.3.2.3.4   LIS1, NDE1, NDEL1 and DISC1

LIS1 and NDE1/NDEL1 were first implicated in the DISC1 interaction network through yeast two-hybrid screens (Morris et al., 2003; Ozeki et al., 2003; Brandon et al., 2004). All three proteins bind to the C-terminal region of DISC1 and disturbances in that region specifically inhibit the interactions (Brandon et al., 2004). Unlike LIS1, which binds to the N-terminal region of NDE1/NDEL1, DISC1 binding to these homologues is facilitated through the conserved C-terminal α-helix (**Figure 9**) (Feng et al., 2000; Sasaki et al., 2000; Brandon et al., 2004). This DISC1 interaction domain also corresponds to the binding site for cytoplasmic dynein heavy chain (Sasaki et al., 2000), implicating the role of DISC1 in regulation of dynein pathway through NDE1/NDEL1. Furthermore, co-transfection and immunoprecipitation studies showed that DISC1 can form a protein complex with LIS1, and such complexes contain increased amounts of DISC1 in the presence of NDEL1, confirming that NDEL1 is capable of bringing the two proteins together. The DISC1-NDEL1 complex also exists in murine brain, where it is developmentally regulated (Brandon 2004). Inhibition of this interaction directly disturbs neurite outgrowth through redistribution of NDEL1 (Kamiya et al., 2006).

DISC1, LIS1 and NDE1/NDEL1 all localise to the centrosome (Morris et al., 2003), suggesting a role of DISC1 in microtubule dynamics and organisation, as well as neuronal migration. DISC1 upregulates the dynein motor complex, which includes LIS1 and NDE1/NDEL1, by accumulating and stabilising it at the centrosome. Consistent with this role, truncating DISC1 at the C-terminus results in destabilisation and relocation of the complex, thus affecting neurite outgrowth and neuronal migration (Kamiya et al., 2005). Interestingly, another known DISC1 interaction partner, PDE4B, also associates with this complex at the centrosome, as well as the synapse (Bradshaw et al., 2008, 2011), in concordance with known DISC1 localisation (Kirkpatrick et al., 2006). PDE4B facilitates phosphorylation of NDE1 by PKA in close proximity to the DISC1 and dynein binding domain at the conserved α-helix, which may in turn affect its interactions. As such, PDE4B presents another way or regulating the DISC1/LIS1/NDE1/NDEL1 complex, and by extension, a range of critical neural processes (Bradshaw et al., 2008, 2011).

1.3.3 Protein aggregation of DISC1

1.3.3.1 Protein aggregation

Protein homeostasis, or proteostasis, serves to regulate the concentration, conformation, binding, and location of proteins (Balch et al., 2008), as well as removal of misfolded species in order to avoid accumulation of aggregates (**Figure 10**). Correct folding of proteins and maintenance of overall domain architecture is critical for successful performance of biological functions (Hipp et al., 2019). However, proteostasis, especially in post-mitotic neurons, is sensitive to functional disruption, which can lead to impaired clearance and, subsequently, accumulation of insoluble or incorrectly folded protein (Korth, 2012). Such disturbances, often termed "proteinopathies", are a hallmark of various pathological conditions, most prominently including neurodegenerative disorders.

1.3.3.1.1 Formation and accumulation of pathological aggregates

Misfolded proteins can arise from multiple sources, such as genetic mutations, aberrant transcription or translation, post-translational modifications or environmental stressors (Balch et al., 2008; Hipp et al., 2019). In addition, proteins containing intrinsically disordered regions possess a heightened capacity for formation of pathologic aggregates. Such aggregates either cause a loss of function or gain of a new, toxic property (Hipp et

al., 2019; Zaharija & Bradshaw, 2024). Based on their structural organisation, pathological aggregates can be distinguished into two categories: amyloid fibrils or amorphous aggregates (**Figure 10**). The former possess an ordered structure characterised by parallel or anti-parallel β-strands lying perpendicular to the elongated main fibril axis. While amorphous aggregates may also contain β-strands, they lack higher-ordered structure and morphology present in amyloid fibrils (Hipp et al., 2019).

If proteostasis is well-maintained, aggregated or misfolded proteins will undergo degradation via one of the two major interconnected proteolytic pathways, the ubiquitin-proteasome system (UPS) or the autophagosomal-lysosomal system. The UPS predominately degrades single, unfolded polypeptides and soluble misfolded proteins capable of entering the narrow proteasomal channel. In contrast, lysosomal degradation includes macromolecules, toxic aggregates and cellular organelles that undergo a multi-step process including protein-lipid and protein-protein interactions (Pohl & Dikic, 2019; Zhao et al., 2022). Any disruptions of proteolytic pathways can result in inability to target and degrade aberrant proteins, thus leading to accumulation of toxic aggregates (**Figure 10**).
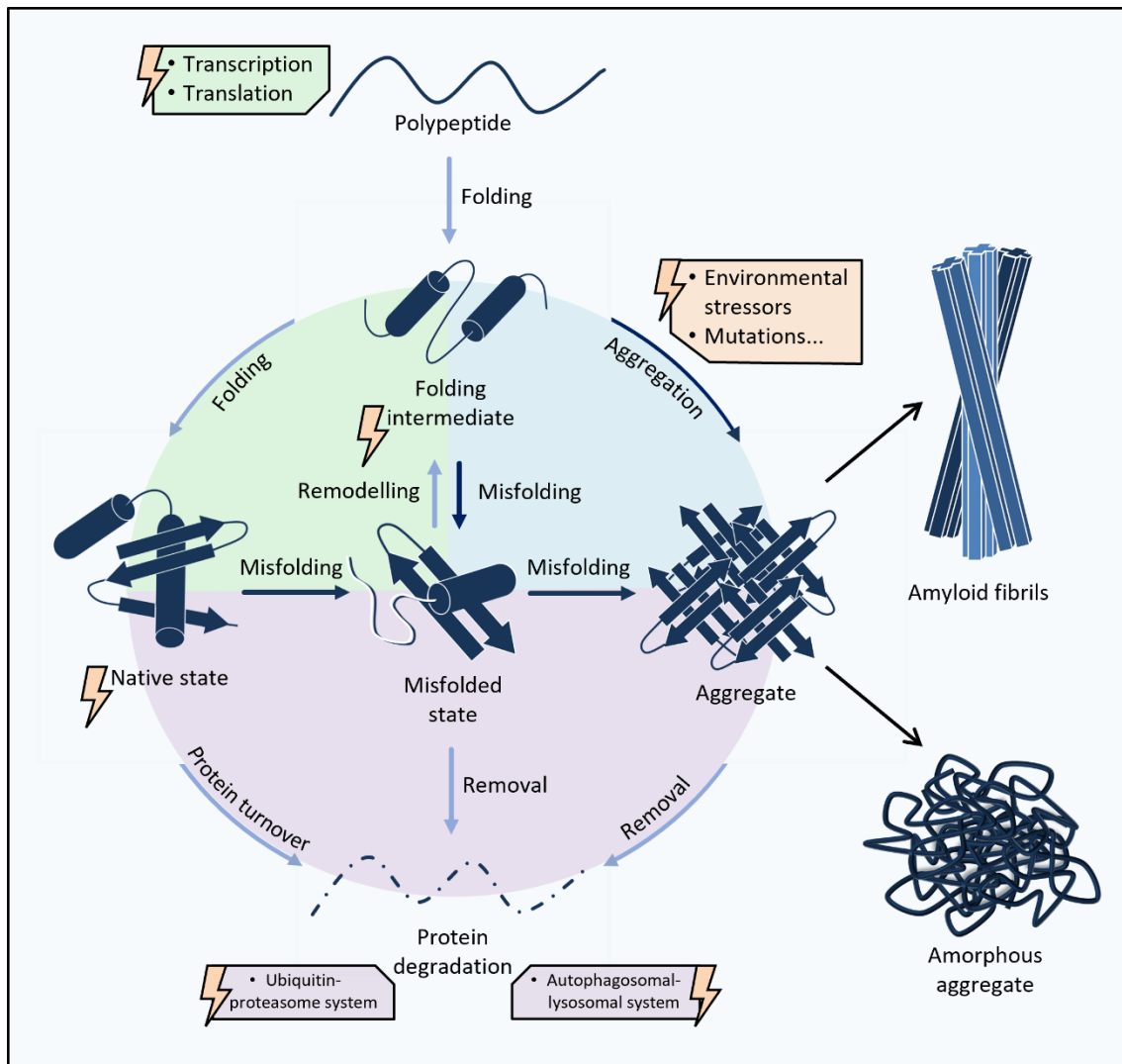
Figure 10. Schematic representation of proteostasis and aggregate development.
Well-maintained proteostasis serves to regulate proteins and their functionality in their
native state (light arrows) and minimise misfolding/aggregation (dark arrows), which can
lead to either loss of functionality, or gain of a new toxic function. Proteostasis regulates
three main processes: protein biogenesis and folding (green), conformational
maintenance (blue) and protein degradation (purple). Misfolded proteins and aggregates
undergo clearance via one of two degradation pathways: ubiquitin-proteasome system or
autophagosomal-lysosomal system. Aberrations (orange, lightning symbol) occurring
either during protein synthesis, degradation, folding, or due to environmental influences,
can lead to production and accumulation of misfolded protein and toxic aggregates
(amorphous or amyloid), resulting in disbalanced proteostasis and, consequentially,
disease development. Adapted from Hipp et al, 2019.

1.3.3.1.1 Protein aggregation in mental illness

It is well established that protein abnormalities can lead to neurological disorders. For instance, Alzheimer's disease is characterised by the accumulation of misfolded tau proteins and amyloid-beta peptides (Barmaki et al., 2023), while Huntington's disease is characterised by aggregation of mutant huntingtin (Herrmann et al., 2021). Such diseases share many clinical traits with CMIs, including cognitive, emotional and behavioural deficits. Moreover, comorbidity of CMIs with various neurodegenerative disorders has been well documented (Weamer et al., 2009; Emanuel et al., 2011; Byrne et al., 2013; Gabilondo et al., 2017; Ellis et al., 2020). Considering the shared symptomatology and comorbidity incidence between CMIs and neurodegenerative disorders, research focus soon shifted to the existence of misfolded insoluble protein aggregates in the brains of patients suffering from CMIs (Leliveld et al., 2008, 2009; Ottis et al., 2011; Bader, Tomppo, et al., 2012; Bradshaw et al., 2014; Nucifora et al., 2016).

While no large, aggregated protein structures were found to exist in major mental illnesses, a hypothesis suggesting formation of micro-aggregates of specific proteins within the brain was put forward, which may account for the chronic onset of the diseases (Leliveld et al., 2008; Korth, 2012). However, unlike neurodegenerative disorders, which are characterised by large neuronal and synaptic losses, aggregation in mental illness does not lead to neuronal apoptosis, but likely acts through loss and gain of function effects and recruitment of other proteins into aggresomes (Hui et al., 2022). Accumulation of protein aggregates in brains of patients suffering from neuropsychiatric disorders can also occur due to the disruption of other processes, such as disruption to the endoplasmic reticulum (Bown et al., 2000; Bengesser et al., 2018; Kim et al., 2018), autophagy processes (Merenlender-Wagner et al., 2013; Kang et al., 2022; Barmaki et al., 2023; Song et al., 2023) or ubiquitin-proteasome system (Altar et al., 2005; Scott et al., 2016; Meiklejohn et al., 2019; Kim et al., 2021). For example, some studies showed that patients with schizophrenia have diminished proteasome function and increased levels of ubiquitinated protein, indicative of misfolded protein clearance (Bousman et al., 2019; Scott & Meador-Woodruff, 2019).

Although the investigation of protein aggregation in the context of CMIs is still in its early stages, researching the mechanisms behind this process may help in elucidating novel therapeutic treatments of these disorders. As such, a role of DISC1 in aberrant

proteostasis represents a putative target for further research into pathophysiology of schizophrenia and recurrent disorders.

1.3.3.2 DISC1 aggregation in mental illness

1.3.3.2.1 Post-mortem studies in CMI patients

As the protein product of a major gene implicated in the pathophysiology of CMIs, with a prominent role in behavioural control, DISC1 presented an excellent target for research of aberrant proteostasis in CMIs (Korth, 2012). Investigation of post-mortem brains of patients with schizophrenia, bipolar disorder and major depressive disorder revealed that approximately twenty percent of patients had DISC1 aggregates within the cingular cortex, while none were present in healthy controls (Leliveld et al., 2008), nor patients suffering from neurodegenerative diseases (Ottis et al., 2011). Insoluble DISC1, a product of aggregates large enough to exceed solubility, also led to dysfunctional molecular interaction with NDEL1, leading to a loss-of-function phenotype similar to described familial cases carrying a DISC1 mutation (Leliveld et al., 2008). Interestingly, aggregating DISC1 also demonstrated the ability to recruit dysbindin, a protein involved in dendritic spine formation, to cell-invasive aggresomes in multiple systems, including post-mortem brains for a subgroup of patients with CMIs (Ottis et al., 2011). DISC1 can also co-recruit soluble endogenous DISC1 into aggresomes, depleting the functional pool, thus resulting in compromised normal neuronal function and mitochondrial transport (Ottis et al., 2011; Atkin et al., 2012). Inhibition of autophagosomal pathway enhanced formation of such aggresomes, indicating that disruptions to the pathway can have negative effects on neuronal function and intracellular transport of organelle cargo (Atkin et al., 2012). The latter is of significant importance, considering the role of DISC1 in regulation of synaptic vesicle transport (Flores et al., 2011).

1.3.3.2.2 *In vivo* studies in CMI patients

A single *in vivo* study on the presence of DISC1 aggregates in patients suffering from mental illness has been performed to date. Cerebrospinal fluid (CSF) samples were collected from patients with first-episode psychosis and healthy controls, and assayed using the highly-sensitive surface-based fluorescence intensity distribution analysis that enables detection of single aggregates. Subsequent analysis showed elevated levels of DISC1 aggregates in CSF, specifically in a subset of patients suffering from schizophrenia

or schizoaffective disorder (Pils et al., 2023). The possibility of *in vivo* detection of aggregated proteins in patients suffering from mental illness can thus prove invaluable in the future as a diagnostic biomarker of CMIs, in at least a subset of patients.

1.3.3.2.3 Transgenic murine model studies

A transgenic rat model, overexpressing the full-length *DISC1* transgene and common variants S704C and L607P, displayed not only DISC1 aggregates within neurons, but behavioural phenotypes consistent with disruption of dopamine neurotransmission as well. These include high sensitivity to amphetamine, hyperexploratory behaviour and motor deficits (Trossbach et al., 2016), as well as deficits in cognitive flexibility (Wang et al., 2022) and social performance (Seidisarouei et al., 2022; Wang et al., 2022). Furthermore, elevation in cytosolic dopamine levels increased DISC1 multimerization and insolubility, as well as complex formation with the dopamine transporter (Trossbach et al., 2016).

Morphological aberrations reported in the same tg*DISC1* model include a decrease of dopaminergic neurons in substantia nigra pars compacta (Hamburg et al., 2016) and dopamine content in the dorsal striatum (Trossbach et al., 2016). Both are a part of the nigrostriatal pathway responsible for locomotor behaviour and reward functions. Taken together, these results establish a causal connection between DISC1 aggregation and altered dopamine homeostasis, consequently supporting its role in the pathology of CMIs.

Further research conducted on the tg*DISC1* rat demonstrated that DISC1 aggregation leads to alteration in the CA1 region of hippocampus proper. Deficits include impairments in encoding of location-independent information, as well as impaired neuronal response during sleep and/or rest and network synchrony, which have previously been reported for schizophrenia patients (Kaefer et al., 2019). Another study demonstrated that the tg*DISC1* rat features a dysregulated immune-related network of genes that can be detected through peripheral blood testing, thus providing a diagnostic tool to identify of subsets of CMI patients by reverse translation (Trossbach et al., 2019).

1.3.3.2.4 Neuronal culture studies

Abnormalities in glutamatergic pathway, including hypofunction of glutamate-gated NMDA (N-methly-D-aspartate) receptors and their modulator D-serine (Hashimoto et al.,

2003), are distinctly associated with psychosis in schizophrenia patients (Ma et al., 2012). Formation of D-serine is catalysed by serine racemase (SR), which is stabilised by its binding to DISC1 (Ma et al., 2012). Curiously, SR has also been shown to associate with DISC1 aggresomes in cortical neurons. This interaction is enhanced in the presence of D-serine, which augments the formation of large DISC1 aggregates, facilitated by NMDA receptors (Jacobi et al., 2019). Such interaction provides an insight into convergence of pathways between aberrant proteostasis and glutamatergic dysregulation, implicated in the aetiology of schizophrenia.

1.3.3.3 DISC1 aggregation in neurodegenerative diseases

DISC1 aggregates were also detected in the murine models and brains of patients suffering from Huntington's disease (HD). DISC1 and mutant huntingtin (HTT) form pathological complexes, resulting in dysregulation of interaction between soluble DISC1 and PDE4. Loss of interaction leads to aberrant increase in PDE4 activity, which in turn affects cAMP levels and cellular signalling. A decrease in cAMP levels can be detected in cerebrospinal fluid of HD patients, suggesting the role of PDE4 in disease development. Moreover, the loss of the physiological control DISC1 exerts over PDE4 due to the formation of DISC1-HTT complex may also underlie anhedonia seen in a murine model of HD, further confirming the role of abnormal proteostasis in disease development (Tanaka et al., 2017).

DISC1 co-aggregates with another protein of importance in neurodegenerative disorders, TDP-43 (TAR DNA-binding protein 43 kDa). In frontotemporal lobar degeneration (FTLD), TDP-43 aggregation leads to progressive neuronal atrophy, causing severe mental and behavioural deficits. Co-aggregation of TDP-43 and DISC1 results in impaired local translation in dendrites, as well as behavioural and mental deficits in both murine models and post-mortem brains of FTLD patients. Behavioural deficits were improved upon exogenous DISC1 expression in frontal cortex, implicating that the loss of soluble DISC1 is directly responsible for aberrant behaviour relevant to psychiatric conditions (Endo et al., 2018).

1.4 Disrupted in Schizophrenia 1 and *Drosophila*

1.4.1 *Drosophila* as a model for CMI research

CMIs share a complex, elusive aetiology that is dependent on both genetic and environmental component. In order to study the genetic background and pathological mechanisms behind these disorders, animal models across various species have been established. While the fruit fly, *Drosophila melanogaster*, initially seems far removed from mammalian models, numerous fundamental physiological, biological and neurological pathways are conserved between them (Narayanan & Rothenfluh, 2015).

Regardless of the differences in brain morphology, *Drosophila* represents a versatile model used in research for over a century. They are easy to maintain, have a short life cycle and produce large numbers of progenies, with a short generation time that allows sophisticated genetic manipulation and research of gene function at a rapid pace not achievable in other models (Cheng et al., 2018). Following the sequencing of both the fly and human genome, comparisons between the two revealed that approximately 75% of known human genes have functional homologues in *Drosophila*, strengthening its legitimacy as a research model for biological research (Jennings, 2011).

Due to the shared genetics of the human and fly nervous system, genetic manipulation and biological studies in *Drosophila* enabled substantial advances in various neurobiological fields, such as neurogenetics (Bellen et al., 2010). This neurogenetic approach gave way to research of the molecular basis of behaviour, including locomotor activity (Feany & Bender, 2000; Hunter et al., 2021), circadian rhythms (Hendricks et al., 2000; Shaw et al., 2000; Sehgal et al., 2007), information processing, learning (Drain et al., 1991; Lei et al., 2022) and memory (Blum et al., 2009; Furukubo-Tokunaga et al., 2016). Whereas cognitive and mental deficits seen in CMI patients cannot be fully replicated in any animal model, elucidating molecular mechanisms conserved within species and their dysfunctions may help uncover the risk factors and underlying pathology of these diseases. As such, *Drosophila* represents a powerful tool for modelling neuropsychiatric disorders such as social isolation and substance addiction.

1.4.2 *Drosophila* models of DISC1

Although no *DISC1* orthologue can be found in fruit flies, a significantly high (92%) number of genes encoding DISC1-interacting proteins is conserved within the *Drosophila* genome (Furukubo-Tokunaga et al., 2016). Among others, these include PDE4B1, ATF4, LIS1 and NDEL1, as well as the aggregating protein Dysbindin (Furukubo-Tokunaga et al., 2016). Therefore, even if *DISC1* itself is not conserved in flies, transgenic models expressing the human gene can often unveil unique phenotypes through protein-protein interaction.

To date, a limited number of studies examining DISC1 function in *Drosophila* have been conducted, focusing primarily on the circadian rhythm and locomotor activity. Deviations in both are commonly reported in schizophrenia patients (Afonso et al., 2011; Schäppi et al., 2018). For example, motor abnormalities can be observed in up to 80% of patients suffering from schizophrenia (Martin et al., 2022), and are often associated with impairments in social and functional capacity (Nadesalingam et al., 2022). Sleep and circadian rhythm disruption directly correlate to symptom severity in schizophrenia patients, and present one of the most common symptoms of the disorder (Cosgrave et al., 2018). Moreover, dopamine disturbances are closely linked to the circadian clock and can mutually exacerbate abnormalities in one another (Ashton & Jagannath, 2020; Samardžija et al., 2024).

The first transgenic fly model of human *DISC1* generated by Sawamura and colleagues showed that punctate accumulation of exogenous human DISC1 in the nucleus results in disturbance of sleep homeostasis (Sawamura et al., 2008). Interestingly, full-length DISC1, but not a C-terminally truncated counterpart mimicking the Scottish family translocation, exhibited altered sleep time. Upon induction of full-length DISC1 in male fly mushroom bodies, which are important in associative learning and memory formation, animals displayed reduced arousal state during the night. Nevertheless, no alteration in the circadian rhythm nor sleep bout frequency was detected (Sawamura et al., 2008). Normal intrinsic circadian period was also observed in tg*DISC1* mouse model, however, it exhibited lack of sleep rather than the longer sleep bouts seen in flies (Jaaro-Peled et al., 2016).

The variation in *Drosophila* phenotype was attributed to the difference in the cellular localisation, since only the full-length protein localised to the nucleus. Taking into consideration that DISC1 interacts with ATF4 within the nucleus, findings suggest that DISC1 modulates CRE-mediated gene transcription and sleep homeostasis in flies through its interaction with ATF4 (Sawamura et al., 2008). Moreover, cAMP/CREB signalling pathway was previously shown to have a non-circadian role in sleep and waking homeostasis of *Drosophila* (Hendricks et al., 2001), thus further confirming the results.

Another study expressed human DISC1 in developing *Drosophila* neurons to test the effect of overexpression on neurodevelopment and behaviour (Furukubo-Tokunaga et al., 2016). It was shown that DISC1 overexpression results in associative memory defects in fly larvae through suppression of axonal and dendritic neuronal branching. Curiously, the C-terminally truncated DISC1 construct (DISC1 1-597) localised to the nucleus in adult flies, but not the dendrites or axons. In contrast, when expressed in larval neurons, DISC1 1-597 expressed weakly in both axons and dendrites, demonstrating developmentally regulated subcellular dynamics of DISC1 (Furukubo-Tokunaga et al., 2016). Similar results were previously observed in mammalian cells and primary mouse cortical neurons (Millar et al., 2005; Sawamura et al., 2008), suggesting that subcellular dynamics of DISC1 in developing fly neurons is an evolutionally conserved mechanism within species. In another study, DISC1 1-597 was found to exert specific effects on neurodevelopment, neurophysiology and cognitive functions of *Drosophila* through downregulation of multiple disease-risk pathways (Shao et al., 2017).

Larvae expressing full-length DISC1 or DISC1 1-597 in mushroom body neurons also failed to exhibit olfactory memory compared to wild type controls and non-expressing *DISC1* carriers, indicating that memory deficits were a direct result of DISC1 expression. Moreover, this study showed functional interaction of *DISC1* and *Dysbindin*, the fly homologue of the human gene encoding the Dysbindin protein, in the development of glutamatergic synaptogenesis of motor neurons through a genetic interaction study (Furukubo-Tokunaga et al., 2016). Another study confirmed the role of *DISC1* in the development of *Drosophila* glutamatergic synapses through its interaction with the fly homologue of the human *Neurexin* gene, another psychiatric risk factor (Pandey et al., 2017). These results are in concordance with the glutamatergic hypothesis of

schizophrenia, suggesting that cognitive deficits arise from the altered glutamate neurotransmission (Kahn et al., 2015; Nakahara et al., 2021).

While insoluble DISC1 aggregates were also isolated from *Drosophila* cells in the same study, accumulation of DISC1 did not elicit robust neuronal cell death when observed in the compound eyes of the fly, which is highly sensitive to neurodegeneration (Furukubo-Tokunaga et al., 2016). However, it is still unknown whether DISC1 aggregation may affect the developmental and functional phenotypes exhibited in transgenic flies.

Disturbances in sleep, locomotion and cognitive function portray an important aspect of psychiatric disorders. While a number of studies on transgenic DISC1 flies may be limited, they represent a practical and advantageous model for studying disease-related phenotypes and underlying pathologic mechanisms of function.

2. Thesis aims

This thesis represents an exciting new approach in the research of the effects of aggregation in neuropsychiatric disorders. It aims to deepen the knowledge and understanding of structure and functions of the DISC1 protein, known for its involvement in the pathology of mental illness, as well as to utilise the *Drosophila* animal model to assess behavioural consequences of DISC1 expression. Chronic mental illnesses such as schizophrenia and recurrent disorders are amongst leading causes of mental illness worldwide, yet our knowledge of their pathological mechanisms remains limited. As such, it is pivotal to consider approaches other than genetic studies. Thus, we hypothesize that disruption in protein homeostasis presents a potential pathological mechanism behind psychiatric disorders, in a process similar to the one seen in neurodegenerative disorders. The DISC1 protein could therefore become a putative therapeutic target for chronic mental illnesses, while also providing a powerful insight into the mechanisms behind these disorders.

With this work, we aim to answer the following questions:

1) Can empirically attained DISC1 regions be optimized based on bioinformatics predictions to achieve greater stability?
2) What are the distinct expression patterns of DISC1 structural regions, when expressed in mammalian cells?
3) Do DISC1 regions expressed in isolation present stable, functional units capable of binding to known interaction proteins?
4) Which region or regions are crucial for DISC1 aggregation and can deletion of that region or regions abolish DISC1 aggregation propensity?
5) What are the behavioural consequences of DISC1 expression in *Drosophila* animal models and can they be associated with symptoms seen in patients suffering from neuropsychiatric disorders?

3. Materials and methods

3.1 Materials

3.1.1 Chemicals

Table 2. List of chemicals

Chemical	Catalogue no.	Manufacturer
Acetic acid	10192247	Honeywell
Acrylamide	A8887	Sigma-Aldrich
Agar	05040	Sigma-Aldrich
Agar type II for *Drosophila*	66-105	Genesee Scientific
Agarose	10-35-1010	Bio-Budget
Ampicillin sodium salt	K029.4	Carl Roth
Ammonium peroxodisulphate	A3678	Sigma-Aldrich
Bromophenol Blue	114391	Sigma-Aldrich
Calcium chloride	P128210	GRAM-MOL
Chloramphenicol	C0378	Sigma-Aldrich
Cornmeal	-	"Okusi zavičaja"
Dithiothreitol (DTT)	D0632	Sigma-Aldrich
Ethilene tetraacetic acid (EDTA)	20301.186	VWR Chemicals
Ethanol, 96%	133124	KEFO
Ethanol, absolute	P147303	GRAM-MOL
Fluoroshield	F6182	Sigma-Aldrich
Glycerol	P121003	GRAM-MOL
Glycine	33226	Sigma-Aldrich
HEPES	H3375	Sigma-Aldrich
Hydrochloric acid, 37%	20252.290	VWR Chemicals
Isopropyl β-D-1-thiogalactopyranoside (IPTG)	I6758	Sigma-Aldrich
Isopropanol	P100516	GRAM-MOL
Kanamycin sulphate	60615	Sigma-Aldrich
Magnesium chloride 6-hydrate	P139120	GRAM-MOL

Chemical	Catalogue no.	Manufacturer
Manganese (II) chloride tetrahydrate	22129	Sigma-Aldrich
Methanol	414816	Carlo Erba
MG132	CSN11436	CSN Pharma
Mineral oil	8042-47-5	Sigma-Aldrich
N, N, N', N'-Methylenebisacrylamide	43701	Thermo Scientific
NIPAGIN	NC10.1	Roth
Nuclease-free water	83645.290	VWR Chemicals
Phenylmethylsulfonyl fluoride	10837091001	Roche
PIPES	P6757	Sigma-Aldrich
Ponceau S	5938.2	Carl Roth
Potassium acetate	P1190	Sigma-Aldrich
Potassium chloride	P9333	Sigma-Aldrich
Potassium dihydrogen phosphate	26936.293	VWR Chemicals
Propionic acid	402907	Sigma-Aldrich
Sarkosyl (*N*-Lauroylsarcosine sodium salt)	L5125	Sigma-Aldrich
Sodium azide	71289	Sigma-Aldrich
Sodium chloride	P148590	GRAM-MOL
Sodium dihydrogen phosphate	28015.294	VWR Chemicals
Sodium dodecyl sulfate	75746	Sigma-Aldrich
Sodium hydroxide	P147090	GRAM-MOL
Sodium hypochlorite solution (13%)	148022	GRAM-MOL
Spectinomycin dihydrochloride pentahydrate	S4014	Sigma-Aldrich
Sucrose	S9378	Sigma-Aldrich
Sugar "Premijer"	-	Factory Osijek
TEMED (N, N, N', N'-Tetramethylenthylenediamine)	T7024	Sigma-Aldrich
Tris base	93362	Sigma-Aldrich
Triton X-100	9036-19-5	Sigma-Aldrich
Tween-20	P1379	Sigma-Aldrich
Tryptone	95039	Sigma-Aldrich

Chemical	Catalogue no.	Manufacturer
Yeast, dry	101011	Encian
Yeast extract	92144	Sigma-Aldrich

3.1.2 Equipment

Table 3. List of equipment

Product	Details	Manufacturer
Camera	ORCA-R2 CCD camera, used with the Olympus IX83 inverted microscope	Hamamatsu Photonics
ChemiDoc XRS+	Detection system for chemiluminescence, fluorescence, and colorimetric imaging	BioRad
DAM5M Drosophila Activity Monitors	Allows for measurement of 32 flies, four infrared beams per tube (5 mm diam.)	TriKinetics Inc.
DAMS Drosophila Activity Monitors	Allows for measurement of 32 flies, one infrared beam per tube (5 mm diam.)	TriKinetics Inc.
DAMSystem3 LC4 Light Controller	Allows turning the light source on/off by a predetermined schedule	TriKinetics Inc.
Drosophila flow regulator	The Flow Buddy – used to administrate CO_2 for the purpose of anesthetizing flies	Genesee Scientific
Electrophoresis chamber	Mini-PROTEAN Tetra Vertical Electrophoresis Cell	BioRad
Electrophoresis power supply	PowerPac Universal Power Supply, output range 1-500 V	BioRad
Microscope	Olympus IX83 inverted fluorescent microscope	Olympus Europa Holding

Product	Details	Manufacturer
Mini horizontal electrophoresis system	multiSUB Mini with 7 × 7cm, 7 × 10cm gel tray and 8-well combs	Cleaver Scientific
Spectrophotometer	BioDrop μLITE UV/VIS spectrophotometer	Biochrom
Tabletop centrifuge	Centrifuge MiniSpin plus, max RCF: 14,100 × g	Eppendorf
Transfer system	Trans-Blot Turbo Transfer System	BioRad
Ultracentrifuge	Sorvall MTX 150 Micro-Ultracentrifuge S140-AT fixed angle rotor	Thermo Fisher Scientific
UV transilluminator	Compact benchtop UV Transilluminator, MD-20 / HD-20	Wealtec Corp.

3.1.3 Software

Table 4. List of computer programs

Software	Purpose	Developer
cellSens V1.5.	Biological image analysis	Olympus Europa Holding
DAMSystem V3.08	Quantification of Drosophila movement over time; includes DAMSystem3 Data Collection Software and FileScan program	TriKinetics Inc.
GraphPad Prism 10	Graphical depiction and analysis of quantitative data	GraphPad

Software	Purpose	Developer
Fiji ImageJ	Biological image analysis	National Institute of Health
Image Lab	Image capture and analysis software	BioRad

Table 5. List of online software and tools

Software/Tool	Purpose	Developer
AGGRESCAN	Prediction of aggregation hot spots in polypeptides (http://bioinf.uab.es/aggrescan/)	UAB Barcelona
ANuPP	Prediction of aggregation nucleation in peptides and proteins (https://web.iitm.ac.in/bioinfo2/ANuPP/homeseq1/)	Indian Institute of Technology Madras
FoldAmyloid	Prediction of amyloidogenic regions in proteins (http://bioinfo.protres.ru/fold-amyloid/)	The Bioinformatics Group
MetAmyl	Prediction of amyloid aggregation in proteins (https://metamyl.genouest.org/)	GenQuest Bioinformatics
MUSCLE	Multiple sequence comparison by log-expectation tool (https://www.ebi.ac.uk/jdispatcher/msa/muscle?stype=protein)	EMBL-EBI

Software/Tool	Purpose	Developer
NEBcutter v3.0.17	Online DNA restriction mapping (https://nc3.neb.com/NEBcutter/)	New England BioLabs
Oligo Analysis Tool	Evaluation of the oligomer parameters (https://operon.com/tools/oligo-analysis-tool.aspx)	Eurofins Genomics
Pairwise Structural Alignment	Alignment of protein 3D structures (https://www.rcsb.org/alignment)	RCSB PDB
Reverse complement	Computes reverse complement of a nucleotide sequence (https://reverse-complement.com/)	Audrius Meskauskas, PhD
TANGO	Prediction of aggregation nucleating regions in unfolded polypeptide chains (http://tango.crg.es/)	Centre for Genomic Regulation

3.1.4 Plastic and other materials

Table 6. List of plastic materials

Product	Details	Catalogue no.	Manufacturer
Cell culture plates	6-well, sterile	83.3920	Sarstedt
	12-well, sterile	83.3921	Sarstedt
	24-well, sterile	83.3922	Sarstedt
Combs for SDS-PAGE	15-well, thickness: 1.5 mm	1653366	BioRad
	15-well, thickness: 1.0 mm	1653360	BioRad
	10-well, thickness: 1.5 mm	1653365	BioRad
	10-well, thickness: 1.0 mm	1653369	BioRad

Product	Details	Catalogue no.	Manufacturer
Conical tubes	15 mL, sterile	62.554.502	Sarstedt
	50 mL, sterile	62.547.274	Sarstedt
Cell Scraper	16 cm, sterile	83.1832	Sarstedt
Cryogenic tubes	1.80 mL	479-6843	Thermo Fisher Scientific
Drosophila stock bottles	Polypropylene, square bottom	32-130	Genesee Scientific
Drosophila vials	25 × 95 mm	789008	Dutscher
Microcentrifuge tubes	1.5 mL	Z336769	Sigma-Aldrich
PCR tubes	0.2 mL	BR781305-1000EA	Sigma-Aldrich
Petri dishes	92 mm, sterile	82.1472.001	Sarstedt
Pipette tips	100-1200 μL	21.00.610	Ratiolab
	20-200 μL	5131090C	CAPP
	0.1-10 μL	F161631	Fisher Scientific
T25 flasks	25 mL, sterile	83.3910.002	Sarstedt
Serological pipette	10 mL, sterile	86.1254.025	Sarstedt
Syringes	10 mL	309110	BD
	1 mL	303174	BD
Syringe filters	0.2 μm, sterile	83.1826.001	Sarstedt
Ultracentrifuge tubes	11 × 34mm	S5007	Science Services

Table 7. List of other required materials

Product	Details	Catalogue no.	Manufacturer
Blotting sheets	Whatman GB003, size 110 × 140 mm	10427804	Cytiva
Hypodermal needles	Needle gauge: 21G Needle length: 40 mm	304432	BD
Microscope coverslips	Round, thickness: 0.13-0.16 mm, diameter: 12 mm	CB00120RA120MNZ0	Fisher Scientific
Plates for WB	Short plates	1653308	BioRad
	Spacer plates, 1.5 mm	1653312	BioRad
	Spacer plates, 1.0 mm	1653311	BioRad
Transfer membrane	Porablot PVDF, pore size 0.2 μm	741260	Macherey-Nagel

3.1.5 Materials required for cloning, bacterial cultivation, mammalian cell culture and *Drosophila* cultivation

Buffers and solutions are made up to 1L with Milli-Q water, unless otherwise specified. If required, pH was adjusted using either sodium hydroxide or hydrochloric acid.

3.1.5.1 Cloning

3.1.5.1.1 DNA oligonucleotides

Synthetic DNA oligonucleotides (primers) used for cloning purposes were purchased from Eurofins Scientific and Metabion. Upon receiving the primers, 100 μM stock solutions were diluted to working stocks of 10 μM with ultrapure water.

Table 8. DNA oligonucleotides for general cloning and sequencing.

Gene	Description	Primer	Sequence (5'→3')
-	Sequencing - standard	CMV - forward	CGCAAATGGGCGGTAGGCGTG
-	Sequencing - standard	EGFP seq - forward	CATGGTCCTGCTGGAGTTCGTG
-	Sequencing - standard	pENTR - forward	CTACAAACTCTTCCTGTTAGTTAG
-	Sequencing - standard	pENTR - reverse	ATGGCTCATAACACCCCTTG
-	Cloning - Addition of sites	Ext BamKpn - forward	GCTATAAGGATCCGGTACCTAGTCGACATG
-	Cloning - Addition of sites	Ext XhoXba - reverse	GGCACCAGCTCGAGTCTAGAATTCTCATC
-	Sequencing - standard	M13 – forward	CAGGAAACAGCTATGACC
-	Sequencing - standard	M13 - reverse	CAGGAAACAGCTATGAC
-	Sequencing - standard	pPMW-Seq - forward	GACTGTGCGTTAGGTCCTGT
-	Sequencing - standard	T7 – forward	TAATACGACTCACTATAGGG
-	Sequencing - standard	T7 – reverse	GCTAGTTATTGCTCAGCGG
DISC1	Sequencing - DISC1 (middle)	DISC1seq – forward	TCAGTCTCTTGGCTACACGG

Table 9. Gene-specific oligonucleotides used for Gateway cloning

Gene	Name[1]	Sequence (5'→3')
DISC1	DISC1-1 - forward	AATAGCAGGCTTCGCCGCCACCATGCCAGGCG
DISC1	DISC1-249 - reverse	GGCCACCACTTTGTACAAGAAAGCTGGGTCTCAAGCTTTGGCTC
DISC1	DISC1-257 - forward	AATAGCAGGCTTCGCCGCCACCATGGAGGACCCGCG
DISC1	DISC1-383 - reverse	GGCCACCACTTTGTACAAGAAAGCTGGGTCTCACAGGTCTTCTAATC
DISC1	DISC1-539 - forward	AATAGCAGGCTTCGCCGCCACCATGCCACCGGAAAC
DISC1	DISC1-539 - reverse	CACCACTTTGTACAAGAAAGCTGGGTCTCATGGCTCTGCATG
DISC1	DISC1-597 - reverse	GGGCACCACTTTGTACAAGAAAGCTGGGTCTCATGATATGGCATGC
DISC1	DISC1-635 - forward	AGCAGGCTTCGCCGCCACCATGAATGTCAAAAAG
DISC1	DISC1-655 - reverse	CACCACTTTGTACAAGAAAGCTGGGTCTCAGTGCTCCACTTC
DISC1	DISC1-691 - forward	AATAGCAGGCTTCGCCGCCACCATGTGGGAAGCTG
DISC1	DISC1-738 - reverse	CACCACTTTGTACAAGAAAGCTGGGTCTCAGGAGTGGAGC
DISC1	DISC1-807 - reverse	GGGGCACCACTTTGTACAAGAAAGCTGGGTCTCAGAGATCTTCATC
DISC1	DISC1-836 - reverse	CACCACTTTGTACAAGAAAGCTGGGTCTCATCCCGCCTCC
DISC1	DISC1-854 - reverse	CACCACTTTGTACAAGAAAGCTGGGTCTCAGGCTTGTGCTTC

[1] *Gene name – first codon number cloned – primer direction.*

Table 10. Gene-specific oligonucleotides used for restriction cloning

Gene	Name[1]	Sequence (5'→3')
DISC1	DISC1-1-Sal - forward	GTAGTCGACATGCCAGGCGG
DISC1	DISC1-257-Sal - forward	GTAAGTCGACATGGAGGACCCGC
DISC1	DISC1-370-Eco - reverse	GGCGCGAATTCTCATCAATAATCATCATTCTC
DISC1	DISC1-383-Eco - reverse	GGCGAATTCTCATCACAGGTCTTCTAATC
DISC1	DISC1-384-Sal - forward	GGCGTCGACATGGAACAAGAGAAAATC
DISC1	DISC1-383-XbaKpn - reverse	GCGCGTCTAGACTATCAGGTACCCAGGTCTTCTAATC
DISC1	DISC1-390-Eco – reverse	GGGCGAATTCTCATCACAGGCTGATT
DISC1	DISC1-415-SalKpn - forward	GAAAAGTCGACATGGGTACCGCCTTGCGCC
DISC1	DISC1-415-XbaKpn - reverse	GCAAATCTAGACTATCAGGTACCGGCAGCCTGG
DISC1	DISC1-446-SalKpn - forward	GCATAGTCGACATGGGTACCGACAGCTTGCAC
DISC1	DISC1-446-XbaKpn - reverse	GCGAATCTAGACTATCAGGTACCGTCCTGAGCAG
DISC1	DISC1-477-SalKpn - forward	GGGATGTCGACATGGGTACCTTTGTGCTGGAAG
DISC1	DISC1-477-XbaKpn - reverse	GCGCCTCTAGACTATCAGGTACCAAACATCCTTG
DISC1	DISC1-508-SalKpn - forward	GATAAAGTCGACATGGGTACCGTGGGCCAGCTG
DISC1	DISC1-508-XbaKpn - reverse	GCGAATCTAGACTATCAGGTACCCACCAGTGGG
DISC1	DISC1-539-SalKpn - forward	GCAAAGTCGACATGGGTACCCCACCGGAAAC
DISC1	DISC1-538-Eco - reverse	GGCGAATTCTCATCACTCTGCATGG

Gene	Name[1]	Sequence (5'→3')
DISC1	DISC1-539-Sal - forward	GTAGTCGACATGCCACCGGAAAC
DISC1	DISC1-577-Sal - forward	GGCGCGTCGACATGAAAGTTAACG
DISC1	DISC1-597-Sal - forward	GGCGTCGACATGTCAGGAAACC
DISC1	DISC1-597-Eco - reverse	GGGCGAATTCTCATCATGATATGGCATG
DISC1	DISC1-601-Eco - reverse	GCGCGAATTCTCATCAGAAATGGTTTCC
DISC1	DISC1-622-Eco - reverse	GGAGAATTCTCATCACTCCAGCCCT
DISC1	DISC1-635-Sal - forward	GGCGTCGACATGAATGTCAAAAAGCTG
DISC1	DISC1-655-Eco - reverse	GAGGAATTCTCATCAGTGCTCCACTTC
DISC1	DISC1-691-Sal - forward	GGAGTCGACATGTGGGAAGCTG
DISC1	DISC1-738-Eco - reverse	GGAGAATTCTCATCAGGAGTGGAGC
DISC1	DISC1-801-Sal - forward	GGCGTCGACATGCACAGTCATG
DISC1	DISC1-807-Eco - reverse	GGGCGAATTCTCATCAGAGATCTTCATC
DISC1	DISC1-829-Eco - reverse	GACGAATTCTCATCAGAGCTGCAGG
DISC1	DISC1-836-Eco - reverse	GTAGAATTCTCATCATCCCGCCTCC
DISC1	DISC1-854-Eco - reverse	GGAGAATTCTCATCAGGCTTGTGCTTC

[1] *Gene name – first codon number cloned – restriction site(s) added – primer direction.*

Table 11. Plasmid vectors used for cloning and construct expression

Vector backbone	Vector type	Gene insert	Antibiotic resistance	Origin	Publication
pDONR/Zeo	Entry	-	ZEO	Thermo Fisher Scientific	Unpublished
pENTR1A no *ccd*B	Entry	-	KAN	Addgene	(Campeau et al., 2009)
pcDNA3.1-MYO10-HMM-NanoTrap	Expression	-	AMP	Addgene	(Bird et al., 2017)
pdcDNA3.1-FlagMyc	Expression	-	AMP	BCCM/LMBP Plasmid Collection	Unpublished
pDEST-CMV-N-EGFP	Expression	-	AMP	Addgene	(Agrotis et al., 2019)
pDEST-CMV-N-mCherry	Expression	-	AMP/CHL		
pPRW	*Drosophila* expression	-	AMP/CHL	T. Murphy, DRGC	Unpublished

Vector backbone	Vector type	Gene insert	Antibiotic resistance	Origin	Publication
pDONR221	Entry vector	ATF4 (full length)	KAN	DNASU Plasmid Repository	Unpublished
pDONR221	Entry vector	NDE1 (full length)	KAN	N. Bradshaw, D. Soares & D. Porteous, Edinburgh	Unpublished
pDONR221	Entry vector	NDEL1 (full length)	KAN	N. Bradshaw, D. Soares & D. Porteous, Edinburgh	Unpublished
pDONR221	Entry vector	PDE4B1 (full length)	KAN	DNASU Plasmid Repository	Unpublished
pDONR/ZEO	Entry vector	DISC1 (257-383, D)	ZEO	Generated during thesis	(Zaharija & Bradshaw, 2024)
pDONR/ZEO	Entry vector	DISC1 (635-738, S)	ZEO	Generated during thesis	(Zaharija & Bradshaw, 2024)

Vector backbone	Vector type	Gene insert	Antibiotic resistance	Origin	Publication
pENTR1A	Entry vector	DISC1 (1-259, Nterm)	KAN	Generated during thesis	(Zaharija & Bradshaw, 2024)
pENTR1A	Entry vector	DISC1 (1-383, Nterm-D)	KAN	Generated during thesis	(Zaharija & Bradshaw, 2024)
pENTR1A	Entry vector	DISC1 (1-415, Nterm-linker)	KAN	Generated during thesis	(Zaharija & Bradshaw, 2024)
pENTR1A	Entry vector	DISC1 (257-370, D-half UVR)	KAN	Generated during thesis	(Zaharija & Bradshaw, 2024)
pENTR1A	Entry vector	DISC1 (257-390, D- UVR)	KAN	Generated during thesis	(Zaharija & Bradshaw, 2024)
pENTR1A	Entry vector	DISC1 (257-538, D-linker)	KAN	Generated during thesis	(Zaharija & Bradshaw, 2024)
pENTR1A	Entry vector	DISC1 (257-597, D-ST)	KAN	Generated during thesis	(Zaharija & Bradshaw, 2024)

Vector backbone	Vector type	Gene insert	Antibiotic resistance	Origin	Publication
pENTR1A	Entry vector	DISC1 (257-655, D-I)	KAN	Generated during thesis	(Zaharija & Bradshaw, 2024)
pENTR1A	Entry vector	DISC1 (384-538, linker)	KAN	Generated during thesis	(Zaharija & Bradshaw, 2024)
pENTR1A	Entry vector	DISC1 (384-655, linker-I)	KAN	Generated during thesis	(Zaharija & Bradshaw, 2024)
pENTR1A	Entry vector	DISC1 (539-655, I)	KAN	Generated during thesis	(Zaharija & Bradshaw, 2024)
pENTR1A	Entry vector	DISC1 (539-738, I-S)	KAN	Generated during thesis	(Zaharija et al., 2020)
pENTR1A	Entry vector	DISC1 (539-601, I-half UVR)	KAN	Generated during thesis	Unpublished
pENTR1A	Entry vector	DISC1 (539-622, I-UVR)	KAN	Generated during thesis	Unpublished

Vector backbone	Vector type	Gene insert	Antibiotic resistance	Origin	Publication
pENTR1A	Entry vector	DISC1 (539-854, I-C)	KAN	Generated during thesis	(Zaharija & Bradshaw, 2024)
pENTR1A	Entry vector	DISC1 (635-836, S-C)	KAN	Generated during thesis	(Zaharija & Bradshaw, 2024)
pENTR1A	Entry vector	DISC1 (691-807, C-half UVR)	KAN	Generated during thesis	Unpublished
pENTR1A	Entry vector	DISC1 (691-829, C-half UVR)	KAN	Generated during thesis	Unpublished
pENTR1A	Entry vector	DISC1 (691-836, C)	KAN	Generated during thesis	(Zaharija & Bradshaw, 2024)
pENTR1A	Entry vector	DISC1 (Δ384-415)	KAN	Generated during thesis	(Zaharija & Bradshaw, 2024)

Vector backbone	Vector type	Gene insert	Antibiotic resistance	Origin	Publication
pENTR1A	Entry vector	DISC1 (1-655Δ384-415)	KAN	Generated during thesis	(Zaharija & Bradshaw, 2024)
pENTR1A	Entry vector	DISC1 (1-836Δ384-415)	KAN	Generated during thesis	(Zaharija & Bradshaw, 2024)
pENTR223	Entry vector	DISC1 (full length)	SPECT	DNASU Plasmid Repository	Unpublished
pENTR223	Entry vector	LIS1 (full length)	SPECT	DNASU Plasmid Repository	Unpublished
pdcDNA-FlagMyc	Mammalian expression	ATF4 (full length)	AMP	Generated during this thesis	Unpublished
pdcDNA-FlagMyc	Mammalian expression	DISC1 (full length)	AMP	Generated during thesis	(Samardžija et al., 2023)
pdcDNA-FlagMyc	Mammalian expression	DISC1 (1-259, Nterm)	AMP	Generated during thesis	(Zaharija & Bradshaw, 2024)

Vector backbone	Vector type	Gene insert	Antibiotic resistance	Origin	Publication
pdcDNA-FlagMyc	Mammalian expression	DISC1 (1-383, Nterm-D)	AMP	Generated during thesis	(Zaharija & Bradshaw, 2024)
pdcDNA-FlagMyc	Mammalian expression	DISC1 (1-415, Nterm-linker)	AMP	Generated during thesis	(Zaharija & Bradshaw, 2024)
pdcDNA-FlagMyc	Mammalian expression	DISC1 (257-370, D-half UVR)	AMP	Generated during thesis	Unpublished
pdcDNA-FlagMyc	Mammalian expression	DISC1 (257-383, D)	AMP	Generated during thesis	(Zaharija & Bradshaw, 2024)
pdcDNA-FlagMyc	Mammalian expression	DISC1 (257-390, D-UVR)	AMP	Generated during thesis	Unpublished
pdcDNA-FlagMyc	Mammalian expression	DISC1 (257-538, D-linker)	AMP	Generated during thesis	(Zaharija & Bradshaw, 2024)
pdcDNA-FlagMyc	Mammalian expression	DISC1 (257-597, D-ST)	AMP	Generated during thesis	(Zaharija & Bradshaw, 2024)

Vector backbone	Vector type	Gene insert	Antibiotic resistance	Origin	Publication
pdcDNA-FlagMyc	Mammalian expression	DISC1 (257-655, D-I)	AMP	Generated during thesis	(Zaharija & Bradshaw, 2024)
pdcDNA-FlagMyc	Mammalian expression	DISC1 (384-538, linker)	AMP	Generated during thesis	(Zaharija & Bradshaw, 2024)
pdcDNA-FlagMyc	Mammalian expression	DISC1 (384-655, linker-I)	AMP	Generated during thesis	(Zaharija & Bradshaw, 2024)
pdcDNA-FlagMyc	Mammalian expression	DISC1 (539-601, I-half UVR)	AMP	Generated during thesis	Unpublished
pdcDNA-FlagMyc	Mammalian expression	DISC1 (539-622, I-UVR)	AMP	Generated during thesis	Unpublished
pdcDNA-FlagMyc	Mammalian expression	DISC1 (539-655, I)	AMP	Generated during thesis	(Zaharija & Bradshaw, 2024)
pdcDNA-FlagMyc	Mammalian expression	DISC1 (539-738, I-S)	AMP	Generated during thesis	(Zaharija & Bradshaw, 2024)

Vector backbone	Vector type	Gene insert	Antibiotic resistance	Origin	Publication
pdcDNA-FlagMyc	Mammalian expression	DISC1 (539-854, I-C)	AMP	Generated during thesis	(Zaharija & Bradshaw, 2024)
pdcDNA-FlagMyc	Mammalian expression	DISC1 (635-738, S)	AMP	Generated during thesis	(Zaharija & Bradshaw, 2024)
pdcDNA-FlagMyc	Mammalian expression	DISC1 (635-836, S-C)	AMP	Generated during thesis	(Zaharija & Bradshaw, 2024)
pdcDNA-FlagMyc	Mammalian expression	DISC1 (691-807, C-half UVR)	AMP	Generated during thesis	Unpublished
pdcDNA-FlagMyc	Mammalian expression	DISC1 (691-829, C-UVR)	AMP	Generated during thesis	Unpublished
pdcDNA-FlagMyc	Mammalian expression	DISC1 (691-836, C)	AMP	Generated during thesis	(Zaharija & Bradshaw, 2024)
pdcDNA-FlagMyc	Mammalian expression	DISC1 (Δ384-415)	AMP	Generated during thesis	(Zaharija & Bradshaw, 2024)

Vector backbone	Vector type	Gene insert	Antibiotic resistance	Origin	Publication
pdcDNA-FlagMyc	Mammalian expression	DISC1 (1-655Δ384-415)	AMP	Generated during thesis	(Zaharija & Bradshaw, 2024)
pdcDNA-FlagMyc	Mammalian expression	DISC1 (1-836Δ384-415)	AMP	Generated during thesis	(Zaharija & Bradshaw, 2024)
pdcDNA-FlagMyc	Mammalian expression	LIS1 (full length)	AMP	N. Bradshaw, Düsseldorf	Unpublished
pdcDNA-FlagMyc	Mammalian expression	NDE1 (full length)	AMP	N. Bradshaw, Düsseldorf	Unpublished
pdcDNA-FlagMyc	Mammalian expression	NDEL1 (full length)	AMP	N. Bradshaw, Düsseldorf	Unpublished
pdcDNA-FlagMyc	Mammalian expression	PDE4B1 (full length)	AMP	Generated during thesis	Unpublished
pDEST-CMV-N-EGFP	Mammalian expression	ATF4 (full length)	AMP	Generated during thesis	Unpublished

Vector backbone	Vector type	Gene insert	Antibiotic resistance	Origin	Publication
pDEST-CMV-N-EGFP	Mammalian expression	DISC1 (257-383, D)	AMP	Generated during thesis	Unpublished
pDEST-CMV-N-EGFP	Mammalian expression	DISC1 (257-383, I)	AMP	Generated during thesis	Unpublished
pDEST-CMV-N-EGFP	Mammalian expression	DISC1 (691-836, C)	AMP	Generated during thesis	(Zaharija & Bradshaw, 2024)
pDEST-CMV-N-EGFP	Mammalian expression	LIS1 (full length)	AMP	Generated during thesis	Unpublished
pDEST-CMV-N-EGFP	Mammalian expression	NDE1 (full length)	AMP	Generated during thesis	Unpublished
pDEST-CMV-N-EGFP	Mammalian expression	NDEL1 (full length)	AMP	Generated during thesis	Unpublished
pDEST-CMV-N-mCherry	Mammalian expression	ATF4 (full length)	AMP	Generated during thesis	Unpublished

Vector backbone	Vector type	Gene insert	Antibiotic resistance	Origin	Publication
pDEST-CMV-N-mCherry	Mammalian expression	LIS1 (full length)	AMP	Generated during thesis	Unpublished
pDEST-CMV-N-mCherry	Mammalian expression	NDE1 (full length)	AMP	Generated during thesis	Unpublished
pDEST-CMV-N-mCherry	Mammalian expression	NDEL1 (full length)	AMP	Generated during thesis	Unpublished
pDEST-CMV-N-mCherry	Mammalian expression	PDE4B1 (full length)	AMP	Generated during thesis	Unpublished
pETG10A	Entry vector	DISC1 (384-538, linker)	AMP/CHL	Generated during thesis	(Zaharija & Bradshaw, 2024)
pPRW	Drosophila expression	DISC1 (full length)	AMP	Generated during thesis	Unpublished

3.1.5.1.2 Materials required for cloning, DNA extraction and purification

Table 12. Buffers and solutions required for cloning, DNA extraction and purification

Buffer	Reagents	Composition
1% agarose gel solution	Agarose	1% (w/v)
	TAE buffer (1×)	50 mL
	DNA stain	1:100,000
50×TAE buffer (stock, pH 8.6)	Acetic acid	1 M
	EDTA	50 mM
	Tris-HCl	2 M
1× TAE buffer (1:50 dilution)	Acetic acid	20 M
	EDTA	1 mM
	Tris-HCl	40 mM

Table 13. Kits required for DNA cloning, DNA extraction and purification

Name	Details	Catalogue no.	Manufacturer
DNA polymerase kit	Phusion® High-Fidelity DNA Polymerase, 2000 U/mL	M0530L	New England Biolabs
my-Budget Gel Extraction Kit	Isolation of DNA from agarose gels	55-2500-250	BioBudget
QIAprep Spin Miniprep Kit	Isolates up to 20 µg high-purity plasmid	27104	QIAGEN

Table 14. Commercial enzymes and solutions required for cloning, DNA extraction and purification

Name	Details	Catalogue no.	Manufacturer
BP Clonase	Gateway BP Clonase II Enzyme mix	11789020	Thermo Fisher Scientific
Deoxyribonucleotide (dNTP) Solution Mix	10 mM	N0447L	New England Biolabs
FastAP Thermosensitive Alkaline Phosphatase	Thermosensitive Alkaline Phosphatase (1 U/µL)	EF0651	Thermo Fisher Scientific
FastDigest EcoRI	Restriction enzyme	FD0274	Thermo Fisher Scientific
FastDigest KpnI	Restriction enzyme	FD0524	Thermo Fisher Scientific
FastDigest SalI	Restriction enzyme	FD0644	Thermo Fisher Scientific
FastDigest XbaI	Restriction enzyme	FD0685	Thermo Fisher Scientific
LR Clonase	Gateway LR Clonase II Enzyme mix	11791020	Thermo Fisher Scientific
Proteinase K Solution	>600 U/mL	EO0491	Thermo Fisher Scientific
T4 DNA Ligase	4000 U/mL	M0202S	New England Biolabs
T4 DNA Ligase Reaction Buffer	10×	B0202S	New England Biolabs

Table 15. Ladders and DNA stains

Name	Details	Catalogue no.	Manufacturer
100 bp DNA ladder (unstained)	100 bp + 1.5 kb DNA Ladder	85-2150-250	Bio Budget
1 kb DNA ladder (unstained)	my-Budget 1 kb DNA Ladder	85-1000-250	BioBudget
1 kb DNA ladder (stained)	Take5™1kb DNA Ladder	DNL0102	highQu
DNA stain	*my*-Budget DNA/RNA Stain Green	87-1000-G	BioBudget
Loading dye	10× FastDigest Green Buffer	B72	Thermo Fisher Scientific

3.1.5.2 Materials required for bacteral growth, propagation and storage

Table 16. List of bacterial strains

Name	Details	Catalogue no.	Manufacturer
*ccd*B Survival	Designed for use with the Gateway Vector Recombination System	A10460	Thermo Fisher Scientific
NEB 5-alpha (NEB5α)	DH5α derivative. T1 phage resistant and *endA* deficient	C2987I	New England BioLab

Table 17. Buffers and solutions required for competent bacteria growth and storage

Buffer name	Reagents	Composition
Inoue transformation buffer	Calcium chloride	15 mM
	Manganese (II) chloride tetrahydrate	55 mM
	Potassium chloride	250 mM
	PIPES (pH 6.7)	10 mM
LB agar	Agar	0.1 M
	Sodium chloride	85.6 mM
	Tryptone	41 mM
	Yeast extract	0.5% (w/v)
LB media	Sodium chloride	85.6 mM
	Tryptone	41 mM
	Yeast extract	0.5% (w/v)
SOB media (pH 7.0)	Magnesium chloride	5 mM
	Potassium chloride	1.25 mM
	Sodium chloride	4.3 mM
	Tryptone	41 mM
	Yeast extract	0.25% (w/v)

3.1.5.2.1 Other materials used for bacterial growth and propagation

Table 18. List of antibiotics

Name	Stock concentration	Final concentration
Ampicillin	100 mg/mL	100 µg/mL
Chloramphenicol	35 mg/mL	35 µg/mL
Kanamycin	50 mg/mL	50 µg/mL
Spectinomycin	100 mg/mL	100 µg/mL
Zeocin	100 mg/mL	100 µg/mL

3.1.5.3 Materials required for mammalian cell culture

Table 19. List of cell lines used for cell culture

Cell line	Description	Catalogue no.	Manufacturer
HEK293	Human embryonic kidney 293 cells	CRL-1573	American Type Culture Collection
SH-SY5Y	Human neuroblastoma cell line	ACC 209	German Collection of Microorganisms and Cell Cultures GmbH

Table 20. Media and solutions required for cell culture

Name	Details	Catalogue no.	Manufacturer
DMEM	With high glucose, L-glutamine and Phenol Red	41965-039	Thermo Fisher Scientific
DMEM/F12	With high glucose, L-glutamine, HEPES and Phenol Red	31330-038	Thermo Fisher Scientific
Foetal Bovine Serum (FBS)	Sterile-filtered	F1524	Sigma-Aldrich
Formaldehyde solution	3.8-4.2%, buffered, pH 6.7-7.1	1.00496	Sigma-Aldrich
MEM Non-Essential Amino Acids	Non-essential amino acid solution (100×) without L-glutamine	F7524	PAN-Biotech
Penicillin-Streptomycin	10.000 U/ml Penicillin, 10 mg/ml Streptomycin	P06-07100	PAN-Biotech
Trypsin/EDTA	Trypsin 0.05 %/EDTA 0.02 % in DPBS, with Phenol Red	P10-0235SP	PAN-Biotech

Table 21. Buffers required for cell lysis

Buffer	Reagents	Composition
Cell lysis buffer[1]	PBS (10×)	1×
	Triton X-100	1% (v/v)
	Magnesium chloride	20 mM
Cell permeabilising buffer	PBS (10×)	1×
	Triton X-100	0.5% (v/v)

[1] *DNAse I and protease inhibitor cocktail added immediately prior to use. For required dilutions, see* **Table *22***.

Table 22. Commercial reagents required for cell culture

Reagent	Dilution	Catalogue no.	Manufacturer
DNAse I (RNAse-free)	1:1,000	M0303L	New England Biolabs
EDTA-free Protease Inhibitor Cocktail (50×)	1×	11873580001	Merck
Goat serum	10%	G9023	Sigma-Aldrich
Lipofectamine 2000	1:250	11668027	Thermo Fisher Scientific
Metafectene	1:250	T020-1.0	Biontex
Metafectene Pro	1:250	T040-1.0	Biontex

3.1.5.3.1 Materials required for immunocytochemistry (ICC), SDS-PAGE and Western blotting (WB)

Table 23. Buffers and solutions required for SDS-PAGE and WB

Buffer name	Reagents	Composition
30% (w/v) Acrylamide solution	Acrylamide	4.1 M
	N, N, N', N'-Methylenebisacrylamide	64.9 mM
Laemmli buffer	Bromophenol blue	0.004% (w/v)
	Glycerol	25% (v/v)
	SDS	5% (w/v)
	Tris-HCl (pH 6.8)	156 mM
	DTT (add immediately before use)	10% (w/v)
10×PBS (stock solution, pH 7.4)	Disodium hydrogen phosphate	10 mM
	Potassium chloride	2.7 mM
	Potassium dihydrogen phosphate	1.8 mM
	Sodium chloride	137 mM
1× PBS	Disodium hydrogen phosphate	10 mM
	Potassium chloride	2.7 mM
	Potassium dihydrogen phosphate	1.8 mM
	Sodium chloride	137 mM
PBS-T	PBS	1×
	Tween 20 detergent	0.1% (w/v)
PBS-T blocking buffer	Milk powder	5% (w/v)
	PBS-T	95% (v/v)
Ponceau S solution	Acetic acid	0.5% (v/v)
	Ponceau S	2% (w/v)

10× SDS-PAGE running buffer (stock solution)	Glycine	190 mM
	Tris-HCl	25 mM
	SDS	0.1% (w/v)
1× SDS-PAGE running buffer	Glycine	190 mM
	Tris-HCl	25 mM
	SDS	0.1% (w/v)
1× Transfer buffer (semi-dry)	Glycine	39 mM
	Tris-HCl	48 mM
	Methanol	20% (v/v)
	SDS	0.04% (w/v)

Table 24. SDS-PAGE gel composition

Gel	Composition	Volume required
Stacking gel	Water	2.6 mL
	30% Acrylamide solution	1 mL
	1 M Tris-HCl (pH 6.8)	625 μL
	10% SDS	50 μL
	10% APS	50 μL
	TEMED	5 μL
Resolving gel (10%)	Water	4.8 mL
	30% Acrylamide solution	3.9 mL
	1.5 M Tris-HCl (pH 8.8)	3 mL
	10% SDS	120 μL
	10% APS	120 μL
	TEMED	12 μL
Resolving gel (12%)	Water	3.9 mL
	30% Acrylamide solution	2.7 mL
	1.5 M Tris-HCl (pH 8.8)	3 mL
	10% SDS	120 μL
	10% APS	120 μL
	TEMED	12 μL
Resolving gel (15%)	Water	2.7 mL
	30% Acrylamide solution	6 mL
	1.5 M Tris-HCl (pH 8.8)	3 mL
	10% SDS	120 μL
	10% APS	120 μL
	TEMED	12 μL

Table 25. Ladders and substrates required for SDS-PAGE and WB

Product	Details	Catalogue no.	Manufacturer
Protein ladder	*my*-Budget Prestained Protein-Ladder, 10 kDa- 180 kDa	86-1000	BioBudget
Western blotting substrate	Pierce™ ECL Western Blotting Substrate	32209	Thermo Fisher Scientific

3.1.5.3.1.1 Antibodies and stains required for immunocytochemistry (ICC) and Western blotting (WB)

Table 26. List of primary antibodies required for ICC and WB

Immunogen	Host	Dilution	Catalogue no.	Manufacturer
Actin	Mouse	WB 1:5,000	MAB1501	Merck
	Rabbit	WB 1:5,000	A2066	Sigma-Aldrich
FLAG	Mouse	ICC 1:1,000 WB 1:2,000	F1804	Sigma-Aldrich
GFP	Mouse	ICC 1:1,000 WB: 1:2,000	66795	Sigma-Aldrich

Table 27. List of secondary antibodies required for ICC

Antibody	Host	Dye	Dilution	Catalogue no.	Manufacturer
Anti-mouse	Goat	Alexa Fluor 488	1:2,000	A32723	Thermo Fisher Scientific
Anti-mouse	Goat	Alexa Fluor 594	1:2,000	A11005	Thermo Fisher Scientific
Anti-mouse	Goat	Alexa Fluor 555	1:2,000	A32727	Thermo Fisher Scientific
Anti-rabbit	Goat	Alexa Fluor 594	1:2000	A11037	Thermo Fisher Scientific

Table 28. List of fluorescent stains required for ICC

Name	Location	Dilution	Catalogue no.	Manufacturer
DAPI	Cell nucleus	1:2,000	D9542	Sigma-Aldrich
Acti-stain 488 Fluorescent Phalloidin	Cytoskeleton	1:2,000	PHDG1A	Cytoskeleton, Inc

Table 29. List of secondary antibodies required for WB

Antibody	Host	Conjugate	Dilution	Catalogue no.	Manufacturer
Anti-mouse	Goat	HRP	1:10,000	31430	Thermo Fisher Scientific
Anti-rabbit	Goat	HRP	1:10,000	65-6120	Invitrogen

3.1.5.4 Materials required for insoluble protein purification assay

Table 30. Buffers and solutions required for insoluble protein purification assay

Buffer name	Reagents	Composition
Lysis buffer	HEPES (pH 7.5)	50 mM
	Magnesium chloride	5 mM
	Potassium acetate	100 mM
	Sucrose	250 mM
	[1]PMSF	2 mM
	[2]Protease inhibitor cocktail (50×)	1×
A1	HEPES (pH 7.5)	50 mM
	Potassium acetate	100 mM
	Sucrose	1.6 M
	Triton X-100	1% (v/v)
	[1]PMSF	1 mM
B1	HEPES (pH 7.5)	50 mM
	Calcium chloride	30 mM
	Magnesium chloride	20 mM
	Sodium chloride	1 M
	[3]DNAse I	100 U/mL
	[4]Protease inhibitor coctail (50×)	1×
C1	HEPES (pH 7.5)	50 mM
	Sarkosyl	0.5% (w/v)

[1-4] *Reagents added directly prior to use.*

3.1.5.5 Materials required for *Drosophila* cultivation and maintenance

Table 31. List of *Drosophila* strains

Fly strain	Description	Origin
Canton S	Wild type (*wt*) strain, control stock	C. Helfrich Forster, University of Würzburg
elav-GAL4	Flies carrying e*lav*-GAL4 driver used for pan-neuronal expression	Bloomington Drosophila Stock Centre (BDSC_458)
white[1118]	Mutant *wt* strain exhibiting white eyes	Bloomington Drosophila Stock Centre (BDSC_6326)

Table 32. Nutrient medium preparation

	Ingredients	Volume
Mixture A	Tap water	1000 mL
	Sugar	79.3 g
	Agar Type II (cornmeal)	8.5 g
Mixture B	Tap water	400 mL
	Yellow cornmeal	72 g
	Dry yeast	50 g
	Ingredients	**Volume**
Post-preparation	Tap water	200 mL
	Propionic acid	8 mL
	NIPAGIN	15 mL

3.2 Methods

3.2.1 Cloning

3.2.1.1 Primer design

Restriction sites compatible with the gene of interest were chosen using NEBcutter 2.0, an online tool developed by New England BioLabs. Usable restriction sites were chosen from the provided list, based on the selected DNA sequence. a primer template (**Figure 11**) was designed based on the following rules:

1. Both forward and reverse primers need to have a similar melting temperature, preferably within 2°C of each other.
2. The guanidine-cytosine (GC) content of primers needs to be within 50-60%.
3. Both primers need to start/end with either a G or a C base.

In addition to the rules above, complementary regions in primer pairs and long sections of base repeats were avoided while designing the primers. To enable efficient enzymatic cleavage, a 3-6 base clamp was also added before the restriction site, which was then followed by either a start or a stop codon, depending on the primer direction. For reverse primers, an additional stop codon was used to secure termination of the reaction.
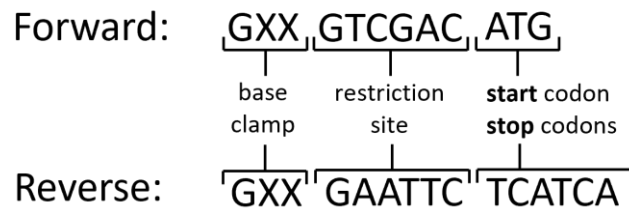
Figure 11. Example of a template used for primer design. X stands for any additional base added to the base clamp. SalI and XbaI were used as an example of restriction sites.

Once the template was created it was used for each primer design, with changes/additions being made to the base clamp according to the abovementioned rules. Next, a gene-specific primer was created by selecting bases from the open reading frame (ORF) of the gene to be cloned. Depending on primer direction, 10-15 bases were added to the template either from the start or from the end of the ORF of our gene of interest. When designing

a reverse primer, the selected nucleotide sequence was made to be a reverse-complement of itself, which can be determined by using the website Reverse complement. Once the primers have been designed, they were further refined to fit the previously mentioned rules by using an online tool (Oligo Analysis Tool, Operon).

3.2.1.2 Polymerase chain reaction (PCR)

Touchdown PCR was used to amplify the specific DNA fragments with increased yield and specificity. The reactions were set up in 0.2 mL PCR tubes, as shown in **Table 1**. All the reagents were kept on ice, apart from Phusion DNA Polymerase that was stored at -20°C until needed. For the first PCR round, sequence-specific primers were used.

Table 33. PCR reaction setup[1]

Reagents	Stock concentrations	Volume (20 µL reaction)	Final concentrations
Ultrapure H_2O	-	< 20.0 µL	-
GC Phusion Buffer	5×	4.0 µL	1×
dNTPs	10 mM	0.4 µL	200 µM each
Forward primer	10 µM	1.0 µL	0.5 µM
Reverse primer	10 µM	1.0 µL	0.5 µM
Template DNA	Variable	0.2-0.5 µL	50 ng
DMSO	100%	0.0-2.0 µL	<10%
Phusion DNA Polymerase	1.0 U	0.2 µL	0.02 U/ µL

[1]Adapted from New England BioLabs, Ltd.

Reaction tubes were then placed into a BioRad PCR Thermal Cycler, with set cycling conditions as shown in **Table 34**. Annealing temperature was set to decrease by 2 °C per cycle, to avoid amplifying nonspecific sequences. Extension time was adapted depending on the DNA fragment size, with fragments consisting of less than 300 base pairs (bp) being set at 15 seconds, 600 bp at 30 seconds, and above 600 bp at 45 seconds, respectively. Upon finishing the cycling, sizes of amplified DNA were verified by agarose gel electrophoresis.

The second round of PCR was done to further limit non-specific products and add additional restriction sites. First round PCR reactions were used as a template, and sequence-specific primers were exchanged for extension primers containing additional restriction sites. In both rounds, same cycling conditions were used. Sizes of the final amplified product were again verified by performing agarose gel electrophoresis, and further confirmed by sequencing (outsourced, Eurofins Genomics).

Table 34. PCR thermal cycling protocol

Step	Temperature	Time	No. of cycles
Initial denaturation	98°C	30 s	1
Denaturation	98°C	10 s	
Annealing	70 – 60°C (2°C ↓ per cycle)	30 s	5
Extension	72°C	Variable	
Denaturation	98°C	10 s	
Annealing	60°C	30 s	30
Extension	72°C	Variable	
Final extension	72°C	Variable	1
End cycle	4°C	∞	1

3.2.1.3 Agarose gel electrophoresis

Agarose gel suspension was heated for approximately 60 seconds, with periodic mixing, then poured into a gel tray. Once cooled, the gel tray was placed inside the electrophoresis tank filled with 1x TAE buffer. For the first round PCR products and purified plasmids, 7 µL of each sample was mixed with 2 µL of loading dye, prior to loading. For second round PCR products, 18 µL of each sample mixed with 2 µL of loading dye was made prior to loading. In all cases, DNA ladder of the corresponding size was prepared by mixing 2.5 µL with 1 µL of loading dye. Loading dye was omitted when using a pre-stained ladder. The gel was run at 150 V for 20 minutes.

3.2.1.3.1 Gel extraction

Following agarose gel electrophoresis of PCR products, DNA bands of the corresponding sizes were visualised and cut out on an UV transilluminator, transferred into sterile 1.5 mL tubes and processed according to manufacturer's instructions (*my*-Budget Gel

Extraction Kit). Briefly, 650 µL of Gel Solubilizer was added to gel fragments and warmed at 50°C for 10 min, or until the fragment was completely dissolved. Next, 50 µL of Binding Optimizer was added to the solution, mixed, then applied onto a Spin Filter placed inside a Receiver Tube. The sample was centrifuged at 11,000 rpm for 1 min, after which the filtrate was discarded. The filter was then washed twice with 700 µL of Washing Solution, with a centrifugation step following each wash. Finally, the sample was centrifuged again at maximum speed for 2 min, and Spin Filter was placed into a clean 1.5 mL tube prior to elution. Elution was carried out with 30 µL of ultrapure water, previously incubated at 50°C to increase DNA yield. Following 1 min incubation at room temperature (RT), the sample was subjected to another centrifugation. The purified DNA was then gently resuspended, and its concentration was measured at 260 nm using BioDrop µLITE spectrophotometer.

3.2.1.4 Restriction cloning using Gateway vectors

3.2.1.4.1 Restriction digest of plasmids and vectors

Restriction enzyme cloning was used to subclone fragments of *DISC1* gene form existing vectors into pENTR1A vector with no death cassette (*ccd*B), at the *SalI* and *XbaI* or *EcoRI* sites. Prior to ligation, both vector and purified DNA sample were subjected to restriction digest with restriction enzymes corresponding to primer restriction sites. Reactions were set up as shown in **Table 35**, and incubated at 37°C overnight.

Table 35. Restriction digest protocol for vectors and purified DNA.

Components	Vector	DNA insert
Vector/DNA	40 µl	30 µl
10× FastDigest Buffer Green	5 µl	4 µl
Restriction enzyme 1 (SalI)	2 µl	2 µl
Restriction enzyme 2 (XbaI)	2 µl	2 µl
FastAP Thermosensitive Alkaline Phosphatase	2 µl	-

The digested vector was run on an agarose gel the following day, as described in Section 3.2.1.3. The gel was visualised on UV transilluminator and a 2.3 kb band corresponding to the vector size was excised from the gel. Both excised vector band and digested DNA were subjected to gel extraction, as described in Section 3.2.1.3.1.

3.2.1.4.2 Ligation

Volume calculations needed to set up a 10 µL ligation reaction were performed as shown in **Figure 12**. The negative control reaction consisted of pENTR1A vector without an insert. Once calculations were completed, reactions were set up on ice, in 0.2 mL PCR tubes. T4 DNA Ligase Buffer was completely thawed and resuspended prior to being added to the reaction, and T4 DNA Ligase was added last.

Insert (PCR)	Restriction enzymes	Plasmid	PCR AA	PCR kbp (AA*0.003)	Plasmid kbp (AA*0.003)	Insert [c]	Plasmid [c]	Insert (µl)	Plasmid (µl)	Ultra-pure H₂O (µl)	Total (µl)
Insert 1	SalI/XbaI	pENTR1A no ccDB	126	0.38	2.27	37.76	42.13	0.4	0.7	7.5	8.5
Insert 2	SalI/XbaI	pENTR1A no ccDB	415	1.25	2.27	30.36	42.13	1.5	0.7	6.3	8.5
Insert 3	SalI/XbaI	pENTR1A no ccDB	446	1.33	2.27	31.08	42.13	1.6	0.7	6.2	8.5
Negative control	SalI/XbaI	pENTR1A no ccDB		2.27			42.13		0.6	7.9	8.5

$$Insert\ (\mu l - unadjusted) = \frac{m}{[c]}insert * \frac{insert\ kbp}{1\ kbp} = \frac{37.5\ ng}{37.76\ ng/\mu l} * \frac{0.38\ kbp}{1\ kbp} = 0.38$$

$$Plasmid\ (\mu l - unadjusted) = \frac{m}{[c]}plasmid * \frac{plasmid\ kbp}{4\ kbp} = \frac{50\ ng}{42.13\ ng/\mu l} * \frac{2.27\ kbp}{4\ kbp} = 0.67$$

$$Total\ (\mu l - unadjusted) = 0.38 + 0.67 = 1.05$$

$$Insert\ (\mu l) = \frac{insert\ (\mu l - unadjusted)}{total\ (\mu l - unadjusted)} = 0.4$$

$$Plasmid\ (\mu l) = \frac{plasmid\ (\mu l - unadjusted)}{total\ (\mu l - unadjusted)} = 0.7$$

$$UP\ H_2O\ (\mu l) = Total\ (\mu l) - insert\ (\mu l) - plasmid\ (\mu l) = 7.5$$

T4 DNA Ligase Buffer (10X)	1.0
T4 DNA Ligase	0.5
Total reaction	10.0

Figure 12. Example of calculations required for ligation of inserts into pENTR1A vector. Numbers for insert sizes and concentrations are given as an example. Calculations show a ligation reaction using a molar ratio 1:3 vector to insert for the indicated DNA sizes. umbers shown in yellow fields are the results obtained by calculations shown below the table. PCR – polymerase chain reaction. AA – amino acid. Vector/PCR kbp – Vector/PCR kilobase pairs. UP H₂O – ultrapure water. $[c]$ – concentration. m – mass. Protocol adapted from New England BioLabs.

Ligation was performed in a BioRad PCR Thermal Cycler. Cycling conditions are shown in **Table 36**. Following ligation, reactions were chilled on ice and 5 µL of each reaction, including the negative control, were transformed into competent NEB5α bacteria, as described in Section 3.2.1.6.2. Ligations were deemed successful if no growth was found

on a negative control reaction plate. Colonies selected from ligated reaction plates were grown and purified as previously described, and obtained entry plasmids were transferred into expression vectors using Gateway recombination cloning system.

Table 36. Ligation cycling conditions

Step	Temperature	Time	No. of cycles
1	16°C	60 s	
2	22°C	60 s	264 ×
3	37°C	60 s	
4	65°C	10 min	1×
5	4°C	∞	1×

3.2.1.5 Gateway recombination cloning

Gateway Technology represents a universal cloning method based on the site-specific recombination properties of a lambda bacteriophage (Landy, 1989), which facilitates its integration into *E. coli* chromosome (Ptashne, 1992). This technology is widely used to transfer heterologous DNA sequences flanked by modified *att* sites into multiple vector systems in a rapid and highly efficient manner (Hartley et al., 2000). Gateway Technology consists of two reactions, the recombinant BP Clonase reaction and recombinant LR Clonase reaction.

3.2.1.5.1 Recombinant BP Clonase reaction

The BP Clonase reaction includes recombination between a PCR product flanked by the *att*B sites, and an *att*P-containing donor vector, to create an entry clone containing *att*L sites. This reaction is catalysed by the BP Clonase enzyme mix, and as a reaction by-product, the death cassette (*ccd*B gene) is excised from the donor vector (**Figure 13**). This reaction, and subsequently the LR reaction described in Section 3.2.1.5.2, were used to subclone the D and S regions of DISC1 into expression vectors of interest. Following manufacturer's instructions, 150 ng of an entry vector (pDONR/Zeo) was mixed with 50 ng of a PCR product. Next, TE buffer (provided with the gel extraction kit) was added to

91

the reaction to the total volume of 9 μL. Finally, 1 μL of the Gateway BP Clonase II Enzyme Mix was added to catalyse the recombination. Upon adding the Clonase Enzyme mix, the reaction was incubated at 25°C for 1 hour. Following incubation, the reaction was terminated by the addition of 1 μL of the Proteinase K solution. Solution was then incubated for additional 5-7 minutes at 37°C. Half of the reaction was then used to transform NEB5α cells, while the rest was stored at -20°C. The remaining constructs described in this thesis were cloned into entry vectors using restriction digest, as described in Section 3.2.1.4.1, due to a low success rate of BP Clonase reactions.
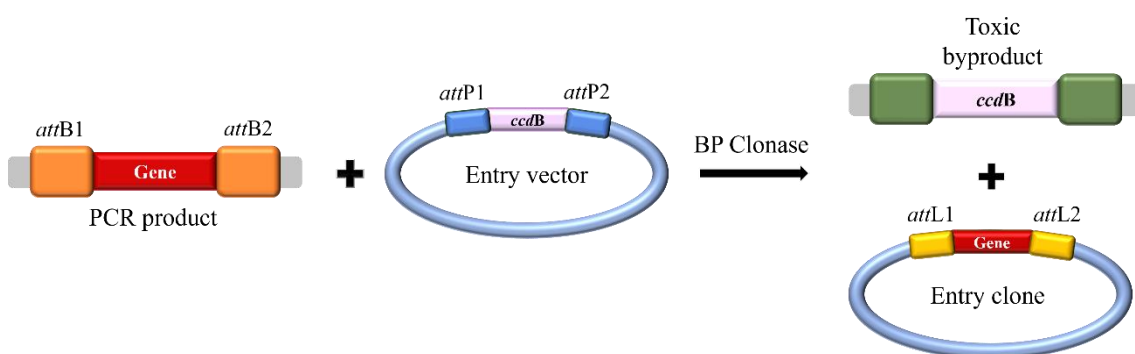
Figure 13. Schematic of the recombinant BP Clonase reaction. PCR product containing the gene of interest that is flanked by *att*B sites, undergoes recombination with the entry vector flanked by *att*P sites, in a reaction catalysed by the BP Clonase enzyme mix. This generates an *att*L – containing entry clone, as well as the toxic byproduct created by the excision of the *ccd*B gene from the entry vector, that drives the clone selectivity. *att*B – bacterial attachment site. *att*P – phage attachment site. *att*L – left attachment site. *ccd*B – death cassette gene.

3.2.1.5.2 Recombinant LR Clonase reaction

The recombinant LR Clonase reaction was used to subclone genes of interest into any expression system of choice. Briefly, an entry clone containing the gene of interest, that is flanked by the attachment sites *att*L, is recombined with an empty Gateway expression vector with attachment sites R (**Figure 14**). Expression vector also contains a *ccd*B gene and an antibiotic-resistance gene different to the entry vector. The presence of the *ccd*B gene allows negative selection of the donor and destination vector, while antibiotic-resistance gene allows for specific clone selection. Expression vectors used for the

purpose of this thesis were pdcDNA3.1-FlagMyc, pDEST-CMV-N-EGFP and pPRW. 150 ng of entry plasmid containing a gene of interest was mixed with the equal amount of expression vector. TE buffer was added to the reaction to the total volume of 9 μL. Lastly, 1 μL of the Gateway LR Clonase II Enzyme Mix was added as a catalyst for the in vitro recombination between the entry clone and an expression vector. The reaction was incubated for 1 hour at 25°C, and subsequently terminated by adding 1 μL of the Proteinase K solution to the reaction. Following a 7-minute incubation at 37°C, 5 μL of the reaction were used to transform NEB5α cells, while the rest was stored at -20°C. Entry and expression vectors which were used and generated are listed in **Table 9**.
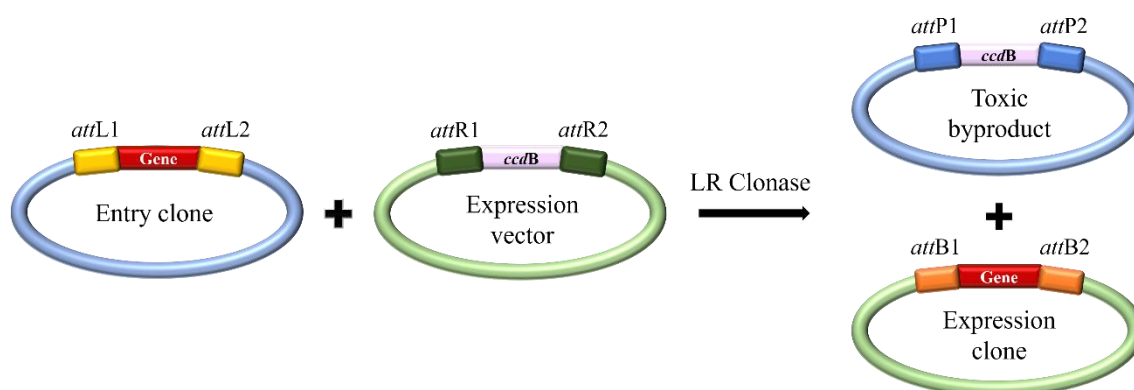
Figure 14. Schematic of the recombinant LR Clonase reaction. Entry clone, containing the gene of interest that is flanked by *att*L sites, undergoes recombination with the expression vector flanked by *att*R sites, in a reaction catalysed by the LR Clonase enzyme mix. This generates an *att*B – containing expression clone, as well as the toxic by-product created by the excision of the *ccd*B gene from the expression vector, that drives the clone selectivity. *att*L – left attachment site. *att*R – right attachment site. *att*P – phage attachment site. *att*B – bacterial attachment site. *ccd*B – death cassette gene.

3.2.1.6 Plasmid preparation

3.2.1.6.1   Preparation of high-efficiency NEB5α cells

Upon thawing a vial of NEB5α competent *E. coli* cells, 50 μL of cells was immediately inoculated onto a petri dish containing 15 mL of pre-poured Lysogeny Broth (LB) agar without antibiotics. The corresponding negative control plate was made in the same manner but streaked with a sterile pipette tip instead. Both plates were then incubated

overnight at 37°C. Following 16 hours of growth, a single colony of ultracompetent cells was used to inoculate 15 mL of Super Optimal Broth (SOB) media containing no antibiotics. The liquid culture was then incubated for 6 hours at 37°C, with continuous shaking at 250 rpm. Following incubation, three conical flasks, each containing 100 mL of SOB with no antibiotics, were inoculated with 10, 50 and 100 µL of liquid culture respectively. Cultures were then incubated overnight for approximately 16 hours at 22°C, with moderate shaking (170 rpm). Following incubation, optical density (OD) of the cultures was measured using BioPhotometer Plus UV/Vis Photometer. Optical density (OD) measurements were performed at 600 nm wavelength (OD_{600}), with SOB media used as a reference measurement. The first culture to reach the OD_{600} of 0.55 was evenly transferred into four sterile 50 mL tubes and centrifuged for 10 minutes at 4°C and 3,700 rpm (Eppendorf, Centrifuge 5920R). Following centrifugation, the supernatant was discarded, and pellet was air-dried for 2 minutes. Next, pellets were resuspended in 10 mL of ice-cold Inoue buffer per tube, after which the suspensions were pooled. Cells were again harvested by centrifugation using the same conditions, and the resulting pellet was air-dried. Upon drying, pellet was resuspended in 10 mL of ice-cold Inoue buffer with an addition 750 µL of dimethyl sulfoxide (DMSO) and incubated on ice for 10 minutes. Following incubation, the resulting suspension of ultracompetent cells was quickly dispensed into 1.5 mL tubes as 120 µL aliquots and snap-frozen using liquid nitrogen. Aliquots were stored at -80°C.

3.2.1.6.2   Bacterial transformation of vectors and plasmids

For plasmid transformation, either 5 µL (new constructs) or 1 µL (re-transformations) of construct of interest (*DISC1*, or its interaction partners) was gently resuspended with 50 µL of NEB5α ultracompetent *E. coli* cells in a sterile 1.5 µL tube. Suspension was incubated on ice for 30 minutes, then subjected to heat shock transformation at 42°C for 30 seconds, followed by a 5 min recovery on ice. Next, each bacterial suspension was incubated for 60 min at 37°C, with continuous shaking at 250 rpm. In the case of kanamycin-resistant plasmids, 250 µL of sterile LB media was added to bacterial suspension prior to incubation. Transformed bacteria were streaked onto LB agar plates containing appropriate antibiotics, which were then incubated overnight at 37°C.

Vectors were transformed into *ccd*B competent *E. coli* cells in the same manner, with the exception that the heat shock was performed for the duration of 45 seconds.

3.2.1.6.3 Bacterial propagation and purification of plasmid DNA from *E. coli*

Following overnight incubation, single colonies were selected from the plates and inoculated into 3 mL of LB media containing appropriate antibiotic. These liquid cultures were then incubated overnight in a shaking incubator at 37°C/250 rpm. Isolation of plasmid DNA was done using the QIAprep Spin Miniprep Kit, according to manufacturer's instructions. Briefly, liquid bacterial cultures were grown overnight, then centrifuged the following morning at 3,700 rpm for 15 min/4°C. After discarding the supernatant, pellet was resuspended in buffer P1 and lysed with buffer P2 immediately after. The lysing reaction was then neutralised using buffer N3 and subjected to centrifugation (13,000 rpm/10 min). Next, supernatant was applied to the commercial spin column and briefly centrifuged (1 min, Eppendorf, MiniSpin). The column was then washed with buffer PB followed by centrifugation, an addition of PE buffer, and another centrifugation. Additional centrifugation was used to remove residual washing buffer from the sample. Supernatant was discarded following every subsequent centrifugation. Sample was then incubated in elution buffer (EB) for one minute and centrifuged for the final time, to elute the plasmid from the column membrane.

3.2.1.7 Micro-measurement of plasmid DNA

The concentration of purified plasmid DNA was measured using a BioDrop μLITE spectrophotometer. The absorbance wavelength was set at 260 nm. EB was used as a blank probe. Plasmid concentrations, expressed in μg/mL, were measured using 1 μL of a sample. For size confirmation, plasmids were run on an agarose gel as described in Section 3.2.1.3 and visualised using BioRad Chemi-Doc MP Imaging System.

3.2.2 Mammalian cell culture

3.2.2.1 Cell culture growth and maintenance

3.2.2.1.1 SH-SY5Y

An immortalised human neuroblastoma-derived cell line, SH-SY5Y, was selected due to its neuronal properties, while also avoiding the limitations of primary mammalian neurons. Cells were kept in a standard humidified incubator at 37°C and 5% CO_2 under sterile conditions, in T25 flasks containing Dulbecco's Modified Eagle Medium F12 (DMEM F12) with the addition of foetal bovine serum (FBS), non-essential amino acids and appropriate antibiotics (later referred to as +/+ media). Once the cells have reached confluency of approximately 80%, they were either subcultured into new flasks to maintain the line, or into cell culture plates for experimentation purposes. This process involves subjecting the cells to trypsinization by removing the media from the flask and adding 1 mL trypsin solution, pre-heated to 37°C. Cells are then incubated in trypsin for approximately 5 minutes at 37°C/5% CO_2 and further detached from the surface by applying external force to flask walls. Trypsinization is terminated by adding 4 mL of preheated +/+ media to the flask. The suspension is then subcultured into a new flask, containing up to 5 mL of preheated +/+ media. In the case of seeding into 12- or 24-well plates for the purpose of immunocytochemistry (ICC), microscopy coverslips were inserted into wells with 1 mL +/+ media prior to the addition of cells.

The volume of cells transferred to a flask as a stock solution depended on the intended use and a timeframe in which cells are expected to reach confluency. In general, cells were diluted in a 1:10 ratio per seeded flask. For a transfection, presuming 70-90% confluency was reached, cells were diluted in a 1:5 ratio.

3.2.2.1.2 HEK293

Immortalised human embryonic kidney 293 (HEK293) cells were selected mainly for the purpose of WB, due to the ease of transfection and rapid growth rate. These cells were cultured and maintained in the same manner as described for SH-SY5Y cells, although DMEM without the addition of Ham's F12 media was used instead. Cells were either subcultured into T25 flasks, or 6-/12-well plates for the experimental purposes. When subculturing into 6-well plates, volumes of cells and media added were tripled. In general, cells were diluted in a 1:50 ratio per seeded flask, and a 1:5 ratio per well.

3.2.2.2 Cell storage

For the purposes of storing and reusing the line, flasks of approximately 60-70% confluency were subjected to trypsinization, then neutralised as previously described. Pooled cells were transferred into a sterile 15 mL tube and centrifuged at 1,000 rpm for 5 minutes. Next, media was carefully removed, and cells were gently resuspended in 2 mL of freezing media per tube. Cell suspension was then transferred to cryogenic tubes, in 1 mL aliquots. Cells were subjected to a slow freezing method by first being cooled at 4°C for 2 hours, then frozen overnight at -20°C. Finally, cells were frozen at -80°C for long-term storage.

3.2.2.3 Transfection

3.2.2.3.1 Transfection of SH-SY5Y cells

Once cells were seeded into a 12- or 24-well plate for the purpose of ICC, they were transfected with DNA plasmid(s) of interest the following day, in sterile conditions. Preheated DMEM/F12 media without the antibiotics was used instead (hereby referred to as -/- media), to facilitate plasmid integration into the cell. For single transfections, a transfectant solution was made by using 100 μL of -/- media and 2 μL of either Lipofectamine 2000 or Metafectene Pro (1:50 dilution) per well. While the transfectant solution was incubating at RT, a DNA solution was prepared by mixing 100 μL of -/- media and 0.5 μg of plasmid per well. Both solutions were mixed to the total volume of 200 μL per well and incubated at 37°C for 30 minutes. In the meantime, +/+ media was removed from the plate and cells were washed with 500 μL of -/- media per well, to remove any remnants of antibiotics. Again, the media was removed, and 300 μL were added instead. Following incubation, 200 μL of plasmid/transfectant solution was added to corresponding wells to a total of 500 μL per well. Transfected plate was incubated in a standard humidified incubator, at 37°C/5% CO_2 for 6 hours. When designated incubation time has passed, -/- media was removed from the cells and instead replaced with 1mL of +/+ media. Plate was then incubated at 37°C overnight before being subjected to ICC.

For co-transfections of two plasmids, a DNA solution was made with 100 μL -/- media and 0.5 μg of each plasmid per well.

3.2.2.3.1.1 Nanoscale Pulldown assay (NanoSPD)

Triple transfections were performed in neuroblastoma cells for the purpose of employing a NanoSPD assay. This assay is described in more detail in Section 4.2.3 of the Results.

A transfectant solution was made by using 100 μL of -/- media and 4 μL of Metafectene Pro (1:25 dilution), while a DNA solution was made with 100 μL -/- media and 0.5 μg of NanoTrap vector, DISC1 region and assumed interaction partner, respectively. Suitable control reactions were included as well. EGFP control (pDEST-CMV-N-EGFP) was co-transfected with the NanoTrap vector (pcDNA3.1-MYO10-HMM-NanoTrap) to show that NanoTrap indeed does bind EGFP and is able to traffic it to filopodial tips. Other control reactions included co-transfection of Flag-tagged DISC1 regions with the NanoTrap vector, to show that NanoTrap will exclusively bind EGFP-fused protein, not the Flag-tagged interaction partners. Final control reaction was co-transfecting NanoTrap vector, EGFP control and Flag-tagged interactors, to show that interaction partners will not be trafficked to the filopodial tips by binding to the EGFP tag itself.

3.2.2.3.2 Immunocytochemistry

Following transfection, neuroblastoma cells were prepared for the immunofluorescence analysis. First, cells were washed once with $1\times$ PBS, then fixed in 4% formaldehyde solution for 15 minutes. After fixation, cells were subsequently permeabilised for 10 minutes with cell permeabilising buffer and washed three times with $1\times$ PBS. Next, cells were blocked with 10% goat serum/$1\times$ PBS for up to an hour, then incubated in primary antibodies diluted in blocking buffer overnight, at 4°C. Cells were washed three times with 1X PBS for 15 minutes the following day, then incubated in the dark with secondary antibodies and DAPI stain diluted in blocking buffer for 1 hour. When required, Acti-stain 488 stain was also added to the secondary antibody solution. In the case of GFP-fused protein transfection, cells were kept in the dark during the whole process. Finally, cells were washed three more times with $1\times$ PBS for 15 minutes and mounted onto glass slides with Fluoroshield mounting media. Cells were imaged using $60\times$ objective on the Olympus IX83 inverted microscope, using an ORCA-R2 CCD camera and cellSens Imaging Software. Further analysis was performed using Fiji software.

3.2.2.3.3 Transfection of HEK293 cells

After seeding HEK293 cells into a 12-well plate, cells were transfected in a manner similar to neuroblastoma cells, only by using DMEM -/- media and Metafectene instead of DMEM/F12 and Lipofectamine 2000/Metafectene Pro. In the case of cells being seeded into a 6-well plate, a transfectant solution was made by using 300 μL of -/- media and 6 μL of Metafectene (1:50 dilution) per well. DNA solution was prepared by mixing 300 μL of -/- media and 1.5 μg of plasmid per well. Both solutions were mixed to the total volume of 600 μL per well and incubated at 37°C for 30 minutes. In the meantime, +/+ media was removed from the plate and cells were washed with 1 mL of -/- media per well. Again, the media was removed, and 900 μL were added instead. Following incubation, 600 μL of plasmid/transfectant solution was added to corresponding wells to a total of 1.5 mL per well. Transfected plate was incubated in a standard humidified incubator, at 37°C/5% CO_2 for 6 hours. When designated incubation time has passed, -/- media was removed from the cells and instead replaced with 3 mL of +/+ media. Plate was then incubated at 37°C overnight, in a standard humidified incubator.

3.2.2.3.4 Proteasomal inhibition assay

Proteosomal inhibition assay was used to test the stability of plasmids encoding the empirical ESPRIT DISC1 regions (D, I and C, respectively) against their theoretical counterparts containing either a whole UVR-like repeat (D/I/C_{UVR}), or only its half (D/I/$C_{half\ UVR}$). These theoretical counterparts were cloned for the purpose of this thesis, based on the bioinformatics data kindly provided by Luis Sanchez-Pulido. Plasmids were transfected into HEK293 cells as described previously, in two identical sets with appropriate negative controls. Following a 6-hour incubation, 1 μL of 10 μM MG132 proteasome inhibitor was added to one set of transfected cells. Cells were harvested and subjected to cell lysis after overnight incubation, and obtained samples were analysed by Western blotting.

3.2.2.3.5 Cell lysis

Following the transfection of HEK293 cells, media was removed, and cells were washed twice in 1× PBS. Next, cells were incubated in 100 μL cell lysis buffer for approximately 5 minutes. Immediately prior to use, 2 units of RNAse-free DNAse I and 50× protease inhibitor cocktail (diluted to the final concentration of 1×) were added to the lysis buffer.

Cells were gently scraped from the surface of the wells and lysed suspensions were transferred into sterile 1.5 mL tubes. Cell suspensions were incubated on ice for 1 hour, with periodical vortexing, then prepared for SDS-PAGE by diluting 1:1 in Laemmli buffer and adding 1M DTT (10% of the cell lysis buffer volume). Finally, samples were subjected to protein denaturation at 95°C for 5 minutes, then cooled on ice.

3.2.2.3.6 SDS-PAGE and Western blot

The SDS-PAGE (sodium dodecyl sulfate-polyacrylamide gel electrophoresis) method was used to separate protein samples based on their molecular weight. Previously prepared samples were loaded onto polyacrylamide gels of corresponding acrylamide percentage, together with a protein ladder marker. Gels were run in $1\times$ SDS running buffer at 180 V until the dye front has reached the bottom of the gel. Gels were then briefly washed with $1\times$ transfer buffer and transferred onto polyvinylidene fluoride (PVDF) membranes using Trans-Blot Turbo Transfer System, at 25 V/0.5 A for 30 minutes.

After protein transfer, membranes were washed with distilled H_2O and stained with Ponceau S, to visualise total protein. Following the removal of Ponceau S stain, membranes were blocked for 1 hour in $1\times$ PBS-T/5% milk solution with continuous shaking. Next, membranes were incubated in primary antibodies diluted in 1X PBS-T overnight, at 4°C. Membranes were washed with $1\times$ PBS-T three times over the course of 30 minutes the following day, then incubated in secondary antibodies/$1\times$ PBS-T for 1 hour with continuous shaking. Again, membranes were washed with $1\times$ PBS-T for 30 minutes and visualised with Pierce ECL Western Blotting Substrate, using ChemiDoc Imaging System.

3.2.2.3.7 Insoluble protein purification assay

Protein aggregation in transfected HEK293 cells was investigated by lysing the cells and subjecting them to a set of ultracentrifugation steps based on a previously published (Leliveld et al., 2008) and adapted protocol (Zaharija et al., 2022), in which soluble protein in the supernatant was separated from insoluble protein in the pellet. Buffers used to solubilise the protein between centrifugations are described in detail in **Table *30***. Briefly, cells were lysed with 200 μL of Lysis Buffer per well. Following lysis, 60 μL of each homogenate was separated and prepared for Western blotting, as described in

Section 3.2.2.3.5. Samples were stored at -20°C until required. The rest of the homogenised samples were transferred into ultracentrifuge tubes, with 2.5 µL of Triton-X 100 added to each tube. Samples were centrifuged at 4°C, 20,000 × g for 20 minutes. After supernatant was removed, pellet was lysed and centrifuged in the same manner.

Next, pellets were resuspended in 200 µL of A1 buffer and centrifuged at 4°C, 130,000 × g for 45 minutes. This process was repeated once more before resuspending the pellet in buffer B1 and incubating the samples at 4°C overnight. Samples were centrifuged at 4°C, 130,000 × g for 45 minutes the following day. Pellet was again resuspended in buffer B1, without the addition of DNAse I, and centrifuged under the same conditions. Next, pellet was dissolved in 200 µL of buffer C1 using a hypodermal insulin needle. Samples were incubated on ice for 1 hour with continuous shaking and centrifugated at 4°C, 112,000 × g for 45 minutes. Again, buffer C1 was added to the pellet and the process was repeated. Centrifugation yielded insoluble protein fraction, which was dissolved in 20 µL of Laemmli buffer and 2 µL DTT. Samples were denatured at 95°C for 5 minutes, cooled on ice, and used for SDS-PAGE/WB analysis as described in Section 3.2.2.3.6, together with previously prepared homogenate samples.

3.2.3 Statistical analyses

3.2.3.1 Protein expression quantification and statistical analysis

Following proteasomal inhibition assay, expression levels of visualised proteins were quantified using the BioRad Image Lab software. Quantification was performed using an exposure time that did not lead to signal saturation, to retain the proportional relationship between signal strength and protein concentration. Band lanes were manually adjusted, with automatized subsequent analysis. Volumes of expression were obtained via integrated normalisation for both Flag-tagged proteins and corresponding β-actin controls, to account for cell count variability. Further statistical analysis of biological replicates was done using Microsoft Excel and GraphPad Prism software. Firstly, obtained volumes for Flag-tagged samples were divided by corresponding β-actin controls. Obtained volumes were then normalised by mean and subjected to further analysis, using ordinary one-way ANOVA with Tukey's multiple comparison post-hoc test. A p-value of < 0.05 was considered statistically significant.

3.2.3.2 Colocalization analysis

Colocalization between DISC1 regions and their interaction partners, as well as colocalization with the endoplasmic reticulum, was analysed using Fiji ImageJ software. Colocalization images in .tif format were imported into the program and split to channels based on fluorescent signal, where correlation was determined between the red and green channels. For the purpose of correlation analysis, two plugins were employed: JACoP (Bolte & Cordelières, 2006) and Colocalization Finder (credited authors: Christophe Laummonerie, Jerome Mutterer, Philippe Carl). Analyses performed by JACoP included calculation of Pearson's coefficient, overlap coefficient, Manders' coefficients M1 and M2 and Costes' automatic threshold. Threshold parameters were then further adjusted as necessary. Colocalization Finder was used for the purpose of generating cytofluorograms, as well as for the confirmation of Pearson's coefficient values.

3.2.3.3 Aggregate number and size quantification

Aggregating constructs spanning the D region plus linker, linker + I region, as well as the linker region alone, were used to analyse the difference in aggregate number and size. Analysis was performed on 12 images of aggregating cells per construct, obtained across four independent experiments. Quantification was performed using Fiji ImageJ software (Schindelin et al., 2012), with an aggregate defined as any compact accumulation of antibody signal of at least 1 μm in diameter. Original diameter length was obtained in pixels by using a built-in Measure tool, which was later converted into μm units using Microsoft Excel. Graphs were generated using GraphPad Prism software, which was also used to perform further analysis using one-way ANOVA with Tukey's multiple comparison post-hoc test. A p-value of < 0.05 was considered statistically significant.

3.2.3.4 Prediction of aggregating domains

The amino acid sequence of full-length human L variant DISC1 (NP_061132.2) was used to investigate potential aggregating and/or amyloid-forming regions of the said protein. Several online prediction tools were used for this purpose: AGGRESCAN (Conchillo-Solé et al., 2007), ANuPP (Prabakaran et al., 2021), FoldAmyloid (Garbuzynskiy et al., 2010), MetAmyl (Emily et al., 2013), and TANGO (Fernandez-Escamilla et al., 2004; Linding et al., 2004; Rousseau et al., 2006). In total, these tools employ six different algorithms for aggregation and/or amyloid formation prediction. Analysis conditions

were used at default parameters for every algorithm, after which a consensus was determined for each amino acid, as to whether it was expected to aggregate or not.

3.2.4 *Drosophila melanogaster* research model

3.2.4.1 Fly husbandry

Flies (*Drosophila melanogaster*) were raised either in vials or stock bottles with standard cornmeal-based agar medium, and maintained at 25°C and 70% relative humidity, on a 12-hour on/off light cycle (lights on at 08:00, lights off at 20:00). Nutrient medium was prepared following a recipe found in **Table *32***. Briefly, Mixture B was added to Mixture A and periodically mixed while cooking on medium-high heat. Once suspension was brought to a boil, heat was turned down and cooking continued for another 20 minutes. Food was supplemented with additional 200 mL of tap water, due to evaporation. Once finished, propionic acid and p-hydroxybenzoic acid methyl ester (NIPAGIN) in 95% ethanol were added to the food to prevent unwanted microorganism growth. Stock bottles were populated with adult flies at densities that were certain to produce a comparable number of progenies. Flies were transferred to vials containing fresh food at least once a week.

3.2.4.2 Fly collection

When collecting flies for behavioural assessment or crossing, flies were briefly anesthetized with CO_2 and sorted by gender. Prior to performing behavioural assays, flies were left to recover from anaesthesia for at least 18 hours at 25°C and 70% relative humidity under a 12 h light/12 h dark cycle. All behavioural tests were performed on three to five days old males, the day after flies were placed in vials with fresh food.

3.2.4.3 Fly strains

The wild type *(wt)* flies of the *Canton S* (CS) background were used as a primary control stock. Transgenic flies were generated by microinjecting a pPRW plasmid containing full length human *DISC1* (h*DISC1*) and a P element helper plasmid into *white^1118^ Drosophila* embryos. *DISC1* gene was injected downstream of the transgenic construct UAS (promoter), which prevented DISC1 expression unless activated by a *Gal4* driver. Transformant chromosomes were balanced by using *SM6a* (second chromosome balancer), on flies *w[1118][iso]/y[+]Y;Sco/SM6a; 3[iso]*, and *TM6c* (third chromosome

balancer), on flies *w[1118][iso]/y[+]Y;2[iso];TM2/TM6c,Sb*. Two fly strains were generated using this approach: hemizygote flies carrying UAS fused with *DISC1* balanced on the second chromosome (*SM6a*, UAS-*DISC1-2nd*), or third chromosome (*TM6c*, UAS-*DISC1-3rd*). Anatomical specificity of DISC1 expression was achieved by crossing UAS-*DISC1* flies with transgenic flies that had a *Gal4* activator downstream of the pan-neuronal *elav* driver. 3-to-5-day old males carrying the UAS-*DISC1* transgene on either 2nd or 3rd chromosome were mated with virgins carrying the pan-neuronal *elav-Gal4* driver. First generation progenies (*elav-Gal4* x UAS-*DISC1*) were then collected and used for behavioural testing.

3.2.4.4 Behavioural assays

3.2.4.4.1 Negative geotaxis assay

The negative geotaxis assay was performed for the purpose of measuring climbing ability of control flies (*wt*, UAS-*DISC1-2nd*, UAS-*DISC1-3rd* and *elav-Gal4*, relative to UAS>*Gal4* progeny). A day prior to the assay, 50 males from both transgenic and control lines were selected and transferred in groups of 10 into vials containing 3 mL nutrient media. The following day, flies were transferred into vials without nutrients and a line drawn halfway up the tube height. Five vials were then placed in a rectangular frame with a secure lid to retain an upright position and placed in front of a white background. Following a 30-minute acclimation, the frame was tapped three times in rapid succession, ensuring that all flies fall to the bottom of the tube, which induced the negative geotaxis response. After 5 seconds the flies' position was captured with a camera and the process was repeated after a 1-minute recovery period, five times in total. Flies were then transferred back into the food vials and maintained under standard conditions (25°C and 70% relative humidity, on a 12-hour on/off light cycle). The assay was repeated each week with the same set of flies, until flies reached 4 weeks of age. For the statistical analysis, the average number of flies that crossed the horizontal line was divided by an average number of flies within each vial. The total performance across the 5 vials for each fly strain was calculated as the average percentage of five consecutive measurements.

3.2.4.4.2 Sleep and activity

Drosophila Activity Monitoring System (DAMS), a system which counts the number of breaks of an infrared beam that bisects the midline of a glass tube housing a single fly

(Pfeiffenberger et al., 2010), was used to detect and quantify the activity and sleep behaviour. Sixteen males of each line (control flies (*wt*, UAS-*DISC1-2ⁿᵈ*, UAS-*DISC1-3ʳᵈ* and *elav-Gal4*) and UAS>*Gal4* progeny) were recorded in the 65 mm × 5 mm glass tubes, that had food on one end and a porous plug on the other, placed inside the TriKinetics monitors. Monitor holds 32 tubes, and was used to collect the fly activity data (a number of infrared beam crossings) in one-minute intervals for each fly, using the DAMSystem3 software. Data was then exported into Microsoft Excel. Sleep was defined as no beam interruption for 5 minutes. The activity and sleep patterns were monitored continuously for five consecutive days at 25°C, under a 12 h light/12 h dark cycle. Data was collected using DAMSystem3 Data Collection Software. Data was exported as .txt files using DAMFileScan and analysed using a software developed by Andretić-Waldowski lab group (Rigo et al., 2021). From the recorded data, the total average activity (number of glass tube crossings in a 24-hour period) and sleep duration (in minutes during a 1-hour period) were calculated for each experiment. Data analysis was performed with the help of Milan Petrović (Faculty of Informatics and Digital Technologies, University of Rijeka). Statistical analysis was performed with GraphPad Prism 10, using ordinary one-way ANOVA followed by Tukey's multiple comparison post-hoc test. A *p*-value of < 0.05 was considered statistically significant.

4. Results

4.1 Structural analysis of DISC1

4.1.1 Domain refinement

4.1.1.1 Reanalysing conserved UVR-like repeat regions of DISC1

While the origins of *DISC1* may be obscured, potentially due to its unusually rapid sequence evolution that is still hindering the process of accurately investigating its homology, another possible explanation of its origins has previously been discovered (Sanchez-Pulido & Ponting, 2011). Specifically, it has been shown that the *DISC1* gene contains several homologous sequence repeats conserved even among non-vertebrae species, of which two (UVR1 and UVR2, **Figure 15**, A) can be found within the central part of the protein (Sanchez-Pulido & Ponting, 2011). These repeats showed statistically significant resemblance to a UVR domain of the UvrB protein, which consists of two anti-parallel α-helices associated via structural loop (Alexandrovich et al., 1999, 2001; Sohi et al., 2000). A third putative UvrB-like repeat (UVR3, **Figure 15**, A) may be found near the C-terminal part of the DISC1 protein (Sanchez-Pulido & Ponting, 2011).

Recently, two solution NMR structures of a C-terminal part of DISC1, corresponding to UVR3, have been solved in solution with its interaction partners NDEL1 (Protein Data Bank (PDB) code: 5YI4) (Ye et al., 2017) and ATF4 (PDB code: 6IRR) (Wang et al., 2019). Interestingly, when both structures of C-terminal DISC1 are superimposed onto the solution structure of UvrB (PDB code: 1E52, Alexandrovich, A 2001), a striking correspondence can be seen (**Figure 15**, B/C). Alignment and comparison of all three sequences further confirms the similarities, as shown in **Figure 15**, C/D. This further confirms the original prediction of Sanchez-Pulido and Ponting.

It is also interesting to note that these three theoretically predicted UvrB-like repeats significantly overlap with the empirical, ESPRIT-derived regions of DISC1 (Yerabham et al., 2017), specifically with regions D, I and C (**Figure 15**, A). UVR1 can be seen overlapping with the C-terminal part of the D region, and partially stretching below it, while both UVR2 and UVR3 can be found fully within the I and C regions, respectively. Thus, we hypothesized that these UVR-like repeats represent key structural elements of the experimentally determined regions of DISC1, and as such can be used to further refine region boundaries.
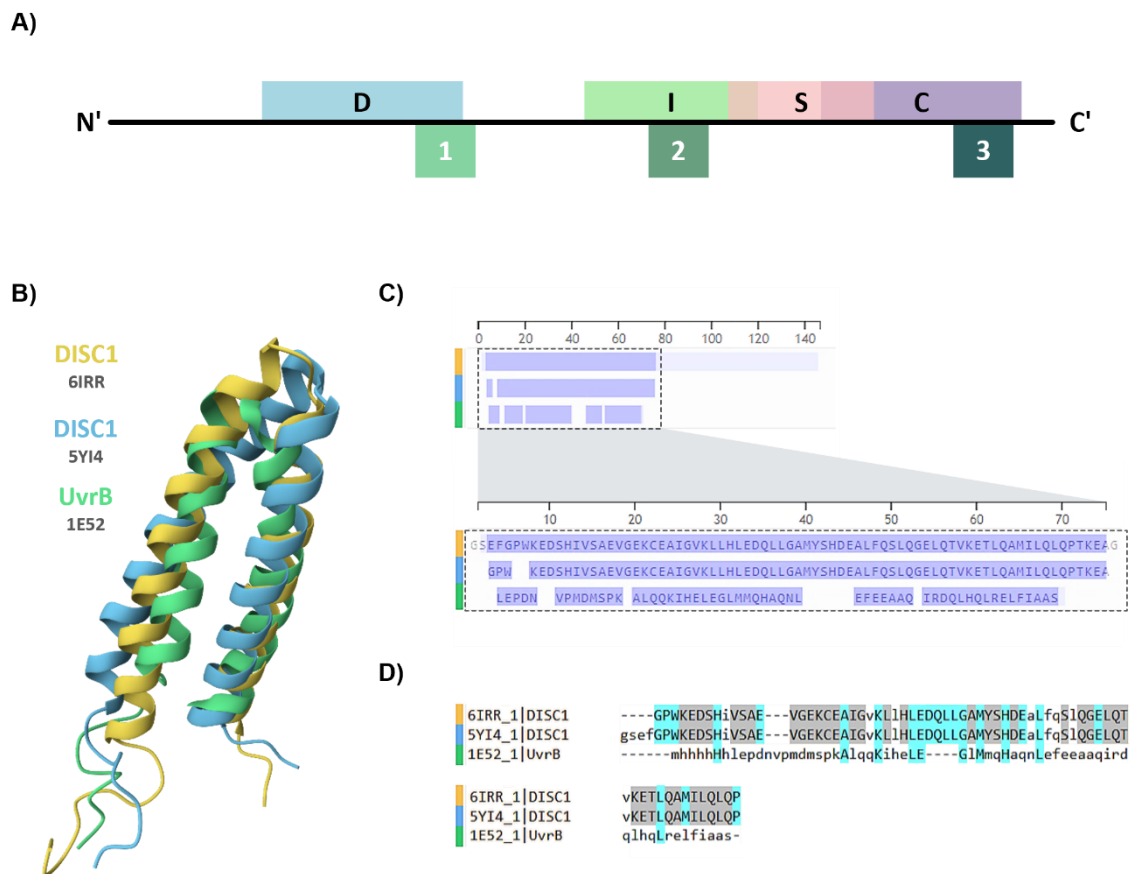
Figure 15. The predicted UvrB-like repeats of DISC1. A) Schematic one-dimensional representation of experimentally defined DISC1 regions (D, I, S and C) (Yerabham et al., 2017) and the predicted corresponding UvrB-like regions (UVR1, UVR2 and UVR3) (Sanchez-Pulido & Ponting, 2011). **B)** Two solution NMR structures of the predicted UVR3 repeat of DISC1 (PDB: 5YI4 (Ye et al., 2017), PDB: 6IRR (Wang et al., 2019)) superimposed on a UvrB repeat (Alexandrovich et al., 2001), using RCSB PDB: Structure Alignment and Comparison online tool. **C)** Sequence alignment and comparison of superimposed structures shown in B), generated using the same tool. Upper part of the figure shows sequence comparison of all three structures, with colour-coding on the left corresponding to the structures shown in B). Lower part of the figure is enlarged to show the exact amino acid sequences of the compared structures. Purple highlights indicate high similarities between the three structures. **D)** Sequence alignment of the structures shown in B), generated using Multiple Sequence Comparison by Log-Expectation tool (ref). Amino acids highlighted in blue show complete alignment, while those highlighted in grey indicate partial alignment. Lower case characters represent unaligned amino acid residues. Colour codes found on the left side of the sequences correspond to the colour codes of the structures shown in B).

4.1.1.2 Redefining the experimentally determined domains of DISC1, based on the UVR-like repeats

The current boundaries of DISC1 regions were identified using the high-throughput ESPRIT technique, by expressing almost 28,000 randomly generated truncated clones of DISC1 in *Escherichia coli* (Yerabham et al., 2017). However, while the employment of this technique was highly successful in identifying stable, folded regions of DISC1, it is important to note that the fragments expressed in bacteria cannot be fully representative of the endogenous human DISC1 protein. Moreover, the constructs tested ranged from 150-400 AA, which covers a relatively small portion of all possible construct variations within an 854 AA-long protein (4% of all possible combinations). Taking these caveats into account, it is reasonable to conclude that the ESPRIT-determined domain boundaries may not represent the exact boundary limits. We therefore set to optimize the empirically known boundaries of DISC1 regions through integration with theoretical positions of UVR-like repeats within their respective regions (**Figure 15**, A).

For each region, three DISC1 constructs were cloned: one representing the empirically determined region ("ESPRIT"), one shortened to end immediately after the structural loop of the UVR-like repeat ("half UVR"), thus truncating it in the middle, and one ending immediately after the UVR-like repeat ("full UVR"). The relative stability of the constructs was confirmed by Western blot, following the expression in HEK293 cells. Two major points of interest were investigated: the total level of expression of each protein fragment normalised to β-actin, and the stability of each fragment against proteasomal degradation. The latter was analysed based on the fragment expression levels either in the absence or presence of proteasome inhibitor MG132, which allows protein accumulation by reducing its degradation. As such, only stable, folded proteins will not undergo protein degradation over time. Seven biological replicates were obtained for each result, with each replicate consisting of four technical replicates.

4.1.1.2.1 D region stability increases with proteasome inhibition

Three of the D region-based constructs (ESPRIT D: AA 257-393, $D_{half\ UVR}$: AA 257-370, $D_{full\ UVR}$: AA 257-390) cells showed a variable degree of expression both in the presence and absence of MG132 (**Figure 16**, A-C). While all showed similar resilience to proteasomal degradation, the construct that was extended to include the full UVR1 repeat showed an increase in expression relative to its ESPRIT-derived equivalent when

subjected to proteasomal degradation, as well as in the presence of the inhibitor. Interestingly, the construct ending halfway through UVR1 showed similar stability in the absence of the inhibitor as its ESPRIT-derived counterpart, with a slight increase in expression noted in its presence. Taken together, these results suggest that the UvrB-like repeat is part of, but not essential to the structure of D region, and that the C-terminal boundary of the region may be extended to encompass the entirety of the UVR1.
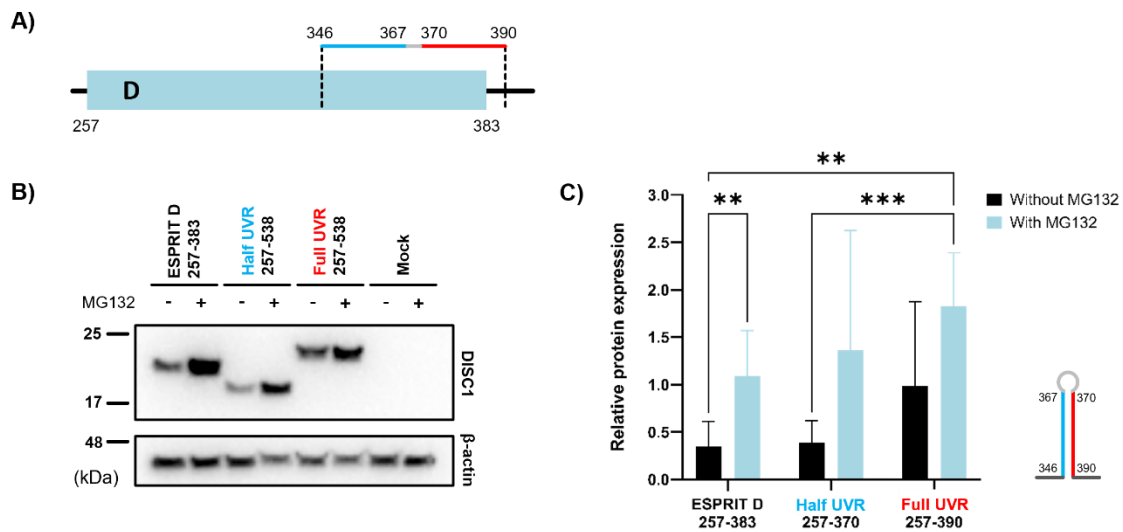
Figure 16. D region stability increases with proteasome inhibition. A) Schematic representation of the ESPRIT-derived D region, with detail of the location of the UVR1 repeat, relative to the region. The two helices of the repeat are indicated in blue and red, with a connecting structural loop shown in grey. Numbers on the schematic indicate amino acid positions. **B)** Western blot of fragments based on the ESPRIT-D region. Text colours correspond to the schematic shown in A), with amino acid boundaries of each fragment written below. β-actin protein levels were used as a loading control. Testing the stability of the ESPRIT-derived D region was accomplished by expressing Flag-tagged DISC1 fragments in HEK293 cells, in the presence and absence of the proteasome inhibitor MG132. Seven biological replicates of each experiment were performed, each comprising four technical replicates. **C)** Quantification of the blot shown in B), displaying the relative resistance of fragments to proteasome degradation, corrected to β-actin. Statistical analysis was performed for all possible combinations using one-way ANOVA with Tukey's multiple comparison post-hoc test. **: $p < 0.01$, ***: $p < 0.001$. Schematic depiction of the UVR1 is shown next to the graph. The two helices of the repeat are indicated in blue and red, with a connecting structural loop shown in grey.

4.1.1.2.1   I region does not represent a stable domain

Surprisingly, all three constructs based on the I region (ESPRIT I: AA 539-655, $I_{\text{half UVR}}$: AA 539-601, $I_{\text{full UVR}}$: AA 539-622) expressed extremely poorly in HEK293 cells relative to the D and C constructs, which greatly hindered quantitative analysis (**Figure 17**, A-C). In fact, the expression levels of fragments that did not undergo MG132 treatment were almost impossible to detect, regardless of the number of replicates, resulting in only four out of seven blots being quantifiable. However, quantification of these blots strongly indicated that the ESPRIT-derived I region does not represent a self-sufficient, folded unit in mammalian cells, as shown by a high increase in stability in the presence of proteasomal inhibitor. Similar, albeit more subtle results can be seen in the cases of $I_{\text{half UVR}}$ and $I_{\text{full UVR}}$. Both fragments expressed extremely poorly on their own, with marginally higher expression levels seen in the presence of MG132. Considering that the UVR-like repeat occupies the middle of the I region, it is reasonable to assume that the truncations within the repeat, or of the region itself, lead to further destabilization. Taken together, these results strongly indicate that, in spite of the results yielded by the ESPRIT screen in bacteria, the I region does not represent a self-sufficient, stable domain when expressed in isolation in mammalian cells, and any further truncation will lead to even more prominent destabilization.
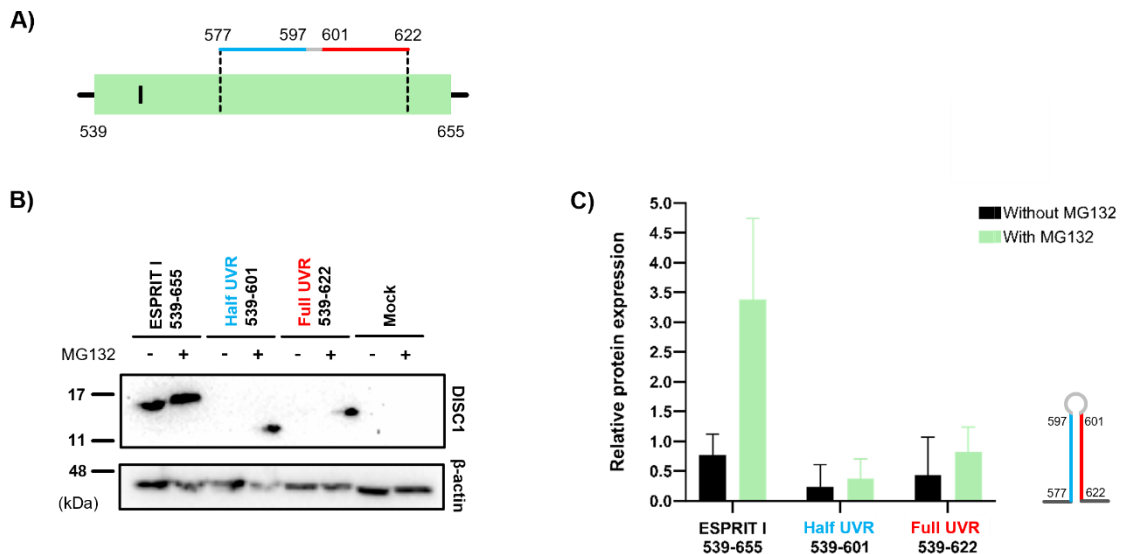
Figure 17. I region does not represent a stable domain. A) Schematic representation of the ESPRIT-derived I region, with detail of the location of the UVR2 repeat, relative to the region. The two helices of the repeat are indicated in blue and red, with a connecting structural loop shown in grey. Numbers on the schematic indicate amino acid positions. **B)** Western blot of fragments based on the ESPRIT-I region. Text colours correspond to the schematic shown in A), with amino acid boundaries of each fragment written below. β-actin protein levels were used as a loading control. Testing the stability of the ESPRIT-derived I region was accomplished by expressing Flag-tagged DISC1 fragments in HEK293 cells, in the presence and absence of the proteasome inhibitor MG132. Seven biological replicates of each experiment were performed, each comprising four technical replicates. **C)** Quantification of the blot shown in B), displaying the relative resistance of fragments to proteasome degradation, corrected to β-actin. Statistical analysis was performed for all possible combinations using one-way ANOVA with Tukey's multiple comparison post-hoc test. No statistical significance was seen between the results. Schematic depiction of the UVR2 is shown next to the graph. The two helices of the repeat are indicated in blue and red, with a connecting structural loop shown in grey.

4.1.1.2.1.1 I region shows increased stability while in complex with other C-terminal regions

To assess whether the I region can be stabilised by other C-terminal regions of DISC1, we expressed all three (I, S and C region, respectively) in isolation. Next, we expressed a combination of the I and S region, and a combination of all three regions, terminating at AA 854. All the constructs were sequenced, and expressed both in the presence and absence of MG132 (**Figure 18**). While the I region alone still barely expressed, and was detectable only in the presence of a proteasome inhibitor, both S and C region expressed similarly well in either case. However, a construct encoding the I and S regions in combination consistently showed a complete lack of expression across three replicates, implicating destabilisation of the S region by the I region. In contrast, a construct encoding I, S and C displayed remarkable stability, especially in the presence of MG132.

Taking into consideration the results obtained for the I region, alone and in combination with the S region, we can conclude that adding the C region to the complex hinders the S region destabilisation by the I region, and further acts as a stabiliser to both.
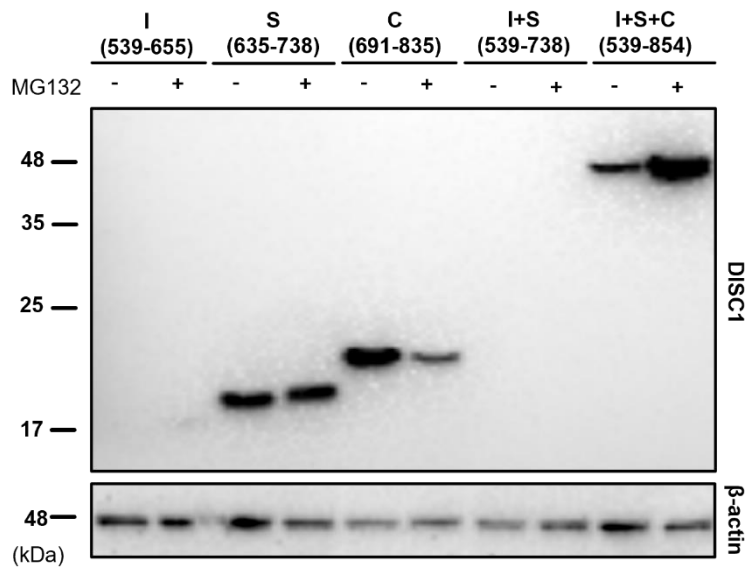
Figure 18. I region shows increased stability while in complex with other C-terminal regions. Western blot of constructs encoding DISC1 I, S, and C regions, respectively, as well as the combinations of I+S and all three C-terminal constructs (I+S+C). The stability of the constructs was tested by expressing Flag-tagged DISC1 fragments in HEK293 cells, in the presence and absence of the proteasome inhibitor MG132.

4.1.1.2.2 C region presents a stable domain that can be further refined

Curiously, both the ESPRIT-derived C region (ESPRIT C: AA 691-836), and a version of it that was truncated immediately after UVR3 ($C_{full\ UVR}$: AA 691-829), showed lesser resilience to the proteasomal degradation over time than the other two DISC1 regions (**Figure 19**, A-C). However, the $C_{full\ UVR}$ construct did exhibit higher expression levels than its empirical counterpart, implying that the final seven amino acids of the ESPRIT-derived C region are dispensable for its structure. As such, redefining the boundaries of this region to end at amino acid 829 could further improve its stability.

In contrast, a construct ending halfway through the UVR3 repeat ($C_{half\ UVR}$: AA 691-807) showed significantly lower protein expression both in the presence and absence of proteasome inhibitor, strongly supporting the idea that UVR3 represents a crucial part of the C region.
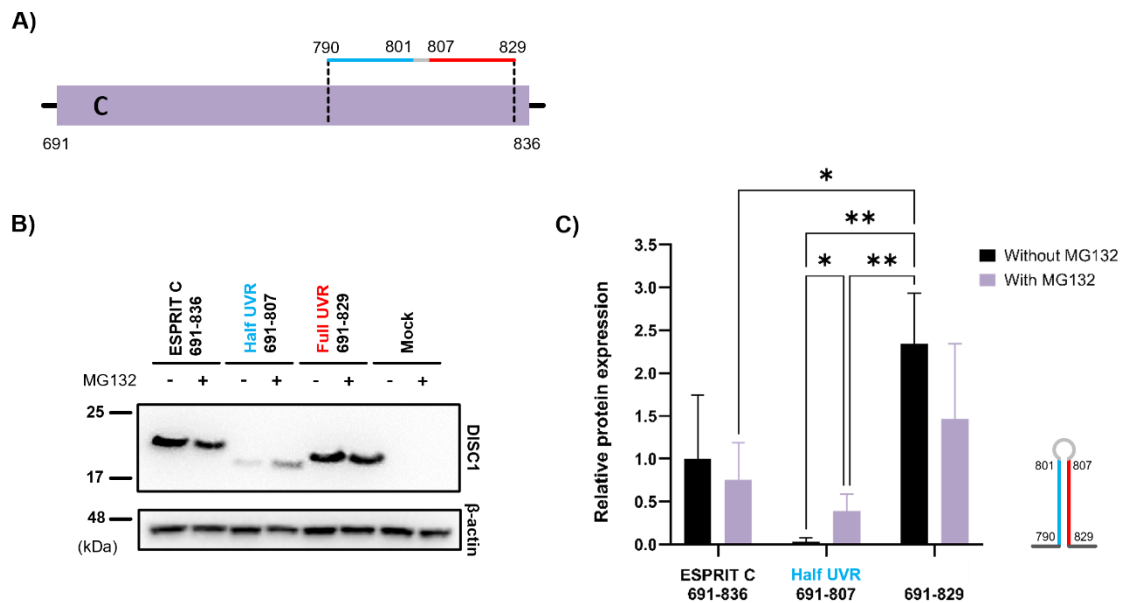
Figure 19. C region represents a stable domain that can be further refined. A) Schematic representation of the ESPRIT-derived C region, with detail of the location of the UVR3 repeat, relative to the region. The two helices of the repeat are indicated in blue and red, with a connecting structural loop shown in grey. Numbers on the schematic indicate amino acid positions. **B)** Western blot of fragments based on the ESPRIT-C region. Text colours correspond to the schematic shown in A), with amino acid boundaries of each fragment written below. β-actin protein levels were used as a loading control. Testing the stability of the ESPRIT-derived Cc region was accomplished by expressing Flag-tagged DISC1 fragments in HEK293 cells, in the presence and absence of the proteasome inhibitor MG132. Seven biological replicates of each experiment were performed, each comprising four technical replicates. **C)** Quantification of the blot shown in B), displaying the relative resistance of fragments to proteasome degradation, corrected to β-actin. Statistical analysis was performed for all possible combinations using one-way ANOVA with Tukey's multiple comparison post-hoc test. *: $p < 0.1$, **: $p < 0.01$. Schematic depiction of the UVR3 is shown next to the graph. The two helices of the repeat are indicated in blue and red, with a connecting structural loop shown in grey.

113

4.2 Functional analysis of DISC1

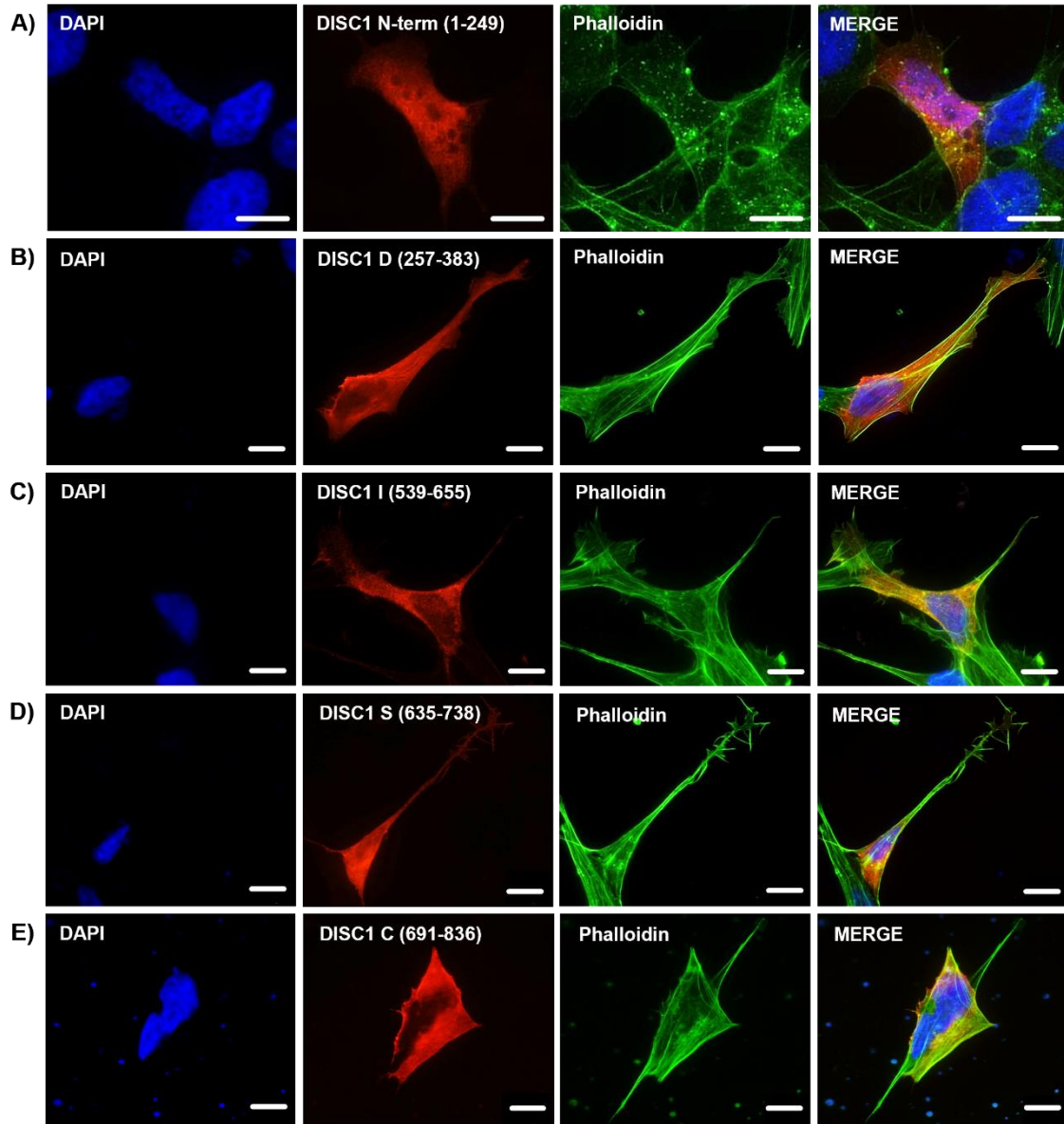### 4.2.1 DISC1 regions primarily localise to the cell cytoplasm

The DISC1 domain structure is comprised of four structural regions named D, I, S, and C, respectively, which present stable, functional units in bacteria (Yerabham et al., 2017) (**Figure 20**). However, not much was known of their stability nor localization outside of this system. To assess whether these regions present functional structural units when expressed in mammalian cell culture, as well as their common expression patterns, we cloned constructs encoding for each region based on the ESPRIT-predicted boundaries, using a combination of Gateway cloning and restriction enzyme cloning. Constructs encoding for each were transfected into SH-SY5Y neuroblastoma cells and further confirmed by Western blotting (**Figure 21**, F) in HEK293 cells.
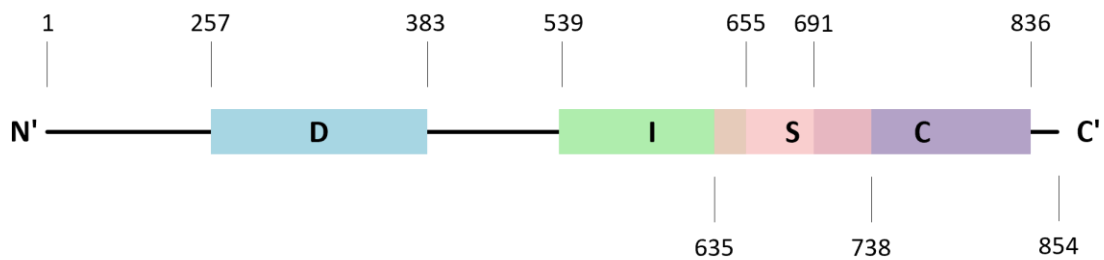
Figure 20. Schematic representation of the one-dimensional domain structure of DISC1, featuring the four structured regions (D, I, S and C). Numbers represent amino acid boundaries of each region. Adapted from Yerabham et al, 2017.

Following the expression in neuroblastoma cells, Flag-tagged domain constructs emitting red fluorescence could be seen to localise exclusively in the cell cytoplasm, predominately in the perinuclear area (**Figure 21**, B-E). Stable cytoplasmic expression could be seen for all the regions throughout multiple replicates, with the exception of the I region. In most cases, transfection rate of the construct encoding for the I region was low, and often followed by cell death or severe disruption of cytoskeleton. This finding suggests that the I region itself might not be as stable as previously predicted and could potentially be toxic to cells when overexpressed. Western blot of the I region further

114

confirmed these results (**Figure 21**, F), in which the band corresponding the I region showed diminished expression despite the strong and consistent expression of β-actin loading control. These results are also in agreement with our previous experiments that tested the stability of the ESPRIT-derived I region versus its theoretical counterparts, in the presence or absence of MG132.

Additionally, we expressed the presumably unstructured N-terminal part of the protein as well, encoding amino acids 1-249 (**Figure 21**, A). Much like its domain counterparts, this construct was also seen to have a stable, cytoplasmic expression.

Some, notably the D and C region, also overlapped with a marker of the endoplasmic reticulum (ER) (**Figure 22**, A, D), with Pearson's correlation coefficient for both regions showing high statistical significance (**Figure 22**, E, H). This is consistent with the reported role of DISC1 in the regulation of ER calcium dynamics (Park et al., 2015). However, a more detailed analysis of these findings is necessary to fully confirm localisation of these regions to the ER.
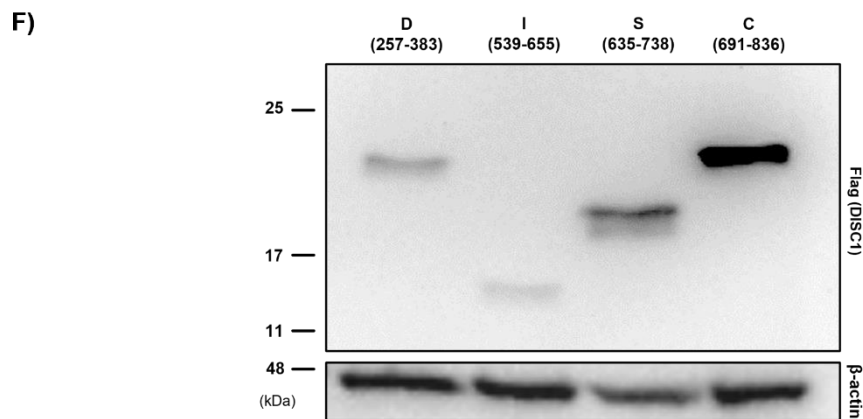
Figure 21. DISC1 regions primarily localise to the cell cytoplasm. A) N-terminal region of the protein shows stable cytoplasmic expression in neuroblastoma cells. **B)** D region shows stable cytoplasmic expression in neuroblastoma cells. **C)** I region shows cytoplasmic expression in neuroblastoma cells. **D)** S region shows stable cytoplasmic expression in neuroblastoma cells. **E)** C region shows stable cytoplasmic expression in neuroblastoma cells. **F)** Western blot of constructs encoding individual regions of DISC1, with β-actin protein levels used as a loading control. All DISC1 constructs shown here are Flag-tagged and visualised using an anti-Flag antibody. Amino acid boundaries of each region are indicated next to, or below the corresponding region. Cytoskeleton was visualised using Acti-stain 488 (Phalloidin). Western blot was performed using HEK293 cell lysates. Microscopy images are obtained from SH-SY5Y cells and are typical of three independent experiments. Scale bars represent 10 μm.
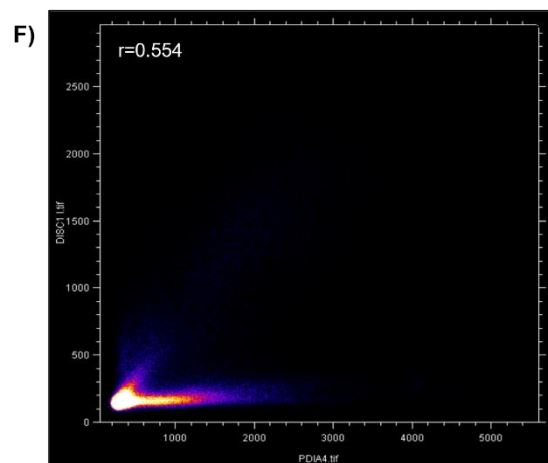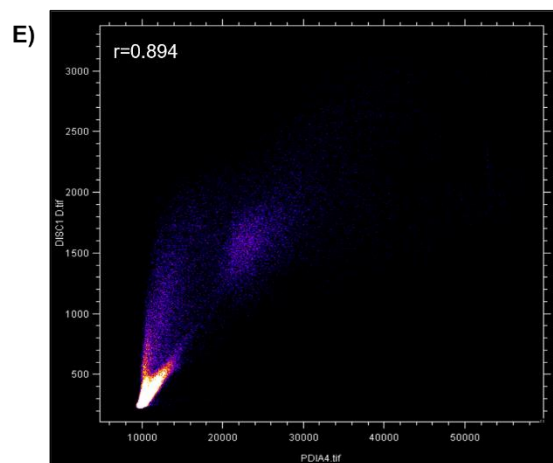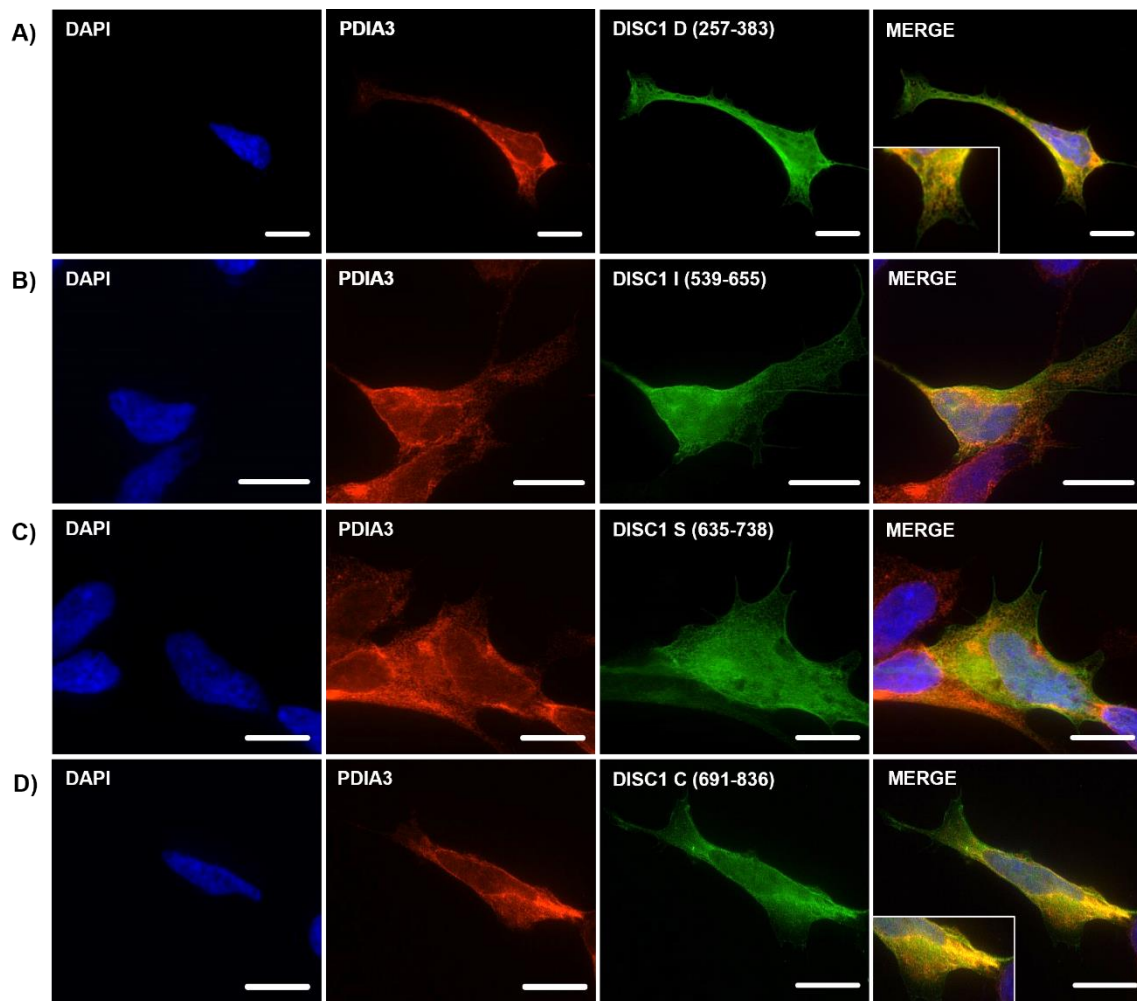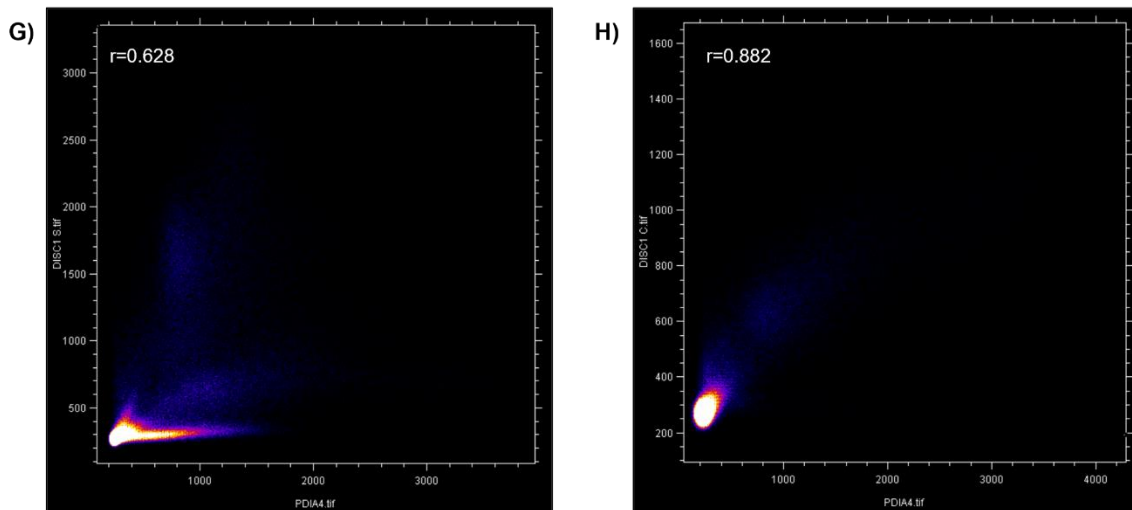
Figure 22. Basic subcellular expression pattern of the four ESPRIT-derived DISC1 regions. A) The D region expression is indicative of colocalization with the ER (yellow, shown enlarged). **B)** The I region expression is indicative of partial colocalization with the ER. **C)** The S region is indicative of partial colocalization with the ER. **D)** The C region expression is indicative of colocalization with the ER (yellow, shown enlarged). **E)** Cytofluorogram used for visualization of colocalization shown in A). High colocalization can be seen by a predominately linear pixel distribution between the two axis (white), and a Pearson's coefficient of 0.894. **F)** Cytofluorogram used for visualization of colocalization shown in B). Low colocalization can be seen by a horizontal pixel distribution between the two axis (white), and a Pearson's coefficient of 0.554. **G)** Cytofluorogram used for visualization of colocalization shown in C). Low colocalization can be seen by a horizontal pixel distribution between the two axis (white), and a Pearson's coefficient of 0.628. **H)** Cytofluorogram used for visualization of colocalization shown in A). High colocalization can be seen by a fairly linear pixel distribution between the two axis (white), and a Pearson's coefficient of 0.882. All DISC1 constructs shown here are Flag-tagged and visualised using an anti-Flag antibody (green). Anti-PDIA3 (red) was used as an ER marker. Amino acid boundaries of each region are indicated next to the corresponding region. Microscopy images are obtained from SH-SY5Y cells and are typical of three independent experiments. Scale bars represent 10 μm. Pearson's coefficient is indicated as "r".

4.2.2 Preliminary studies indicate that most regions of DISC1 are capable of binding interaction partners

If DISC1 regions inferred from the ESPRIT screening indeed represent stable, folded units, then they are also expected to have functionality. As a multifunctional scaffolding protein that lacks any known enzymatic activity, most of the known functions of DISC1 are exerted through protein-protein interactions. Notably, several interaction partners have previously been inferred to bind to DISC1 near to the ESPRIT-derived regions. As such, we hypothesized that if these regions are indeed functional, then they should also be able to interact with known DISC1 interaction proteins.

To address this, we initially tested four known DISC1 interaction partners: PDE4B1, ATF4, NDE1, and NDEL1. PDE4B1 is known to interact within the ESPRIT-determined D domain boundaries (Millar et al., 2005), ATF4 has been implied to bind near the I domain as well as the C domain (Morris et al., 2003), while NDE1 and NDEL1 were shown to interact near the end of the C domain (Brandon et al., 2004) (**Figure 23**). Additionally, another DISC1 interaction partner, LIS1, was tested for its binding capabilities within the S and C region (**Figure 23**) (Brandon et al., 2004).
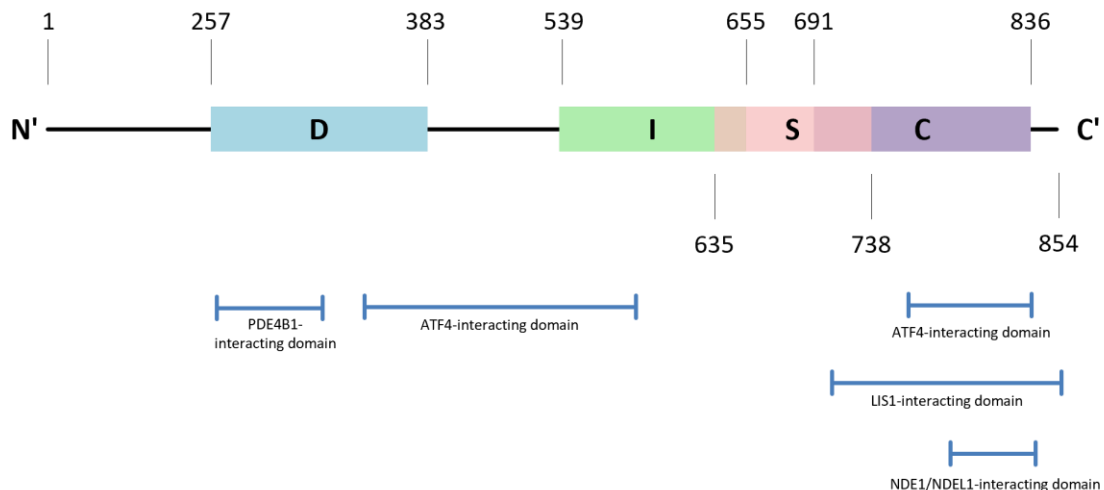
Figure 23. Protein interaction domains of DISC1. PDE4B1 is known to interact within the D domain. ATF4 is known to bind near the I domain, as well as the C domain. LIS1 is known to interact within the S and C domain overlap. NDE1 and NDEL1 are known to bind near the C domain. Blue lines represent binding regions of DISC1 interactors.

Initially, we tested the expression pattern yielded by each of the four EGFP-tagged DISC1 region when expressed alone in neuroblastoma cells, where all four were found to localize within the cell cytoplasm (**Figure 24**). Next, preliminary testing of interaction was conducted by co-expressing a construct encoding the EGFP DISC1 region with its respective mCherry-tagged interaction partner, to which it is predicted to bind. Colocalization between the regions and their interaction partners was then assessed by fluorescent microscopy. Interestingly, when expressed, the D region showed almost complete colocalization with PDE4B1 within the cell cytoplasm (**Figure 24**, C). These results were further supported by a high value of Pearson's coefficient and almost completely linear distribution shown in a cytofluorogram (**Figure 24**, D).
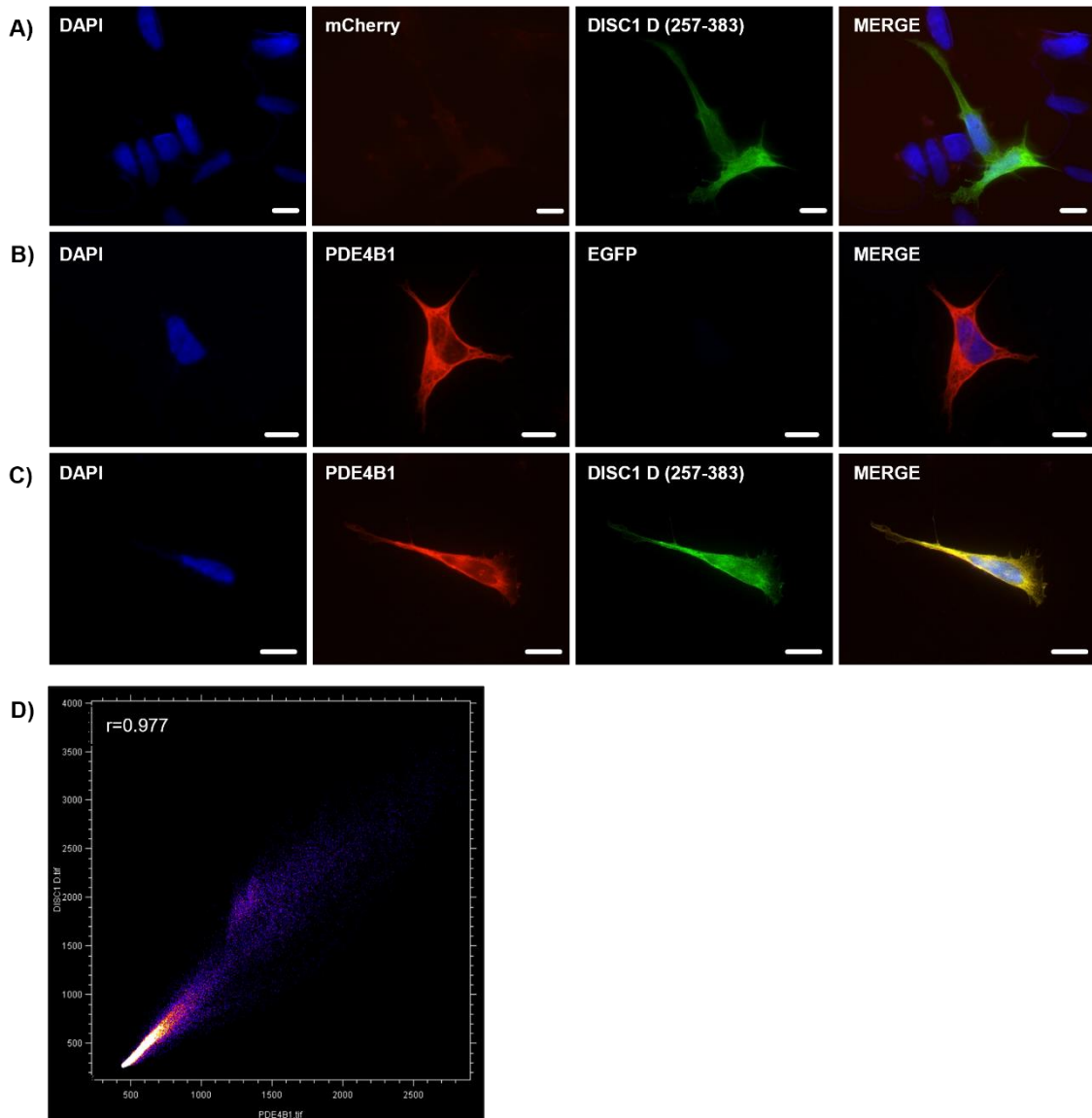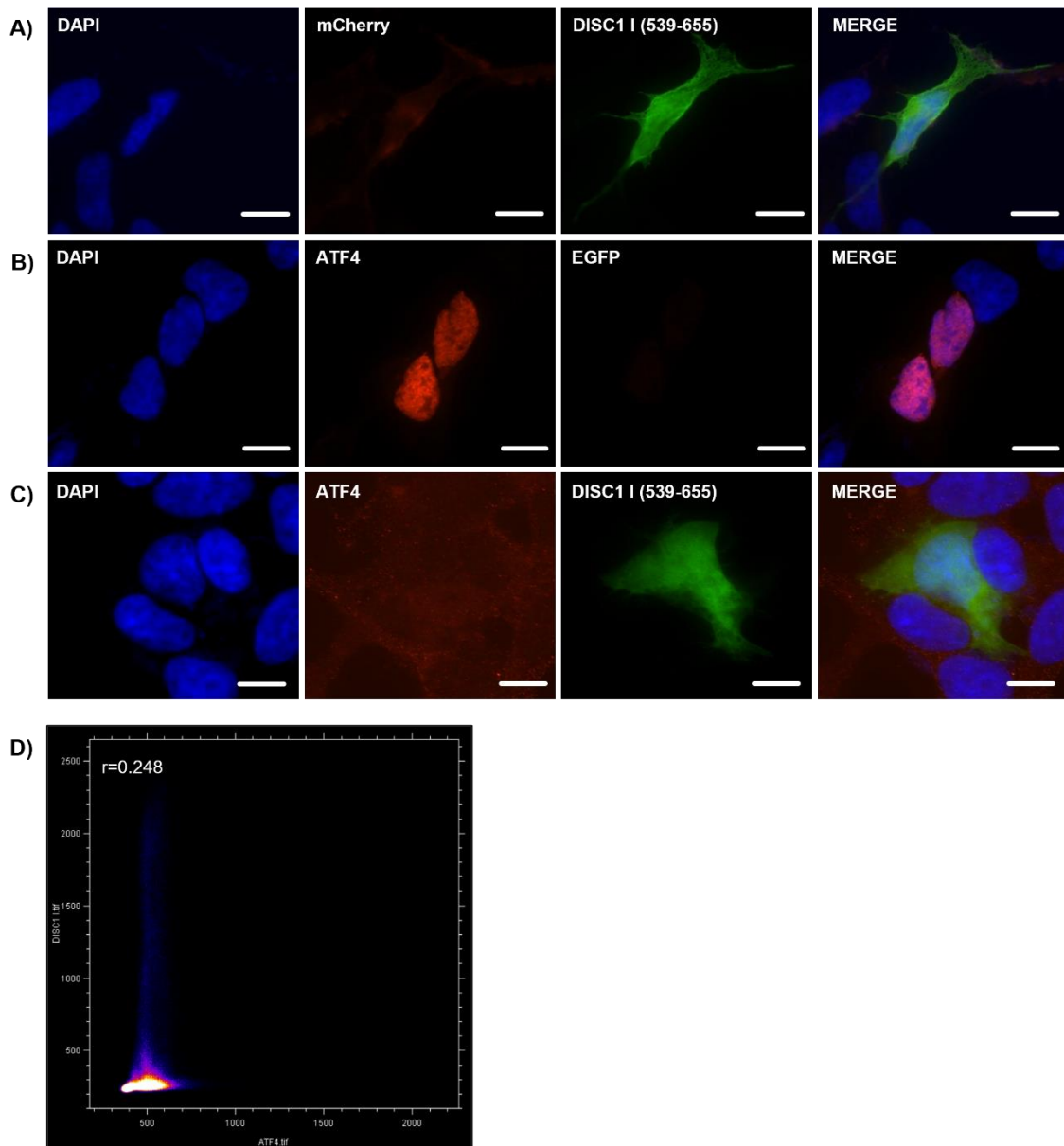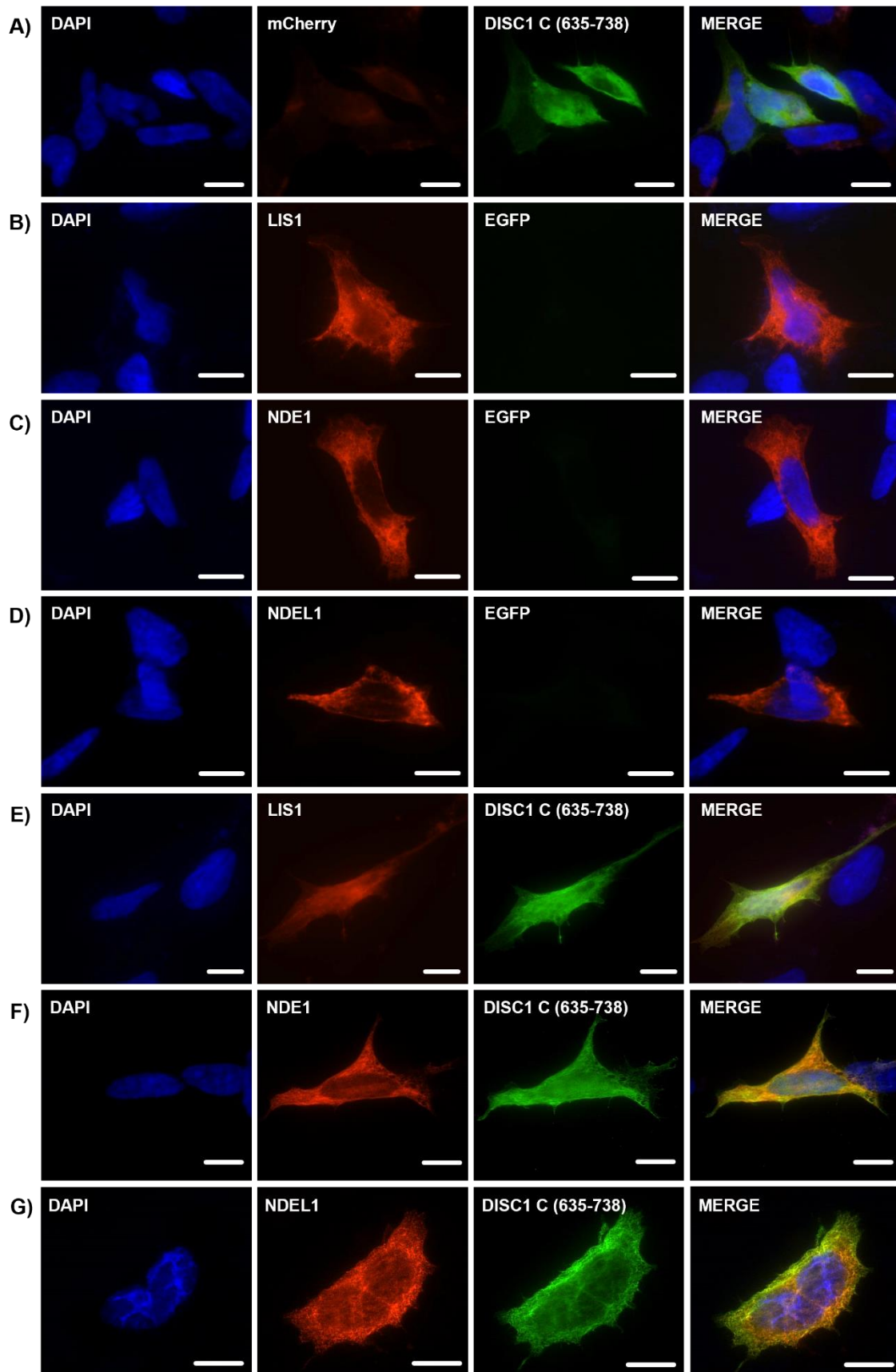
Figure 24. DISC1 D region is shown to colocalize with PDE4B1. A) DISC1 D construct fused with EGFP (green) shows cytoplasmic localization when expressed in isolation. **B)** DISC1 interaction partner PDE4B1 fused with mCherry (red) shows cytoplasmic localization when expressed in isolation. **C)** PDE4B1 shows high colocalization with the D region (yellow) within the cell cytoplasm. **D)** Cytofluorogram used for visualization of colocalization shown in C). High colocalization can be seen by linear pixel distribution between the two axis (white), and a Pearson's coefficient of 0.977. Amino acid boundaries of the D region are shown in brackets. Microscopy images are obtained from SH-SY5Y cells and are typical of three independent experiments. Scale bars represent 10 μm. Pearson's coefficient is indicated as "r".

In contrast, while ATF4 successfully expressed within the nucleus (**Figure 25**, B), it was markedly difficult to co-express with the I region (**Figure 25**, C) due to the low expression levels seen from either, or both constructs across multiple experiments. Consistently low expression of the I region was also recorded in previous experiments (Section 4.1.1.2.2).

Unlike the I region and ATF4, LIS1 was seen to almost completely colocalize with the C region within the cell cytoplasm, with an expression pattern highly similar to that seen when the C region was expressed in isolation (**Figure 26**, E).

Finally, the C region was seen to colocalize with both NDE1 (**Figure 26**, F) and NDEL1 (**Figure 26**, G). Interestingly, Pearson's correlation coefficient was slightly higher in the case of colocalization with NDE1, which was also visible in a more uniform signal distribution and lower signal-to-noise ratio (**Figure 26**, I).

Figure 25. DISC1 I region does not seem to colocalize with ATF4. A) DISC1 construct fused with EGFP (green) shows cytoplasmic localization when expressed in isolation. **B)** DISC1 interaction partner ATF4 fused with mCherry (red) shows nuclear localization when expressed in isolation. **C)** ATF4 shows poor expression when co-transfected with the I region, indicating that ATF4 does not bind within the I region. **D)** Cytofluorogram used for visualization of colocalization shown in C). Low colocalization can be seen by horizontal pixel distribution between the two axis (white), and a low Pearson's coefficient of 0.248. Amino acid boundaries of the I region are shown in brackets. Microscopy images are obtained from SH-SY5Y cells and are typical of three independent experiments. Scale bars represent 10 µm. Pearson's coefficient is indicated as "r".
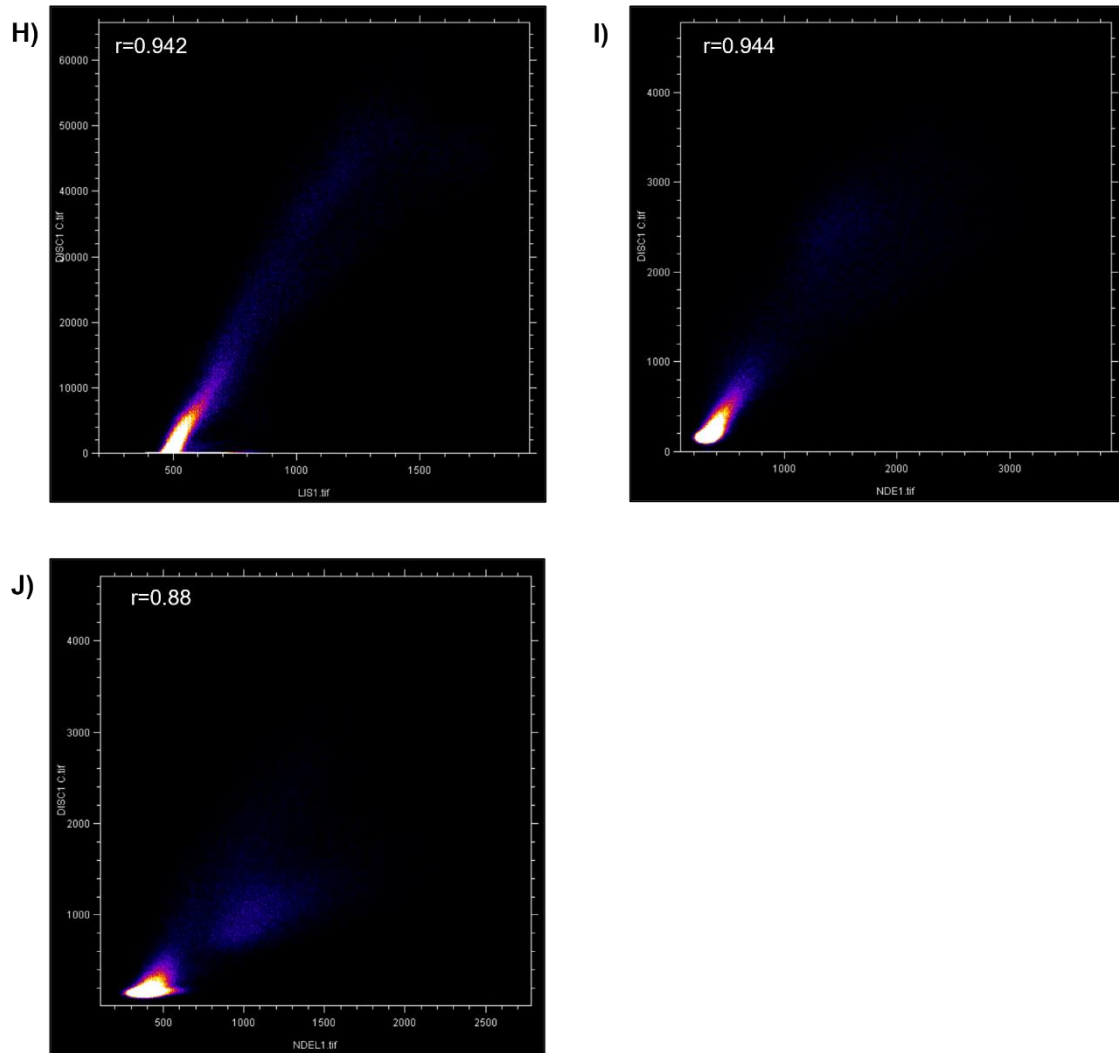
Figure 26. DISC1 C is shown to colocalize with LIS1, NDE1 and NDEL1. A) DISC1 construct fused to EGFP (green) shows cytoplasmic localization when expressed in isolation. **B)** DISC1 interaction partner LIS1 shows cytoplasmic localization when expressed in isolation. **C)** DISC1 interaction partner NDE1 shows cytoplasmic localization when expressed in isolation. **D)** DISC1 interaction partner NDEL1 shows cytoplasmic localization when expressed in isolation. **E)** LIS1 shows high colocalization with the C region (yellow) within the cell cytoplasm. **F)** NDE1 shows slightly lower colocalization with the C region (yellow) than what can be seen with its paralogue, NDE1. **G)** NDEL1 shows high colocalization with the C region (yellow) within the cell cytoplasm. **H)** Cytofluorogram used for visualization of colocalization shown in E). High colocalization can be seen by linear pixel distribution between the two axis (white), and a Pearson's coefficient of 0.942. **I)** Cytofluorogram used for visualization of colocalization shown in F). High colocalization can be seen by linear pixel distribution between the two axis (white), and a Pearson's coefficient of 0.944. **J)** Cytofluorogram used for visualization of colocalization shown in F). Slightly lower colocalization is indicated by the less linear pixel distribution (white) and a Pearson's coefficient of 0.880.

All interaction partners are fused with mCherry and are depicted in red. Amino acid boundaries of the D region are shown in brackets. Microscopy images are obtained from SH-SY5Y cells and are typical of three independent experiments. Scale bars represent 10 μm. Pearson's coefficient is indicated as "r".

4.2.3 Binding capability of DISC1 regions assessed by Nanoscale Pulldown assay

NanoSPD, or Nanoscale Pulldown assay, is a method based on a standard affinity pulldown assay that was miniaturised for the purpose of being performed within a native cell cytoplasm. It exerts its function by hijacking the normal intercellular trafficking process by myosin motors to forcibly pull fluorescently-tagged proteins along filopodial actin filaments (Bird et al., 2017). Based on the formation of "bait-prey" complex between the class 10 myosin motor fused to the NanoTrap vector (MYO10-NanoTrap), protein of interest and an interactor protein, molecular signal crowds at filopodial tips and amplifies fluorescence (Bird et al., 2017). Using this assay enables analysing protein-protein interactions within a single cell, by using fluorescent microscopy to determine whether the bait and prey proteins are indeed found in the tips of filopodia.

Here, triple transfections were performed in which the NanoTrap vector and EGFP-tagged DISC1 regions acted as a "bait", and Flag-tagged DISC1 interaction partners acted as "prey". MYO10-NanoTrap vector, which specifically interacts with EGFP, non-covalently binds the EGFP-DISC1 region, which in turn binds the Flag-tagged interaction protein, and this complex is then accumulated at the filopodial tips, creating an overlapping signal (**Figure 27**, A).

In the case of a control reaction, or a reaction in which there is no protein-protein interaction, only EGFP-DISC1 would be transported into filopodial tips, while the Flag signal would be expressed solely in the cytoplasm (**Figure 27**, B).

NanoSPD assay was utilized with the purpose of further confirming the results of preliminary colocalization assays described in Section 4.2.2. Based on those results, we hypothesized that at least three regions of the protein, D, S and C, will be able to forcibly pull their respective interaction partners to the filopodial tips.
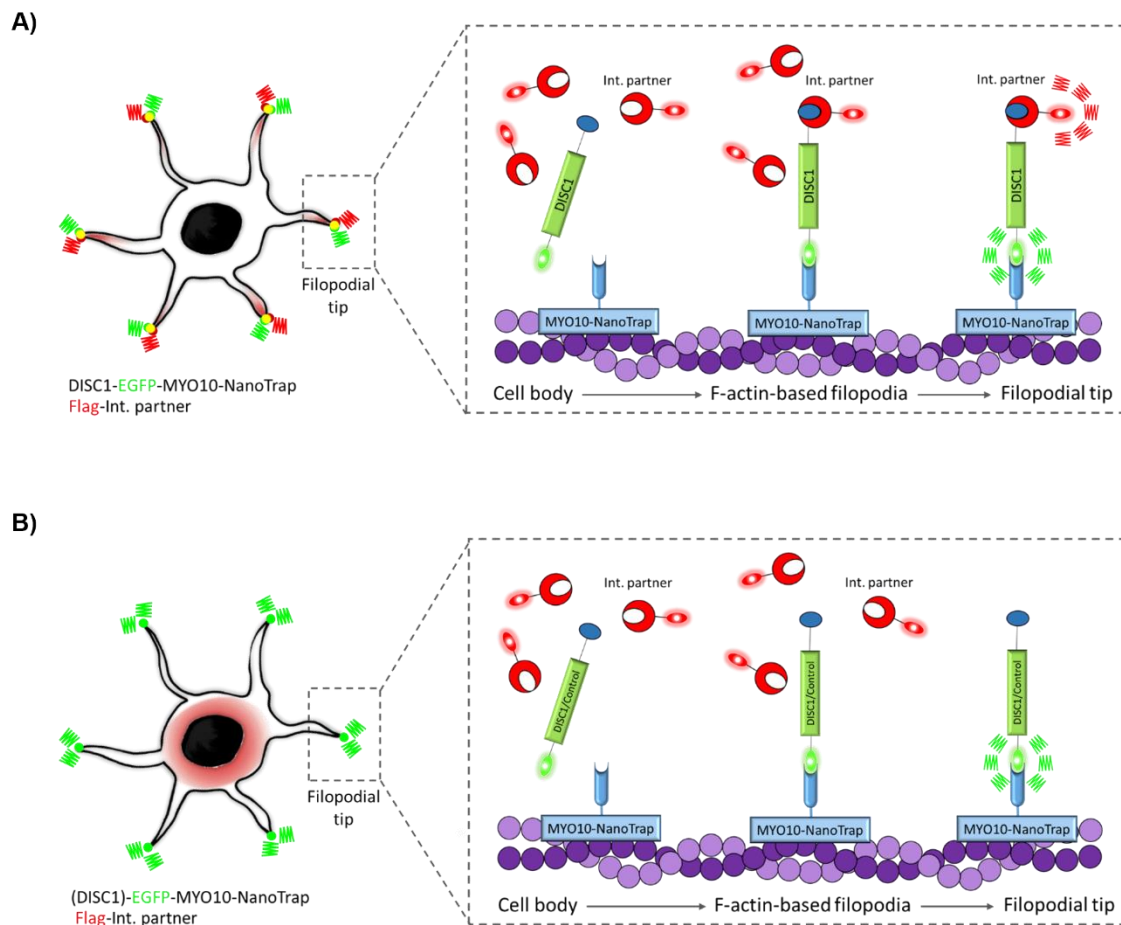
126

Figure 27. Schematic depiction of NanoSPD assay. A) Protein complex formation between NanoTrap, DISC1 and interaction partner. MYO10-NanoTrap vector (shown in blue) hijacks the normal process of intracellular trafficking by trapping the fluorescently tagged protein (EGFP DISC1, labelled green) and forcibly pulling it toward the filopodial tip. If another fluorescently tagged protein (Flag-tagged interaction partner, labelled red) interacts with DISC1, formed complex is jointly accumulated at the filopodial tip, and an overlap between the green and the red fluorescence results in a magnified yellow signal (smaller box). **B)** Protein complex formation between NanoTrap and EGFP control, or DISC1, showing no protein-protein interaction. NanoTrap vector is shown in blue, EGFP control, or EGFP-tagged DISC1, are shown in green. In case of a control reaction, when no binding ensues, NanoTrap motor will traffic the EGFP control alone to the filopodial tips, accumulating the green signal (small box). Flag-tagged proteins (shown in red) will remain unbound in the cytoplasm. In the same manner, if a NanoTrap-bound EGFP-DISC1 does not form protein-protein interactions, it will be trafficked along the filopodia alone, with Flag-tagged proteins remaining in the cytoplasm. Adapted from Bird et al, 2017.

4.2.3.1 DISC1 D region alone is not capable of pulling PDE4B1 into filopodial tips

First, we used the NanoSPD assay to investigate interactions between the DISC1 D region and PDE4B1 protein. To confirm that the NanoTrap motor will only transport EGFP-fused proteins to the filopodia, Flag-tagged DISC1 D was co-transfected with this motor protein into SH-SY5Y cell line. As expected, this resulted in a normal cytoplasmic expression of the D region (**Figure 28**, A) with no filopodial accumulation. On the other hand, when EGFP alone was co-transfected with the NanoTrap motor, the green EGFP signal has readily accumulated in the filopodial tips (**Figure 28**, B), thus proving that EGFP can indeed be trafficked by a myosin motor.

Next, to show that EGFP alone is not capable of binding PDE4B1, the two were co-transfected together with the NanoTrap motor. While Flag-tagged PDE4B1 could only be found in the cell body, EGFP could be seen in both the cell cytoplasm and filopodial tips, thus confirming that EGFP alone is not capable of binding PDE4B1 (**Figure 28**, C).

Finally, the D region fused with EGFP was co-transfected with the NanoTrap motor and Flag-tagged PDE4B1. Curiously, while both constructs expressed within the cell cytoplasm, only the D region was accumulated at the filopodia (**Figure 28**, D). While this does not necessarily mean that the D region is completely unable to bind the PDE4B1 protein, based on the close colocalization seen in previous data, it might indicate that this region alone does not have sufficient binding capabilities to interact with other proteins.
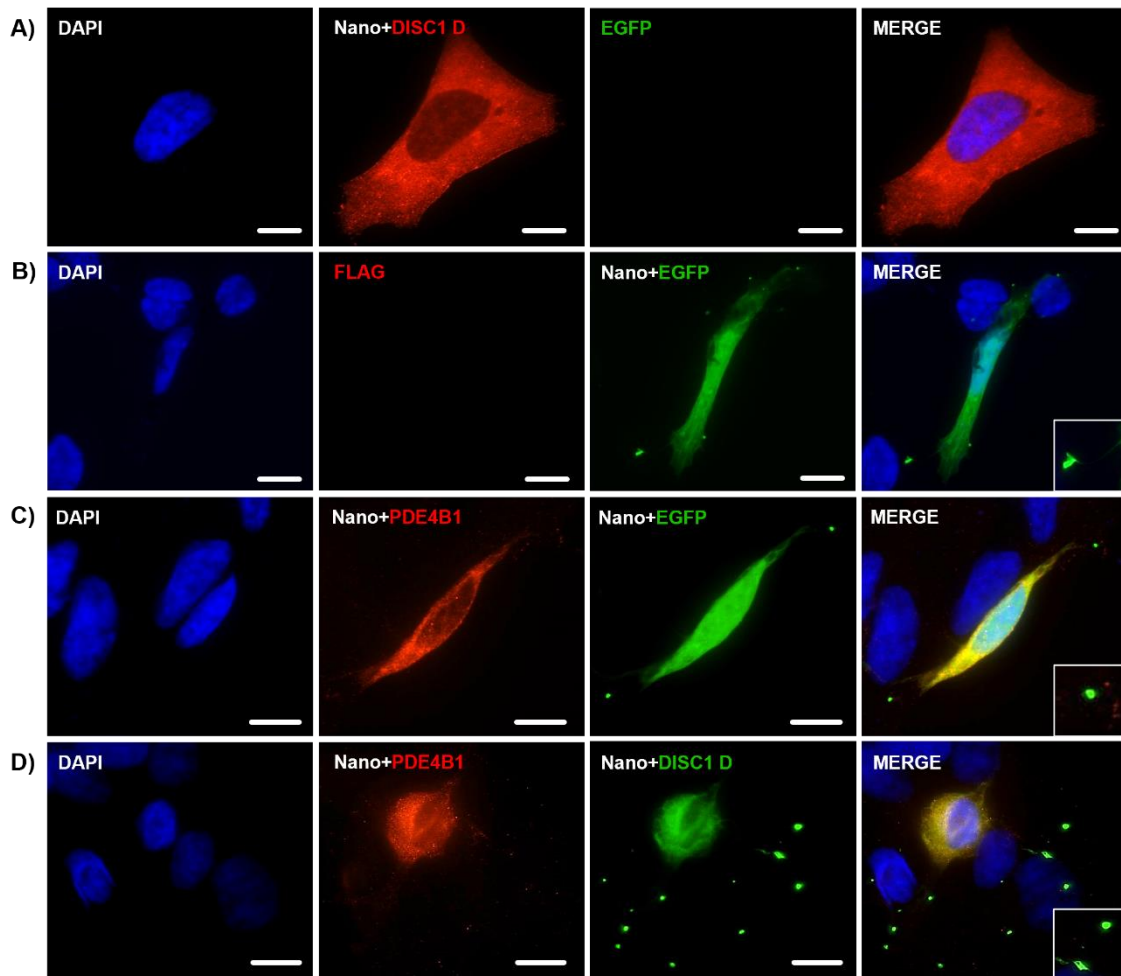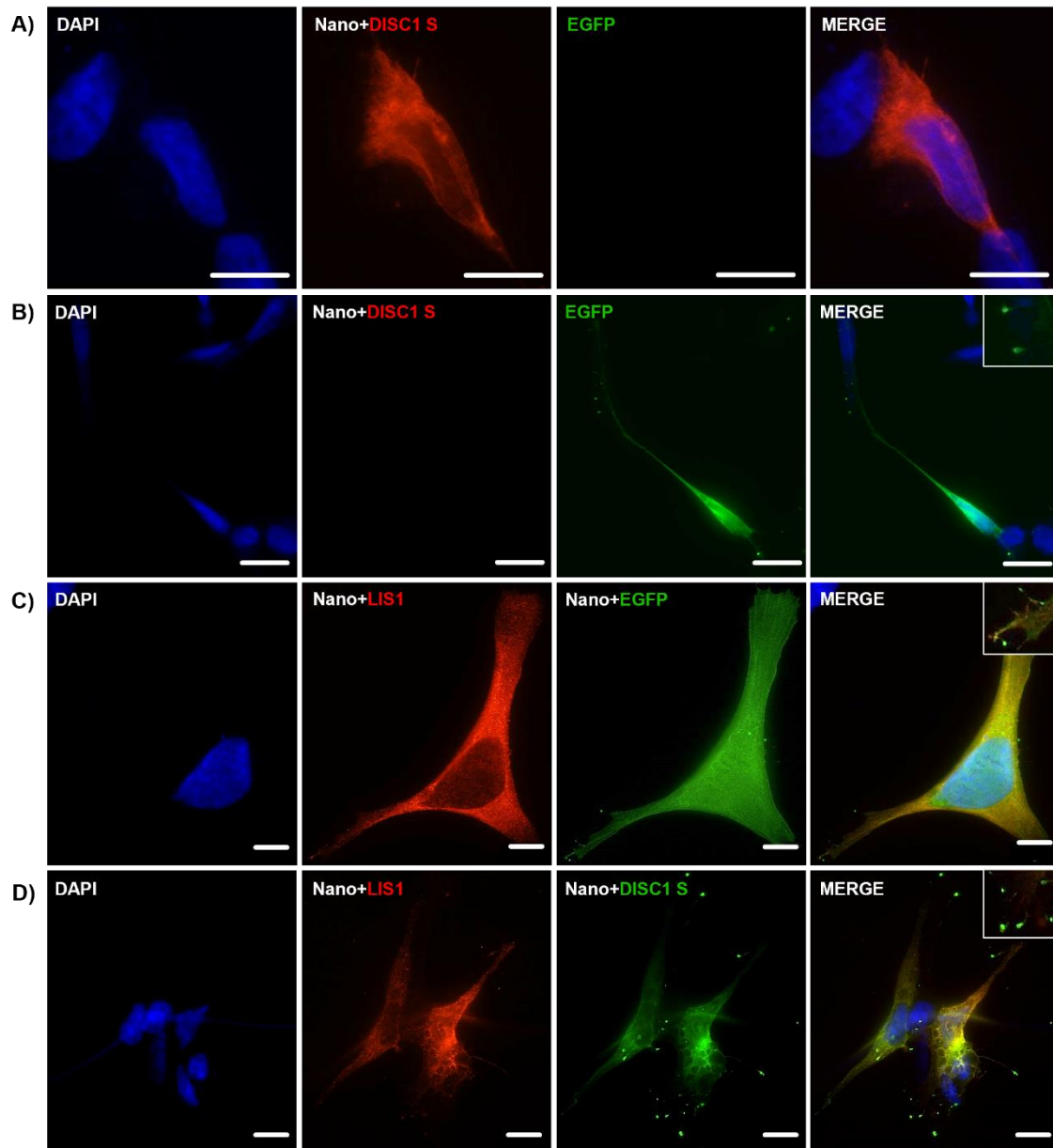
Figure 28. DISC1 D region alone is not capable of pulling PDE4B1 into filopodial tips. A) Flag-tagged DISC1 D region (red) co-transfected with the NanoTrap vector expresses solely within the cell cytoplasm. **B)** EGFP control (green) co-expressed with the NanoTrap vector expresses within the cell cytoplasm, as well as accumulates at the filopodial tips (green, enlarged). **C)** EGFP control (green) co-expressed with Flag-tagged DISC1 interaction partner PDE4B1 and the NanoTrap vector. While both PDE4B1 and EGFP control express within the cell cytoplasm, only EGFP is capable of binding to the NanoTrap vector and accumulating at the filopodial tips (green, enlarged). **D)** Co-expression of NanoTrap vector, Flag-tagged PDE4B1 (red) and EGFP-fused DISC1 D (green). While both PDE4B1 and DISC1 D express within the cell cytoplasm, only DISC1 D accumulates at the filopodial tips (green, enlarged). Text colours reflect either the red or the green channel imaged. Microscopy images are from SH-SY5Y cells, and are representative of three independent experiments. Scale bars represent 10 μm. Nano – pcDNA3.1-MYO10-HMM-Nanotrap vector, where MYO10 stands for myosin class 10 molecular motor, and HMM refers to heavy meromyosin.

4.2.3.2 DISC1 S region alone is not capable of pulling LIS1 into filopodial tips

Similar to the assessment of colocalization between the D region and PDE4B1, we also tested whether the S region is capable of binding and accumulating LIS1 at the filopodial tips. Again, several control reactions were performed first to ensure that only EGFP-fused proteins will bind to the NanoTrap motor. For these reasons, Flag-tagged S region of DISC1 was co-transfected with the NanoTrap motor, to show that S region retains its normal cytoplasmic expression in neuroblastoma cells (as previously shown in Section 4.2.1) void of signal accumulation at the filopodia (**Figure 29**, A).

In contrast, co-transfection of the NanoTrap vector with the EGFP control resulted with both the cytoplasmic expression, and the accumulation of green signal within the filopodial tips (**Figure 29**, B). When co-transfecting LIS1 and EGFP control together with the NanoTrap motor, cytoplasmic expression is seen by both LIS1 and EGFP (**Figure 29**, C), although only EGFP was able to accumulate at the tips of filopodia (**Figure 29**, C - enlarged).

Finally, the EGFP-fused S region and Flag-tagged LIS1 were co-expressed together with the NanoTrap vector (**Figure 29**, D). Again, while both constructs readily expressed within the cell cytoplasm, no joint accumulation of signal was seen at the filopodia. Instead, only the S region was travelled along the filopodia, indicating that no protein-protein interaction was happening between the said region and LIS1. Taking into consideration that the S region alone is only 103 AA long, these results might indicate that a bigger region of DISC1, or multiple regions working together, might be necessary to successfully bind interactor proteins.
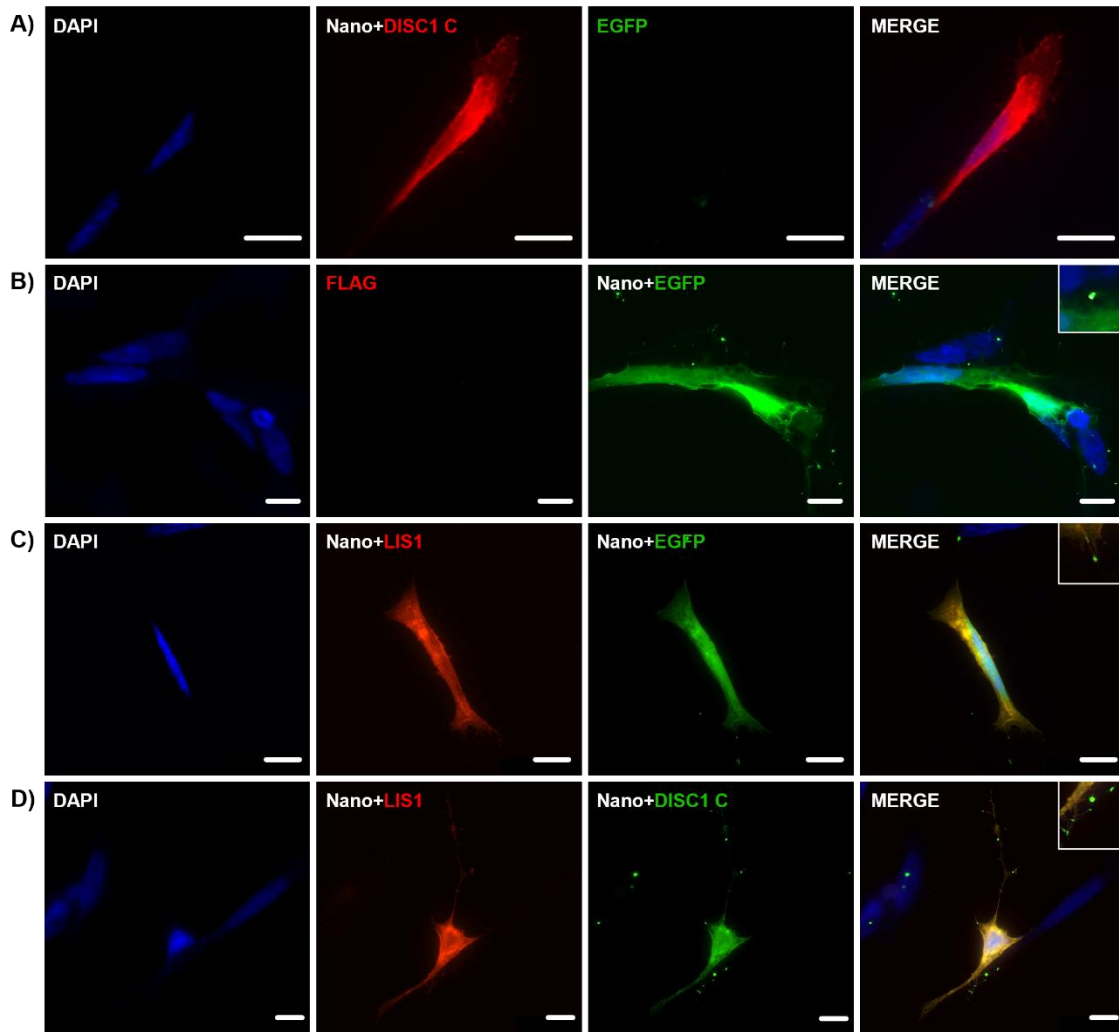
Figure 29. DISC1 S region alone is not capable of pulling LIS1 into filopodial tips.
A) Flag-tagged DISC1 S region (red) co-transfected with the NanoTrap vector expresses solely within the cell cytoplasm. **B)** EGFP control (green) co-expressed with the NanoTrap vector expresses within the cell cytoplasm, as well as accumulates at the filopodial tips (green, enlarged). **C)** EGFP control (green) co-expressed with Flag-tagged DISC1 interaction partner LIS1 and the NanoTrap vector. While both PDE4B1 and EGFP control express within the cell cytoplasm, only EGFP is capable of binding to the NanoTrap vector and accumulating at the filopodial tips (green, enlarged). **D)** Co-expression of NanoTrap vector, Flag-tagged LIS1 (red) and EGFP-fused DISC1 S (green). While both LIS1 and DISC1 S express within the cell cytoplasm, only DISC1 S accumulates at the filopodial tips (green, enlarged). Text colours reflect either the red or

the green channel imaged. Microscopy images are from SH-SY5Y cells, and are representative of three independent experiments. Scale bars represent 10 μm. Nano – pcDNA3.1-MYO10-HMM-Nanotrap vector, where MYO10 stands for myosin class 10 molecular motor, and HMM refers to heavy meromyosin.

4.2.3.3 DISC1 C region alone is not capable of pulling LIS1 into filopodial tips

Considering that LIS1 protein was shown to bind within the amino acid boundaries of both the S and the C region (**Figure 30**), we tested its interaction with the latter as well. To follow the consistency of performing control reactions within each NanoSPD assay, Flag-tagged DISC1 C region was co-transfected with the NanoTrap vector in neuroblastoma cells.

As shown in Section 4.2.2, construct encoding the C region of the protein exhibited cytoplasmic expression, with no indication of signal accumulation at the filopodial tips (**Figure 30**, A). EGFP control was co-expressed with the NanoTrap in isolation as well, exhibiting both cytoplasmic expression and the ability of travelling along the filopodia (**Figure 30**, B). Next, LIS1 was co-transfected with EGFP control and NanoTrap vector. Previous results displayed that both were equally expressed within the native cell cytoplasm, with EGFP being gathered at the filopodial tips as well (**Figure 30**, C).

Lastly, LIS1 co-expression with the EGFP DISC1 C region and NanoTrap vector (**Figure 30**, D) yielded the same results as seen with LIS1 and DISC1 S (Section 4.2.3.2). Both constructs retained cytoplasmic expression, but only EGFP-fused C region was accumulated at the filopodial ends. These results imply that the C region alone is not capable of binding LIS1, and further alternatives such as co-expression with the combination of S and C regions need to be explored.

Figure 30. DISC1 C region alone is not capable of pulling LIS1 into filopodial tips.
A) Flag-tagged DISC1 C region (red) co-transfected with the NanoTrap vector expresses solely within the cell cytoplasm. **B)** EGFP control (green) co-expressed with the NanoTrap vector expresses within the cell cytoplasm, as well as accumulates at the filopodial tips (green, enlarged). **C)** EGFP control (green) co-expressed with Flag-tagged DISC1 interaction partner LIS1 and the NanoTrap vector. While both PDE4B1 and EGFP control express within the cell cytoplasm, only EGFP is capable of binding to the NanoTrap vector and accumulating at the filopodial tips (green, enlarged). **D)** Co-expression of NanoTrap vector, Flag-tagged LIS1 (red) and EGFP-fused DISC1 C (green). While both LIS1 and DISC1 C express within the cell cytoplasm, only DISC1 C accumulates at the filopodial tips (green, enlarged). Text colours reflect either the red or the green channel imaged. Microscopy images are from SH-SY5Y cells, and are representative of three independent experiments. Scale bars represent 10 μm. Nano – pcDNA3.1-MYO10-HMM-Nanotrap vector, where MYO10 stands for myosin class 10 molecular motor, and HMM refers to heavy meromyosin.

4.2.3.4 DISC1 C region is capable of forming protein-protein interactions with NDE1

Another DISC1 interaction partner, NDE1, was investigated for its binding abilities within the C region of the protein using the NanoSPD approach. As shown in previous experiments, the assay was performed with the inclusion of all control reactions.

First reaction combines DISC1 C region in Flag with the NanoTrap vector (**Figure 31**, A), again showing that Flag-tagged constructs do not bind to the myosin motor-based vector. The following control included co-expression of EGFP and NanoTrap (**Figure 31**, B), where EGFP exhibited its ability to bind to the myosin motor-based vector, which then travelled it along the filopodia until signal accumulation at the tips. Finally, NDE1 was co-expressed with EGFP control and NanoTrap vector, where both expressed within the native cytoplasm and EGFP additionally accumulated at the filopodial ends as well (**Figure 31**, C).

Curiously, unlike in previous cases of interaction with DISC1 domains, when the construct encoding the C region fused with EGFP was introduced in place of the EGFP control, both the C region omitting the green fluorescence and NDE1 omitting the red fluorescence were seen as accumulation of yellow signal at the filopodial tips (**Figure 31**, D). Both constructs also retained their cytoplasmic expression, however accumulation of a double-signal strongly indicated that the C region is, in fact, able to act as a stable, functional region capable of interaction with NDE1 even when expressed in isolation.
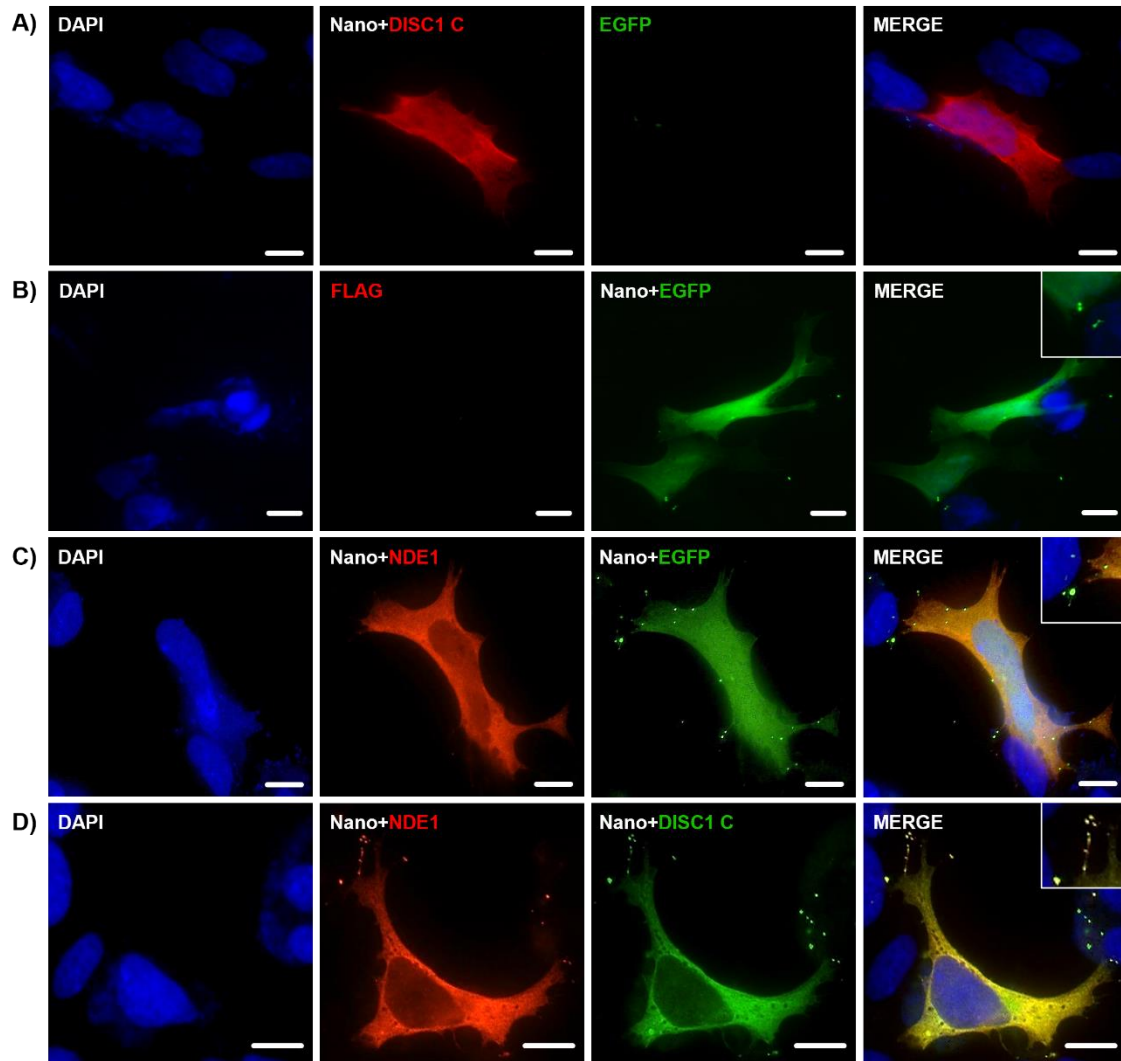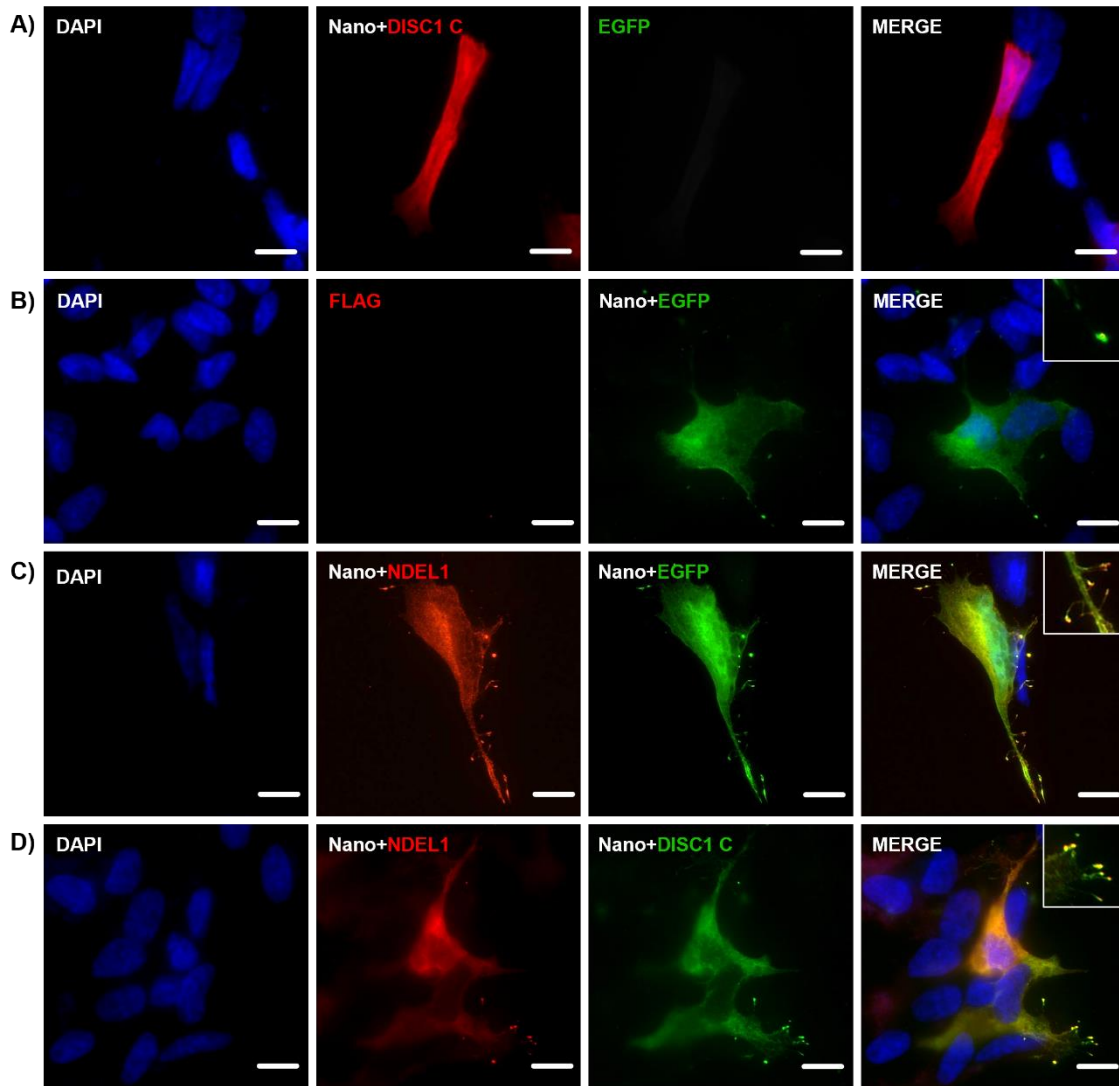
Figure 31. DISC1 C region is capable of forming protein-protein interactions with NDE1. A) Flag-tagged DISC1 C region (red) co-transfected with the NanoTrap vector expresses solely within the cell cytoplasm. **B)** EGFP control (green) co-expressed with the NanoTrap vector expresses within the cell cytoplasm, as well as accumulates at the filopodial tips (green, enlarged).**C)** EGFP control (green) co-expressed with Flag-tagged DISC1 interaction partner NDE1 and the NanoTrap vector. While both NDE1 and EGFP control express within the cell cytoplasm, only EGFP is capable of binding to the NanoTrap vector and accumulating at the filopodial tips (green, enlarged). **D)** Co-expression of NanoTrap vector, Flag-tagged NDE1 (red) and EGFP-fused DISC1 C (green). NDE1 binds to the C region of DISC1, and both constructs are then travelled along the filopodia, resulting in accumulating yellow signal at the filopodial tips (enlarged, yellow). Text colours reflect either the red or the green channel imaged. Microscopy images are from SH-SY5Y cells, and are representative of three independent experiments. Scale bars represent 10 μm. Nano – pcDNA3.1-MYO10-HMM-Nanotrap vector, where MYO10 stands for myosin class 10 molecular motor, and HMM refers to heavy meromyosin.

135

4.2.3.5 DISC1 C region is capable of forming protein-protein interactions with NDEL1

A NDE1 paralogue, NDEL1, was also studied for its binding abilities within the C region of the DISC1 protein. Much like in the case of its paralogue, control reactions previously described in detail were performed to assure consistency across all experiments.

As such, Flag-tagged DISC1 region (**Figure 32**, A), EGFP control (**Figure 32**, B) as well as the EGFP control and Flag-tagged NDEL1 (**Figure 32**, C) were all co-expressed with the NanoTrap vector, where all constructs showed cytoplasmic expression. However, while co-expressing EGFP control in the absence of NDEL1 predictably resulted in EGFP accumulation at the filopodial ends, the following control reaction including both EGFP control and NDE1 resulted in the accumulation of both signals (**Figure 32**, C - enlarged).

Unexpectedly, NDEL1 exhibited an interesting ability to travel along the filopodia even in the absence of DISC1 region. Considering that none of the other interaction partners showed any binding affinity towards EGFP, a question remains whether NDEL1 was able to bind to the sections of myosin found in the NanoTrap motor itself. As such, a role of NDEL1 in intracellular trafficking by myosin motors requires further exploration.

Lastly, NDEL1 was co-expressed with DISC1 C and NanoTrap vector, in which both NDEL1 and the C region were seen accumulated at the filopodial tips in the form of a strong yellow signal, suggesting that NDEL1 can also potentially form interactions with the C region, much like its paralogue NDE1 (**Figure 32**, D). However, considering that NDEL1 has also been seen to interact either with the NanoTrap vector, or the EGFP, further confirmation of this result is needed.

Figure 32. DISC1 C region is capable of forming protein-protein interactions with NDEL1. A) Flag-tagged DISC1 C region (red) co-transfected with the NanoTrap vector expresses solely within the cell cytoplasm. **B)** EGFP control (green) co-expressed with the NanoTrap vector expresses within the cell cytoplasm, as well as accumulates at the filopodial tips (green, enlarged).**C)** EGFP control (green) co-expressed with Flag-tagged DISC1 interaction partner NDEL1 and the NanoTrap vector. While also showing cytoplasmic expression, both NDEL1 and EGFP seem to be capable of binding to the NanoTrap vector and accumulating at the filopodial tips (yellow, enlarged). **D)** Co-expression of NanoTrap vector, Flag-tagged NDEL1 (red) and EGFP-fused DISC1 C (green). Both NDEL1 and DISC1 C are accumulated at the filopodial tips, suggesting interaction (enlarged, yellow). Text colours reflect either the red or the green channel imaged. Microscopy images are from SH-SY5Y cells, and are representative of three independent experiments. Scale bars represent 10 μm. Nano – pcDNA3.1-MYO10-HMM-Nanotrap vector, where MYO10 stands for myosin class 10 molecular motor, and HMM refers to heavy meromyosin.

4.3 DISC1 aggregation

4.3.1 Some combinations of DISC1 regions are capable of aggregate formation

As previously described, full length DISC1 protein formed clear cytoplasmic aggregates when expressed in SH-SY5Y cells (**Figure 33**, A). In contrast, the four structured regions showed exclusively cytoplasmic expression without any indication of aggregate formation when expressed under the same conditions, as described in Section 4.2.1. This indicates that none of these structured regions, nor the N-terminal section of the protein, is capable of inducing aggregation. Considering these results, we next investigated whether different combinations of these regions may form aggregates. Thus, constructs spanning the pairs of neighbouring domains (D and I, I and S, S and C, respectively), as well as the combination of all C-terminal domains (I, S and C) were cloned and expressed in neuroblastoma cells. Curiously, while neither the combination of regions I and S (**Figure 33**, B), nor S and C (**Figure 33**, C) resulted in aggregation, the combination of all three regions (**Figure 33**, D) did show consistent propensity for aggregation throughout multiple experiments.

Alongside the combination of all three C-terminal regions, another combination was found to form cytoplasmic aggregates. A construct encoding both the D and I regions, along with the uncharacterised region linking the two, demonstrated consistent aggregation when overexpressed in cells (**Figure 33**, E).

Cytoplasmic aggregates were also found present in a construct spanning the D region and extending to a known Scottish translocation breakpoint in the middle of the I region (AA 597), that segregates with high incidence of CMIs (**Figure 33**, F). It is therefore indicated that DISC1 can aggregate through at least two distinct mechanisms, one based on the central part of the protein, and one based on its C-terminal section.
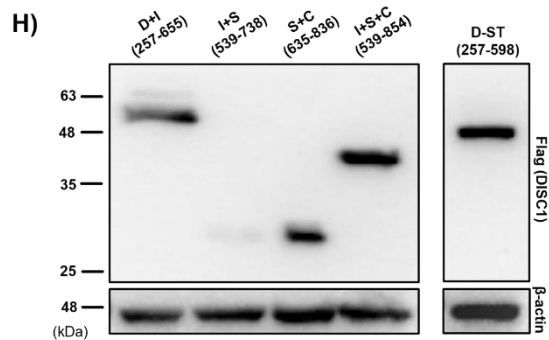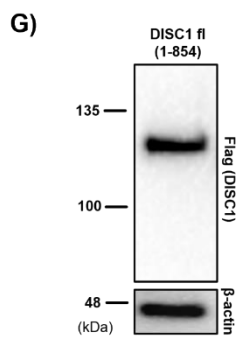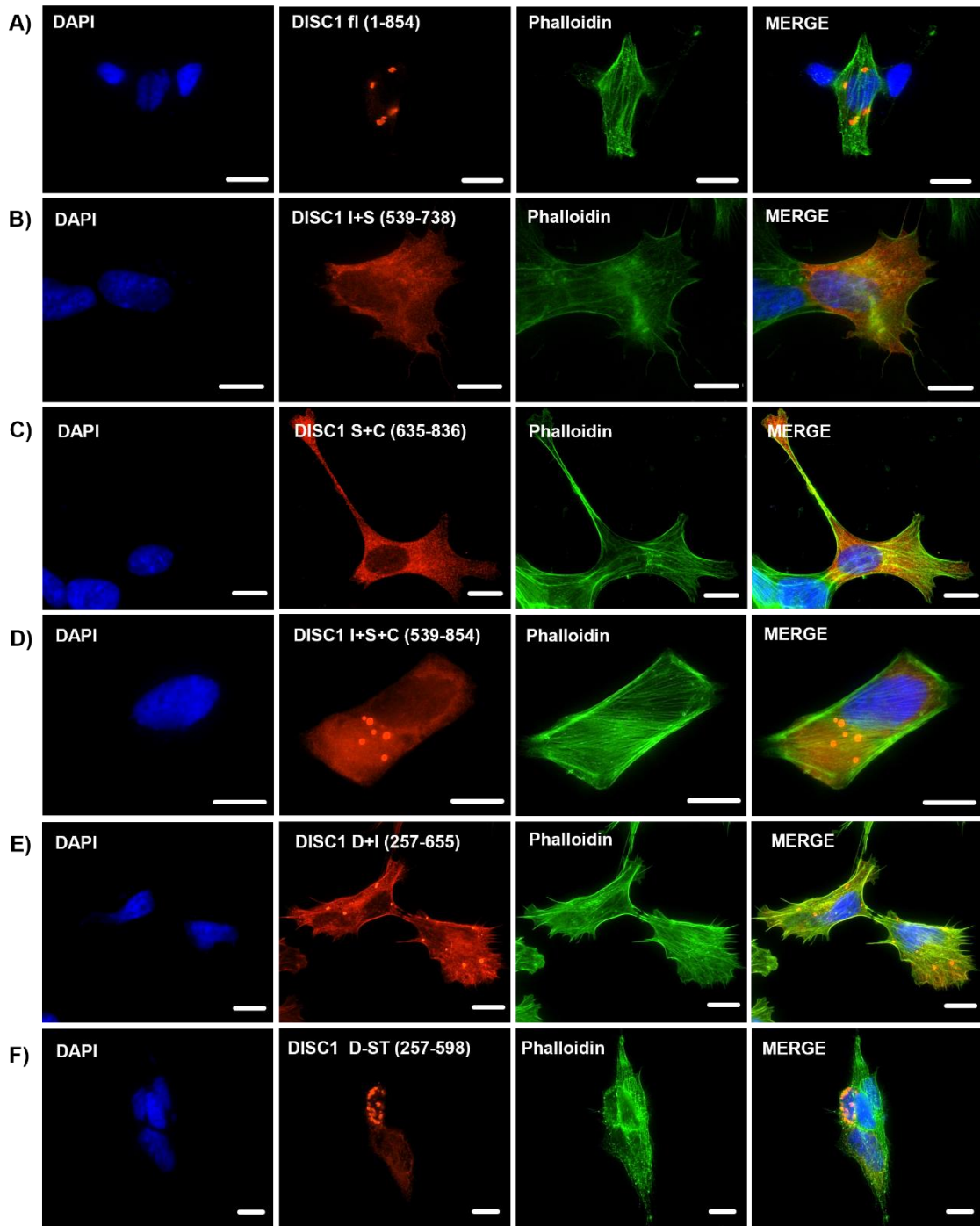
A)
| DAPI | DISC1 fl (1-854) | Phalloidin | MERGE |

B)
| DAPI | DISC1 I+S (539-738) | Phalloidin | MERGE |

C)
| DAPI | DISC1 S+C (635-836) | Phalloidin | MERGE |

D)
| DAPI | DISC1 I+S+C (539-854) | Phalloidin | MERGE |

E)
| DAPI | DISC1 D+I (257-655) | Phalloidin | MERGE |

F)
| DAPI | DISC1 D-ST (257-598) | Phalloidin | MERGE |

G) DISC1 fl (1-854)

135 —
100 —
48 —
(kDa)

Flag (DISC1)
β-actin

H)
D+I (257-655) I+S (539-738) S+C (635-836) I+S+C (539-854) D-ST (257-598)

63 —
48 —
35 —
25 —
48 —
(kDa)

Flag (DISC1)
β-actin

139

Figure 33. Some combinations of DISC1 regions are capable of aggregate formation. A) Full length DISC1 protein forms cytoplasmic aggregates when expressed in neuroblastoma cells. **B)** A DISC1 construct encoding the I and S regions does not readily aggregate when expressed. **C)** A DISC1 construct encoding for the S and C regions does not readily aggregate when expressed. **D)** A DISC1 construct encoding the I, S and C regions shows consistent aggregation propensity when expressed. **E)** A DISC1 construct encoding the D and I regions, together with the linker region between them, shows consistent aggregation propensity when expressed. **F)** A DISC1 construct spanning the D region and terminated in the middle of the I region, at the Scottish translocation (ST) breakpoint, shows consistent aggregation propensity when expressed. **G)** Confirmation of full length DISC1 expression by Western blot, with β-actin protein levels used as a loading control. **H)** Confirmation of construct expression by Western blot, with β-actin protein levels used as a loading control. All DISC1 constructs shown here are Flag-tagged and visualised using an anti-Flag antibody. Amino acid boundaries of each construct are indicated next to, or below the corresponding construct. Cytoskeleton was visualised using Acti-stain 488 (Phalloidin). Western blots were performed using HEK293 cell lysates. Microscopy images are from SH-SY5Y cells, and are representative of three independent experiments. Scale bars represent 10 μm.

4.3.2 Simultaneous transfection of multiple DISC1 regions does not result in co-aggregation

Previous work performed by our collaborators (Cukkemane et al., 2021), demonstrated the ability of the C region to form β-fibrils in the bacterial system. To test whether the aggregation of the construct encoding all three C-terminal regions is a result of the C region recruiting other regions, or their combinations, into aggregates, we co-expressed them together with appropriate single transfection controls in mammalian cells (**Figure 34**, A-E).

Interestingly, while co-expressing C with either the I region alone (**Figure 34**, F), or in combination with S (**Figure 34**, H), resulted in poor expression of the latter two, the C region did colocalise with both the S region alone (**Figure 34**, G), and with a combination of I, S and C (**Figure 34**, I). Notably, co-expression of the C region with a combination of I, S and C did not result in aggregation, despite of I, S and C showing a strong aggregation propensity when expressed alone (**Figure 34**, E).
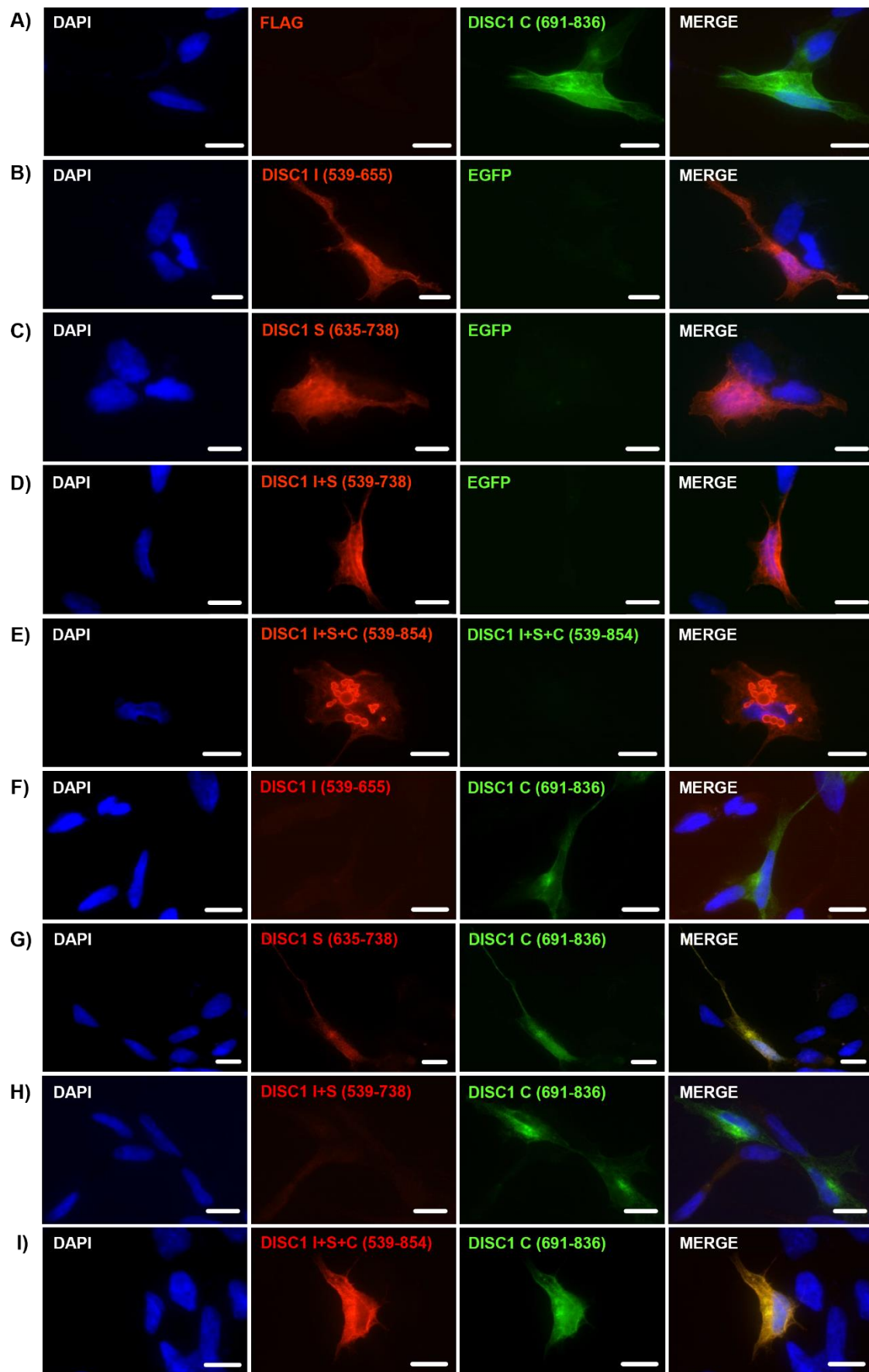
Figure 34. C region does not recruit other C-terminal, nor their combinations, into aggregates. When expressed in isolation, neither the C region **(A)**, I region **(B)** nor S region **(C)** form aggregates. **D)** A construct encoding both the I and S regions does not aggregate. **E)** A construct encoding a combination of I, S and C regions forms clear cytoplasmic aggregates. **F)** Co-expression of a construct encoding the C region and one encoding the I region does not show propensity to aggregate, although signal strength of the I region is very weak. **G)** Co-expression of a construct encoding the C region and one encoding the S region does not show propensity to aggregate, although the constructs do colocalise. **H)** Co-expression of a construct encoding the C region and one encoding both the I and S region does not show propensity to aggregate, although signal strength of the I+S region construct is very weak. **I)** Co-expression of a construct encoding the C region and one encoding the I, S and C regions combined does not show aggregation propensity, although the constructs do colocalise. In all images, proteins listed in green are fused to EGFP, while proteins listed in red are Flag-tagged. Amino acid boundaries of each construct are indicated next to the corresponding construct. Experiments were performed using SH-SY5Y neuroblastoma cells. Scale bars represent 10 μm.

4.3.3 The linker region of DISC1 is sufficient to induce its aggregation

Considering that neither the D region alone, nor the I region, were able to form aggregates when expressed in isolation, we hypothesized that the unstructured linker region between D and I is the one responsible for DISC1 aggregation propensity. To confirm this, we created constructs spanning the D region and linker, linker and I region and linker region only (**Figure 35**, E). When expressed, the combination of the D region and linker readily formed aggregates (**Figure 35**, A). The same could be seen for the construct encoding linker and I region (**Figure 35**, B). As expected, when expressed in isolation, the linker region has also shown significant aggregate formation. Taken together, these results strongly implicate that the linker region itself is the principal cause of DISC1 aggregation.

For further confirmation, we performed an insoluble protein purification assay by transfecting HEK293 cells with a plasmid encoding either the D region alone, its combination with linker, or the linker region alone. Following transfection, cells were lysed, and insoluble protein fractions were purified in different buffers through multiple ultracentrifugation steps. While all three protein fragments were present in the original homogenous cell lysate, both fragments containing either the linker region alone or its combination with the D region were also visible in the final insoluble fraction (**Figure 35**, F). In contrast, the D region alone was not present in the purified insoluble fraction

(**Figure 35**, F). Considering that protein aggregates usually have significantly higher degree of insolubility than their correctly folded counterparts, these results support the hypothesis that the linker region is responsible for the aggregation propensity of DISC1.
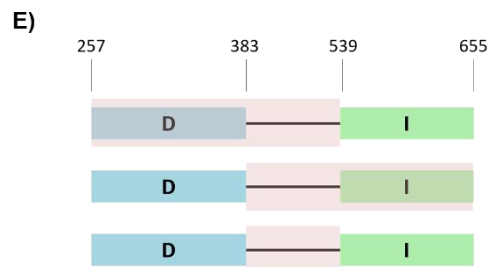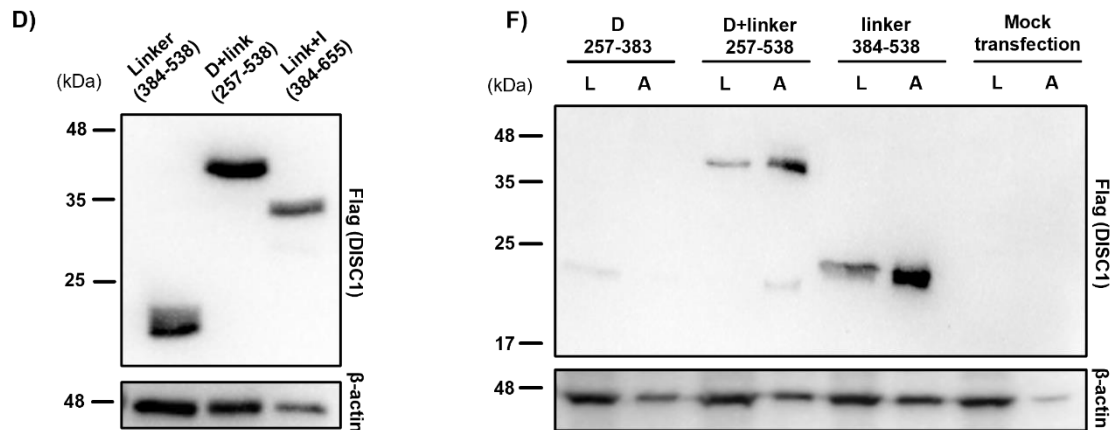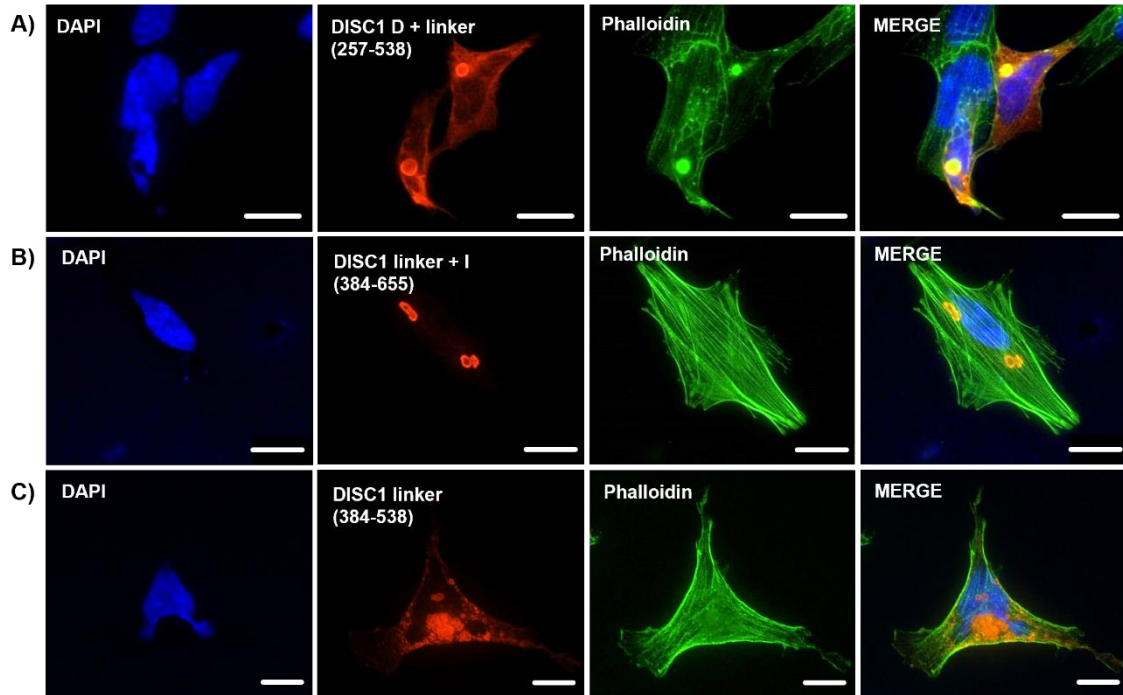
Figure 35. The linker region of DISC1 is sufficient to induce its aggregation. A) A construct consisting of the D region and linker region consistently forms cytoplasmic aggregates when expressed in neuroblastoma cells. **B)** A construct consisting of the linker region and I region consistently forms cytoplasmic aggregates when expressed in neuroblastoma cells. **C)** A construct consisting of the linker region alone consistently forms cytoplasmic aggregates when expressed. **D)** Constructs encoding the linker region alone, with or without the D or I regions, shown by Western blot. **E)** Constructs encoding the linker region alone, with or without the D or I regions, shown in schematic form. **F)** An insoluble protein purification assay, in which HEK293 cells are transfected with DISC1 constructs, lysed, and then subjected to a series of solubilisation and ultracentrifugation steps to obtain purified insoluble protein faction. All DISC1 fragments are visible in the crude cell lysates (L), while only those containing the linker region are enriched in the purified insoluble fraction, where aggregates are expected to be found (A). All DISC1 constructs shown here are Flag-tagged and visualised using an anti-Flag antibody. Cytoskeleton was visualised using Acti-stain 488 (Phalloidin). Amino acid boundaries of each construct are indicated next to, or below the corresponding construct. Western blots were performed using HEK293 cell lysates, with β-actin protein levels used as a loading control. Microscopy images are from SH-SY5Y cells, and are representative of three independent experiments. Scale bars represent 10 μm.

Interestingly, while expressing these constructs containing the linker region, a clear distinction in aggregate number, size and morphology could be seen across multiple experiments. To investigate such variability, we performed a blinded assay in which we quantified the average number of aggregates seen across random cells for each construct, including a full length DISC1, as well as the average diameter of the largest aggregate, performed across the same set of cells. Notably, shorter constructs including the linker region yielded either larger, or more numerous aggregates in contrast to full length DISC1 (**Figure 36**, A-B). The increase in the average number of aggregates was especially striking in the case of the linker region expressed alone and in combination with the I region (**Figure 36**, A). In contrast, while the combination of D region and the linker region exhibited the smallest number of aggregates per cell, the diameter of those aggregates was shown on average to be higher than the other constructs analysed (**Figure 36**, B). While the variability seen in these aggregates will require further investigation, especially in terms of morphological variety, we can assume that it likely comes as a result of these constructs lacking other regions of the protein that would otherwise bring structural stability.
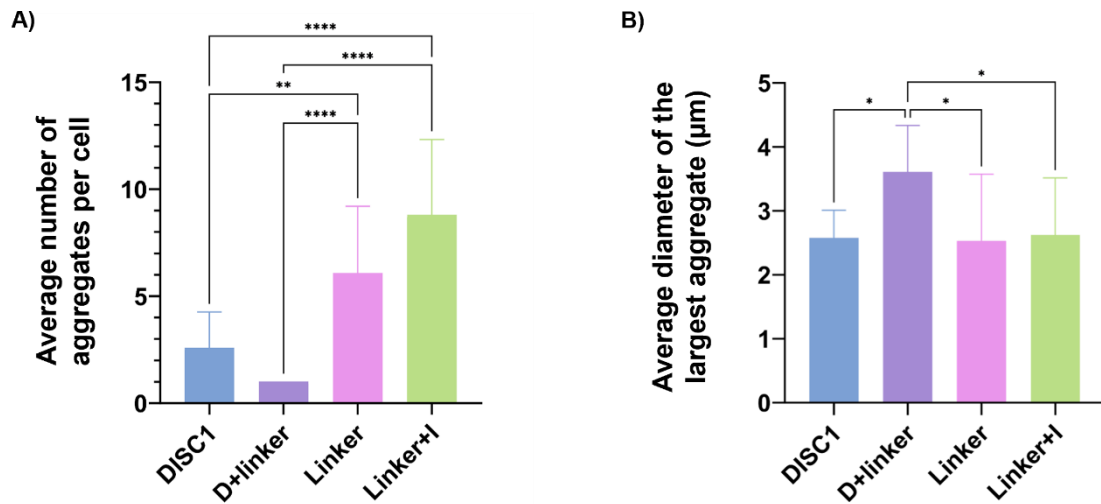
Figure 36. Constructs flanked at the linker region show variability in aggregate number and size. A) The average number of aggregates seen per cell for full length DISC1, linker region in combination with either D or I region, and linker region alone. Number of aggregates was averaged across 12 cells per construct, from four independent experiments. **B)** The average diameter of the largest aggregate seen per cell. Diameter of the largest aggregate was averaged across the same set of cells mentioned in B). Statistical significance was calculated for all possible combinations, using a one-way ANOVA, with a p value (*) < 0.05 being considered statistically significant.

4.3.3.1 An aggregation-critical region of DISC1 lies immediately C-terminal of the D region

After showing that DISC1 linker region plays a key role in DISC1 aggregation, we set to further investigate this finding by refining the said region by systematically shortening it, for the purpose of determining the exact cluster of amino acids responsible for DISC1 aggregation propensity. We cloned a number of constructs encoding the N-terminal part of the protein and terminating throughout the linker region at different lengths. First created construct encoded DISC1 from its N-terminus to the AA 383, which marks the C-terminal ESPRIT-determined boundary of the D region. From there, every subsequent construct was extended for additional 31 amino acids until the end of the region was reached, as shown in **Figure 37**, B. The linker region was similarly mapped for the C-terminal part of the protein, starting with the construct encoding AA 415 to 854, a C-terminus of DISC1. Every subsequent construct was then shortened for 31 aa at the N-terminal part until most of the region was mapped through (**Figure 37**, C).

145

The first two N-terminal constructs encoding amino acids 1-383 and 1-415 were successfully subcloned into both bacterial and mammalian expression vectors, and subsequently tested in SH-SY5Y cells. A C-terminal construct encoding amino acids 415-854 was also successfully subcloned into a bacterial expression vector and was later used to create a full length DISC1 construct, with a deletion in the linker region. As the results were obtained using these constructs, obtaining the others was not necessary.
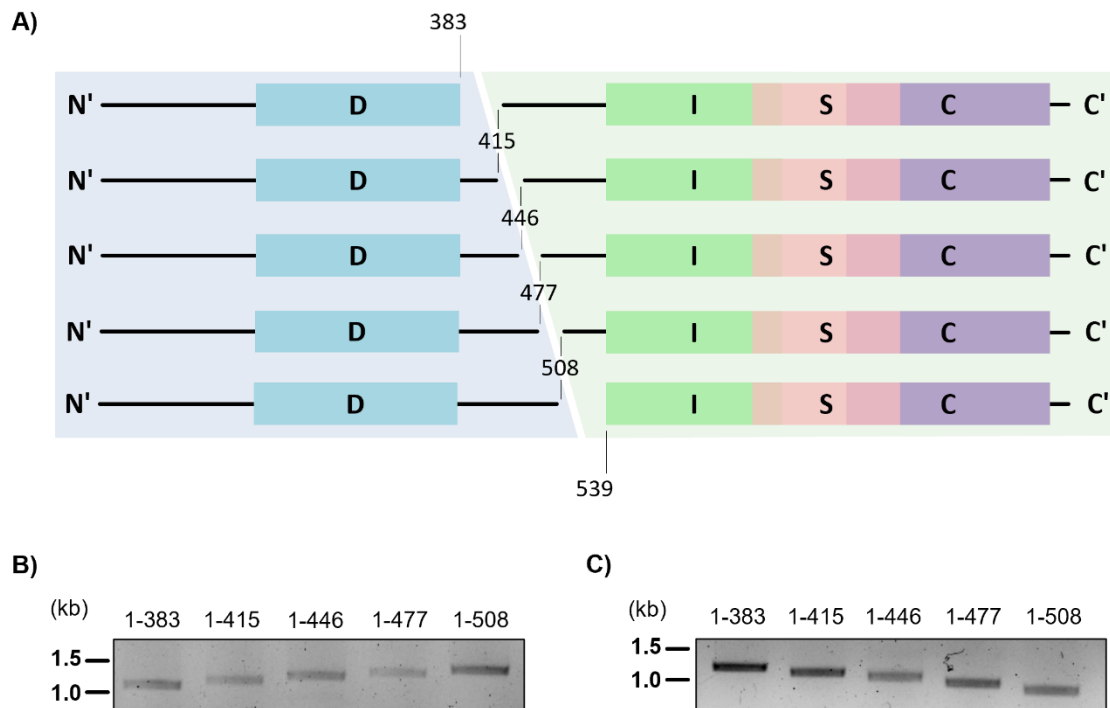

Figure 37. Refining the aggregating linker region of DISC1. A) Schematic representation of the constructs created for the purpose of mapping the DISC1 linker region and its aggregation properties. N-terminal constructs (left, in blue) were designed to map the linker region by spanning the N-terminus plus the D region, and terminating at a 31 AA distance from each other, starting with AA 383. C-terminal constructs (right, in green) were created to span the different lengths of the linker region and terminate at the C-terminal end of the protein. Starting at AA 415, every subsequent construct was shortened for additional 31 AA until the beginning of the I region was reached, at AA 539. **B)** DNA fragments of C-terminal truncations of the linker region, visualised on 1% agarose gel. **C)** DNA fragments of N-terminal truncations of the linker region, visualised on 1% agarose gel.

146

When expressed in cells, as expected, a construct ending at the classic C-terminal end of the D region (AA 1-383) did not form aggregates (**Figure 38**, A). In a striking contrast, a construct ending 32 amino acids later showed obvious aggregation propensity (**Figure 38**, B). While this finding might indicate that the short 32 AA sequence of the linker region is sufficient to cause DISC1 aggregation, further investigation was necessary to confirm this claim.
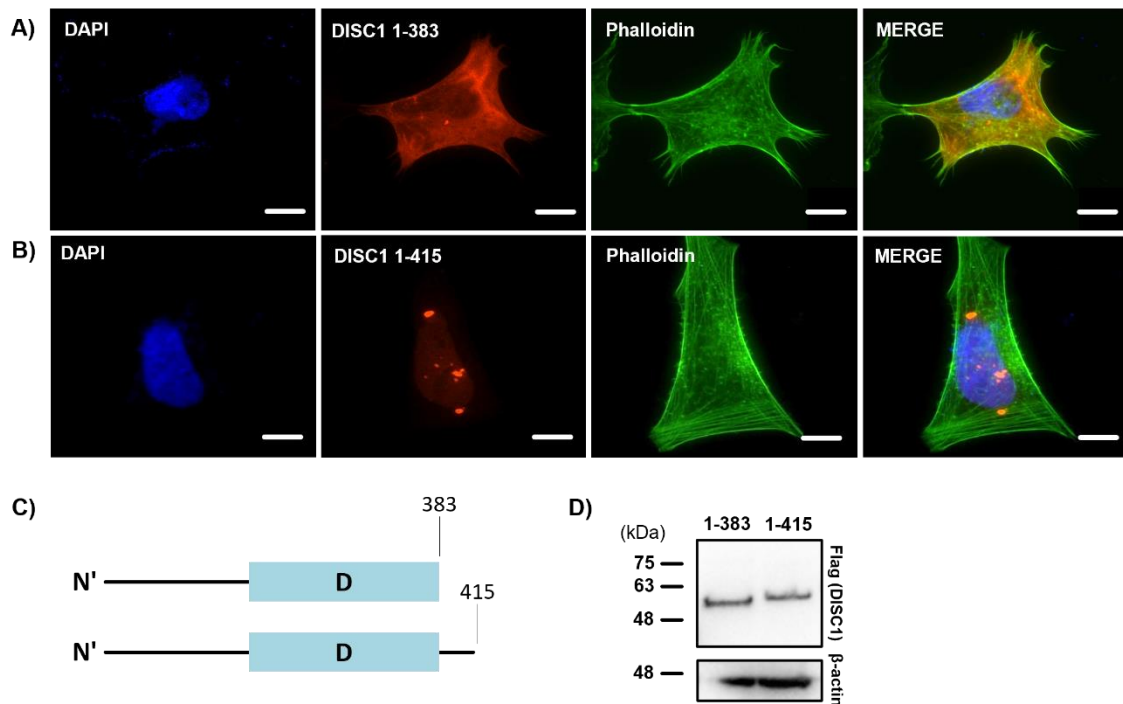

Figure 38. An aggregation-critical region of DISC1 lies immediately C-terminal of the D region. A) DISC1 construct encoding the N-terminal part of the protein, and the D region does not cause aggregation when expressed. **B)** DISC1 construct encoding the N-terminal part of the protein and terminating 32 AA after the end of D region shows aggregation propensity when expressed. **C)** Schematic representation of the constructs used in this experiment. **D)** Confirmation of construct expression by Western blot. All DISC1 constructs shown here are Flag-tagged and visualised using an anti-Flag antibody. Cytoskeleton was visualised using Acti-stain 488 (Phalloidin). Amino acid boundaries of each construct are indicated next to, or below the corresponding construct. Western blots were performed using HEK293 cell lysates, with β-actin protein levels used as a loading control. Microscopy images are from SH-SY5Y cells, and are representative of three independent experiments. Scale bars represent 10 μm.

4.3.4 Deleting a part of the linker region abolishes the aggregation propensity of DISC1

To confirm that the short, 32 amino acid cluster in the N-terminus of the linker region is indeed a key for DISC1 aggregation, we generated a full length DISC1 construct with a deletion in this part of the protein. A previously mentioned N-terminal truncation clone spanning amino acids 415-854 was ligated to a C-terminal truncation terminating at the end of the D region (AA 1-383), thus creating a full-length construct missing the amino acid cluster thought to be the driving force of DISC1 aggregation (DISC1 fl (Δ384-415)). Following the full-length variant, we also generated a couple of C-terminally truncated constructs missing this region (DISC1 1-836 (Δ384-415) and DISC1 1-655 (Δ384-415), respectively), to confirm that the C-terminal part of the protein does not affect the aggregation seen in the linker region. Based on the previously collected data, we hypothesized that by deleting the 32 AA within the linker region, we will successfully abolish DISC1 aggregation.

To confirm our hypothesis, a construct encoding the entirety of DISC1, except for AA 384-415, was expressed in SH-SY5Y neuronal cells (**Figure 39**, A). Strikingly, this construct indeed consistently failed to aggregate, as did the rest of the C-terminally truncated constructs lacking this region (**Figure 39**, B-C, E), while full length DISC1 continued to form aggregates under the same circumstances (**Figure 39**, D). With these results, we fully confirmed that this part of the linker region is indeed a driving force behind DISC1 aggregation.
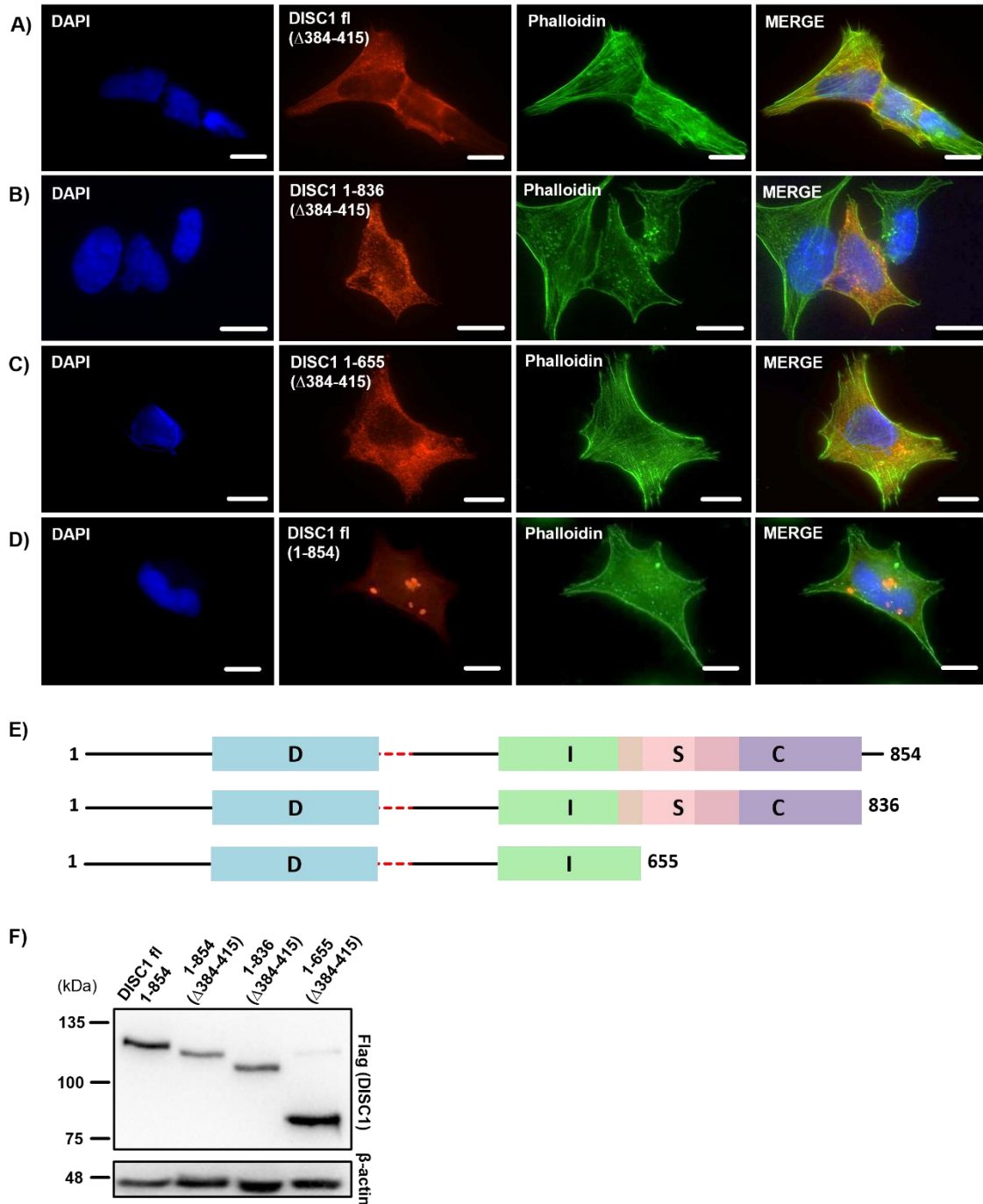
Figure 39. Deleting a part of the linker region abolishes the aggregation propensity of DISC1. A) Full length DISC1 construct missing the first 32 amino acids of the linker region does not readily form aggregates. **B)** Full length DISC1 construct missing the first 32 amino acids of the linker region and a sequence following the C region does not readily form aggregates. **C)** DISC1 construct truncated at the end of the I region and missing the first 32 amino acids of the linker region does not readily form aggregates. **D)** Full length DISC1 construct retains its aggregation propensity. **E)** Schematic representation of the

149

constructs used in this experiment. **D)** Confirmation of construct expression by Western blot. All DISC1 constructs shown here are Flag-tagged and visualised using an anti-Flag antibody. Cytoskeleton was visualised using Acti-stain 488 (Phalloidin). Amino acid boundaries of each construct are indicated next to, or below the corresponding construct. Western blots were performed using HEK293 cell lysates, with β-actin protein levels used as a loading control. Microscopy images are from SH-SY5Y cells, and are representative of three independent experiments. Scale bars represent 10 μm.

4.3.5 Assessing aggregating potential of the linker region using online prediction tools

Having identified a region required for aggregation, we next wanted to investigate how this might function by assessing the aggregating potential of the linker region. For this purpose we employed five different online prediction tools: AGGRESCAN (Conchillo-Solé et al., 2007) (**Figure 40**, A), TANGO (Fernandez-Escamilla et al., 2004; Linding et al., 2004; Rousseau et al., 2006) (**Figure 40**, B, C), FoldAmyloid (Garbuzynskiy et al., 2010) (Figure , D), MetAmyl (Emily et al., 2013) (**Figure 40**, E), and ANuPP (Prabakaran et al., 2021) (**Figure 40**, F). These tools were designed to predict the propensity of the protein to either form aggregates or amyloids, or both, based on the protein sequence. Interestingly, while most predictions done throughout the employment of these tools yielded similar results, showing aggregation/amyloid formation hotspots dispersed throughout the entirety of the protein sequence (**Figure 40**, A-E; **Figure 41**, B), ANuPP most strongly implicated the aggregation within the linker region (**Figure 40**, F). Specifically, this tool is used to predict regions of the protein most likely to be involved in aggregate nucleation by considering atomic-level features of hexapeptides (Prabakaran et al., 2021). It suggested that AA 387-395 and AA 400-415 have the highest nucleation capacity within the protein (**Figure 41**, C). These predictions complement our findings stating that deleting AA 384-315 of DISC1 is sufficient to abolish its aggregation propensity.

It is also notable that the linker region is rich in glutamine residues, which can be involved in aggregation. Moreover, the linker region contains an abundance of charged amino acids, which would make it prone to forming protein complexes (**Figure 41**, C).
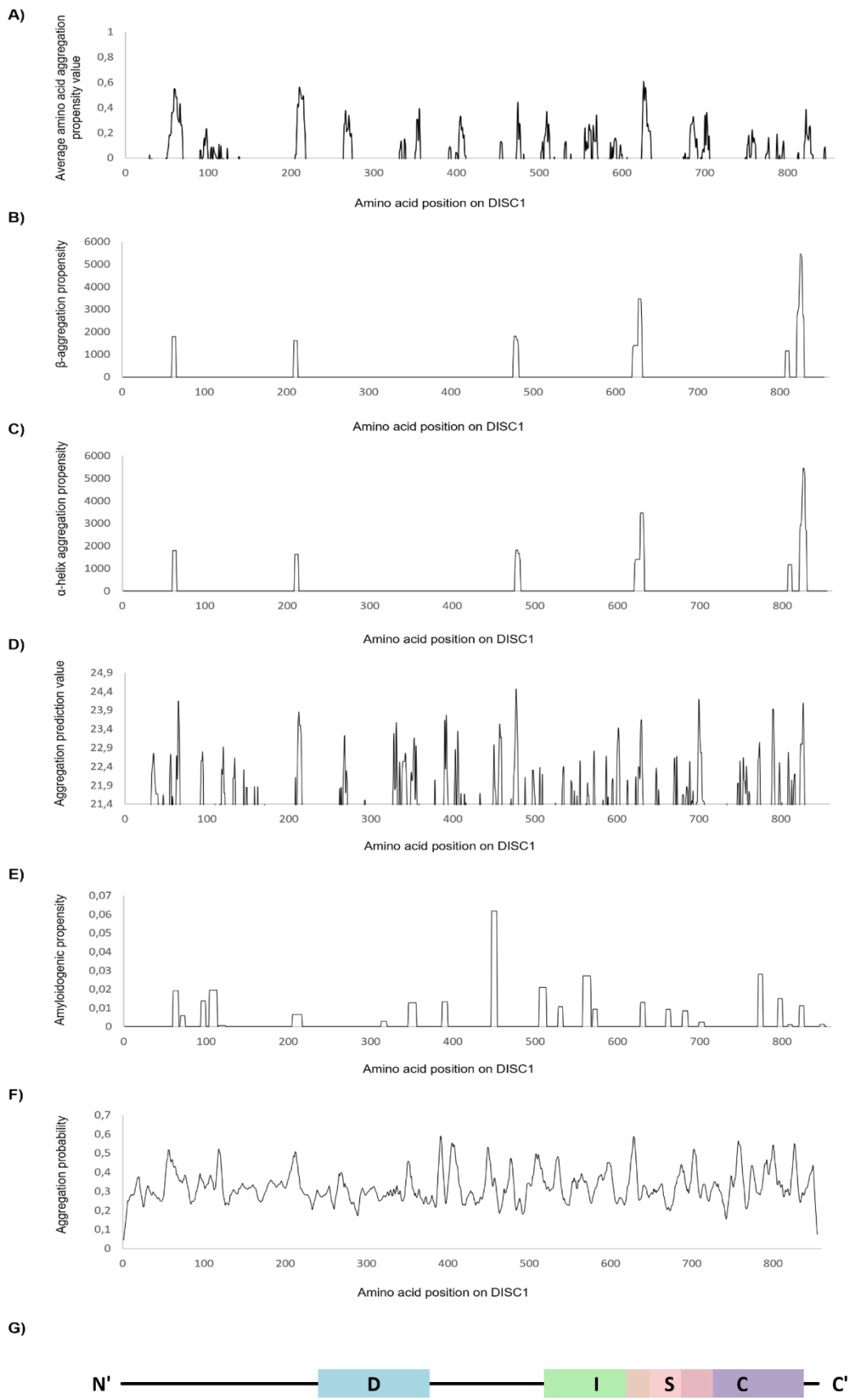
Figure 40. Sequence analysis of DISC1 sequence and its aggregation and/or amyloid formation propensity. A) Graph showing average amino acid aggregation propensity value for each amino acid in DISC1 sequence, calculated using AGGRESCAN online tool. **B)** Graph showing β-aggregation propensity of each amino acid in DISC1 sequence, calculated using TANGO online tool. **C)** Graph showing α-helix aggregation propensity of each amino acid in DISC1 sequence, calculated using TANGO online tool. **D)** Graph showing aggregation prediction value of each amino acid in DISC1 sequence, calculated using FoldAmyloid online tool. **E)** Graph showing amyloidogenic propensity of each amino acid in DISC1 sequence, calculated using MetAmyl online tool. **F)** Graph showing aggregation probability for each amino acid in DISC1 sequence, calculated using ANuPP online tool. **G)** Structure of DISC1, drawn to scale.

A)

B)

C)

```
301   SSSSLDPSLAGCGGDGSSGSGDAHSWDTLLRKWEPVLRDCLLRNRRQMEVISLRLKLQKL   360

361   QEDAVENDDYDKAETLQQRLEDLEQEKISLHFQLPSRQPALSSFLGHLAAQVQAALRRGA   420

421   TQQASGDDTHTPLRMEPRLLEPTAQDSLHVSITRRDWLLQEKQQLQKEIEALQARMFVLE   480

481   AKDQQLRREIEEQEQQLQWQGCDLTPLVGQLSLGQLQEVSKALQDTLASAGQIPFHAEPP   540

541   ETIRSLQERIKSLNLSLKEITTKVCMSEKFCSTLRKKVNDIETQLPALLEAKMHAISGNH   600
```

Figure 41. Aggregation potential of the linker region. A) Main structure of the DISC1 protein drawn to scale. **B)** Five online prediction tools of protein aggregation and/or amyloid formation propensity were employed to analyse the amino acid sequence of DISC1. Graph shows accumulated data (**Figure 40**, A-F) from all tools that predicted aggregation at each amino acid position. **C)** Amino acid sequence of the linker region, spanning amino acids 384-528, with surrounding amino acids shown for context (grey). Glutamate residues are shown in green, while charged amino acids are shown in blue. The purple bar above amino acids indicates the region predicted by ANuPP to have aggregate nucleation potential.

153

4.4 Behavioural studies of DISC1

4.4.1 Establishing a *Drosophila* model expressing DISC1

Many biological processes have been evolutionarily conserved between vertebrates and invertebrates (Therianos et al., 1995; Reichert, 2002). As such, *Drosophila melanogaster* has been successfully used as a genetic model for studying a range of complex behaviours and their underlying molecular mechanisms, including memory (Blum et al., 2009), learning (Drain et al., 1991), locomotion (Jordan et al., 2006) and sleep (French et al., 2021). While an orthologue of *DISC1* is not present in flies, the DISC1-binding proteins are. Creating transgenic *DISC1* models that express the DISC1 protein, and analysis of resulting behavioural phenotypes can thus help in further elucidation of molecular pathways underlying schizophrenia and other mental disorders.

Targeted expression of human genes in the fly brain can be achieved through various approaches (McGuire et al., 2004), such as *Gal4*/UAS (Upstream Activating Sequence), which allows the selective activation of any cloned gene in a cell-specific manner (Brand & Perrimon, 1993) (**Figure 42**). In this thesis, we utilised the binary expressing system *Gal4*/UAS to express DISC1 pan-neuronally, using the *elav-Gal4* (Embryonic Lethal, Abnormal Vision) promoter. We used two UAS-*DISC1* lines with gene insertion either on the second or the third chromosome (*SM6a* and *TM6c*, respectively).
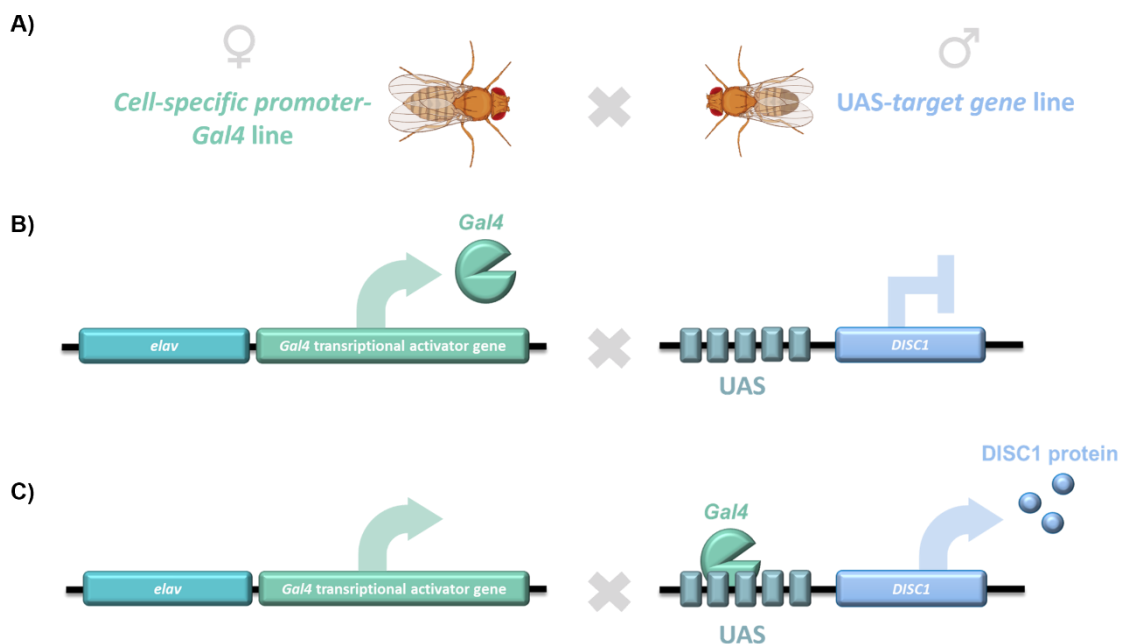
Figure 42. Schematic of the *Gal4/*UAS system used to generate DISC1-expressing progenies. A) Female flies carrying inserted *Gal4* gene and a cell specific promoter *elav* are crossed with male flies carrying the target gene subcloned behind a tandem array of five optimized *Gal4* binding sites (UAS – Upstream Activating Sequence) (Brand & Perrimon, 1993). **B)** In the absence of *Gal4*, target gene is not expressed in male flies. **C)** Crossing flies expressing *Gal4* (*elav-Gal4* line) with flies carrying the target gene (UAS-*DISC1* line) activates UAS-gene expression in progenies, in a specific cluster of cells which express *Gal4*. The effect of expression can be observed by analysing resulting phenotypes through various stages of development. Adapted from Brand and Perrimon, 1993.

4.4.2 Locomotor activity and sleep analysis

4.4.2.1 UAS-DISC1 transgenic lines express the DISC1 protein, affecting *Drosophila* climbing ability

As a preliminary assessment of locomotor activity, and an indicator of neurodegenerative processes occurring during aging, young males from the non-expressing lines containing *DISC1* gene on both chromosomes (*UAS*-DISC1-2nd and *UAS*-DISC1-3rd), as well as the *wt Canton S* control line were subjected to negative geotaxis once a week over the course of three weeks. Negative geotaxis is a term used to describe an innate escape response found in *Drosophila*, during which flies climb the cylinder walls upon being forced to the bottom, usually by a mechanical startle (Gargano et al., 2005). To evaluate climbing abilities, the percentage of flies that managed to climb above the horizontal threshold line halfway up the tube in five seconds post-startle was measured. In order to minimize variability, fifty flies per line (ten per vial) were assessed over the course of five measurements, with one-minute recuperation time between each measurement.

Surprisingly, both supposedly non-expressing transgenic lines exhibited higher locomotor activity with age, compared to the *wt* control (**Figure 43**). The highest increase in vertical climbing was seen in flies carrying the *DISC1* gene on the 3rd chromosome (*UAS*-DISC1-3rd), with more than 60% of the flies passing the threshold post-startle on both weeks 2 and 4. Compared to *wt*, the *UAS*-DISC1-2nd line displayed a more subtle increase in locomotor activity than its *UAS*-DISC1-3rd counterpart, with the highest increase measured at 4 weeks of age.
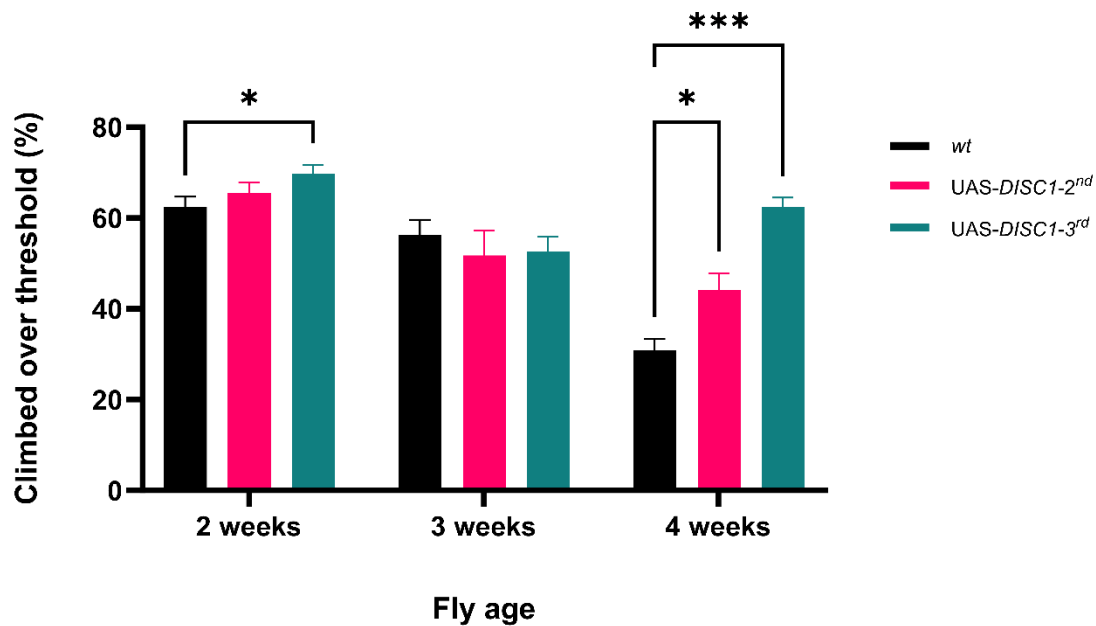
Figure 43. Flies containing non-expressing DISC1 show an increase in locomotor activities with age. A graph depicting the negative geotaxis response (a number of flies crossing the threshold 5s post-startle) of aging UAS-*DISC1* transgenic flies carrying the non-expressing DISC1 gene on the second (UAS-*DISC1-2nd*) and third (UAS-*DISC1-3rd*) chromosome, and *Canton S* wild type (*wt*) control flies. A set of 2-week-old male flies (n=50 per line) from both transgenic and *wt* control stocks was used to assess negative geotaxis response over the course of 3 weeks. The total performance across the five vials (n=10 per vial) for each fly strain was calculated as the average percentage of five consecutive measurements. Statistical analysis was performed for all possible combinations, using one-way ANOVA with Tukey post-hoc test. A *p*-value of < 0.05 was considered statistically significant (*).

While it is known that locomotor activity of flies declines with age (Ganetzky & Flanagan, 1978; Le Bourg & Lints, 1992), it was surprising to see that more than 40% of the 4 weeks-old transgenic flies managed to climb over the threshold during allocated time. Considering the altered, possibly neuroprotective behaviour of both UAS-*DISC1* lines compared to *wt* control, we hypothesized that the source of this behaviour arises either from the site of the genomic insertion, or a leaky construct displayed as background expression of DISC1 in the absence of *Gal4*. To assess whether the difference in negative geotaxis between UAS-*DISC1* transgenic flies and *wt* is due to a leaky expression of transgenic flies, a Western blot analysis was performed on samples of homogenised heads and bodies of flies (credit: Bobana Samardžija), using anti-human DISC1 antibody. Both

transgenic lines exhibited bands at ~180 kDa in flies' bodies, which corresponds to a dimeric DISC1 species also visible in the control line expressing human DISC1 (**Figure 44**). Higher expression in flies' bodies versus brains may be indicative of a higher DISC1 expression in motor neurons and ventral nerve cord (equivalent of a human spinal nerve cord), which could explain observed negative geotaxis phenotypes. Albeit weak, the UAS-*DISC1-3rd* transgenic line shows higher expression than its UAS-*DISC1-2nd* counterpart, in both heads and bodies. This is in correspondence with our negative geotaxis results, which show a protective effect of UAS-*DISC1-3rd* on age-dependent increase in negative geotaxis.
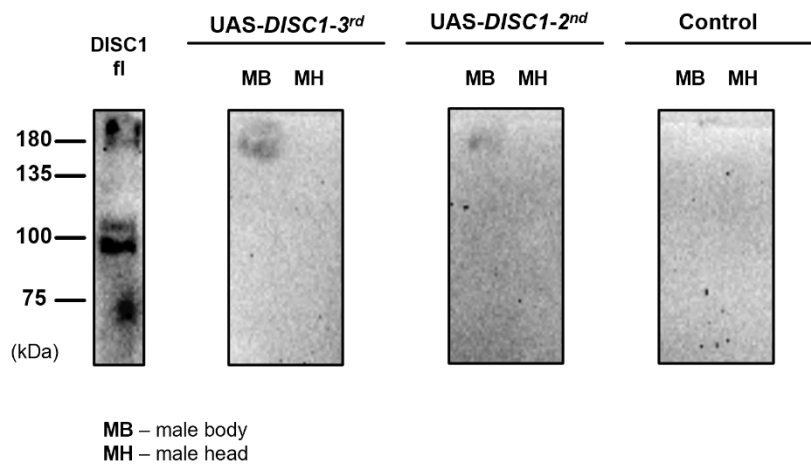
Figure 44. UAS-*DISC1* transgenic lines express the DISC1 protein. Five bodies (without heads) per fly line were used for body homogenates preparation, and twenty heads for head homogenates. Protein extraction was performed on 3-5 days old adult male flies from the mutant *wt* (wild type) control line (*Canton S*), UAS-*DISC1-2nd* and UAS-*DISC1-3rd*. Full length human DISC1 (DISC1 fl) was used as an additional control. This experiment was performed by Bobana Samardžija, to whom we offer sincere thanks.

Curiously, compared to the second chromosome, the third *Drosophila* chromosome harbours a higher number of genes corresponding to human ones that belong to the *DISC1* interaction network (Samardžija et al., 2024), suggesting that chromosomal location of gene insertion could play a significant role in *Drosophila* behaviour. Taken together, these results confirmed our previous hypothesis that transgenic UAS-*DISC1* lines, which are not expected to, do in fact express DISC1, in correlation with the changes in negative geotaxis during aging.

4.4.2.2 Expression of DISC1 affects average locomotor activity in *Drosophila*

4.4.2.2.1 *DISC1* insertion on the third chromosome affects average locomotor activity in *Drosophila*

Considering the negative geotaxis results, we have decided to measure locomotor activity of UAS-*DISC1* transgenic lines versus control lines (*wt – Canton S*, *elav-Gal4*) over the course of five days. To determine whether the activation of *DISC1* expression has an additional effect on locomotor phenotype, we facilitated *DISC1* expression pan-neuronally. This was achieved by crossing the UAS-*DISC1* with *elav-Gal4* flies, and measuring locomotor activity of the first-generation UAS>*Gal4* progenies. Locomotion was measured using the Drosophila Activity Monitoring System (DAMS), in one-minute intervals, and expressed as an average number of beam-breaks per minute over a five-day period, in L/D (light/dark) conditions (**Figure 45**, B).

Our results showed that both the leaking UAS-*DISC1-3rd* line and the corresponding UAS>*Gal4* progeny line exhibit heightened locomotor activity compared to controls. The UAS-*DISC1-3rd* line exhibited higher average 24-h activity than its *UAS>Gal4* counterpart when compared to *wt* control, but no significant difference was measured in comparison to *UAS>Gal4* line itself (**Figure 45**, A). However, both transgenic lines showed higher activity during dark hours compared to *wt* control (**Figure 45,** D-E), with UAS-*DISC1-3rd* line exhibiting higher peak activity than UAS>*Gal* (**Figure 45**, B). These results confirm our previous finding that supposedly inactivated UAS-*DISC1-3rd* line indeed produces protein, much like the UAS>*Gal4* progeny line. Our data thus presents an unexpected effect of UAS-*DISC1-3rd* on locomotor behaviour phenotype, which differs significantly from UAS>*Gal4* during the dark hours across all days.

Varying changes in overall locomotor behaviour were observed in all DISC1 transgenic flies (both UAS and UAS>*Gal4*), regardless of the gene insertion location (**Appendix I**). However, no significant difference in the activity during dark hours was observed in transgenic lines expressing DISC1 on the second chromosome (**Appendix I**). Third chromosome insertion had a stronger overall effect on the increase in locomotor activity, suggesting that gene insertion location does, in fact, play a role in behavioural phenotype. Taken together, our data indicates that DISC1 expression modulates the locomotor behaviour in *Drosophila* models.
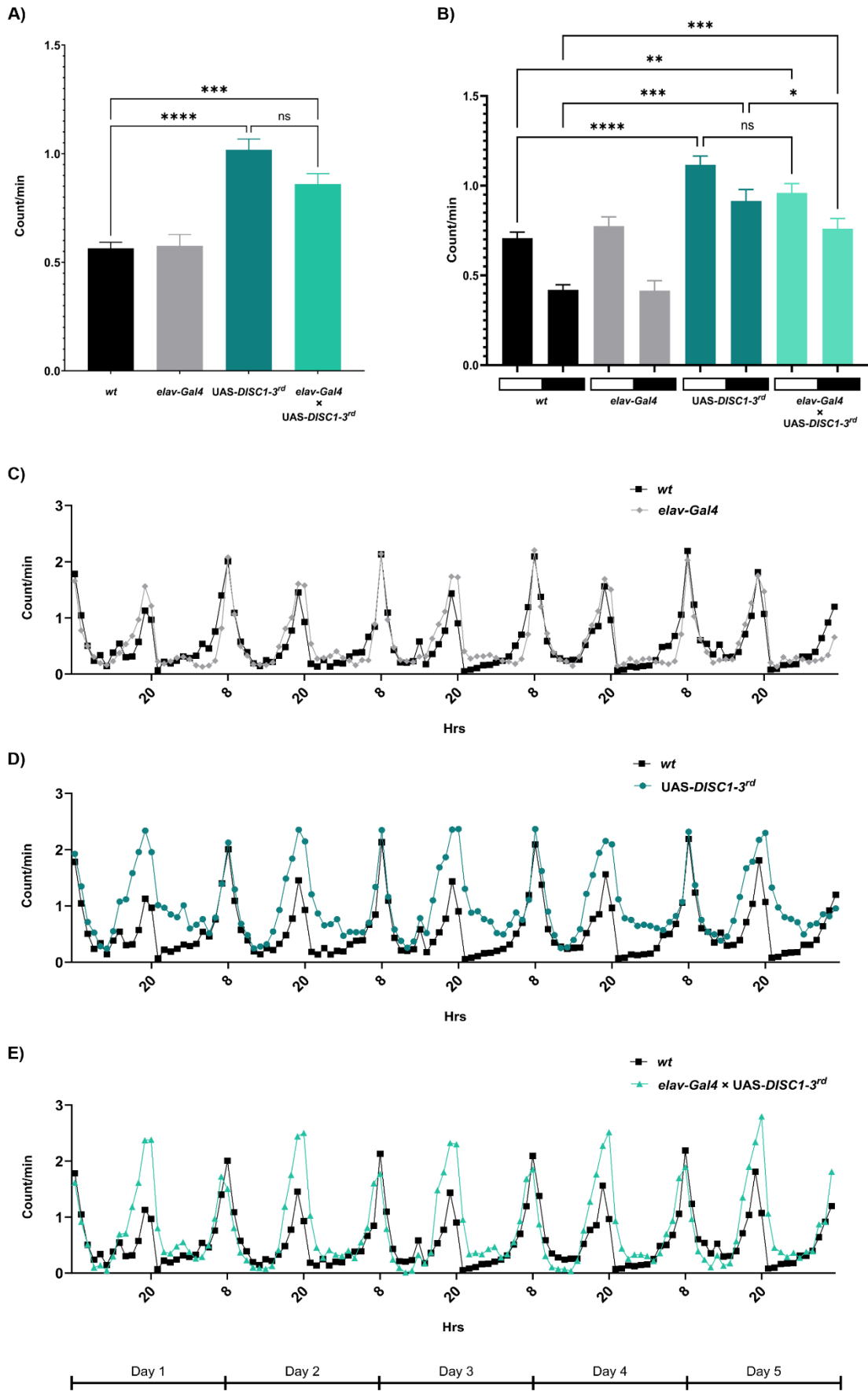
Figure 45. Increased 24-hour locomotor activity in pan-neuronal DISC1 expression line and UAS-*DISC1-3rd* control line. The average locomotor activity per minute was measured in 3-5 days old first generation male transgenic flies (UAS-*DISC1-3rd*, *elav-Gal4* × UAS-*DISC1*/*TM6c* progenies (UAS>*Gal4*)) and controls (*wt*, *elav-Gal4*) over the course of five consecutive days, in L/D (light/dark) conditions. Statistical analysis was performed on n=48 flies per line, using one-way ANOVA with Tukey post-hoc test. $p < 0.05$ = statistically significant (*); $p > 0.05$ = not significant (ns). **A)** Average 24-h locomotor activity of transgenic UAS-*DISC1-3rd* and UAS>*Gal4* versus *wt* control. **B)** Average 24-h activity of all lines, divided into 12-h L/D periods (white/black boxes). **C)** Comparison of *wt* and *elav-Gal4* controls over the 5-day period. **D)** Comparison of UAS-*DISC1-3rd* and *wt* over the 5-day period. **E)** Comparison of the UAS>*Gal4* progeny line and *wt*, over the 5-day period. *wt* – wild type line (*Canton S*); *elav-Gal4* – pan-neuronal driver line.

4.4.2.3 The amount of sleep in UAS-*DISC1* flies decreases at night, not during the day

In schizophrenia, disrupted circadian rhythms and sleep are closely related to changes in locomotor behaviour (Cosgrave et al., 2018; Waters & Manoach, 2012). Patients suffering from schizophrenia often exhibit changes in sleep latency and sleep phases, thus negatively affecting normal daily locomotor patterns (Wulff et al., 2012; Cosgrave et al., 2018). For these reasons, we also monitored sleep patterns of our DISC1 *Drosophila* models using DAMS. Our prediction, based on the results showing increased locomotor activity in DISC1-expressing fly lines, was that the amount of sleep will be decreased in flies that express DISC1 pan-neuronally.

While it is difficult to measure sleep directly in the fruit fly, rest periods that last five or more minutes have been shown empirically to represent sleep. In our study, the average amount of sleep over five consecutive days under L/D conditions was derived from the frequency of infrared beam interruptions recorded with DAMS. We measured sleep in both UAS-*DISC1* transgenic control lines with insertions on second (UAS-*DISC1-2nd*) (**Appendix II**) and third (UAS-*DISC1-3rd*) chromosome, *wt* and *elav-Gal4* controls, as well as UAS>*Gal4* progenies.

4.4.2.3.1 UAS-*DISC1-3rd* line, but not UAS>*Gal4* progenies, exhibit decrease in total sleep amount

When analysing average sleep over a 5-day period in transgenic lines carrying *DISC1* on the third chromosome, UAS-*DISC1-3rd* but not UAS>*Gal4* (*elav-Gal4* × UAS-*DISC1-3rd*) progenies showed a statistically significant drop in the amount of sleep compared to the *wt* (*Canton S*) control (**Figure 46**, A).

In correspondence with our previous results measuring locomotor activity, rest periods measured in UAS-*DISC1* flies were significantly shorter than in *wt* controls, especially during the dark hours (**Figure 46,** B, D). This finding supports our hypothesis that pan-neuronal DISC1 expression results in a decrease of sleep amount in *Drosophila*. In contrast, the UAS>*Gal4* progenies exhibited no significant difference in the amount of sleep compared to *wt*, in both L and D conditions (**Figure 46,** B, E), indicating that crossing the flies to activate targeted gene expression to does not result in a higher expression compared to the UAS-*DISC1* line. Similar results were seen in flies with *DISC1* insertion on the second chromosome, albeit to a lesser extent (**Appendix II**).

Taken together, these findings support the role of DISC1 in sleep-related disturbances shown in previous studies (Furukubo-Tokunaga et al., 2016; Sawamura et al., 2008). However, more research is needed to elucidate the stronger effects of the UAS-*DISC1-3rd* line compared to the corresponding UAS>*Gal4* line.
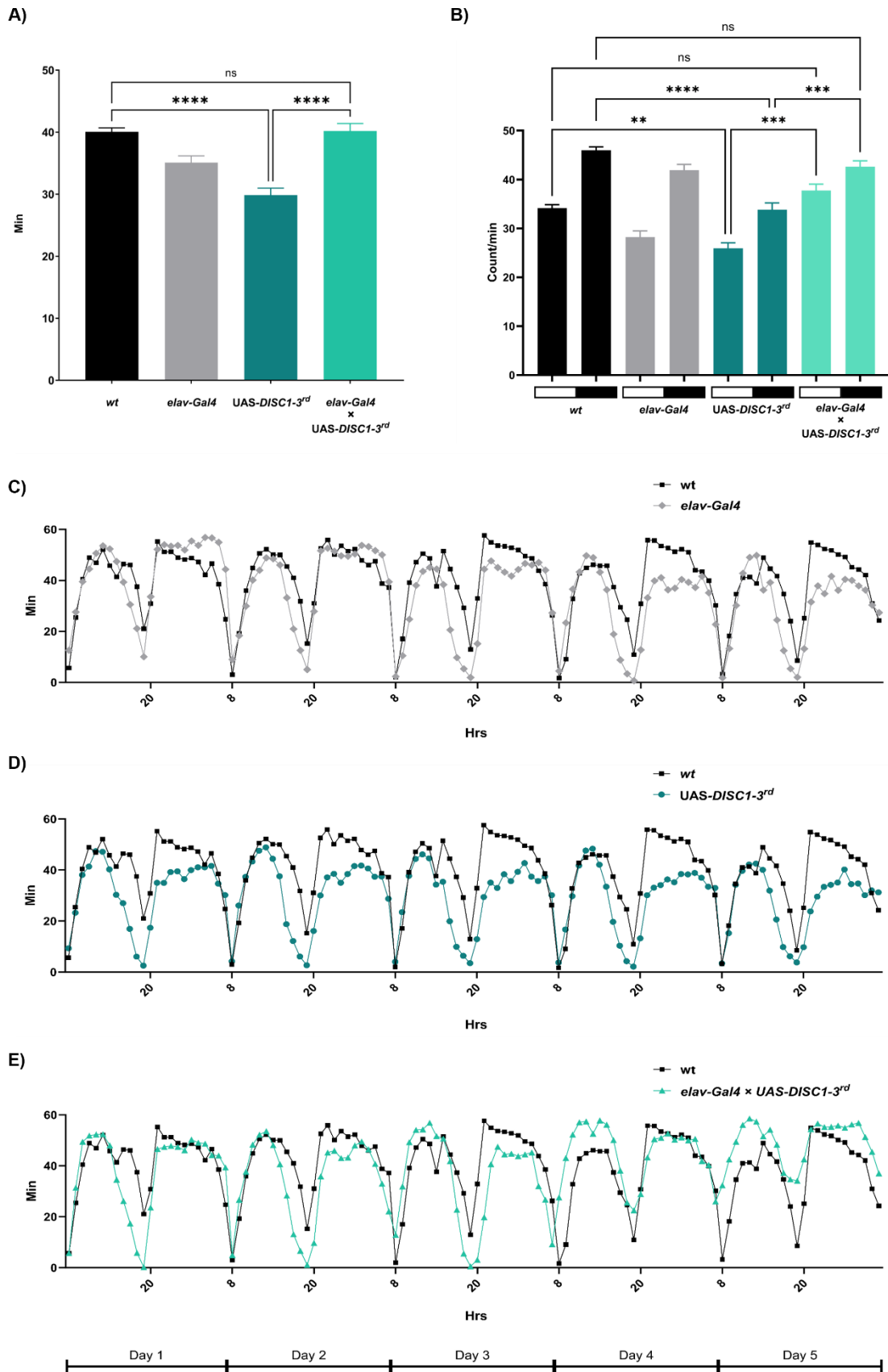
Figure 46. UAS-*DISC1-3rd* line, but not UAS>*Gal4* progenies, exhibit decrease in total sleep amount. The average duration of sleep, shown in minutes, was measured in 3-5 days old first generation male transgenic flies with gene insertion on the third chromosome (UAS-*DISC1-3rd* and *elav-Gal4* × UAS-*DISC1-3rd* progenies (UAS>*Gal4*)), and corresponding controls (*wt*, *elav-Gal4*) during the 5-day period, in L/D (light/dark) conditions. Sleep was defined as no beam interruption for five or more minutes. Results are depicted as an average of a 24-hour period. Statistical analysis was performed on n=48 flies per line, using one-way ANOVA with Tukey post-hoc test. $p < 0.05$ = statistically significant (*); $p > 0.05$ = not significant (ns). **A)** Average overall sleep amount of UAS-*DISC1-3rd* and UAS>*Gal4* progeny lines versus *wt*. **B)** Average sleep amount of all lines, divided into 12-h L/D periods (white/black boxes). **C)** Comparison of *wt* and *elav-Gal4* controls over the 5-day period. **D)** Comparison of UAS-*DISC1-3rd* and *wt* over the 5-day period. **E)** Comparison of the UAS>*Gal4* progeny line and *wt*, over the 5-day period. *wt* – wild type line (*Canton S*); *elav-Gal4* – pan-neuronal driver line.

5. Discussion

5.1 Structural organisation of DISC1

5.1.1 Experimentally derived DISC1 regions can be redefined based on bioinformatics predictions

DISC1 is a widely expressed scaffolding protein with a number of crucial roles in biological processes (Chubb et al., 2008; Thomson et al., 2013). While extensively studied throughout the years due to its genetic link to major mental illness, the tridimensional structure of DISC1 still remains largely unknown. Owing to its low homology with known proteins, rapid sequence evolution, as well as high aggregation propensity (Yerabham et al., 2017), experimental studies of DISC1 have been lacking for years after its initial discovery. While some groups have performed experiments using full-length recombinant DISC1 (Narayanan et al., 2011; Tanaka et al., 2017), solved structures have been limited to small fragments at the extreme C-terminal part of the protein (Ye et al., 2017; Wang et al., 2021). To date, only two contrasting approaches have yielded results on a larger scale; the in silico delineation of regions resembling an UVR domain of the UvrB protein within the highly conserved parts of DISC1 (Sanchez-Pulido & Ponting, 2011), and the experimental determination of putative folded domains acquired through a high-throughput deletion screen performed in bacteria (Yerabham et al., 2017). Interestingly, while contrasting, these two approaches partially converge in their respective results. Three of the four experimentally determined regions overlap with the three predicted UVR-like repeats, suggesting that bioinformatics predictions could be integrated into the empirically obtained domain data of DISC1. However, the empirical approach has several caveats that need to be addressed. Firstly, the extent of protein expression in bacteria cannot be fully representative of the endogenous *in vivo* expression of the full-length DISC1 protein. Secondly, the shortness (150-400 AA) of constructs screened does not represent all viable construct variation of a full-length protein, which may account for two of the regions being represented by more than one soluble construct (Yerabham et al., 2017). Knowing that this experimental model can be less reliable due to the differences between the bacterial and endogenous expression in cells, we attempted to amalgamate empirical and bioinformatics data to assess whether the UVR-like repeats represent key structural elements of the empirical DISC1 regions, and if, by integration

164

of these repeats, we can further optimize region boundaries to achieve higher stability (**Figure 47**).
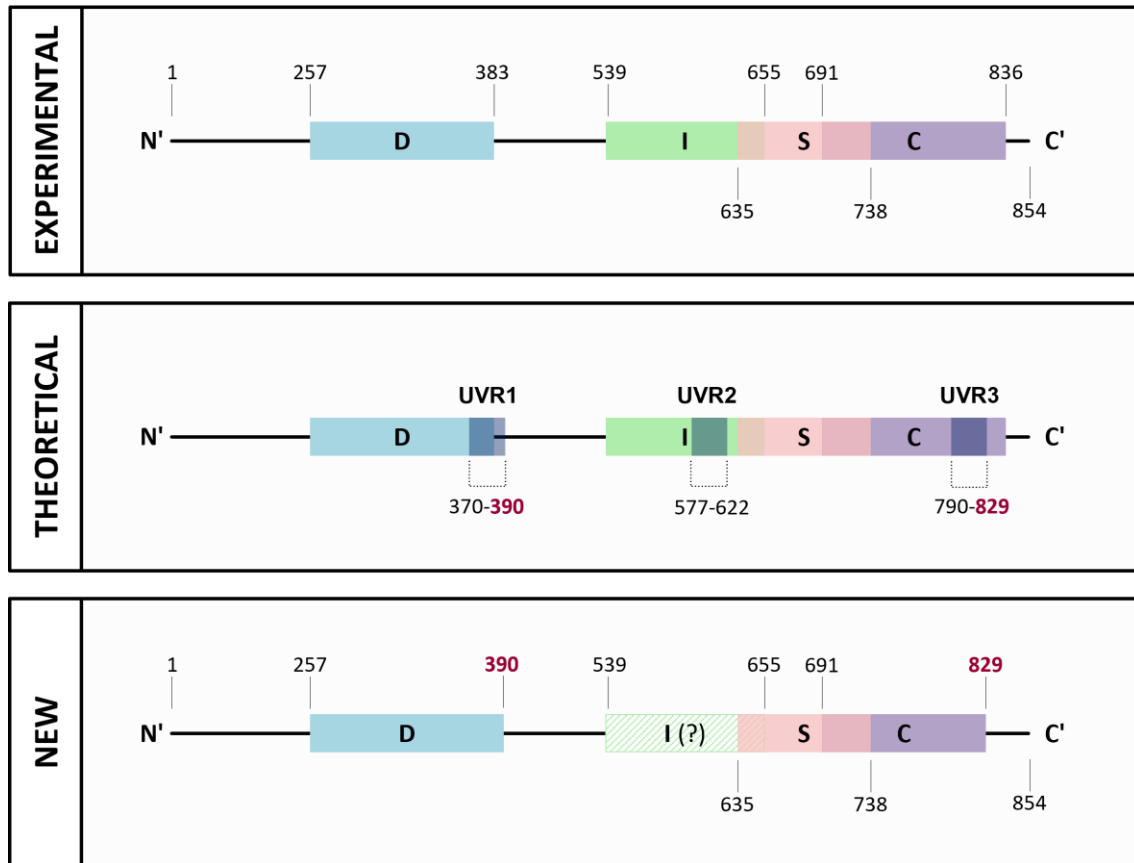

Figure 47. Summary of the structural data presented in this thesis. The first panel shows DISC1 domain structure, experimentally obtained in a bacterial system (Yerabham et al., 2017). It consists of four stable, folded domains named D, I, S and C. The numbers represent amino acid boundaries of the protein and each region. The second panel shows three bioinformatically predicted UvrB-like structural elements (Sanchez-Pulido & Ponting, 2011), superimposed on the experimentally obtained DISC1 domain structure. The numbers below each repeat (UVR1, UVR2 and UVR3) represent amino acid boundaries. The third panel shows the new DISC1 domain structure proposed in this thesis. Two out of four experimentally obtained regions (D and C) were modified based on the bioinformatics predictions, showing increased stability in mammalian expression system. The D region was lengthened to include the entirety of the UVR1, while the C region was shortened at the C-terminal to end at the UVR3 (red, bolded). The I region was shown to be unstable when expressed in mammalian cells, which strongly implicates that the I region does not represent a stable, structural region by itself.

The high-throughput screen predicted four putative DISC1 regions which were named, from N- to C-terminus, D, I, S and C, respectively (Yerabham et al., 2017). Curiously, the D region, represented by two soluble constructs primarily expressed as α-helical dimers in vitro, was found within the N-terminal part of the protein previously thought to be unstructured (Yerabham et al., 2017). Through expression in mammalian cell culture, we have confirmed that the D region is stable within its empirically determined boundaries (AA 257-383), and that it likely partially conserves the previously predicted UVR-like repeat (UVR1, AA 346-390) at its far C-terminal end. The region could still be efficiently expressed while containing only half of the repeat (AA 257-370), indicating that it is not integral for region stability. However, expressing the region with the C-terminal boundary optimized to include the UVR1 in its entirety (AA 257-390), revealed a rise in construct stability. Our results thus indicate that, while the UVR1 is likely part of the D region, it is not necessarily integral for its function. Nevertheless, to achieve higher stability, the region boundaries can be optimized to include the repeat in its entirety.

In contrast to the isolated N-terminal D region, the remaining regions overlap, yet were considered as distinct due to their stability in isolation as purified recombinant proteins. As each region exhibits unique oligomerisation states (dimeric, tetrameric and monomeric for I, S and C, respectively) (Yerabham et al., 2017), it is assumed that their combinations account for the multiple oligomerisation states seen in the full-length DISC1 protein (Narayanan et al., 2011). All the C-terminal regions are predominantly α-helical in structure, with the C region, represented by two soluble constructs, being most stable as a purified protein (Yerabham et al., 2017). Moreover, it is the region of DISC1 for which most success has been achieved by structural approaches (Ye et al., 2017; Yerabham et al., 2017; Cukkemane et al., 2021; Wang et al., 2021), and the only region with solved crystal structure to date (Ye et al., 2017; Wang et al., 2021). Out of the three C-terminal regions, the C region (AA 691-836) was also the easiest to express in mammalian cell culture, and exhibited highest stability in the absence of proteasome inhibitor MG132. The presence of the predicted UVR-like repeat (UVR3, AA 790-821) near its C-terminus has been confirmed by solution NMR (Ye et al., 2017; Wang et al., 2021), which corresponds to the results presented in this thesis. Construct created to represent the C region ending halfway through the UVR3 (AA 691-807), which coincidentally corresponds to the AA site of the reported American frameshift mutation

(Sachs et al., 2005), exhibited significantly lower protein expression both in the presence and absence of MG132. However, the construct truncated at the C-terminal end immediately after UVR3 displayed higher stability than its empirical counterpart in both the presence and absence of MG132, suggesting that the empirically determined borders can be shortened to exclude the final seven amino acids. The region of the protein representing UVR3, spanning AA 807 and 829, was previously shown to represent a leucine zipper domain important for binding NDE1/NDEL1 proteins (Brandon et al., 2004). Taken together, these results serve as a confirmation that UVR3 is an indispensable structural element of the C region. Another interesting observation regarding this region of DISC1 is that its expression was lower in the presence of proteasome inhibitor for both constructs containing UVR3 in its entirety. It could be hypothesised that upon proteasome inhibition the C region undergoes degradation through another pathway, such as the autophagosomal-lysosomal system. However, additional experiments are required to confirm this hypothesis.

The last region of DISC1 predicted to contain the UVR-like repeat (UVR2, AA 577-622) is the I region (AA 539-655). Unlike in other regions identified via high-throughput analysis, there is an upper limit to the I region solubility when concentrated above 30 µM (Yerabham et al., 2017). It is the least stable region upon expression as a recombinant protein (Yerabham et al., 2017), which is in correspondence with our results in mammalian cell culture, precluding analysis of whether UVR2 formed an integral part of it or not. Similar results were seen when expressing the region in the absence of proteasome inhibitor. Stability of the empirical region did rise significantly upon proteasome inhibition. This could be explained by the region's instability and precipitation at higher concentrations, as noted by Yerabham and colleagues, which in turn triggers the UPS-mediated degradation.

In the case of the I region, UVR2 is located nearer to the middle of the region. As such, truncating the empirical region to end at UVR2 (AA 539-622), or halfway through it (AA 539-601), resulted in marked decrease in expression. The I region could however be stabilised when co-expressed as a part of a unit with the S and C regions, but not when in combination with the S region only. The S and C regions, however, exhibited highly stable expression on their own, both in the presence and absence of MG132. The instability of the I and S region in combination could arise due to the overlap between them, thought

to drive the oligomerisation states of DISC1 (Yerabham et al., 2017). Hypothetically, if the intrinsically unstable I region is dominant as the intermolecular interaction domain, it may affect the stability of the S region. In turn, since the S region also overlaps in part with the very stable C region, the latter may serve to stabilise both former regions. Another possible cause of the I region instability could be due to its high aggregation propensity seen upon purification from *E. coli* (Yerabham et al., 2017). When translated into mammalian system, it is possible that the region undergoes aberrant multimerization toxic to the cell, resulting in cell death and, consequently, low or non-existent expression. Frequent cell death upon the I region expression was also seen during the functional assays performed by our group, described in the later section. However, this phenomenon requires further investigation. For instance, cytotoxicity of the constructs may be tested by calcein AM assay, which uses a cell-permeant dye to measure cell viability. Another option includes quantification of lactate dehydrogenase as a measure of potential toxicity. It is a cytoplasmic enzyme released into the cell in response to cellular damage. As lactate dehydrogenase remains stable in cell culture medium, it serves as a useful tool for measuring the presence of toxicity in tissues and cells, including primary cells (Kaja et al., 2017).

While our results confirm the structural importance of UVR2 for the I region stability, they also strongly implicate that this part of DISC1 is unlikely to represent a distinct folded region when expressed in isolation. It therefore appears likely that the C region represents a stable functional unit, while I and S seemingly add to it, but require the C region for their structural stability. Alternatively, I, S and C may interact together as a single structural unit of DISC1 and could potentially be considered as a single structural domain.

5.1.2 Most DISC1 regions are functional in isolation, with the C region being capable of forming protein-protein interactions

5.1.2.1 Localisation and function of DISC1 regions

Protein domains represent basic protein units capable of folding, structural stability, and independent function (Wang et al., 2021). Elucidating the function of single domains can be at least partly achieved by observing their subcellular localisation patterns within the cell. For this purpose, we expressed all four DISC1 regions in human neuroblastoma (SH-

SY5Y) cells. Similar to the expression of fl DISC1, isolated regions localised exclusively within the cell cytoplasm. However, two of the regions, D and C, exhibited in parts a distinctive diffused pattern corresponding to localisation within the endoplasmic reticulum (ER). Previous literature demonstrated localisation of fl DISC1 in the ER (Park et al., 2015), as well as in the mitochondria-associated endoplasmic reticulum membrane (Park et al., 2017), where it was shown to regulate ER calcium dynamics and ER-mitochondria calcium transfer (Park et al., 2015, 2017). Upon staining the cells expressing single DISC1 regions with an antibody against PDIA4 (Protein Disulfide Isomerase Family A, Member 4), a member of the disulfide isomerase family of ER proteins with an N-terminal ER signal sequence (National Center for Biotechnology Information, 2024), we observed colocalization within two regions – D and C. While these results require further confirmation by confocal immunofluorescence, they present an area of interest considering ER-mediated calcium dynamics are required for regulation of neuronal processes such as axonal growth, neuronal excitability and synaptic plasticity (Park et al., 2015). Moreover, ER stress and oxidative stress cause dysregulation of the unfolded protein response (UPR), a highly conserved mechanism which ensures three-dimensional conformation of proteins (Muneer & Khan, 2019) and is known to regulate cell differentiation, survival and death (Kim et al., 2019a). While ER chaperone proteins serve as a protection against misfolded proteins, their accumulation within the ER activates compensatory mitochondrial UPR mechanism through mitochondria-associated ER membrane. However, persistent oxidative stress facilitates generation of reactive oxygen species and build-up of intracellular calcium ions, further exacerbating ER-mitochondrial stress, which consequently leads to even bigger accumulation of toxic aggregates that cannot be degraded via proteasomal or autophagosomal system (Muneer & Khan, 2019). Both ER/oxidative stress and aggregation are well documented in patients suffering from schizophrenia (Leliveld et al., 2008; Ottis et al., 2011; Nucifora et al., 2016; Kim et al., 2018, 2019a, 2019b) and, as such, further research into dysregulation of ER dynamics makes a compelling target for the study of pathological mechanisms behind neuropsychiatric disorders.

Another interesting aspect of the UPR is its connection to ATF4. Namely, ATF4 functions as a transcription factor of UPR target genes and promotes expression of proteins associated with apoptosis and autophagy via PERK (protein kinase RNA-like ER kinase)

signalling cascade of UPR (Fusakio et al., 2016; Kim et al., 2019a). ATF4 has been shown previously to interact with the C region of DISC1 (Wang et al., 2021), and observing this interaction in the context of ER and mitochondrial stress could prove beneficial for future research.

5.2   Protein interactions of DISC1 regions

Another aspect of a domain function is its ability to form interactions with other proteins. For a protein to function, its sequence must contain explicit interacting sites while simultaneously showing a balance between structural stability and flexibility (Nerattini et al., 2020). Empirically determined DISC1 regions are consistent with established interacting sites for several of the key interaction partners of DISC1 (Yerabham et al., 2017), which is sufficient to consider them as functional protein domains. We set to confirm this claim by co-expressing these regions with several known interaction partners in mammalian cell culture. The area of DISC1 corresponding to the D region, spanning AA 277-383, is known to be involved in interactions with TNIK (Wang et al., 2011), Kalirin-7 (Hayashi-Takagi et al., 2010) and PDE4B1 (Millar et al., 2005; Murdoch et al., 2007). We were able to confirm the latter of these interactions by co-expressing the D region alone with PDE4B1 in neuroblastoma cells, which was assessed by immunofluorescence. PDE4B1 and DISC1 D localised within the cell cytoplasm, both in isolation and when co-expressed, which corresponded to the previously published results obtained by immunofluorescence and confocal immunofluorescence, using full-length DISC1 (Millar et al., 2005).

We assessed the I region in a similar manner using ATF4, which was previously shown in yeast-two hybrid and luciferase assay to interact with the C-terminal part of DISC1 (Morris et al., 2003). The I region expressed in isolation showed high instability, with limited transfection and high percentage of cell death. While ATF4 modestly expressed in isolation, within the cell nucleus, upon co-transfection with the I region there was no indication of interaction between the two. Interestingly, Morris and colleagues showed that, while the full length DISC1 can interact with ATF4, the interaction is lost upon DISC1 truncation at the translocation breakpoint (Morris et al., 2003). Another study by Sawamura and colleagues showed that the predicted leucine zipper domain found within exon 9 (AA 607-628) of DISC1 is the minimum domain required for ATF4 binding

(Sawamura et al., 2008), which is consistent with the data obtained by Morris et al. However, a C-terminal region of DISC1 spanning AA 765-835 was recently shown to be sufficient for interaction with ATF4 (Wang et al., 2019). This data indicates that the C region of DISC1 is also required for ATF4 binding, and is in corroboration with our previous assessment that the I region does not represent a stable, functional unit outside of the C-terminal DISC1 complex.

The highest number of different DISC1 interaction partners binds within the C region, including LIS1, NDE1 and NDEL1 (Morris et al., 2003; Ozeki et al., 2003; Brandon et al., 2004). Using immunofluorescence, we have demonstrated this region to be sufficient for these interactions in isolation. Our results are in concordance with previously published data demonstrating that these interactions fail to happen upon C-terminal truncation of DISC1 (Brandon et al., 2004), or are severely weakened (Kamiya et al., 2006). Kamiya and colleagues further demonstrated that the crucial region for DISC1-NDEL1 interaction encompasses AA 802-835 of DISC1, based on systematic C-terminal truncation (Kamiya et al., 2006; Bradshaw, 2017). This part of the protein corresponds to the C-terminal part of the empirical C region, which we have confirmed can be further truncated to end at AA 829 without the loss of interaction.

One caveat of observing protein interactions using immunofluorescence only is our inability to confirm with certainty that overlapping signals do not arise from overlayed cells, instead of a genuine interaction. While these types of interactions would typically be assessed using confocal immunofluorescence, lack of access to the equipment prompted us to employ a different method. Nanoscale Pulldown (NanoSPD) assay is a miniaturised version of the standard affinity pulldown assay that can be performed within a native cell cytoplasm (Bird et al., 2017). The method is based on hijacking the normal intercellular trafficking process by myosin motors to forcibly pull fluorescently tagged proteins along filopodial actin filaments (Bird et al., 2017), hence representing a powerful tool to study protein-protein interactions. By employing NanoSPD we once again assessed putative DISC1 regions, apart from the I region which we previously showed to be intrinsically unstable.

While the D region signal did accumulate at the filopodia, it did not colocalise with PDE4B1. There are several possible explanations as to why this occurred. One possibility

is that the D region can form protein interactions only in the context of the three-dimensional structure, where specific conditions such as hydrophobic effect and electrostatic forces are met. This corresponds to previous findings by Millar and colleagues, which shows that patient-derived lymphoblastoid cell lines carrying a t(1;16) translocation breakpoint exhibit a 50% decrease in PDE4B1 expression (Millar et al., 2005). Following this logic, further truncation of the protein might result in complete abolishment of the interaction. Moreover, by probing fl DISC1 peptide arrays with the PDE4B1 fusion protein, Murdoch and colleagues demonstrated that these two proteins interact through multiple binding sites. Some of these sites can be found within the far N-terminal part of the protein (AA 31-65 and AA 101-135), and even within what is known today as the I region (AA 611-650) (Murdoch et al., 2007). As our construct representing the D region contains only one of the PDE4B1-specific binding sites identified (AA 266-290) (Murdoch et al., 2007), the absence of additional binding regions may account for the lack of interaction.

Another reasoning assumes that the interaction between DISC1 and PDE4B1 is of a transient type, meaning that certain cellular context is required for binding (de Las Rivas & Fontanillo, 2010). Lack of the proper context, or its disruption by a forcible pull of DISC1 D into the filopodia might thus result in the absence of binding. Transient interactions are common for proteins involved in signalling cascades, a category of proteins to which PDE4B1 belongs to, as well (Soares et al., 2011). Finally, several studies suggested that both the self-association domain and the C-terminal region of DISC1 are necessary for functional oligomer formation (Kamiya et al., 2005; Young-Pearse et al., 2010), which exists in a delicate equilibrium between dimeric and octameric species thought to be modulated by PKA-induced phosphorylation (Narayanan et al., 2011; Roche & Potoyan, 2019). This oligomer formation is essential for binding of certain proteins, which might be the case for PDE4B1 as well. Hypothetically, if certain higher order species are required for PDE4B1 binding due to their modulation by PKA, and formation of these species is somehow disrupted during the pulldown assay, it might result in the absence of PDE4B1 binding. Furthermore, past research showed that dimeric N-terminal DISC1 fragments exhibit a decrease in conformational heterogeneity, as well as an increase in local disorder likely driven by the absence of contacts formed with the central domain of the protein (Roche & Potoyan, 2019), which could account for the lack

of PDE4B1 binding in this specific case. In support of this, a study investigating the ternary complex of mutated huntingtin, DISC1 and PDE4B1 displayed significant effects upon DISC1-PDE4B1 interactions following deletion of AA 201-208 of DISC1 (Tanaka et al., 2017).

Although it may principally function as the basis of the higher order oligomerisation of DISC1 (Leliveld et al., 2009; Yerabham et al., 2017), the role of the S region within the context of DISC1 is less clear. However, most of the LIS1 interaction with DISC1 has been observed through the LIS1/NDE1/NDEL1 complex (Brandon et al., 2004), with limited research dedicated to study of DISC1-LIS1 interaction separate of the NDE1/NDEL1 effects. For these reasons, we set out to study its interaction with LIS1 using NanoSPD. Unfortunately, we met with the same results previously seen with the D region: DISC1 S was not capable of pulling LIS1 into filopodial tips. Possible explanation for the lack of binding can be drawn from the biophysical data obtained by Yerabham and colleagues (Yerabham et al., 2017). Their work suggests that an overlap between the I and the S region is responsible for different oligomeric states of DISC1, where the S region represents higher oligomeric states. Based on this hypothesis, it is possible that LIS1 does not directly bind to the S region, but S is instead required to set DISC1 into a proper oligomeric state for facilitating the interaction.

Another explanation may arise from the overlap between the S and C regions, the functional interconnectivity of LIS1 with NDE1/NDEL1, as well as previously obtained structural information on the C-terminal part of DISC1. This specific lack of interaction is suggestive of our hypothesis that I, S and C interact together as a single structural unit in DISC1, with the C region being the most integral part of the domain. The latter hypothesis is further strengthened by the fact that DISC1 C was the only construct that tested positive for interaction with NDE1 and NDEL1, but not LIS1, upon nanoscale pulldown. In the future, LIS1 interaction should be tested with both S+C and I+S+C constructs, to confirm the hypothesis suggesting existence of a singular C-terminal DISC1 unit. However, the interaction with I+S+C could be severely hindered by its aggregation propensity and may require a different approach.

Despite the high homology between the two, NDEL1, but not NDE1, was able to accumulate in filopodial tips in the absence of DISC1. This particular transfection

included EGFP control, Flag-tagged NDEL1 and a NanoTrap vector containing myosin class 10 (MYO10) molecular motor. Considering that during our previous experiments NDEL1 did not show any indication of binding to EGFP control, we reasoned that NDEL1 was travelled to filopodial tips by directly interacting with MYO10. MYO10 consists of an ATPase motor domain which binds to actin filaments, a neck domain associated with regulatory light chains, a coiled-coil motif and a C-terminal tail domain responsible for binding of cargo proteins (Kerber & Cheney, 2011; Bird et al., 2017). In addition to its functions in filopodia, MYO10 was shown to be crucial for proper assembly and orientation of the mitotic spindle, as well as growth cone migration and synapse formation in *Xenopus laevis* (Kerber & Cheney, 2011). Curiously, while loss of NDE1 affects spindle assembly and function (Feng & Walsh, 2004), and LIS1 has a crucial role in mytotic spindle orientation (Moon et al., 2014), interaction between the two and MYO10 not was seen during our experiments. However, LIS1 was shown to exert its control over mitotic spindle organisation via the LIS1-NDEL1-dynein complex (Moon et al., 2014). Additionally, another member of the myosin family, myosin II, and cytoplasmic dynein were shown to affect neuronal migration and growth-cone motility in indirect manner (Vallee et al., 2009). Taken together, these findings may provide a new insight into the role of NDEL1 in cytoskeleton organisation and neurodevelopment.

5.3 DISC1 aggregation

5.3.1 An aggregation-critical region of DISC1 is found in the central part of the protein

Recently, aberrant proteostasis has been suggested as an underlying pathological mechanism for psychiatric disorders (Korth, 2012), in addition to the traditional genetic approach. The pathology of many other chronic brain disorders, such as neurodegenerative disorders, can be characterised by the presence of misfolded or aggregated protein. This knowledge suggests that a similar mechanism may occur in chronic mental disorders, as well (Leliveld et al., 2008; Korth, 2012). In the following years, several proteins were found to aggregate in this manner (Ottis et al., 2011; Bader, Ottis, et al., 2012; Bradshaw et al., 2014; Nucifora et al., 2016) in the post-mortem brains of patients suffering from chronic neuropsychiatric disorders, including DISC1 (Leliveld et al., 2008, 2009). Furthermore, expression of aggregating DISC1 in murine models led

to a variety of significant changes in biochemical, neuroanatomical and behavioural phenotypes closely related to the dopamine system, in correspondence to phenotypes observed in schizophrenia patients (Trossbach et al., 2016; Zhu et al., 2017; Sialana et al., 2018; Kaefer et al., 2019). In this thesis, by using human neuroblastoma cells, we investigated whether one of the recently discovered DISC1 regions is responsible for its aggregation propensity.

Our results demonstrated that a short section of the protein lying immediately C-terminal of the D region, spanning AA 384-415, was sufficient for aggregation. Moreover, deletion (Δ384-415) of this section resulted in complete abolishment of DISC1 aggregation, thus defining it as aggregation-critical. It was not found within any of the most stable DISC1 fragments yielded by the ESPRIT screening, but would be predicted to have α-helical content with coiled coil potential (for AA 384-393) based on bioinformatics prediction (Soares et al., 2011). Further refinement of this region may be a possibility in the future, as similar work has already been performed by our group using TRIOBP-1, another protein found to aggregate in CMIs. There, we were able to narrow down the length of the aggregating region from 24 to just 8 amino acids, by systematic truncation of constructs (Zaharija et al., 2022; Zaharija & Bradshaw, 2024).

Our findings are in concordance with the results obtained from the brains of patients with sporadic cases of chronic psychiatric conditions, in which an insoluble DISC1 species of approximately 72 kDa was detected using an antibody specific to part of the C region (Leliveld et al., 2008). The exact nature of this DISC1 species is unknown, but based on its size and the presence of C-terminus, it would be expected to have lost the first N-terminal ~200 AA, possibly through the posttranslational modification process. In theory, such species would contain all known structured regions, including the aggregation-critical region we described. While the artificial system of overexpressing purified recombinant DISC1 may be substantially different from the endogenous DISC1 expression in the brains of affected patients, it serves as a good initial model for study of aggregation mechanisms. However, generation of a high-quality antibody against the N-terminus of DISC1 is needed for further confirmation of our conclusions.

Another study performed in HeLa cells found that a truncated DISC1 construct spanning AA 357-854 exhibits a "punctate" phenotype akin to smaller-sized aggregates. In terms

of ESPRIT-determined regions, this would approximate to a protein missing the N-terminal disordered region and a better part of the D region. Interestingly, this phenotype was lost with truncation of what is now known as the I region (Brandon et al., 2005), thus considering it responsible for such expression. The difference in our results may arise from the fact that their construct boundaries were defined prior to the uncovering of the DISC1 domain structure, meaning that their constructs represented partial, thus unstable, domains.

A recent study on a mouse model expressing Huntington's disease (HD)-associated human *huntingtin* (*HTT*) mutant, implicated a short section of the DISC1 N-terminus (AA 209-227) preceding the D region, as critical for aggregation with HTT (Tanaka et al., 2017). Moreover, DISC1 aggregation was significantly accelerated in the presence of HTT due to co-aggregation, but not by an increased rate of spontaneous DISC1 aggregation. This implicates that spontaneous DISC1 aggregation likely occurs through distinct mechanisms separate from those induced by its co-aggregation with HTT, as suggested by our findings of an independent aggregation-critical region. Similar conclusions can be drawn from the way in which DISC1 can induce TRIOBP-1 co-aggregation, even in the absence of the TRIOBP-1 regions responsible for its spontaneous aggregation, through a separate mechanism involving the N-terminal untranslated region (Zaharija et al., 2022; Samardžija et al., 2023).

Curiously, another region of DISC1 was also found to be capable of aggregation in our system, separate from the effects of the linker region. This region encompasses the three C-terminal regions of DISC1, I, S and C (AA 539-854). However, no such propensity was seen when the I and S (AA 539-738) or the S and C regions (AA 635-836) were expressed. Our results broadly align with the study by Leliveld and colleagues, which demonstrated that a C-terminal region of DISC1 approximate to the S and C regions (AA 640-854) was capable of aggregation in cells (Leliveld et al., 2009). Purification of insoluble material from the brains of psychiatric patients also resulted in detection of C-terminal DISC1 fragments (Leliveld et al., 2008), however, while distinct, a mechanism by which this region of the protein aggregates is yet undetermined. While it cannot be formally ruled out that the extreme C-terminal tail (AA 836-854) of DISC1 plays a role in its aggregation, there is indication that the I region may be complicit as well. The construct spanning AA 440-597, which includes the N-terminal part of the I region ahead of the

breakpoint, was shown to produce the punctate expression (Brandon et al., 2005). In contrast, further study of truncated DISC1 constructs with "punctate" phenotype observed the lack of said phenotype in the construct bisecting the I region at the translocation breakpoint (AA 598-854). This construct includes the extreme C-terminal amino acids, but exhibits no sign of aggregate formation (Brandon et al., 2005). Interestingly, other studies showed that this particular fragment of DISC1 is capable of self-association (Leliveld et al., 2008, 2009) and can exist as dimeric, octameric and multimeric species under physiologically relevant conditions (Leliveld et al., 2009). Both the dimerization (AA 765-854) and oligomerization (AA 668-747) domains can be found predominately within the C region of DISC1 (Leliveld et al., 2009). The latter is a part of the well-conserved coiled-coil domain which contains another self-association site at AA 403-504 (Kamiya et al., 2005), corresponding to a part of the linker found between the regions D and I. While oligomerization may represent a natural self-interaction, accumulation of higher order species can also lead to aberrant multimerization and formation of insoluble aggregates, which corresponds to our data regarding the C-terminal region of DISC1. Taken together, these results indicate the existence of at least two distinct mechanisms of DISC1 aggregation – one driven by the central region, and the other arising from the C-terminus of DISC1.

Albeit our group did not find any indication that the C region alone is capable of aggregation, recent biophysical characterisation performed in an in vitro bacterial system showed it to be capable of forming fibrillar aggregates (Cukkemane et al., 2021). This self-association and aggregation of the C region was driven by a β-core (AA 716-761) region, a tightly packed region of β-fibrils (Cukkemane et al., 2021), in a way similar to what has been observed in the interaction of DISC1 with HTT (Tanaka et al., 2017). While the two different aggregating regions of DISC1 are not necessarily conflicting, given the difference between the expression systems, the linker region between D and I shows the highest aggregation capacity of any individual section of DISC1 examined in neuroblastoma cells, diminishing any effect of aggregation of the C region alone. Expression and purification of the linker region from *Escherichia coli* is comparatively harder to achieve under the same conditions, than it is the case for the C region, which is sufficiently stable and easy to express (Zaharija & Bradshaw, 2024). It is therefore reasonable to conclude that the linker region has inherently larger aggregation propensity

when studied in isolation. However, given that both regions were determined using model systems rather than endogenous DISC1, pathological relevance of aggregation in both cases needs to be further confirmed.

In this thesis, we demonstrated that in mammalian cell systems, aggregation of DISC1 is dependent upon a short linker region found between D and I. Moreover, we have shown that removing the region abolished aggregation propensity of DISC1 in its entirety (**Figure 48**). Together with previous knowledge that aggregation could arise through the recombinant C region of the protein (Cukkemane et al., 2021), our data implicates the existence of more than one distinct molecular mechanism of aggregation.

Our results, as well as generation of the DISC1 (Δ384-415) deletion construct, can help in creating better model systems for future studies of DISC1 aggregation, separate from the effects of overexpression. This could be addressed, to a significant extent, in a system involving three lines of animals: one control lacking a transgene, one expressing full-length aggregating DISC1, and one expressing a mutant version of the protein that lacks the ability to aggregate (DISC1 Δ384-415). Furthermore, a gain of insight into possible pathological mechanisms of DISC1 aggregation may serve as a stepping stone towards the discovery of alternative therapy options for at least a subset of patients suffering from chronic and debilitating psychiatric disorders, such as schizophrenia, bipolar disorder and depression.
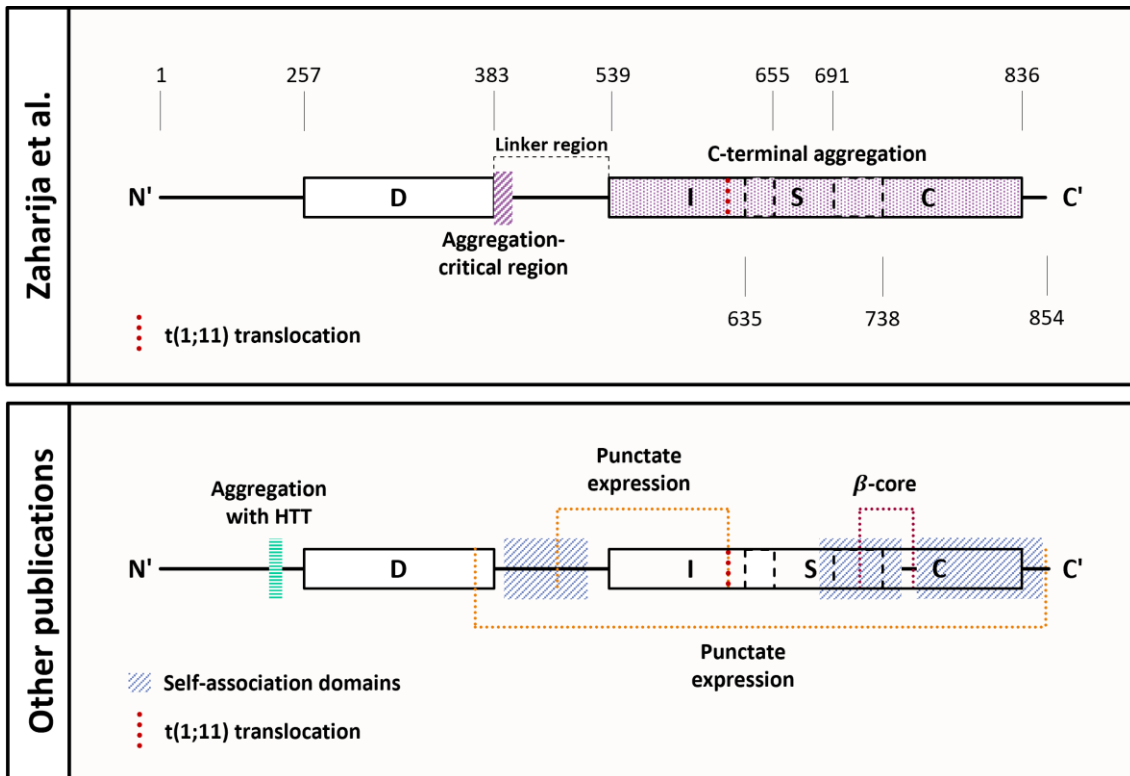
Figure 48. Summary of aggregation data presented in this thesis. Upper panel depicts aggregating parts of DISC1 as shown in the Results section of this thesis (Zaharija & Bradshaw, 2024). The DISC1 protein seems to aggregate through at least two distinct mechanisms: one arising from the central part of the protein (aggregation-critical region, purple/striped), and one arising from the C-terminal part of the protein (purple/dotted). The aggregation-critical region (AA 383-415) can be found within the linker region between D and I. Deletion of this region results in complete abolishment of DISC1 aggregation propensity. Lower panel depicts various parts of DISC1 indicative of aggregation and/or self-association, as shown by other research groups. Green/horizontal stripes – DISC1 aggregation with huntingtin (HTT) (Tanaka et al., 2017); orange/dotted lines – punctate DISC1 expression (Brandon et al., 2005); blue/diagonal stripes – DISC1 self-association domains (Kamiya et al., 2005; Leliveld et al., 2009); dark red/dotted lines – β-core aggregation (Cukkemane et al., 2021); red vertical broken line – Scottish t(1;11) translocation (Millar et al., 2000).

179

5.4 DISC1 expression in *Drosophila*

5.4.1 Gene insertion of *DISC1* affects locomotor activity and sleep patterns in *Drosophila* fruit fly

The fruit fly, *Drosophila melanogaster*, has been successfully used for decades as a tool to study human genetics and disease, with significant advancements made particularly in neurodegeneration (Furukubo-Tokunaga, 2009; Lessing & Bonini, 2009). Although fly models possess the same limitations as other animal models regarding the study of distinguishingly human diseases, conservation of biological pathways amongst the species can be used to study complex disease functions through exhibited endophenotypes (Furukubo-Tokunaga, 2009; Furukubo-Tokunaga et al., 2016). While flies do not express complex phenotypes equivalent to symptoms of schizophrenia, the genes relevant to basic biological processes such as arousal, sleep, learning and memory can be manipulated, and the effect on behavioural phenotypes can be objectively quantified in a fly model (Furukubo-Tokunaga, 2009). Moreover, interactions between conserved components involved in molecular processes can be used to identify underlying cognitive deficits in patients suffering from psychiatric conditions. Considering the equivalent molecular mechanisms in brain development (Lessing & Bonini, 2009), as well as the vast number of transgenic techniques available to study human disease in fly models (Furukubo-Tokunaga et al., 2016), we set out to study the behavioural consequences of *DISC1* expression and aggregation in *Drosophila* models expressing the transgenic DISC1 protein.

Although *DISC1* does not have a homologous gene in *Drosophila* (Bord et al., 2006), multiple genes encoding its protein interactors are highly conserved within the fly genome (Furukubo-Tokunaga, 2009). Due to this, several groups have previously studied the effects of transgenic DISC1 in flies, showing its role in regulation of sleep homeostasis (Sawamura et al., 2008), neurodevelopment and associative memory (Furukubo-Tokunaga et al., 2016), development of glutamatergic synapses (H. Pandey et al., 2017), as well as its involvement in multiple disease-risk pathways (Shao et al., 2017). Our study was thus conducted to confirm the role of DISC1 in sleep and locomotor activity of fruit flies by using our new transgenic lines, which will then be utilised for future research on DISC1 aggregation.

In our preliminary assessment of locomotor activity by negative geotaxis in ageing flies, we tested non-expressing transgenic fly lines with human *DISC1* insertions on the second (UAS-*DISC1*-2nd) and third chromosome (UAS-*DISC1*-3rd) versus the *Canton S* (CS) *wt* controls. Subsequent data analysis uncovered a surprising increase in activity in 4-weeks-old transgenic UAS flies compared to the *wt* controls, particularly in the case of the UAS-*DISC1*-3rd line. Further investigation revealed leaky UAS constructs evident as background DISC1 expression in in the absence of *Gal4*, a driver that activates protein expression upon its interaction with the UAS promoter. As such, altered behavioural phenotype of UAS transgenic lines likely arises from the background DISC1 expression.

The median lifespan of CS flies is 50 days (Qiu et al., 2017). At 4 weeks, flies are considered to be of an advanced age, which results in decreased locomotor performance (Qiu et al., 2017). A marked increase in locomotor ability of 4-weeks-old UAS-*DISC1* flies compared to CS may indicate a possible neuroprotective effect of DISC1 in advance age, consistent with reported neuroprotective role of DISC1 in age-related diseases such as Alzheimer's (Deng et al., 2016; Wang et al., 2018; Lu et al., 2022). DISC1 was previously reported to protect synaptic plasticity from Aβ-induced toxicity in a transgenic mouse model of Alzheimer's disease (Wang et al., 2018). Additionally, DISC1 overexpression was shown to reduce the levels and density of Aβ plaques through its interaction with BACE1 (β-site amyloid precursor protein cleaving enzyme 1), resulting in a rescue of cognitive deficits in a murine Alzheimer's model (Deng et al., 2016). A neuroprotective role of DISC1 was also demonstrated in post-mortem brains of CMI patients, where the loss of DISC1 led to a reduction of VGF (non-acronymic), a neuroprotective peptide precursor important for synaptic plasticity and neurogenesis (Ramos et al., 2014). A follow-up study showed that DISC1 regulates VGF expression through PI3K (Phosphoinositide 3-kinase), an enzyme involved in AKT/CREB signalling pathway (Rodríguez-Seoane et al., 2015).

The increase in locomotor activity of UAS-*DISC1* transgenic flies may thus be contributed to its neuroprotective effect. However, it is important to note that our UAS-*DISC1* lines are of a mutant *white^{1118}* background rather than CS. While *white^{1118}* strain has a similar lifespan as CS (median of lifespan 54 days), a study of age-dependent performance between the two demonstrated that old (40-45 days) *white^{1118}* flies display faster travel time and higher percentage recovery of locomotion after anoxia (Qiu et al.,

2017). As such, age-related difference in locomotor activity of UAS-*DISC1* flies may be a result of the *white* mutation. This limitation can be addressed in future experiments by including a *white^(1118)* control together with the *wt* CS.

To determine whether the activation of *DISC1* expression has an additional effect on locomotor abilities of *Drosophila*, we measured locomotor activity of UAS-*DISC1* flies together with UAS>*Gal4* progenies expressing *DISC1* pan-neuronally over the course of five days, using the *Drosophila* Activity Monitoring System.

While the DISC1-expressing *Gal4* lines also exhibited a range of different phenotypes compared to controls, phenotype severity was stronger in the fly lines containing leaky UAS constructs. Moreover, the third chromosome insertion continuously had a stronger effect than that of a second during the assessment of both the locomotor activity and sleep, indicating that genomic insertion is closely related to phenotype severity. This may be explained by the fact that the third chromosome carries more genes analogous to human that interact with *DISC1* compared to the second chromosome, thus highlighting the significant impact of chromosomal location on behaviour (Furukubo-Tokunaga et al., 2016; Samardžija et al., 2024).

Locomotor activity in the UAS flies with a third chromosome insertion was markedly higher than *wt* during the dark/night hours, and a significant decrease in sleep was also measured during the same period. This is consistent with the reports from schizophrenia patients, most of which experience sleep difficulties during nighttime (Freeman & Waite, 2025). However, while the UAS-*DISC1*-3^(rd) flies shared a fairly similar locomotor phenotype with their corresponding UAS>*Gal4* progeny line, UAS-*DISC1*-3^(rd) displayed a highly significant decrease in sleep amount both during the light and dark hours, compared to UAS>*Gal4*. At this moment, we cannot explain the differences in sleep phenotypes between the UAS and UAS>*Gal4* lines. To address this issue, a Western blot analysis of both the UAS and UAS>*Gal4* line should be performed in the future, to assess whether a notable difference in DISC1 expression levels is present in either of the two lines.

Contrary to our results, a study assessing the sleep homeostasis of transgenic DISC1 flies did not mark any alterations in sleep patterns or motor disturbances in UAS-*DISC1* controls (Sawamura et al., 2008). This may potentially arise due to the difference in the

expression systems. The GeneSwitch (GS) system utilised by Sawamura and colleagues differs from the conventional *Gal4/UAS* system used in this thesis in that it allows both temporal and spatial regulation of inducible transgene expression (McGuire et al., 2004). Furthermore, the GS system allows expression only in the mushroom bodies of the fly, in comparison to the pan-neuronal driver used in this thesis. As such, while leaks in the GS system may be present (Scialo et al., 2016), they may be negligent compared to the compound leaky expression present in the whole brain, and thus have no visible effect on the phenotype.

Another discrepancy between our results and those previously published arises from the altered phenotype observed in flies expressing DISC1. While we observed no discernible difference in sleep phenotypes between DISC1-expressing (UAS>*Gal4*) lines and *wt* controls, Sawamura and colleagues reported increased sleep time per day in male flies following induced expression (Sawamura et al., 2008). Apart from the different expression system used, altered sleep phenotypes observed by Sawamura and colleagues were directly associated with subcellular localisation of DISC1 in the nucleus. Acknowledging different roles of DISC1 based on its subcellular localisation and interactions, we may tentatively conclude that the expression of DISC1 in different brain areas and/or neuronal clusters can result in different sleep phenotypes. However, this hypothesis requires further investigation.

The phenotypes we observed in UAS-*DISC1* flies do, however, correspond to those previously reported in transgenic mice overexpressing wild-type DISC1, which were found to be awake longer than wild type controls, even though no difference in locomotor activity was noted (Jaaro-Peled et al., 2016). The results presented in the aforementioned study suggest that DISC1 affects signalling cascades associated with sleep regulation, such as the monoamine systems (Jaaro-Peled et al., 2016). This hypothesis is further supported by dopaminergic abnormalities seen in a transgenic rat model of human DISC1 (Trossbach et al., 2016). Moreover, sleep deprivation was shown to impair cAMP signalling in the hippocampus through an increased activity of PDE4 family members (Vecsey et al., 2009), known to interact with DISC1 (Millar et al., 2005). Thus, DISC1 may also affect sleep homeostasis through cAMP signalling. Another study into the oscillatory patterns of *Disc1* showed that *Disc1* expression levels are enhanced during

late nighttime to early daytime (Lee et al., 2021), which is in agreement with the nighttime phenotype observed in our study.

Novel results published by our group during the generation of this thesis support the hypothesis that DISC1 affects signalling cascades associated with sleep regulation. Notably, we showed that both UAS-*DISC1* lines exhibit significant elevation of hydrogen peroxide, a reactive oxygen species associated with oxidative stress. DISC1 dysfunction was previously linked to oxidative stress in several studies (Park et al., 2017; Fuentes-Villalobos et al., 2019; Watanabe et al., 2023), and schizophrenia patients often show abnormalities in oxidative stress-related biomarkers (Cuenod et al., 2021; Chen et al., 2023). Elevated levels of hydrogen peroxide suggest disruptions in cellular redox signalling pathways, which could in turn affect signalling cascades and neurotransmitter systems known to regulate behaviour (Samardžija et al., 2024), in concordance with the results obtained from transgenic rat models.

Although preliminary, our results have several limitations that need to be acknowledged: mainly, while the CS stock was used as the initial wild type control, a comparison to the *white* (w^{1118}) control stock is required as well due to the genetic background of our transgenic lines. Furthermore, the negative geotaxis assay and Western blot of fly homogenates require at least two more replicates to be statistically significant. Finally, while we conducted separate assessment and statistical analysis of UAS-*DISC1-2nd* and UAS-*DISC1-3rd* effects on fly phenotypes, a direct comparison between the two is required to fully assess the impact of chromosomal insertion location. However, during the writing of this thesis our research group expanded on the preliminary results shown here, resolving most of the limitations addressed and providing further insight into an array of UAS-*DISC1* phenotypes (Samardžija et al., 2024). Curiously, some results were highly contradictory, while some remained largely similar. Namely, the DISC1 protein was found to be present both in the bodies and heads of UAS-*DISC1* transgenic strains, while our initial analysis shows it to be present only in the heads; this indicates that DISC1 expression is present in both the brain and the ventral nerve cord of transgenic flies (Samardžija et al., 2024). Negative geotaxis assay provided results similar to the preliminary ones, with a display of decreased climbing ability in 3-5 days old UAS-*DISC1-3rd* flies (Samardžija et al., 2024). However, a discrepancy arises from both sleep and locomotor activity data. Our latest results show that 3-5 days old UAS-*DISC1* lines

display decreased sleep and lower locomotor activity during the day compared to the w^{1118} control (Samardžija et al., 2024), while the initial results compared to the wild type CS control implied the contrary. However, the CS control displays markedly lower total activity in comparison to the w^{1118} control, indicating that the difference in controls may account for the data discrepancy. Further research should thus aim to use the w^{1118} stock outcrossed with CS at ten times as the standard, to avoid the potential effects of *white* mutation on the phenotype.

Our preliminary study serves as a further investigation of DISC1 expression in flies, in light of the recently determined aggregation-critical region, as well as to present another glance into the role of DISC1 in regulation of sleep and locomotor activity. Furthermore, this study lays the foundation for future generation of transgenic fly models expressing both the aggregating and non-aggregating DISC1, hence providing the ability to directly compare phenotypes and assess the effects on DISC1 aggregation on behaviour.

6. Conclusions

DISC1 is a multifunctional scaffolding protein with critical roles in a vast array of disease-related pathways. However, the lack of structural understanding of DISC1 has impeded analysis of its roles in neurodevelopment, as well as the consequences for chronic neuropsychiatric conditions such as schizophrenia, major depressive disorder and bipolar disorder. This thesis thus focused on improving the understanding of DISC1 from both structural and functional perspective, with the following findings:

1. Bioinformatically predicted UVR-like repeats are compatible with the three experimentally determined DISC1 regions: D, I and C.
   1.1. UVR1 is a part of, but not essential to the structure of D region, and the C-terminal boundary of the region may be extended to encompass the entirety of the UVR1.
   1.2. UVR2 is an essential structural element of the I region. However, the I region probably does not represent a self-sufficient, stable domain when expressed in isolation in mammalian cells.
       1.2.1. The stability of the I region increases while in complex with both S and C, in mammalian cells. However, expression of the I region in complex with the S region destabilizes the latter.
   1.3. UVR3 is a crucial structural element of the C region, and the boundaries of this region can be further refined to end at the C-terminal end of UVR3.
2. The experimentally determined DISC1 regions primarily localize to the cell cytoplasm when expressed in mammalian cells. Three out of the four (D, I and C) regions express stably, while the I region retains poor expression.
   2.1. The D and C regions overlap with a marker of the endoplasmic reticulum with high statistical significance.
   2.2. The D region expressed in isolation appears to not have sufficient binding capabilities to interact with PDE4B1, in contrast to the preliminary results.
   2.3. The S region expressed in isolation appears to not have sufficient binding capabilities to bind LIS1, in contrast to the preliminary results.

2.4. The C region expressed in isolation does not bind LIS1, but interacts with the NDE1 and NDEL1 proteins; however, the interaction with NDEL1 needs to be revisited.

3. The DISC1 aggregation propensity arises from two different parts of the protein.

   3.1. An aggregation-critical region of DISC1 (AA 384-415) lies immediately C-terminal to the D region; deletion of this region results in complete abolishment of aggregation.

   3.2. A combination of C-terminal DISC1 regions (I+S+C) is capable of aggregate formation; no other C-terminal combination (I+S or S+C) has the same ability.

4. Young transgenic *Drosophila* models carrying inactive human *DISC1* exhibit leaky protein expression, resulting in an early decline of locomotor abilities; expression is higher depending on the location of the chromosomal insertion.

   4.1. Transgenic flies with chromosomal insertion of *DISC1* on the third chromosome exhibit higher expression compared to the insertion on the second chromosome.

5. Expression of DISC1 in *Drosophila* results in higher locomotor activity during the night, particularly in transgenic flies with the insertion on the third chromosome.

6. Expression of DISC1 in *Drosophila* results in reduction of average sleep, particularly in transgenic flies with insertion on the third chromosome.

In light of our conclusions, future research of DISC1 should primarily focus on obtaining the tridimensional structure of DISC1. Elucidating the tertiary structure will enable a closer look into the way DISC1 interacts with multiple proteins within its network, which will in turn allow closer inspection of its functions and distinctive molecular mechanisms by which it exerts them. Another important aspect of DISC1 research arises from its ability to form pathological aggregates in the brains of psychiatric patients. With our recent finding of an aggregation-critical region of DISC1, future experiments should aim to create animal models which express both aggregating and non-aggregating DISC1, and use them to assess the effects of aggregation, as well as co-aggregation, on behaviour. Taking into account the lack of biological testing for CMI patients, testing for aggregation of not only DISC1, but of other aggregating proteins as well, may provide a much-needed biological marker for these diseases. As such, our focus should also be on finding a way to monitor aggregation-prone proteins through blood samples of CMI patients, with the final goal of discovering efficient and personalised therapies for each distinct condition.

7. Literature

1) Abdel-Nour, M., Carneiro, L. A. M., Downey, J., Tsalikis, J., Outlioua, A., Prescott, D., Da Costa, L. S., Hovingh, E. S., Farahvash, A., Gaudet, R. G., Molinaro, R., van Dalen, R., Lau, C. C. Y., Azimi, F. C., Escalante, N. K., Trotman-Grant, A., Lee, J. E., Gray-Owen, S. D., Divangahi, M., … Girardin, S. E. (2019). The heme-regulated inhibitor is a cytosolic sensor of protein misfolding that controls innate immune signaling. *Science (New York, N.Y.)*, *365*(6448). https://doi.org/10.1126/SCIENCE.AAW4144

2) Afonso, P., Brissos, S., Figueira, M. L., & Paiva, T. (2011). Schizophrenia patients with predominantly positive symptoms have more disturbed sleep-wake cycles measured by actigraphy. *Psychiatry Research*, *189*(1), 62–66. https://doi.org/10.1016/J.PSYCHRES.2010.12.031

3) Agrotis, A., Pengo, N., Burden, J. J., & Ketteler, R. (2019). Redundancy of human ATG4 protease isoforms in autophagy and LC3/GABARAP processing revealed in cells. *Autophagy*, *15*(6), 976–997. https://doi.org/10.1080/15548627.2019.1569925

4) Alexandrovich, A., Czisch, M., Frenkiel, T. A., Kelly, G. P., Goosen, N., Moolenaar, G. F., Chowdhry, B. Z., Sanderson, M. R., & Lane, A. N. (2001). Solution structure, hydrodynamics and thermodynamics of the UvrB C-terminal domain. *Journal of Biomolecular Structure & Dynamics*, *19*(2), 219–236. https://doi.org/10.1080/07391102.2001.10506734

5) Alexandrovich, A., Sanderson, M. R., Moolenaar, G. F., Goosen, N., & Lane, A. N. (1999). NMR assignments and secondary structure of the UvrC binding domain of UvrB. *FEBS Letters*, *451*(2), 181–185. https://doi.org/10.1016/S0014-5793(99)00542-6

6) Alkuraya, F. S., Cai, X., Emery, C., Mochida, G. H., Al-Dosari, M. S., Felie, J. M., Hill, R. S., Barry, B. J., Partlow, J. N., Gascon, G. G., Kentab, A., Jan, M., Shaheen, R., Feng, Y., & Walsh, C. A. (2011). Human Mutations in NDE1 Cause Extreme Microcephaly with Lissencephaly. *American Journal of Human Genetics*, *88*(5), 536. https://doi.org/10.1016/J.AJHG.2011.04.003

7) Altar, C. A., Jurata, L. W., Charles, V., Lemire, A., Liu, P., Bukhman, Y., Young, T. A., Bullard, J., Yokoe, H., Webster, M. J., Knable, M. B., & Brockman, J. A. (2005). Deficient hippocampal neuron expression of proteasome, ubiquitin, and mitochondrial genes in multiple schizophrenia cohorts. *Biological Psychiatry*, *58*(2), 85–96. https://doi.org/10.1016/J.BIOPSYCH.2005.03.031

8) Ameri, K., & Harris, A. L. (2008). Activating transcription factor 4. *The International Journal of Biochemistry & Cell Biology*, *40*(1), 14–21. https://doi.org/10.1016/J.BIOCEL.2007.01.020

9) American Psychiatric Association. (2013). *DIAGNOSTIC AND STATISTICAL MANUAL OF MENTAL DISORDERS* (5th ed.). American Psychiatric Publishing.

10) Ashton, A., & Jagannath, A. (2020). Disrupted Sleep and Circadian Rhythms in Schizophrenia and Their Interaction With Dopamine Signaling. *Frontiers in Neuroscience*, *14*. https://doi.org/10.3389/FNINS.2020.00636

11) Atkin, T. A., Brandon, N. J., & Kittler, J. T. (2012). Disrupted in schizophrenia 1 forms pathological aggresomes that disrupt its function in intracellular transport. *Human Molecular Genetics*, *21*(9), 2017–2028. https://doi.org/10.1093/hmg/dds018

12) Austin, C. P., Ky, B., Ma, L., Morris, J. A., & Shughrue, P. J. (2004). Expression of disrupted-in-schizophrenia-1, a schizophrenia-associated gene, is prominent in the mouse hippocampus throughout brain development. *Neuroscience*, *124*(1), 3–10. https://doi.org/10.1016/j.neuroscience.2003.11.010

13) Bader, V., Ottis, P., Pum, M., Huston, J. P., & Korth, C. (2012). Generation, purification, and characterization of cell-invasive DISC1 protein species. *Journal of Visualized Experiments*, *66*. https://doi.org/10.3791/4132

14) Bader, V., Tomppo, L., Trossbach, S. V., Bradshaw, N. J., Prikulis, I., Rutger Leliveld, S., Lin, C. Y., Ishizuka, K., Sawa, A., Ramos, A., Rosa, I., García, Å., Requena, J. R., Hipolito, M., Rai, N., Nwulia, E., Henning, U., Ferrea, S., Luckhaus, C., … Korth, C. (2012). Proteomic, genomic and translational approaches identify CRMP1 for a role in schizophrenia and its underlying traits. *Human Molecular Genetics*, *21*(20), 4406. https://doi.org/10.1093/HMG/DDS273

15) Balch, W. E., Morimoto, R. I., Dillin, A., & Kelly, J. W. (2008). Adapting proteostasis for disease intervention. *Science (New York, N.Y.)*, *319*(5865), 916–919. https://doi.org/10.1126/SCIENCE.1141448

16) Baleriola, J., Walker, C. A., Jean, Y. Y., Crary, J. F., Troy, C. M., Nagy, P. L., & Hengst, U. (2014). Axonally synthesized ATF4 transmits a neurodegenerative signal across brain regions. *Cell*, *158*(5), 1159–1172. https://doi.org/10.1016/J.CELL.2014.07.001

17) Barmaki, H., Nourazarian, A., & Khaki-Khatibi, F. (2023). Proteostasis and neurodegeneration: a closer look at autophagy in Alzheimer's disease. *Frontiers in Aging Neuroscience*, *15*, 1281338. https://doi.org/10.3389/FNAGI.2023.1281338/BIBTEX

18) Beeraka, N. M., Avila-Rodriguez, M. F., & Aliev, G. (2022). Recent Reports on Redox Stress-Induced Mitochondrial DNA Variations, Neuroglial Interactions, and NMDA Receptor System in Pathophysiology of Schizophrenia. *Molecular Neurobiology*, *59*(4), 2472–2496. https://doi.org/10.1007/S12035-021-02703-4

19) Bellen, H. J., Tong, C., & Tsuda, H. (2010). 100 years of Drosophila research and its impact on vertebrate neuroscience: a history lesson for the future. *Nature Reviews. Neuroscience*, *11*(7), 514. https://doi.org/10.1038/NRN2839

20) Bengesser, S. A., Reininghaus, E. Z., Dalkner, N., Birner, A., Hohenberger, H., Queissner, R., Fellendorf, F., Platzer, M., Pilz, R., Hamm, C., Rieger, A., Kapfhammer, H. P., Mangge, H., Reininghaus, B., Meier-Allard, N., Stracke, A., Fuchs, R., & Holasek, S. (2018). Endoplasmic reticulum stress in bipolar disorder? - BiP and CHOP gene expression- and XBP1 splicing analysis in peripheral blood. *Psychoneuroendocrinology*, *95*, 113–119. https://doi.org/10.1016/J.PSYNEUEN.2018.05.029

21) Bertolino, A., Crippa, D., Didio, S., Fichte, K., Musmeci, G., Porro, V., Rapisarda, V., Sastre-Y-Hernandez, M., & Schratzer, M. (1988). Rolipram versus imipramine in inpatients with major, "minor" or atypical depressive disorder: a double-blind double-dummy study aimed at testing a novel therapeutic approach. *International Clinical Psychopharmacology*, *3*(3), 245–253. https://doi.org/10.1097/00004850-198807000-00006

22) Bird, J. E., Barzik, M., Drummond, M. C., Sutton, D. C., Goodman, S. M., Morozko, E. L., Cole, S. M., Boukhvalova, A. K., Skidmore, J., Syam, D., Wilson, E. A., Fitzgerald, T., Rehman, A. U., Martin, D. M., Boger, E. T., Belyantseva, I. A., Friedman, T. B., & Blanchoin, L. (2017). Harnessing molecular motors for nanoscale pulldown in live cells. *Molecular Biology of the Cell*, *28*(3), 463–475. https://doi.org/10.1091/MBC.E16-08-0583

23) Blackwood, R., Fordyce, D. H., Walker, A., St Clair, M. T., Porteous, D. J., & Muir, W. J. (2001). Schizophrenia and Affective Disorders-Cosegregation with a Translocation at Chromosome 1q42 That Directly Disrupts Brain-Expressed Genes: Clinical and P300 Findings in a Family. In *Am. J. Hum. Genet* (Vol. 69).

24) Bleuler, E. (1911). Dementia praecox, oder Gruppe der Schizophrenien. *Franz Deuticke*.

25) Blum, A. L., Li, W., Cressy, M., & Dubnau, J. (2009). Short- and Long-Term Memory in Drosophila Require cAMP Signaling in Distinct Neuron Types. *Current Biology*, *19*(16), 1341–1350. https://doi.org/10.1016/J.CUB.2009.07.016

26) Bolger, G. B. (1994). Molecular biology of the cyclic AMP-specific cyclic nucleotide phosphodiesterases: a diverse family of regulatory enzymes. *Cellular Signalling*, *6*(8), 851–859. https://doi.org/10.1016/0898-6568(94)90018-3

27) Bolte, S., & Cordelières, F. P. (2006). A guided tour into subcellular colocalization analysis in light microscopy. *Journal of Microscopy*, *224*(Pt 3), 213–232. https://doi.org/10.1111/J.1365-2818.2006.01706.X

28) Bord, L., Wheeler, J., Paek, M., Saleh, M., Lyons-Warren, A., Ross, C. A., Sawamura, N., & Sawa, A. (2006). Primate disrupted-in-schizophrenia-1 (DISC1): high divergence of a gene for major mental illnesses in recent evolutionary history. *Neuroscience Research*, *56*(3), 286–293. https://doi.org/10.1016/J.NEURES.2006.07.010

29) Bousman, C. A., Luza, S., Mancuso, S. G., Kang, D., Opazo, C. M., Mostaid, M. S., Cropley, V., McGorry, P., Shannon Weickert, C., Pantelis, C., Bush, A. I., & Everall, I. P. (2019). Elevated ubiquitinated proteins in brain and blood of individuals with schizophrenia. *Scientific Reports 2019 9:1*, *9*(1), 1–8. https://doi.org/10.1038/s41598-019-38490-1

30) Bown, C., Wang, J. F., MacQueen, G., & Young, L. T. (2000). Increased temporal cortex ER stress proteins in depressed subjects who died by suicide. *Neuropsychopharmacology : Official Publication of the American College of Neuropsychopharmacology*, *22*(3), 327–332. https://doi.org/10.1016/S0893-133X(99)00091-3

31) Bradshaw, N. J. (2017). The interaction of schizophrenia-related proteins DISC1 and NDEL1, in light of the newly identified domain structure of DISC1. *Communicative & Integrative Biology*, *10*(4), e1335375. https://doi.org/10.1080/19420889.2017.1335375

32) Bradshaw, N. J., Bader, V., Prikulis, I., Lueking, A., Müllner, S., & Korth, C. (2014). Aggregation of the protein TRIOBP-1 and its potential relevance to schizophrenia. *PloS One*, *9*(10). https://doi.org/10.1371/JOURNAL.PONE.0111196

33) Bradshaw, N. J., Christie, S., Soares, D. C., Carlyle, B. C., Porteous, D. J., & Millar, J. K. (2009). NDE1 and NDEL1: Multimerisation, alternate splicing and DISC1 interaction. *Neuroscience Letters*, *449*(3), 228–233. https://doi.org/10.1016/j.neulet.2008.10.095

34) Bradshaw, N. J., & Hayashi, M. A. F. (2017). NDE1 and NDEL1 from genes to (mal)functions: parallel but distinct roles impacting on neurodevelopmental disorders and psychiatric illness. In *Cellular and Molecular Life Sciences* (Vol. 74, Issue 7, pp. 1191–1210). Birkhauser Verlag AG. https://doi.org/10.1007/s00018-016-2395-7

35) Bradshaw, N. J., Hennah, W., & Soares, D. C. (2013). NDE1 and NDEL1: Twin neurodevelopmental proteins with similar "nature" but different "nurture." In *Biomolecular Concepts* (Vol. 4, Issue 5, pp. 447–464). https://doi.org/10.1515/bmc-2013-0023

36) Bradshaw, N. J., & Korth, C. (2019). Protein misassembly and aggregation as potential convergence points for non-genetic causes of chronic mental illness. *Molecular Psychiatry*, *24*(7), 936–951. https://doi.org/10.1038/S41380-018-0133-2

37) Bradshaw, N. J., Ogawa, F., Antolin-Fontes, B., Chubb, J. E., Carlyle, B. C., Christie, S., Claessens, A., Porteous, D. J., & Millar, J. K. (2008). DISC1, PDE4B, and NDE1 at the centrosome and synapse. *Biochemical and Biophysical Research Communications*, *377*(4), 1091–1096. https://doi.org/10.1016/j.bbrc.2008.10.120

38) Bradshaw, N. J., & Porteous, D. J. (2012). DISC1-binding proteins in neural development, signalling and schizophrenia. *Neuropharmacology*, *62*(3), 1230–1241. https://doi.org/10.1016/J.NEUROPHARM.2010.12.027

39) Bradshaw, N. J., Soares, D. C., Carlyle, B. C., Ogawa, F., Davidson-Smith, H., Christie, S., Mackie, S., Thomson, P. A., Porteous, D. J., & Millar, J. K. (2011). Pka phosphorylation of NDE1 is DISC1/PDE4 dependent and modulates its interaction with LIS1 and NDEL1. *Journal of Neuroscience*, *31*(24), 9043–9054. https://doi.org/10.1523/JNEUROSCI.5410-10.2011

40) Bradshaw, N. J., Ukkola-Vuoti, L., Pankakoski, M., Zheutlin, A. B., Ortega-Alonso, A., Torniainen-Holm, M., Sinha, V., Therman, S., Paunio, T., Suvisaari, J., Lönnqvist, J., Cannon, T. D., Haukka, J., & Hennah, W. (2017). The NDE1 genomic locus can affect treatment of psychiatric illness through gene expression changes related to microRNA-484. *Open Biology*, *7*(11). https://doi.org/10.1098/rsob.170153

41) Brand, A. H., & Perrimon, N. (1993). Targeted gene expression as a means of altering cell fates and generating dominant phenotypes. *Development (Cambridge, England)*, *118*(2), 401–415. https://doi.org/10.1242/DEV.118.2.401

42) Brandon, N. J., Handford, E. J., Schurov, I., Rain, J. C., Pelling, M., Duran-Jimeniz, B., Camargo, L. M., Oliver, K. R., Beher, D., Shearman, M. S., & Whiting, P. J. (2004). Disrupted in Schizophrenia 1 and Nudel form a neurodevelopmentally regulated protein complex: Implications for schizophrenia and other major neurological disorders. *Molecular and Cellular Neuroscience*, *25*(1), 42–55. https://doi.org/10.1016/j.mcn.2003.09.009

43) Brandon, N. J., Kirsty Millar, J., Korth, C., Sive, H., Singh, K. K., & Sawa, A. (2009). *Understanding the Role of DISC1 in Psychiatric Disease and during Normal Development*. https://doi.org/10.1523/JNEUROSCI.3355-09.2009

44) Brandon, N. J., & Sawa, A. (2011). Linking neurodevelopmental and synaptic theories of mental illness through DISC1. In *Nature Reviews Neuroscience* (Vol. 12, Issue 12). https://doi.org/10.1038/nrn3120

45) Brandon, N. J., Schurov, I., Camargo, L. M., Handford, E. J., Duran-Jimeniz, B., Hunt, P., Millar, J. K., Porteous, D. J., Shearman, M. S., & Whiting, P. J. (2005). Subcellular targeting of DISC1 is dependent on a domain independent from the Nudel binding site. *Molecular and Cellular Neurosciences*, *28*(4), 613–624. https://doi.org/10.1016/J.MCN.2004.11.003

46) Burdick, K. E., Kamiya, A., Hodgkinson, C. A., Lencz, T., Derosse, P., Ishizuka, K., Elashvili, S., Arai, H., Goldman, D., Sawa, A., & Malhotra, A. K. (2008). Elucidating the relationship between DISC1, NDEL1 and NDE1 and the risk for schizophrenia: evidence of epistasis and competitive binding. *Human Molecular Genetics*, *17*(16), 2462–2473. https://doi.org/10.1093/HMG/DDN146

47) Byrne, S., Heverin, M., Elamin, M., Bede, P., Lynch, C., Kenna, K., Maclaughlin, R., Walsh, C., Al Chalabi, A., & Hardiman, O. (2013). Aggregation of neurologic and neuropsychiatric disease in amyotrophic lateral sclerosis kindreds: a population-based case-control cohort study of familial and sporadic amyotrophic lateral sclerosis. *Annals of Neurology*, *74*(5), 699–708. https://doi.org/10.1002/ANA.23969

48) Calarco, C. A., & Lobo, M. K. (2021). Depression and substance use disorders: Clinical comorbidity and shared neurobiology. *International Review of Neurobiology*, *157*, 245–309. https://doi.org/10.1016/BS.IRN.2020.09.004

49) Callicott, J. H., Straub, R. E., Pezawas, L., Egan, M. F., Mattay, V. S., Hariri, A. R., Verchinski, B. A., Meyer-Lindenberg, A., Balkissoon, R., Kolachana, B., Goldberg, T. E., & Weinberger, D. R. (2005). Variation in DISC1 affects hippocampal structure and function and increases risk for schizophrenia. *Proceedings of the National Academy of Sciences of the United States of America*, *102*(24), 8627. https://doi.org/10.1073/PNAS.0500515102

50) Camargo, L. M., Collura, V., Rain, J. C., Mizuguchi, K., Hermjakob, H., Kerrien, S., Bonnert, T. P., Whiting, P. J., & Brandon, N. J. (2007). Disrupted in Schizophrenia 1 Interactome: evidence for the close connectivity of risk genes and a potential synaptic basis for schizophrenia. *Molecular Psychiatry*, *12*(1), 74–86. https://doi.org/10.1038/SJ.MP.4001880

51) Campeau, E., Ruhl, V. E., Rodier, F., Smith, C. L., Rahmberg, B. L., Fuss, J. O., Campisi, J., Yaswen, P., Cooper, P. K., & Kaufman, P. D. (2009). A versatile viral system for expression and depletion of proteins in mammalian cells. *PloS One*, *4*(8). https://doi.org/10.1371/JOURNAL.PONE.0006529

52) Carlyle, B. C., MacKie, S., Christie, S., Millar, J. K., & Porteous, D. J. (2011). Co-ordinated action of DISC1, PDE4B and GSK3β in modulation of cAMP signalling. *Molecular Psychiatry*, *16*(7), 693–694. https://doi.org/10.1038/MP.2011.17

53) Cetin-Karayumak, S., Di Biase, M. A., Chunga, N., Reid, B., Somes, N., Lyall, A. E., Kelly, S., Solgun, B., Pasternak, O., Vangel, M., Pearlson, G., Tamminga, C., Sweeney, J. A., Clementz, B., Schretlen, D., Viher, P. V., Stegmayer, K., Walther, S., Lee, J., … Kubicki, M. (2019). White matter abnormalities across the lifespan of schizophrenia: a harmonized multi-site diffusion MRI study. *Molecular Psychiatry 2019 25:12*, *25*(12), 3208–3219. https://doi.org/10.1038/s41380-019-0509-y

54) Chen, A., Muzzio, I. A., Malleret, G., Bartsch, D., Verbitsky, M., Pavlidis, P., Yonan, A. L., Vronskaya, S., Grody, M. B., Cepeda, I., Gilliam, T. C., & Kandel, E. R. (2003). Inducible enhancement of memory storage and synaptic plasticity in transgenic mice

expressing an inhibitor of ATF4 (CREB-2) and C/EBP proteins. *Neuron*, *39*(4), 655–669. https://doi.org/10.1016/S0896-6273(03)00501-4

55) Chen, D., Fan, Z., Rauh, M., Buchfelder, M., Eyupoglu, I. Y., & Savaskan, N. (2017). ATF4 promotes angiogenesis and neuronal cell death and confers ferroptosis in a xCT-dependent manner. *Oncogene*, *36*(40), 5593. https://doi.org/10.1038/ONC.2017.146

56) Chen, M., Liu, Y., Yang, Y., Qiu, Y., Wang, Z., Li, X., & Zhang, W. (2022). Emerging roles of activating transcription factor (ATF) family members in tumourigenesis and immunity: Implications in cancer immunotherapy. *Genes & Diseases*, *9*(4), 981. https://doi.org/10.1016/J.GENDIS.2021.04.008

57) Chen, M. Y., Zhang, Q., Liu, Y. F., Zheng, W. Y., Si, T. L., Su, Z., Cheung, T., Jackson, T., Li, X. H., & Xiang, Y. T. (2023). Schizophrenia and oxidative stress from the perspective of bibliometric analysis. *Frontiers in Psychiatry*, *14*, 1145409. https://doi.org/10.3389/FPSYT.2023.1145409/BIBTEX

58) Chen, Y. M., Lin, C. H., & Lane, H. Y. (2022). Distinctively lower DISC1 mRNA levels in patients with schizophrenia, especially in those with higher positive, negative, and depressive symptoms. *Pharmacology Biochemistry and Behavior*, *213*, 173335. https://doi.org/10.1016/J.PBB.2022.173335

59) Cheng, L., Baonza, A., & Grifoni, D. (2018). Drosophila Models of Human Disease. *BioMed Research International*, *2018*. https://doi.org/10.1155/2018/7214974

60) Chérasse, Y., Maurin, A. C., Chaveroux, C., Jousse, C., Carraro, V., Parry, L., Deval, C., Chambon, C., Fafournoux, P., & Bruhat, A. (2007). The p300/CBP-associated factor (PCAF) is a cofactor of ATF4 for amino acid-regulated transcription of CHOP. *Nucleic Acids Research*, *35*(17), 5954. https://doi.org/10.1093/NAR/GKM642

61) Cherry, J. A., & Davis, R. L. (1999). Cyclic AMP phosphodiesterases are localized in regions of the mouse brain associated with reinforcement, movement, and affect. *The Journal of Comparative Neurology*, *407*(2), 287–301. https://doi.org/10.1002/(SICI)1096-9861(19990503)407:2<287::AID-CNE9>3.0.CO;2-R

62) Chong, H. Y., Teoh, S. L., Wu, D. B. C., Kotirum, S., Chiou, C. F., & Chaiyakunapruk, N. (2016). Global economic burden of schizophrenia: a systematic review. *Neuropsychiatric Disease and Treatment*, *12*, 357–373. https://doi.org/10.2147/NDT.S96649

63) Chubb, J. E., Bradshaw, N. J., Soares, D. C., Porteous, D. J., & Millar, J. K. (2008). The DISC locus in psychiatric illness. In *Molecular Psychiatry* (Vol. 13, Issue 1, pp. 36–64). https://doi.org/10.1038/sj.mp.4002106

64) Chuhma, N., Mingote, S., Moore, H., & Rayport, S. (2014). Dopamine neurons control striatal cholinergic neurons via regionally heterogeneous dopamine and glutamate signaling. *Neuron*, *81*(4), 901. https://doi.org/10.1016/J.NEURON.2013.12.027

65) Clapcote, S. J., Lipina, T. V., Millar, J. K., Mackie, S., Christie, S., Ogawa, F., Lerch, J. P., Trimble, K., Uchiyama, M., Sakuraba, Y., Kaneda, H., Shiroishi, T., Houslay, M. D., Henkelman, R. M., Sled, J. G., Gondo, Y., Porteous, D. J., & Roder, J. C. C. (2007). Behavioral phenotypes of Disc1 missense mutations in mice. *Neuron*, *54*(3), 387–402. https://doi.org/10.1016/J.NEURON.2007.04.015

66) Clark, L. A., Cuthbert, B., Lewis-Fernández, R., Narrow, W. E., & Reed, G. M. (2017). Three Approaches to Understanding and Classifying Mental Disorder: ICD-11, DSM-5,

and the National Institute of Mental Health's Research Domain Criteria (RDoC). *Psychological Science in the Public Interest*, *18*(2), 72–145. https://doi.org/10.1177/1529100617727266/ASSET/IMAGES/LARGE/10.1177_152910 0617727266-FIG1.JPEG

67) Conchillo-Solé, O., de Groot, N. S., Avilés, F. X., Vendrell, J., Daura, X., & Ventura, S. (2007). AGGRESCAN: A server for the prediction and evaluation of "hot spots" of aggregation in polypeptides. *BMC Bioinformatics*, *8*(1), 1–17. https://doi.org/10.1186/1471-2105-8-65/FIGURES/1

68) Cosgrave, J., Wulff, K., & Gehrman, P. (2018). Sleep, circadian rhythms, and schizophrenia: where we are and where we need to go. *Current Opinion in Psychiatry*, *31*(3), 176–182. https://doi.org/10.1097/YCO.0000000000000419

69) Cuenod, M., Steullet, P., Cabungcal, J. H., Dwir, D., Khadimallah, I., Klauser, P., Conus, P., & Do, K. Q. (2021). Caught in vicious circles: a perspective on dynamic feed-forward loops driving oxidative stress in schizophrenia. *Molecular Psychiatry 2021 27:4*, *27*(4), 1886–1897. https://doi.org/10.1038/s41380-021-01374-w

70) Cukkemane, A., Becker, N., Zielinski, M., Frieg, B., Lakomek, N. A., Heise, H., Schröder, G. F., Willbold, D., & Weiergräber, O. H. (2021). Conformational heterogeneity coupled with β-fibril formation of a scaffold protein involved in chronic mental illnesses. *Translational Psychiatry*, *11*(1). https://doi.org/10.1038/s41398-021-01765-1

71) Dai, H., Shen, K., Yang, Y., Su, X., Luo, Y., Jiang, Y., Shuai, L., Zheng, P., Chen, Z., & Bie, P. (2019). PUM1 knockdown prevents tumor progression by activating the PERK/eIF2/ATF4 signaling pathway in pancreatic adenocarcinoma cells. *Cell Death & Disease*, *10*(8). https://doi.org/10.1038/S41419-019-1839-Z

72) de Las Rivas, J., & Fontanillo, C. (2010). Protein–Protein Interactions Essentials: Key Concepts to Building and Analyzing Interactome Networks. *PLoS Computational Biology*, *6*(6), e1000807. https://doi.org/10.1371/JOURNAL.PCBI.1000807

73) Deng, Q. S., Dong, X. Y., Wu, H., Wang, W., Wang, Z. T., Zhu, J. W., Liu, C. F., Jia, W. Q., Zhang, Y., Schachner, M., Ma, Q. H., & Xu, R. X. (2016). Disrupted-in-Schizophrenia-1 Attenuates Amyloid-β Generation and Cognitive Deficits in APP/PS1 Transgenic Mice by Reduction of β-Site APP-Cleaving Enzyme 1 Levels. *Neuropsychopharmacology : Official Publication of the American College of Neuropsychopharmacology*, *41*(2), 440–453. https://doi.org/10.1038/NPP.2015.164

74) Derewenda, U., Tarricone, C., Choi, W. C., Cooper, D. R., Lukasik, S., Perrina, F., Tripathy, A., Kim, M. H., Cafiso, D. S., Musacchio, A., & Derewenda, Z. S. (2007). The structure of the coiled-coil domain of Ndel1 and the basis of its interaction with Lis1, the causal protein of Miller-Dieker lissencephaly. *Structure (London, England : 1993)*, *15*(11), 1467–1481. https://doi.org/10.1016/J.STR.2007.09.015

75) DeRosse, P., Hodgkinson, C. A., Lencz, T., Burdick, K. E., Kane, J. M., Goldman, D., & Malhotra, A. K. (2007). Disrupted in schizophrenia 1 genotype and positive symptoms in schizophrenia. *Biological Psychiatry*, *61*(10), 1208–1210. https://doi.org/10.1016/J.BIOPSYCH.2006.07.023

76) Di Giorgio, A., Blasi, G., Sambataro, F., Rampino, A., Papazacharias, A., Gambi, F., Romano, R., Caforio, G., Rizzo, M., Latorre, V., Popolizio, T., Kolachana, B., Callicott,

J. H., Nardini, M., Weinberger, D. R., & Bertolino, A. (2008). Association of the Ser704Cys DISC1 polymorphism with human hippocampal formation gray matter and function during memory encoding. *The European Journal of Neuroscience*, *28*(10), 2129. https://doi.org/10.1111/J.1460-9568.2008.06482.X

77) Dickerson, F., Jones-Brando, L., Ford, G., Genovese, G., Stallings, C., Origoni, A., O'Dushlaine, C., Katsafanas, E., Sweeney, K., Khushalani, S., & Yolken, R. (2019). Schizophrenia is Associated With an Aberrant Immune Response to Epstein–Barr Virus. *Schizophrenia Bulletin*, *45*(5), 1112–1119. https://doi.org/10.1093/SCHBUL/SBY164

78) Drain, P., Folkers, E., & Quinn, W. G. (1991). cAMP-dependent protein kinase and the disruption of learning in transgenic flies. *Neuron*, *6*(1), 71–82. https://doi.org/10.1016/0896-6273(91)90123-H

79) Dujardin, D. L., Barnhart, L. E., Stehman, S. A., Gomes, E. R., Gundersen, G. G., & Vallee, R. B. (2003). A role for cytoplasmic dynein and LIS1 in directed cell movement. *The Journal of Cell Biology*, *163*(6), 1205. https://doi.org/10.1083/JCB.200310097

80) Ekelund, J., Hennah, W., Hiekkalinna, T., Parker, A., Meyer, J., Lönnqvist, J., & Peltonen, L. (2004). Replication of 1q42 linkage in Finnish schizophrenia pedigrees. *Molecular Psychiatry*, *9*(11), 1037–1041. https://doi.org/10.1038/SJ.MP.4001536

81) Ekelund, J., Lichtermann, D., Hovatta, I., Ellonen, P., Suvisaari, J., Terwilliger, J. D., Juvonen, H., Varilo, T., Arajärvi, R., Kokko-Sahin, M. L., Lönnqvist, J., & Peltonen, L. (2000). Genome-wide scan for schizophrenia in the Finnish population: evidence for a locus on chromosome 7q22. *Human Molecular Genetics*, *9*(7), 1049–1057. https://doi.org/10.1093/HMG/9.7.1049

82) Ellis, N., Tee, A., McAllister, B., Massey, T., McLauchlan, D., Stone, T., Correia, K., Loupe, J., Kim, K. H., Barker, D., Hong, E. P., Chao, M. J., Long, J. D., Lucente, D., Vonsattel, J. P. G., Pinto, R. M., Elneel, K. A., Ramos, E. M., Mysore, J. S., … Holmans, P. (2020). Genetic Risk Underlying Psychiatric and Cognitive Symptoms in Huntington's Disease. *Biological Psychiatry*, *87*(9), 857–865. https://doi.org/10.1016/j.biopsych.2019.12.010

83) Elpers, H., Teismann, H., Wellmann, J., Berger, K., Karch, A., & Rübsamen, N. (2023). Major depressive disorders increase the susceptibility to self-reported infections in two German cohort studies. *Social Psychiatry and Psychiatric Epidemiology*, *58*(2), 277. https://doi.org/10.1007/S00127-022-02328-5

84) Emanuel, J. E., Lopez, O. L., Houck, P. R., Becker, J. T., Weamer, E. A., Demichele-Sweet, M. A. A., Kuller, L., & Sweet, R. A. (2011). Trajectory of cognitive decline as a predictor of psychosis in early Alzheimer disease in the cardiovascular health study. *The American Journal of Geriatric Psychiatry : Official Journal of the American Association for Geriatric Psychiatry*, *19*(2), 160–168. https://doi.org/10.1097/JGP.0B013E3181E446C8

85) Emes, R. D., & Ponting, C. P. (2001). A new sequence motif linking lissencephaly, Treacher Collins and oral-facial-digital type 1 syndromes, microtubule dynamics and cell migration. *Human Molecular Genetics*, *10*(24), 2813–2820. https://doi.org/10.1093/HMG/10.24.2813

86) Emily, M., Talvas, A., & Delamarche, C. (2013). MetAmyl: A METa-Predictor for AMYLoid Proteins. *PLOS ONE*, *8*(11), e79722. https://doi.org/10.1371/JOURNAL.PONE.0079722

87) Endo, R., Takashima, N., Nekooki-Machida, Y., Komi, Y., Hui, K. K. W., Takao, M., Akatsu, H., Murayama, S., Sawa, A., & Tanaka, M. (2018). TAR DNA-Binding Protein 43 and Disrupted in Schizophrenia 1 Coaggregation Disrupts Dendritic Local Translation and Mental Function in Frontotemporal Lobar Degeneration. *Biological Psychiatry*, *84*(7), 509–521. https://doi.org/10.1016/j.biopsych.2018.03.008

88) Ensembl genome browser 112. (2024). *Gene: DISC1 (ENSG00000162946) - Orthologues - Homo_sapiens*. https://www.ensembl.org/Homo_sapiens/Gene/Compara_Ortholog?db=core;g=ENSG00 000162946;r=1:231626790-232041272

89) Eykelenboom, J. E., Briggs, G. J., Bradshaw, N. J., Soares, D. C., Ogawa, F., Christie, S., Malavasi, E. L. V., Makedonopoulou, P., Mackie, S., Malloy, M. P., Wear, M. A., Blackburn, E. A., Bramham, J., Mcintosh, A. M., Blackwood, D. H., Muir, W. J., Porteous, D. J., & Millar, J. K. (2012). A t(1;11) translocation linked to schizophrenia and affective disorders gives rise to aberrant chimeric DISC1 transcripts that encode structurally altered, deleterious mitochondrial proteins. *Human Molecular Genetics*, *21*(15), 3374–3386. https://doi.org/10.1093/hmg/dds169

90) Eyles, D., Feldon, J., & Meyer, U. (2012). Schizophrenia: do all roads lead to dopamine or is this where they start? Evidence from two epidemiologically informed developmental rodent models. *Translational Psychiatry*, *2*(2), e81. https://doi.org/10.1038/TP.2012.6

91) Fatemi, S. H., King, D. P., Reutiman, T. J., Folsom, T. D., Laurence, J. A., Lee, S., Fan, Y. T., Paciga, S. A., Conti, M., & Menniti, F. S. (2008). PDE4B polymorphisms and decreased PDE4B expression are associated with schizophrenia. *Schizophrenia Research*, *101*(1–3), 36–49. https://doi.org/10.1016/J.SCHRES.2008.01.029

92) Faulkner, N. E., Dujardin, D. L., Tai, C. Y., Vaughan, K. T., O'connell, C. B., Wang, Y. L., & Vallee, R. B. (2000). A role for the lissencephaly gene LIS1 in mitosis and cytoplasmic dynein function. *Nature Cell Biology*, *2*(11), 784–791. https://doi.org/10.1038/35041020

93) Feany, M. B., & Bender, W. W. (2000). A Drosophila model of Parkinson's disease. *Nature 2000 404:6776*, *404*(6776), 394–398. https://doi.org/10.1038/35006074

94) Feng, L., Li, M., Hu, X., Li, Y., Zhu, L., Chen, M., Wei, Q., Xu, W., Zhou, Q., Wang, W., Chen, D., Wang, X., & Jin, H. (2021). CK1δ stimulates ubiquitination-dependent proteasomal degradation of ATF4 to promote chemoresistance in gastric Cancer. *Clinical and Translational Medicine*, *11*(10), e587. https://doi.org/10.1002/CTM2.587

95) Feng, Y., Olson, E. C., Stukenberg, P. T., Flanagan, L. A., Kirschner, M. W., & Walsh, C. A. (2000). LIS1 regulates CNS lamination by interacting with mNudE, a central component of the centrosome. *Neuron*, *28*(3), 665–679. https://doi.org/10.1016/S0896-6273(00)00145-8

96) Feng, Y., & Walsh, C. A. (2004). Mitotic spindle regulation by Nde1 controls cerebral cortical size. *Neuron*, *44*(2), 279–293. https://doi.org/10.1016/j.neuron.2004.09.023

97) Fernandez-Escamilla, A. M., Rousseau, F., Schymkowitz, J., & Serrano, L. (2004). Prediction of sequence-dependent and mutational effects on the aggregation of peptides and proteins. *Nature Biotechnology*, *22*(10), 1302–1306. https://doi.org/10.1038/NBT1012

98) Fertig, B. A., & Baillie, G. S. (2018). PDE4-Mediated cAMP Signalling. *Journal of Cardiovascular Development and Disease*, *5*(1). https://doi.org/10.3390/JCDD5010008

99) Flores, R., Hirota, Y., Armstrong, B., Sawa, A., & Tomoda, T. (2011). DISC1 regulates synaptic vesicle transport via a lithium-sensitive pathway. *Neuroscience Research*, *71*(1), 71–77. https://doi.org/10.1016/J.NEURES.2011.05.014

100) Freeman, D., & Waite, F. (2025). Sleep and circadian difficulties in schizophrenia: presentations, understanding, and treatment. *Psychological Medicine*, *55*, e47. https://doi.org/10.1017/S0033291725000297

101) French, A. S., Geissmann, Q., Beckwith, E. J., & Gilestro, G. F. (2021). Sensory processing during sleep in Drosophila melanogaster. *Nature 2021 598:7881*, *598*(7881), 479–482. https://doi.org/10.1038/s41586-021-03954-w

102) Fuentes-Villalobos, F., Farkas, C., Riquelme-Barrios, S., Armijo, M. E., Soto-Rifo, R., Pincheira, R., & Castro, A. F. (2019). DISC1 promotes translation maintenance during sodium arsenite-induced oxidative stress. *Biochimica et Biophysica Acta. Gene Regulatory Mechanisms*, *1862*(6), 657–669. https://doi.org/10.1016/J.BBAGRM.2019.05.001

103) Furukubo-Tokunaga, K. (2009). Modeling schizophrenia in flies. *Progress in Brain Research*, *179*(C), 107–115. https://doi.org/10.1016/S0079-6123(09)17912-8

104) Furukubo-Tokunaga, K., Kurita, K., Honjo, K., Pandey, H., Ando, T., Takayama, K., Arai, Y., Mochizuki, H., Ando, M., Kamiya, A., & Sawa, A. (2016). DISC1 causes associative memory and neurodevelopmental defects in fruit flies. *Molecular Psychiatry*, *21*(9), 1232–1243. https://doi.org/10.1038/mp.2016.15

105) Fusakio, M. E., Willy, J. A., Wang, Y., Mirek, E. T., Baghdadi, R. J. T. A., Adams, C. M., Anthony, T. G., & Wek, R. C. (2016). Transcription factor ATF4 directs basal and stress-induced gene expression in the unfolded protein response and cholesterol metabolism in the liver. *Molecular Biology of the Cell*, *27*(9), 1536–1551. https://doi.org/10.1091/MBC.E16-01-0039

106) Fusar-Poli, P., & Meyer-Lindenberg, A. (2013). Striatal Presynaptic Dopamine in Schizophrenia, Part II: Meta-Analysis of [18F/11C]-DOPA PET Studies. *Schizophrenia Bulletin*, *39*(1), 33. https://doi.org/10.1093/SCHBUL/SBR180

107) Gabilondo, A., Alonso-Moran, E., Nuño-Solinis, R., Orueta, J. F., & Iruin, A. (2017). Comorbidities with chronic physical conditions and gender profiles of illness in schizophrenia. Results from PREST, a new health dataset. *Journal of Psychosomatic Research*, *93*, 102–109. https://doi.org/10.1016/J.JPSYCHORES.2016.12.011

108) Ganetzky, B., & Flanagan, J. R. (1978). On the relationship between senescence and age-related changes in two wild-type strains of Drosophila melanogaster. *Experimental Gerontology*, *13*(3–4), 189–196. https://doi.org/10.1016/0531-5565(78)90012-8

109) Garbuzynskiy, S. O., Lobanov, M. Y., & Galzitskaya, O. V. (2010). FoldAmyloid: a method of prediction of amyloidogenic regions from protein sequence. *Bioinformatics*, *26*(3), 326–332. https://doi.org/10.1093/BIOINFORMATICS/BTP691

110) García-Bea, A., Miranda-Azpiazu, P., Muguruza, C., Marmolejo-Martinez-Artesero, S., Diez-Alarcia, R., Gabilondo, A. M., Callado, L. F., Morentin, B., González-Maeso, J., & Meana, J. J. (2019). Serotonin 5-HT2A receptor expression and functionality in postmortem frontal cortex of subjects with schizophrenia: Selective biased agonism via Gαi1-proteins. *European Neuropsychopharmacology*, *29*(12), 1453–1463. https://doi.org/10.1016/J.EURONEURO.2019.10.013

111) Garcia-Lopez, R., Pombero, A., Estirado, A., Geijo-Barrientos, E., & Martinez, S. (2021). Interneuron Heterotopia in the Lis1 Mutant Mouse Cortex Underlies a Structural and Functional Schizophrenia-Like Phenotype. *Frontiers in Cell and Developmental Biology*, *9*, 693919. https://doi.org/10.3389/FCELL.2021.693919/BIBTEX

112) Gargano, J., Martin, I., Bhandari, P., & Grotewiel, M. (2005). Rapid iterative negative geotaxis (RING): a new method for assessing age-related locomotor decline in. *Experimental Gerontology*, *40*(5), 386–395. https://doi.org/10.1016/j.exger.2005.02.005

113) Grabham, P. W., Seale, G. E., Bennecib, M., Goldberg, D. J., & Vallee, R. B. (2007). Cytoplasmic Dynein and LIS1 Are Required for Microtubule Advance during Growth Cone Remodeling and Fast Axonal Outgrowth. *Journal of Neuroscience*, *27*(21), 5823–5834. https://doi.org/10.1523/JNEUROSCI.1135-07.2007

114) Greenwood, T. A., Swerdlow, N. R., Gur, R. E., Cadenhead, K. S., Calkins, M. E., Dobie, D. J., Freedman, R., Green, M. F., Gur, R. C., Lazzeroni, L. C., Nuechterlein, K. H., Olincy, A., Radant, A. D., Ray, A., Schork, N. J., Seidman, L. J., Siever, L. J., Silverman, J. M., Stone, W. S., … Braff, D. L. (2013). Genome-Wide Linkage Analyses of 12 Endophenotypes for Schizophrenia From the Consortium on the Genetics of Schizophrenia. *The American Journal of Psychiatry*, *170*(5), 521–532. https://doi.org/10.1176/APPI.AJP.2012.12020186

115) Gusev, A., Mancuso, N., Won, H., Kousi, M., Finucane, H. K., Reshef, Y., Song, L., Safi, A., McCarroll, S., Neale, B. M., Ophoff, R. A., O'Donovan, M. C., Crawford, G. E., Geschwind, D. H., Katsanis, N., Sullivan, P. F., Pasaniuc, B., & Price, A. L. (2018). Transcriptome-wide association study of schizophrenia and chromatin activity yields mechanistic disease insights. *Nature Genetics*, *50*(4), 538. https://doi.org/10.1038/S41588-018-0092-1

116) Hai, T., & Hartman, M. G. (2001). The molecular biology and nomenclature of the activating transcription factor/cAMP responsive element binding family of transcription factors: activating transcription factor proteins and homeostasis. *Gene*, *273*(1), 1–11. https://doi.org/10.1016/S0378-1119(01)00551-0

117) Hall, L. S., Pain, O., O'Brien, H. E., Anney, R., Walters, J. T. R., Owen, M. J., O'Donovan, M. C., & Bray, N. J. (2021). Cis-effects on gene expression in the human prenatal brain associated with genetic risk for neuropsychiatric disorders. *Molecular Psychiatry*, *26*(6), 2082. https://doi.org/10.1038/S41380-020-0743-3

118) Hamburg, H., Trossbach, S. V., Bader, V., Chwiesko, C., Kipar, A., Sauvage, M., Crum, W. R., Vernon, A. C., Bidmon, H. J., & Korth, C. (2016). Simultaneous effects on parvalbumin-positive interneuron and dopaminergic system development in a transgenic rat model for sporadic schizophrenia. *Scientific Reports*, *6*. https://doi.org/10.1038/srep34946

119) Hamshere, M. L., Bennett, P., Williams, N., Segurado, R., Cardno, A., Norton, N., Lambert, D., Williams, H., Kirov, G., Corvin, A., Holmans, P., Jones, L., Jones, I., Gill,

M., O'Donovan, M. C., Owen, M. J., & Craddock, N. (2005). Genomewide linkage scan in schizoaffective disorder: significant evidence for linkage at 1q42 close to DISC1, and suggestive evidence at 22q11 and 19p13. *Archives of General Psychiatry*, *62*(10), 1081–1088. https://doi.org/10.1001/ARCHPSYC.62.10.1081

120) Han, J., Back, S. H., Hur, J., Lin, Y. H., Gildersleeve, R., Shan, J., Yuan, C. L., Krokowski, D., Wang, S., Hatzoglou, M., Kilberg, M. S., Sartor, M. A., & Kaufman, R. J. (2013). ER-stress-induced transcriptional regulation increases protein synthesis leading to cell death. *Nature Cell Biology*, *15*(5), 481–490. https://doi.org/10.1038/NCB2738

121) Hartley, J. L., Temple, G. F., & Brasch, M. A. (2000). DNA Cloning Using In Vitro Site-Specific Recombination. *Genome Research*, *10*(11), 1788. https://doi.org/10.1101/GR.143000

122) Hashimoto, K., Fukushima, T., Shimizu, E., Komatsu, N., Watanabe, H., Shinoda, N., Nakazato, M., Kumakiri, C., Okada, S. I., Hasegawa, H., Imai, K., & Iyo, M. (2003). Decreased serum levels of D-serine in patients with schizophrenia: evidence in support of the N-methyl-D-aspartate receptor hypofunction hypothesis of schizophrenia. *Archives of General Psychiatry*, *60*(6), 572–576. https://doi.org/10.1001/ARCHPSYC.60.6.572

123) Hashimoto, R., Numakawa, T., Ohnishi, T., Kumamaru, E., Yagasaki, Y., Ishimoto, T., Mori, T., Nemoto, K., Adachi, N., Izumi, A., Chiba, S., Noguchi, H., Suzuki, T., Iwata, N., Ozaki, N., Taguchi, T., Kamiya, A., Kosuga, A., Tatsumi, M., … Kunugi, H. (2006). Impact of the DISC1 Ser704Cys polymorphism on risk for major depression, brain morphology and ERK signaling. *Human Molecular Genetics*, *15*(20), 3024–3033. https://doi.org/10.1093/HMG/DDL244

124) Hattori, M., Adachi, H., Tsujimoto, M., Arai, H., & Inoue, K. (1994). Miller-Dieker lissencephaly gene encodes a subunit of brain platelet-activating factor acetylhydrolase [corrected]. *Nature*, *370*(6486), 216–218. https://doi.org/10.1038/370216A0

125) Hawken, E. R., & Beninger, R. J. (2014). The amphetamine sensitization model of schizophrenia symptoms and its effect on schedule-induced polydipsia in the rat. *Psychopharmacology*, *231*(9), 2001–2008. https://doi.org/10.1007/S00213-013-3345-9

126) Hayashi-Takagi, A., Takaki, M., Graziane, N., Seshadri, S., Murdoch, H., Dunlop, A. J., Makino, Y., Seshadri, A. J., Ishizuka, K., Srivastava, D. P., Xie, Z., Baraban, J. M., Houslay, M. D., Tomoda, T., Brandon, N. J., Kamiya, A., Yan, Z., Penzes, P., & Sawa, A. (2010). Disrupted-in-Schizophrenia 1 (DISC1) regulates spines of the glutamate synapse via Rac1. *Nature Neuroscience*, *13*(3), 327–332. https://doi.org/10.1038/NN.2487

127) Hendricks, J. C., Finn, S. M., Panckeri, K. A., Chavkin, J., Williams, J. A., Sehgal, A., & Pack, A. I. (2000). Rest in Drosophila is a sleep-like state. *Neuron*, *25*(1), 129–138. https://doi.org/10.1016/S0896-6273(00)80877-6

128) Hendricks, J. C., Williams, J. A., Panckeri, K., Kirk, D., Tello, M., Yin, J. C. P., & Sehgal, A. (2001). A non-circadian role for cAMP signaling and CREB activity in Drosophila rest homeostasis. *Nature Neuroscience 2001 4:11*, *4*(11), 1108–1115. https://doi.org/10.1038/nn743

129) Hennah, W., Thomson, P., McQuillin, A., Bass, N., Loukola, A., Anjorin, A., Blackwood, D., Curtis, D., Deary, I. J., Harris, S. E., Isometsä, E. T., Lawrence, J., Lönnqvist, J., Muir, W., Palotie, A., Partonen, T., Paunio, T., Pylkkö, E., Robinson, M., … Porteous, D.

(2009). DISC1 association, heterogeneity and interplay in schizophrenia and bipolar disorder. *Molecular Psychiatry*, *14*(9), 865–873. https://doi.org/10.1038/MP.2008.22

130) Hennah, W., Tomppo, L., Hiekkalinna, T., Palo, O. M., Kilpinen, H., Ekelund, J., Tuulio-Henriksson, A., Silander, K., Partonen, T., Paunio, T., Terwilliger, J. D., Lönnqvist, J., & Peltonen, L. (2007). Families with the risk allele of DISC1 reveal a link between schizophrenia and another component of the same molecular pathway, NDE1. *Human Molecular Genetics*, *16*(5), 453–462. https://doi.org/10.1093/HMG/DDL462

131) Herrmann, F., Hessmann, M., Schaertl, S., Berg-Rosseburg, K., Brown, C. J., Bursow, G., Chiki, A., Ebneth, A., Gehrmann, M., Hoeschen, N., Hotze, M., Jahn, S., Johnson, P. D., Khetarpal, V., Kiselyov, A., Kottig, K., Ladewig, S., Lashuel, H., Letschert, S., … Bard, J. A. (2021). Pharmacological characterization of mutant huntingtin aggregate-directed PET imaging tracer candidates. *Scientific Reports 2021 11:1*, *11*(1), 1–19. https://doi.org/10.1038/s41598-021-97334-z

132) Hilker, R., Helenius, D., Fagerlund, B., Skytthe, A., Christensen, K., Werge, T. M., Nordentoft, M., & Glenthøj, B. (2018). Heritability of Schizophrenia and Schizophrenia Spectrum Based on the Nationwide Danish Twin Register. *Biological Psychiatry*, *83*(6), 492–498. https://doi.org/10.1016/j.biopsych.2017.08.017

133) Hill, E. V., Houslay, M. D., & Baillie, G. S. (2005). Investigation of extracellular signal-regulated kinase 2 mitogen-activated protein kinase phosphorylation and regulation of activity of PDE4 cyclic adenosine monophosphate-specific phosphodiesterases. *Methods in Molecular Biology (Clifton, N.J.)*, *307*, 225–237. https://doi.org/10.1385/1-59259-839-0:225

134) Hipp, M. S., Kasturi, P., & Hartl, F. U. (2019). The proteostasis network and its decline in ageing. *Nature Reviews Molecular Cell Biology 2019 20:7*, *20*(7), 421–435. https://doi.org/10.1038/s41580-019-0101-y

135) Hirotsune, S., Fleck, M. W., Gambello, M. J., Bix, G. J., Chen, A., Clark, G. D., Ledbetter, D. H., McBain, C. J., & Wynshaw-Boris, A. (1998). Graded reduction of Pafah1b1 (Lis1) activity results in neuronal migration defects and early embryonic lethality. *Nature Genetics*, *19*(4), 333–339. https://doi.org/10.1038/1221

136) Houslay, M. D., & Adams, D. R. (2003). PDE4 cAMP phosphodiesterases: modular enzymes that orchestrate signalling cross-talk, desensitization and compartmentalization. *The Biochemical Journal*, *370*(Pt 1), 1–18. https://doi.org/10.1042/BJ20021698

137) Hovatta, I., Varilo, T., Suvisaari, J., Terwilliger, J. D., Ollikainen, V., Arajärvi, R., Juvonen, H., Kokko-Sahin, M. L., Väisänen, L., Mannila, H., Lönnqvist, J., & Peltonen, L. (1999). A Genomewide Screen for Schizophrenia Genes in an Isolated Finnish Subpopulation, Suggesting Multiple Susceptibility Loci. *American Journal of Human Genetics*, *65*(4), 1114. https://doi.org/10.1086/302567

138) Howes, O. D., Bose, S. K., Turkheimer, F., Valli, I., Egerton, A., Valmaggia, L. R., Murray, R. M., & McGuire, P. (2011). Dopamine synthesis capacity before onset of psychosis: a prospective [18F]-DOPA PET imaging study. *The American Journal of Psychiatry*, *168*(12), 1311–1317. https://doi.org/10.1176/APPI.AJP.2011.11010160

139) Howes, O. D., Kambeitz, J., Kim, E., Stahl, D., Slifstein, M., Abi-Dargham, A., & Kapur, S. (2012). The nature of dopamine dysfunction in schizophrenia and what this means for

treatment. *Archives of General Psychiatry*, *69*(8), 776–786. https://doi.org/10.1001/ARCHGENPSYCHIATRY.2012.169

140) Howes, O. D., Williams, M., Ibrahim, K., Leung, G., Egerton, A., McGuire, P. K., & Turkheimer, F. (2013). Midbrain dopamine function in schizophrenia and depression: a post-mortem and positron emission tomographic imaging study. *Brain*, *136*(11), 3242. https://doi.org/10.1093/BRAIN/AWT264

141) Hui, K. K., Endo, R., Sawa, A., & Tanaka, M. (2022). A perspective on the potential involvement of impaired proteostasis in neuropsychiatric disorders. *Biological Psychiatry*, *91*(4), 335. https://doi.org/10.1016/J.BIOPSYCH.2021.09.001

142) Hunter, I., Coulson, B., Zarin, A. A., & Baines, R. A. (2021). The Drosophila Larval Locomotor Circuit Provides a Model to Understand Neural Circuit Development and Function. *Frontiers in Neural Circuits*, *15*. https://doi.org/10.3389/FNCIR.2021.684969

143) Hwu, H. G., Liu, C. M., Fann, C. S. J., Ou-Yang, W. C., & Lee, S. F. C. (2003). Linkage of schizophrenia with chromosome 1q loci in Taiwanese families. *Molecular Psychiatry*, *8*(4), 445–452. https://doi.org/10.1038/SJ.MP.4001235

144) IHME. (2024). *Global Health Disease Burden* . https://vizhub.healthdata.org/gbd-results/

145) Imai, Y., Soda, M., Inoue, H., Hattori, N., Mizuno, Y., & Takahashi, R. (2001). An unfolded putative transmembrane polypeptide, which can lead to endoplasmic reticulum stress, is a substrate of Parkin. *Cell*, *105*(7), 891–902. https://doi.org/10.1016/S0092-8674(01)00407-X

146) Ingason, A., Rujescu, D., Cichon, S., Sigurdsson, E., Sigmundsson, T., Pietiläinen, O. P. H., Buizer-Voskamp, J. E., Strengman, E., Francks, C., Muglia, P., Gylfason, A., Gustafsson, O., Olason, P. I., Steinberg, S., Hansen, T., Jakobsen, K. D., Rasmussen, H. B., Giegling, I., Möller, H. J., … Clair, D. M. S. (2011). Copy number variations of chromosome 16p13.1 region associated with schizophrenia. *Molecular Psychiatry*, *16*(1), 17. https://doi.org/10.1038/MP.2009.101

147) Ishizuka, K., Kamiya, A., Oh, E. C., Kanki, H., Seshadri, S., Robinson, J. F., Murdoch, H., Dunlop, A. J., Kubo, K. I., Furukori, K., Huang, B., Zeledon, M., Hayashi-Takagi, A., Okano, H., Nakajima, K., Houslay, M. D., Katsanis, N., & Sawa, A. (2011). DISC1-dependent switch from progenitor proliferation to migration in the developing cortex. *Nature 2011 473:7345*, *473*(7345), 92–96. https://doi.org/10.1038/nature09859

148) Jaaro-Peled, H., Altimus, C., LeGates, T., Cash-Padgett, T., Zoubovsky, S., Hikida, T., Ishizuka, K., Hattar, S., Mongrain, V., & Sawa, A. (2016). Abnormal wake/sleep pattern in a novel gain-of-function model of DISC1. *Neuroscience Research*, *112*, 63–69. https://doi.org/10.1016/j.neures.2016.06.006

149) Jaaro-Peled, H., Niwa, M., Foss, C. A., Murai, R., Reyes, S. de los, Kamiya, A., Mateo, Y., O'Donnell, P., Cascella, N. G., Nabeshima, T., Guilarte, T. R., Pomper, M. G., & Sawa, A. (2013). Subcortical dopaminergic deficits in a DISC1 mutant model: a study in direct reference to human molecular brain imaging. *Human Molecular Genetics*, *22*(8), 1574–1580. https://doi.org/10.1093/HMG/DDT007

150) Jacobi, A. A., Halawani, S., Lynch, D. R., & Lin, H. (2019). Neuronal serine racemase associates with Disrupted-In-Schizophrenia-1 and DISC1 agglomerates: Implications for schizophrenia. *Neuroscience Letters*, *692*, 107–114. https://doi.org/10.1016/j.neulet.2018.10.055

151) James, R., Adams, R. R., Christie, S., Buchanan, S. R., Porteous, D. J., & Millar, J. K. (2004). Disrupted in Schizophrenia 1 (DISC1) is a multicompartmentalized protein that predominantly localizes to mitochondria. *Molecular and Cellular Neuroscience*, *26*(1), 112–122. https://doi.org/10.1016/j.mcn.2004.01.013

152) Jankowsky, J. L., Fadale, D. J., Anderson, J., Xu, G. M., Gonzales, V., Jenkins, N. A., Copeland, N. G., Lee, M. K., Younkin, L. H., Wagner, S. L., Younkin, S. G., & Borchelt, D. R. (2004). Mutant presenilins specifically elevate the levels of the 42 residue beta-amyloid peptide in vivo: evidence for augmentation of a 42-specific gamma secretase. *Human Molecular Genetics*, *13*(2), 159–170. https://doi.org/10.1093/HMG/DDH019

153) Jennings, B. H. (2011). Drosophila-a versatile model in biology & medicine. In *Materials Today* (Vol. 14, Issue 5, pp. 190–195). https://doi.org/10.1016/S1369-7021(11)70113-4

154) Jiang, Z., Belforte, J. E., Lu, Y., Yabe, Y., Pickel, J., Smith, C. B., Je, H. S., Lu, B., & Nakazawa, K. (2010). eIF2alpha Phosphorylation-dependent translation in CA1 pyramidal cells impairs hippocampal memory consolidation without affecting general translation. *The Journal of Neuroscience : The Official Journal of the Society for Neuroscience*, *30*(7), 2582–2594. https://doi.org/10.1523/JNEUROSCI.3971-09.2010

155) Johnstone, M., MacLean, A., Heyrman, L., Lenaerts, A.-S., Nordin, A., Nilsson, L.-G., Rijk, P. De, Goossens, D., Adolfsson, R., Clair, D. M. St., Hall, J., Lawrie, S. M., McIntosh, A. M., Del-Favero, J., Blackwood, D. H. R., & Pickard, B. S. (2015). Copy Number Variations in DISC1 and DISC1-Interacting Partners in Major Mental Illness. *Molecular Neuropsychiatry*, *1*(3), 175. https://doi.org/10.1159/000438788

156) Jordan, K. W., Morgan, T. J., & Mackay, T. F. C. (2006). Quantitative Trait Loci for Locomotor Behavior in Drosophila melanogaster. *Genetics*, *174*(1), 271–284. https://doi.org/10.1534/GENETICS.106.058099

157) Kaefer, K., Malagon-Vina, H., Dickerson, D. D., O'Neill, J., Trossbach, S. V., Korth, C., & Csicsvari, J. (2019). Disrupted-in-schizophrenia 1 overexpression disrupts hippocampal coding and oscillatory synchronization. *Hippocampus*, *29*(9), 802–816. https://doi.org/10.1002/hipo.23076

158) Kahn, R. S., Sommer, I. E., Murray, R. M., Meyer-Lindenberg, A., Weinberger, D. R., Cannon, T. D., O'Donovan, M., Correll, C. U., Kane, J. M., Van Os, J., & Insel, T. R. (2015). Schizophrenia. *Nature Reviews Disease Primers 2015 1:1*, *1*(1), 1–23. https://doi.org/10.1038/nrdp.2015.67

159) Kaja, S., Payne, A. J., Naumchuk, Y., & Koulen, P. (2017). Quantification of lactate dehydrogenase for cell viability testing using cell lines and primary cultured astrocytes. *Current Protocols in Toxicology*, *72*, 2.26.1. https://doi.org/10.1002/CPTX.21

160) Kamiya, A., Kubo, K. I., Tomoda, T., Takaki, M., Youn, R., Ozeki, Y., Sawamura, N., Park, U., Kudo, C., Okawa, M., Ross, C. A., Hatten, M. E., Nakajima, K., & Sawa, A. (2005). A schizophrenia-associated mutation of DISC1 perturbs cerebral cortex development. *Nature Cell Biology*, *7*(12), 1067–1078. https://doi.org/10.1038/NCB1328

161) Kamiya, A., Tan, P. L., Kubo, K. I., Engelhard, C., Ishizuka, K., Kubo, A., Tsukita, S., Pulver, A. E., Nakajima, K., Cascella, N. G., Katsanis, N., & Sawa, A. (2008). Recruitment of PCM1 to the centrosome by the cooperative action of DISC1 and BBS4:

a candidate for psychiatric illnesses. *Archives of General Psychiatry*, *65*(9), 996–1006. https://doi.org/10.1001/ARCHPSYC.65.9.996

162) Kamiya, A., Tomoda, T., Chang, J., Takaki, M., Zhan, C., Morita, M., Cascio, M. B., Elashvili, S., Koizumi, H., Takanezawa, Y., Dickerson, F., Yolken, R., Arai, H., & Sawa, A. (2006). DISC1-NDEL1/NUDEL protein interaction, an essential component for neurite outgrowth, is modulated by genetic variations of DISC1. *Human Molecular Genetics*, *15*(22), 3313–3323. https://doi.org/10.1093/HMG/DDL407

163) Kang, W. S., Lee, S. M., Hwang, D., Park, H. J., Kim, J. W., & Shen., L. (2022). Association between Unc-51-like autophagy activating kinase 2 gene polymorphisms and schizophrenia in the Korean population. *Medicine (United States)*, *101*(5), E28745. https://doi.org/10.1097/MD.0000000000028745

164) Karpinski, B. A., Morle, G. D., Huggenvik, J., Uhler, M. D., & Leiden, J. M. (1992). Molecular cloning of human CREB-2: an ATF/CREB transcription factor that can negatively regulate transcription from the cAMP response element. *Proceedings of the National Academy of Sciences of the United States of America*, *89*(11), 4820–4824. https://doi.org/10.1073/PNAS.89.11.4820

165) Kato, M., & Dobyns, W. B. (2003). Lissencephaly and the molecular basis of neuronal migration. *Human Molecular Genetics*, *12 Spec No 1*(REV. ISS. 1). https://doi.org/10.1093/HMG/DDG086

166) Kelly, S., Jahanshad, N., Zalesky, A., Kochunov, P., Agartz, I., Alloza, C., Andreassen, O. A., Arango, C., Banaj, N., Bouix, S., Bousman, C. A., Brouwer, R. M., Bruggemann, J., Bustillo, J., Cahn, W., Calhoun, V., Cannon, D., Carr, V., Catts, S., … Donohoe, G. (2018). Widespread white matter microstructural differences in schizophrenia across 4322 individuals: results from the ENIGMA Schizophrenia DTI Working Group. *Molecular Psychiatry*, *23*(5), 1261–1269. https://doi.org/10.1038/MP.2017.170

167) Kerber, M. L., & Cheney, R. E. (2011). Myosin-X: a MyTH-FERM myosin at the tips of filopodia. *Journal of Cell Science*, *124*(Pt 22), 3733–3741. https://doi.org/10.1242/JCS.023549

168) Kesby, J. P., Cui, X., Burne, T. H. J., & Eyles, D. W. (2013). Altered dopamine ontogeny in the developmentally vitamin D deficient rat and its relevance to schizophrenia. *Frontiers in Cellular Neuroscience*, *7*(JUNE). https://doi.org/10.3389/FNCEL.2013.00111

169) Kim, J. Y., Duan, X., Liu, C. Y., Jang, M. H., Guo, J. U., Pow-anpongkul, N., Kang, E., Song, H., & Ming, G. li. (2009). DISC1 regulates new neuron development in the adult brain via modulation of AKT-mTOR signaling through KIAA1212. *Neuron*, *63*(6), 761. https://doi.org/10.1016/J.NEURON.2009.08.008

170) Kim, J. Y., Liu, C. Y., Zhang, F., Duan, X., Wen, Z., Song, J., Feighery, E., Lu, B., Rujescu, D., St Clair, D., Christian, K., Callicott, J. H., Weinberger, D. R., Song, H., & Ming, G. L. (2012). Interplay between DISC1 and GABA Signaling Regulates Neurogenesis in Mice and Risk for Schizophrenia. *Cell*, *148*(5), 1051. https://doi.org/10.1016/J.CELL.2011.12.037

171) Kim, P., Scott, M. R., & Meador-Woodruff, J. H. (2018). Abnormal expression of ER quality control and ER associated degradation proteins in the dorsolateral prefrontal

cortex in schizophrenia. *Schizophrenia Research*, *197*, 484–491. https://doi.org/10.1016/J.SCHRES.2018.02.010

172) Kim, P., Scott, M. R., & Meador-Woodruff, J. H. (2019a). Abnormal ER quality control of neural GPI-anchored proteins via dysfunction in ER export processing in the frontal cortex of elderly subjects with schizophrenia. *Translational Psychiatry*, *9*(1). https://doi.org/10.1038/S41398-018-0359-4

173) Kim, P., Scott, M. R., & Meador-Woodruff, J. H. (2019b). Dysregulation of the unfolded protein response (UPR) in the dorsolateral prefrontal cortex in elderly patients with schizophrenia. *Molecular Psychiatry 2019 26:4*, *26*(4), 1321–1331. https://doi.org/10.1038/s41380-019-0537-7

174) Kim, P., Scott, M. R., & Meador-Woodruff, J. H. (2021). Dysregulation of the unfolded protein response (UPR) in the dorsolateral prefrontal cortex in elderly patients with schizophrenia. *Molecular Psychiatry*, *26*(4), 1321–1331. https://doi.org/10.1038/S41380-019-0537-7

175) Kimura, H., Tsuboi, D., Wang, C., Kushima, I., Koide, T., Ikeda, M., Iwayama, Y., Toyota, T., Yamamoto, N., Kunimoto, S., Nakamura, Y., Yoshimi, A., Banno, M., Xing, J., Takasaki, Y., Yoshida, M., Aleksic, B., Uno, Y., Okada, T., … Ozaki, N. (2015). Identification of Rare, Single-Nucleotide Mutations in NDE1 and Their Contributions to Schizophrenia Susceptibility. *Schizophrenia Bulletin*, *41*(3), 744–753. https://doi.org/10.1093/SCHBUL/SBU147

176) Kirkpatrick, B., Xu, L., Cascella, N., Ozeki, Y., Sawa, A., & Roberts, R. C. (2006). DISC1 immunoreactivity at the light and ultrastructural level in the human neocortex. *The Journal of Comparative Neurology*, *497*(3), 436–450. https://doi.org/10.1002/CNE.21007

177) Kitagawa, M., Umezu, M., Aoki, J., Koizumi, H., Arai, H., & Inoue, K. (2000). Direct association of LIS1, the lissencephaly gene product, with a mammalian homologue of a fungal nuclear distribution protein, rNUDE. *FEBS Letters*, *479*(1–2), 57–62. https://doi.org/10.1016/S0014-5793(00)01856-1

178) Köditz, J., Nesper, J., Wottawa, M., Stiehl, D. P., Camenisch, G., Franke, C., Myllyharju, J., Wenger, R. H., & Katschinski, D. M. (2007). Oxygen-dependent ATF-4 stability is mediated by the PHD3 oxygen sensor. *Blood*, *110*(10), 3610–3617. https://doi.org/10.1182/BLOOD-2007-06-094441

179) Korth, C. (2012). Aggregated proteins in schizophrenia and other chronic mental diseases: DISC1opathies. *Prion*, *6*(2), 134. https://doi.org/10.4161/PRI.18989

180) Kuhn, R., & Cahn, C. H. (2004). Eugen Bleuler's concepts of psychopathology. *History of Psychiatry*, *15*(59 Pt 3), 361–366. https://doi.org/10.1177/0957154X04044603

181) Kvajo, M., McKellar, H., Drew, L. J., Lepagnol-Bestel, A. M., Xiao, L., Levy, R. J., Blazeski, R., Arguello, P. A., Lacefield, C. O., Mason, C. A., Simonneau, M., O'Donnell, J. M., MacDermott, A. B., Karayiorgou, M., & Gogos, J. A. (2011). Altered axonal targeting and short-term plasticity in the hippocampus of Disc1 mutant mice. *Proceedings of the National Academy of Sciences of the United States of America*, *108*(49), E1349. https://doi.org/10.1073/PNAS.1114113108/-/DCSUPPLEMENTAL

182) Kyriakopoulos, M., Vyas, N. S., Barker, G. J., Chitnis, X. A., & Frangou, S. (2008). A diffusion tensor imaging study of white matter in early-onset schizophrenia. *Biological Psychiatry*, *63*(5), 519–523. https://doi.org/10.1016/J.BIOPSYCH.2007.05.021

183) Lamptey, R. N. L., Chaulagain, B., Trivedi, R., Gothwal, A., Layek, B., & Singh, J. (2022). A Review of the Common Neurodegenerative Disorders: Current Therapeutic Approaches and the Potential Role of Nanotherapeutics. *International Journal of Molecular Sciences*, *23*(3). https://doi.org/10.3390/IJMS23031851

184) Landy, A. (1989). Dynamic, structural, and regulatory aspects of lambda site-specific recombination. *Annual Review of Biochemistry*, *58*(1), 913–941. https://doi.org/10.1146/ANNUREV.BI.58.070189.004405

185) Lassot, I., Ségéral, E., Berlioz-Torrent, C., Durand, H., Groussin, L., Hai, T., Benarous, R., & Margottin-Goguet, F. (2001). ATF4 Degradation Relies on a Phosphorylation-Dependent Interaction with the SCFβTrCP Ubiquitin Ligase. *Molecular and Cellular Biology*, *21*(6), 2192. https://doi.org/10.1128/MCB.21.6.2192-2202.2001

186) Le Bourg, E., & Lints, F. A. (1992). Hypergravity and Aging in Drosophila melanogaster. 4. Climbing Activity4. Climbing Activity. *Gerontology*, *38*(1–2), 59–64. https://doi.org/10.1159/000213307

187) Lee, S. B., Park, J., Kwak, Y., Park, Y. U., Nhung, T. T. M., Suh, B. K., Woo, Y., Suh, Y., Cho, E., Cho, S., & Park, S. K. (2021). Disrupted-in-schizophrenia 1 enhances the quality of circadian rhythm by stabilizing BMAL1. *Translational Psychiatry 2021 11:1*, *11*(1), 1–13. https://doi.org/10.1038/s41398-021-01212-1

188) Lei, Z., Henderson, K., & Keleman, K. (2022). A neural circuit linking learning and sleep in Drosophila long-term memory. *Nature Communications 2022 13:1*, *13*(1), 1–10. https://doi.org/10.1038/s41467-022-28256-1

189) Leliveld, S. R., Bader, V., Hendriks, P., Prikulis, I., Sajnani, G., Requena, J. R., & Korth, C. (2008). Insolubility of disrupted-in-schizophrenia 1 disrupts oligomer-dependent interactions with nuclear distribution element 1 and is associated with sporadic mental disease. *Journal of Neuroscience*, *28*(15), 3839–3845. https://doi.org/10.1523/JNEUROSCI.5389-07.2008

190) Leliveld, S. R., Hendriks, P., Michel, M., Sajnani, G., Bader, V., Trossbach, S., Prikulis, I., Hartmann, R., Jonas, E., Willbold, D., Requena, J. R., & Korth, C. (2009). Oligomer assembly of the C-terminal DISC1 domain (640-854) is controlled by self-association motifs and disease-associated polymorphism S704C. *Biochemistry*, *48*(32), 7746–7755. https://doi.org/10.1021/BI900901E

191) Lessing, D., & Bonini, N. M. (2009). Maintaining the Brain: Insight into Human Neurodegeneration From Drosophila Mutants. *Nature Reviews. Genetics*, *10*(6), 359. https://doi.org/10.1038/NRG2563

192) Lichtenstein, P., Yip, B. H., Björk, C., Pawitan, Y., Cannon, T. D., Sullivan, P. F., & Hultman, C. M. (2009). Common genetic determinants of schizophrenia and bipolar disorder in Swedish families: a population-based study. *The Lancet*, *373*(9659), 234–239. https://doi.org/10.1016/S0140-6736(09)60072-6

193) Linding, R., Schymkowitz, J., Rousseau, F., Diella, F., & Serrano, L. (2004). A comparative study of the relationship between protein structure and beta-aggregation in

globular and intrinsically disordered proteins. *Journal of Molecular Biology*, *342*(1), 345–353. https://doi.org/10.1016/J.JMB.2004.06.088

194) Lipska, B. K., Peters, T., Hyde, T. M., Halim, N., Horowitz, C., Mitkus, S., Weickert, C. S., Matsumoto, M., Sawa, A., Straub, R. E., Vakkalanka, R., Herman, M. M., Weinberger, D. R., & Kleinman, J. E. (2006). Expression of DISC1 binding partners is reduced in schizophrenia and associated with DISC1 SNPs. *Human Molecular Genetics*, *15*(8), 1245–1258. https://doi.org/10.1093/HMG/DDL040

195) Liu, D., Zinski, A., Mishra, A., Noh, H., Park, G. H., Qin, Y., Olorife, O., Park, J. M., Abani, C. P., Park, J. S., Fung, J., Sawaqed, F., Coyle, J. T., Stahl, E., Bendl, J., Fullard, J. F., Roussos, P., Zhang, X., Stanton, P. K., … Chung, S. (2022). Impact of schizophrenia GWAS loci converge onto distinct pathways in cortical interneurons vs glutamatergic neurons during development. *Molecular Psychiatry 2022 27:10*, *27*(10), 4218–4233. https://doi.org/10.1038/s41380-022-01654-z

196) Liu, Z., Steward, R., & Luo, L. (2000). Drosophila Lis1 is required for neuroblast proliferation, dendritic elaboration and axonal transport. *Nature Cell Biology*, *2*(11), 776–783. https://doi.org/10.1038/35041011

197) Lu, H., Qiao, J., Shao, Z., Wang, T., Huang, S., & Zeng, P. (2021). A comprehensive gene-centric pleiotropic association analysis for 14 psychiatric disorders with GWAS summary statistics. *BMC Medicine*, *19*(1). https://doi.org/10.1186/S12916-021-02186-Z

198) Lu, J., Huang, R., Peng, Y., Wang, H., Feng, Z., Fan, Y., Zeng, Z., Wang, Y., Wei, J., & Wang, Z. (2022). Effects of DISC1 on Alzheimer's disease cell models assessed by iTRAQ proteomics analysis. *Bioscience Reports*, *42*(1), BSR20211150. https://doi.org/10.1042/BSR20211150

199) Ma, T. M., Abazyan, S., Abazyan, B., Nomura, J., Yang, C., Seshadri, S., Sawa, A., Snyder, S. H., & Pletnikov, M. V. (2012). Pathogenic disruption of DISC1-serine racemase binding elicits schizophrenia-like behavior via D-serine depletion. *Molecular Psychiatry 2013 18:5*, *18*(5), 557–567. https://doi.org/10.1038/mp.2012.97

200) MacKenzie, S. J., Baillie, G. S., McPhee, I., Mac Kenzie, C., Seamons, R., McSorley, T., Millen, J., Beard, M. B., van Heeke, G., & Houslay, M. D. (2002). Long PDE4 cAMP specific phosphodiesterases are activated by protein kinase A-mediated phosphorylation of a single serine residue in Upstream Conserved Region 1 (UCR1). *British Journal of Pharmacology*, *136*(3), 421. https://doi.org/10.1038/SJ.BJP.0704743

201) Malavasi, E. L. V., Economides, K. D., Grünewald, E., Makedonopoulou, P., Gautier, P., Mackie, S., Murphy, L. C., Murdoch, H., Crummie, D., Ogawa, F., McCartney, D. L., O'Sullivan, S. T., Burr, K., Torrance, H. S., Phillips, J., Bonneau, M., Anderson, S. M., Perry, P., Pearson, M., … Millar, J. K. (2018). DISC1 regulates N-methyl-D-aspartate receptor dynamics: abnormalities induced by a Disc1 mutation modelling a translocation linked to major mental illness. *Translational Psychiatry 2018 8:1*, *8*(1), 1–16. https://doi.org/10.1038/s41398-018-0228-1

202) Malavasi, E. L. V., Ogawa, F., Porteous, D. J., & Millar, J. K. (2012). DISC1 variants 37W and 607F disrupt its nuclear targeting and regulatory role in ATF4-mediated transcription. *Human Molecular Genetics*, *21*(12), 2779–2792. https://doi.org/10.1093/HMG/DDS106

203) Manni, S., Brancalion, A., Tubi, L. Q., Colpo, A., Pavan, L., Cabrelle, A., Ave, E., Zaffino, F., Di Maira, G., Ruzzene, M., Adami, F., Zambello, R., Pitari, M. R., Tassone, P., Pinna, L. A., Gurrieri, C., Semenzato, G., & Piazza, F. (2012). Protein kinase CK2 protects multiple myeloma cells from ER stress-induced apoptosis and from the cytotoxic effect of HSP90 inhibition through regulation of the unfolded protein response. *Clinical Cancer Research : An Official Journal of the American Association for Cancer Research*, *18*(7), 1888–1900. https://doi.org/10.1158/1078-0432.CCR-11-1789

204) Mao, Y., Ge, X., Frank, C. L., Madison, J. M., Koehler, A. N., Doud, M. K., Tassa, C., Berry, E. M., Soda, T., Singh, K. K., Biechele, T., Petryshen, T. L., Moon, R. T., Haggarty, S. J., & Tsai, L. H. (2009). Disrupted in schizophrenia 1 regulates neuronal progenitor proliferation via modulation of GSK3beta/beta-catenin signaling. *Cell*, *136*(6), 1017–1031. https://doi.org/10.1016/J.CELL.2008.12.044

205) Marques, T. R., Ashok, A. H., Angelescu, I., Borgan, F., Myers, J., Lingford-Hughes, A., Nutt, D. J., Veronese, M., Turkheimer, F. E., & Howes, O. D. (2020). GABA-A receptor differences in schizophrenia: a positron emission tomography study using [11C]Ro154513. *Molecular Psychiatry 2020 26:6*, *26*(6), 2616–2625. https://doi.org/10.1038/s41380-020-0711-y

206) Martin, L., Stein, K., Kubera, K., Troje, N. F., & Fuchs, T. (2022). Movement markers of schizophrenia: a detailed analysis of patients' gait patterns. *European Archives of Psychiatry and Clinical Neuroscience*, *272*(7), 1347. https://doi.org/10.1007/S00406-022-01402-Y

207) Marzo, M. G., Griswold, J. M., & Markus, S. M. (2020). Pac1/LIS1 stabilizes an uninhibited conformation of dynein to coordinate its localization and activity. *Nature Cell Biology 2020 22:5*, *22*(5), 559–569. https://doi.org/10.1038/s41556-020-0492-1

208) Mas, P. J., & Hart, D. J. (2017). ESPRIT: A Method for Defining Soluble Expression Constructs in Poorly Understood Gene Sequences. *Methods in Molecular Biology (Clifton, N.J.)*, *1586*, 45–63. https://doi.org/10.1007/978-1-4939-6887-9_4

209) Mateja, A., Cierpicki, T., Paduch, M., Derewenda, Z. S., & Otlewski, J. (2006). The Dimerization Mechanism of LIS1 and its Implication for Proteins Containing the LisH Motif. *Journal of Molecular Biology*, *357*(2), 621–631. https://doi.org/10.1016/J.JMB.2006.01.002

210) McGuire, S. E., Mao, Z., & Davis, R. L. (2004). Spatiotemporal gene expression targeting with the TARGET and gene-switch systems in Drosophila. *Science's STKE : Signal Transduction Knowledge Environment*, *2004*(220). https://doi.org/10.1126/STKE.2202004PL6

211) McKenney, R. J., Vershinin, M., Kunwar, A., Vallee, R. B., & Gross, S. P. (2010). LIS1 and NudE induce a persistent dynein force-producing state. *Cell*, *141*(2), 304–314. https://doi.org/10.1016/J.CELL.2010.02.035

212) Meiklejohn, H., Mostaid, M. S., Luza, S., Mancuso, S. G., Kang, D., Atherton, S., Rothmond, D. A., Weickert, C. S., Opazo, C. M., Pantelis, C., Bush, A. I., Everall, I. P., & Bousman, C. A. (2019). Blood and brain protein levels of ubiquitin-conjugating enzyme E2K (UBE2K) are elevated in individuals with schizophrenia. *Journal of Psychiatric Research*, *113*, 51–57. https://doi.org/10.1016/J.JPSYCHIRES.2019.03.005

213) Merenlender-Wagner, A., Malishkevich, A., Shemer, Z., Udawela, M., Gibbons, A., Scarr, E., Dean, B., Levine, J., Agam, G., & Gozes, I. (2013). Autophagy has a key role in the pathophysiology of schizophrenia. *Molecular Psychiatry 2015 20:1*, *20*(1), 126–132. https://doi.org/10.1038/mp.2013.174

214) Millar, J. K., Brown, J., Maule, J. C., Shibasaki, Y., Christie, S., Lawson; D, Anderson, S., Wilson-Annan, J. C., Devon, R. S., St Clair, D. M., Blackwood, D. H. R., Muir, W. J., & Porteus, D. J. (1998). A long-range restriction map across 3 Mb of the chromosome 11 breakpoint region of a translocation linked to schizophrenia: localization of the breakpoint and the search for neighbouring genes. *Psychiatric Genetics*, *8*(3), 175–181.

215) Millar, J. K., Christie, S., Anderson, S., Lawson, D., Loh, H.-W., Devon, R. S., Arveiler, B., Muir, W. J., Blackwood, D., & Porteus, D. J. (2001). Genomic structure and localisation within a linkage hotspot of Disrupted In Schizophrenia 1, a gene disrupted by a translocation segregating with schizophrenia. In *Molecular Psychiatry* (Vol. 6). www.nature.com/mp

216) Millar, J. K., Christie, S., & Porteus, D. J. (2003). Yeast two-hybrid screens implicate DISC1 in brain development and function. *Biochemical and Biophysical Research Communications*, *311*(4), 1019–1025. https://doi.org/10.1016/j.bbrc.2003.10.101

217) Millar, J. K., Pickard, B. S., Mackie, S., James, R., Christie, S., Buchanan, S. R., Malloy, M. P., Chubb, J. E., Huston, E., Baillie, G. S., Thomson, P. A., Hill, E. V., Brandon, N. J., Rain, J. C., Camargo, L. M., Whiting, P. J., Houslay, M. D., Blackwood, D. H. R., Muir, W. J., & Porteus, D. J. (2005). DISC1 and PDE4B are interacting genetic factors in schizophrenia that regulate cAMP signaling. *Science (New York, N.Y.)*, *310*(5751), 1187–1191. https://doi.org/10.1126/SCIENCE.1112915

218) Millar, K. J., Wilson-Annan, J. C., Anderson, S., Christie, S., Taylor, M. S., Semple, C. A. M., Devon, R. S., St Clair, D. M., Muir, W. J., Blackwood, D. H. R., & Porteus, D. J. (2000). Disruption of two novel genes by a translocation co-segregating with schizophrenia. In *Human Molecular Genetics* (Vol. 9, Issue 9). http://menu.hgmp.mrc.ac.uk/

219) Miyazaki, T., Nakajima, W., Hatano, M., Shibata, Y., Kuroki, Y., Arisawa, T., Serizawa, A., Sano, A., Kogami, S., Yamanoue, T., Kimura, K., Hirata, Y., Takada, Y., Ishiwata, Y., Sonoda, M., Tokunaga, M., Seki, C., Nagai, Y., Minamimoto, T., … Takahashi, T. (2020). Visualization of AMPA receptors in living human brain with positron emission tomography. *Nature Medicine 2020 26:2*, *26*(2), 281–288. https://doi.org/10.1038/s41591-019-0723-9

220) Miyoshi, K., Asanuma, M., Miyazaki, I., Diaz-Corrales, F. J., Katayama, T., Tohyama, M., & Ogawa, N. (2004). DISC1 localizes to the centrosome by binding to kendrin. *Biochemical and Biophysical Research Communications*, *317*(4), 1195–1199. https://doi.org/10.1016/j.bbrc.2004.03.163

221) Miyoshi, K., Honda, A., Baba, K., Taniguchi, M., Oono, K., Fujita, T., Kuroda, S., Katayama, T., & Tohyama, M. (2003). Disrupted-In-Schizophrenia 1, a candidate gene for schizophrenia, participates in neurite outgrowth. *Molecular Psychiatry*, *8*(7), 685–694. https://doi.org/10.1038/SJ.MP.4001352

222) Mizuguchi, M., Takashima, S., Kakita, A., Yamada, M., & Ikeda, K. (1995). Lissencephaly gene product. Localization in the central nervous system and loss of

immunoreactivity in Miller-Dieker syndrome. *The American Journal of Pathology*, *147*(4), 1142. /pmc/articles/PMC1870994/?report=abstract

223) Moon, H. M., Youn, Y. H., Pemble, H., Yingling, J., Wittmann, T., & Wynshaw-Boris, A. (2014). LIS1 controls mitosis and mitotic spindle organization via the LIS1–NDEL1– dynein complex. *Human Molecular Genetics*, *23*(2), 449–466. https://doi.org/10.1093/HMG/DDT436

224) Morris, J. A., Kandpal, G., Ma, L., & Austin, C. P. (2003). DISC1 (Disrupted-In-Schizophrenia 1) is a centrosome-associated protein that interacts with MAP1A, MIPT3, ATF4/5 and NUDEL: regulation and loss of interaction with mutation. *Human Molecular Genetics*, *12*(13), 1591–1608. https://doi.org/10.1093/HMG/DDG162

225) Muir, W. J., Gosden, C. M., Brookes, A. J., Fantes, J., Evans, K. L., Maguire, S. M., Stevenson, B., Boyle, S., Blackwood, D. H. R., St. Clair, D. M., Porteous, D. J., & Weith, A. (1995). Direct microdissection and microcloning of a translocation breakpoint region, t(1;11)(q42.2;q21), associated with schizophrenia. *Cytogenetics and Cell Genetics*, *70*(1–2), 35–40. https://doi.org/10.1159/000133986

226) Mukherjee, P., Whalley, H. C., McKirdy, J. W., Sprengelmeyer, R., Young, A. W., McIntosh, A. M., Lawrie, S. M., & Hall, J. (2014). Altered Amygdala Connectivity Within the Social Brain in Schizophrenia. *Schizophrenia Bulletin*, *40*(1), 152. https://doi.org/10.1093/SCHBUL/SBT086

227) Muneer, A., & Khan, R. M. S. (2019). Endoplasmic Reticulum Stress: Implications for Neuropsychiatric Disorders. *Chonnam Medical Journal*, *55*(1), 8. https://doi.org/10.4068/CMJ.2019.55.1.8

228) Murdoch, H., Mackie, S., Collins, D. M., Hill, E. V., Bolger, G. B., Klussmann, E., Porteous, D. J., Millar, J. K., & Houslay, M. D. (2007). Isoform-Selective Susceptibility of DISC1/Phosphodiesterase-4 Complexes to Dissociation by Elevated Intracellular cAMP Levels. *The Journal of Neuroscience*, *27*(35), 9513. https://doi.org/10.1523/JNEUROSCI.1493-07.2007

229) Murphy, L. C., & Millar, J. K. (2017). Regulation of mitochondrial dynamics by DISC1, a putative risk factor for major mental illness. *Schizophrenia Research*, *187*, 55–61. https://doi.org/10.1016/J.SCHRES.2016.12.027

230) Nadesalingam, N., Chapellier, V., Lefebvre, S., Pavlidou, A., Stegmayer, K., Alexaki, D., Gama, D. B., Maderthaner, L., von Känel, S., Wüthrich, F., & Walther, S. (2022). Motor abnormalities are associated with poor social and functional outcomes in schizophrenia. *Comprehensive Psychiatry*, *115*. https://doi.org/10.1016/J.COMPPSYCH.2022.152307

231) Nakahara, T., Tsugawa, S., Noda, Y., Ueno, F., Honda, S., Kinjo, M., Segawa, H., Hondo, N., Mori, Y., Watanabe, H., Nakahara, K., Yoshida, K., Wada, M., Tarumi, R., Iwata, Y., Plitman, E., Moriguchi, S., de la Fuente-Sandoval, C., Uchida, H., … Nakajima, S. (2021). Glutamatergic and GABAergic metabolite levels in schizophrenia-spectrum disorders: a meta-analysis of 1H-magnetic resonance spectroscopy studies. *Molecular Psychiatry 2021 27:1*, *27*(1), 744–757. https://doi.org/10.1038/s41380-021-01297-6

232) Nakata, K., Lipska, B. K., Hyde, T. M., Ye, T., Newburn, E. N., Morita, Y., Vakkalanka, R., Barenboim, M., Sei, Y., Weinberger, D. R., & Kleinman, J. E. (2009). DISC1 splice variants are upregulated in schizophrenia and associated with risk polymorphisms.

Proceedings of the National Academy of Sciences of the United States of America, *106*(37), 15873. https://doi.org/10.1073/PNAS.0903413106

233) Narayanan, A. S., & Rothenfluh, A. (2015). I Believe I Can Fly!: Use of Drosophila as a Model Organism in Neuropsychopharmacology Research. *Neuropsychopharmacology 2016 41:6*, *41*(6), 1439–1446. https://doi.org/10.1038/npp.2015.322

234) Narayanan, S., Arthanari, H., Wolfe, M. S., & Wagner, G. (2011). Molecular Characterization of Disrupted in Schizophrenia-1 Risk Variant S704C Reveals the Formation of Altered Oligomeric Assembly. *The Journal of Biological Chemistry*, *286*(51), 44266. https://doi.org/10.1074/JBC.M111.271593

235) National Center for Biotechnology Information. (2024, October 10). *PDIA4 protein disulfide isomerase family A member 4*. National Library of Medicine. https://www.ncbi.nlm.nih.gov/gene/9601

236) Neer, E. J., Schmidt, C. J., Nambudripad, R., & Smith, T. F. (1994). The ancient regulatory-protein family of WD-repeat proteins. *Nature 1994 371:6495*, *371*(6495), 297–300. https://doi.org/10.1038/371297a0

237) Nerattini, F., Figliuzzi, M., Cardelli, C., Tubiana, L., Bianco, V., Dellago, C., & Coluzza, I. (2020). Identification of Protein Functional Regions. *Chemphyschem : A European Journal of Chemical Physics and Physical Chemistry*, *21*(4), 335–347. https://doi.org/10.1002/CPHC.201900898

238) Ng, M. Y. M., Levinson, D. F., Faraone, S. V., Suarez, B. K., Delisi, L. E., Arinami, T., Riley, B., Paunio, T., Pulver, A. E., Irmansyah, Holmans, P. A., Escamilla, M., Wildenauer, D. B., Williams, N. M., Laurent, C., Mowry, B. J., Brzustowicz, L. M., Maziade, M., Sklar, P., … Lewis, C. M. (2009). Meta-analysis of 32 genome-wide linkage studies of schizophrenia. *Molecular Psychiatry*, *14*(8), 774. https://doi.org/10.1038/MP.2008.135

239) Nicodemus, K. K., Callicott, J. H., Higier, R. G., Luna, A., Nixon, D. C., Lipska, B. K., Vakkalanka, R., Giegling, I., Rujescu, D., Clair, D. S., Muglia, P., Shugart, Y. Y., & Weinberger, D. R. (2010). Evidence of statistical epistasis between DISC1, CIT and NDEL1 impacting risk for schizophrenia: biological validation with functional neuroimaging. *Human Genetics*, *127*(4), 441–452. https://doi.org/10.1007/S00439-009-0782-Y

240) Niethammer, M., Smith, D. S., Ayala, R., Peng, J., Ko, J., Lee, M. S., Morabito, M., & Tsai, L. H. (2000). NUDEL is a novel Cdk5 substrate that associates with LIS1 and cytoplasmic dynein. *Neuron*, *28*(3), 697–711. https://doi.org/10.1016/S0896-6273(00)00147-1

241) Nikolaus, S., Mamlins, E., Hautzel, H., & Müller, H. W. (2019). Acute anxiety disorder, major depressive disorder, bipolar disorder and schizophrenia are related to different patterns of nigrostriatal and mesolimbic dopamine dysfunction. *Reviews in the Neurosciences*, *30*(4), 381–426. https://doi.org/10.1515/REVNEURO-2018-0037/PDF

242) Niwa, M., Kamiya, A., Murai, R., Kubo, K. ichiro, Gruber, A. J., Tomita, K., Lu, L., Tomisato, S., Jaaro-Peled, H., Seshadri, S., Hiyama, H., Huang, B., Kohda, K., Noda, Y., O'Donnell, P., Nakajima, K., Sawa, A., & Nabeshima, T. (2010). Knockdown of DISC1 by in utero gene transfer disturbs postnatal dopaminergic maturation in the frontal cortex

and leads to adult behavioral deficits. *Neuron*, *65*(4), 480–489. https://doi.org/10.1016/J.NEURON.2010.01.019

243) Norkett, R., Lesept, F., & Kittler, J. T. (2020). DISC1 Regulates Mitochondrial Trafficking in a Miro1-GTP-Dependent Manner. *Frontiers in Cell and Developmental Biology*, *8*. https://doi.org/10.3389/FCELL.2020.00449/FULL

244) Nucifora, L. G., Wu, Y. C., Lee, B. J., Sha, L., Margolis, R. L., Ross, C. A., Sawa, A., & Nucifora Jr, F. C. (2016). A Mutation in NPAS3 That Segregates with Schizophrenia in a Small Family Leads to Protein Aggregation. *Molecular Neuropsychiatry*, *2*(3), 133–144. https://doi.org/10.1159/000447358

245) Numata, S., Ueno, S. ichi, Iga, J. ichi, Song, H., Nakataki, M., Tayoshi, S., Sumitani, S., Tomotake, M., Itakura, M., Sano, A., & Ohmori, T. (2008). Positive association of the PDE4B (phosphodiesterase 4B) gene with schizophrenia in the Japanese population. *Journal of Psychiatric Research*, *43*(1), 7–12. https://doi.org/10.1016/J.JPSYCHIRES.2008.01.013

246) Nwosu, G. O., Powell, J. A., & Pitson, S. M. (2022). Targeting the integrated stress response in hematologic malignancies. *Experimental Hematology & Oncology 2022 11:1*, *11*(1), 1–15. https://doi.org/10.1186/S40164-022-00348-0

247) O'Donovan, M. C., Craddock, N., Norton, N., Williams, H., Peirce, T., Moskvina, V., Nikolov, I., Hamshere, M., Carroll, L., Georgieva, L., Dwyer, S., Holmans, P., Marchini, J. L., Spencer, C. C. A., Howie, B., Leung, H. T., Hartmann, A. M., Möller, H. J., Morris, D. W., … Owen, M. J. (2008). Identification of loci associated with schizophrenia by genome-wide association and follow-up. *Nature Genetics 2008 40:9*, *40*(9), 1053–1055. https://doi.org/10.1038/ng.201

248) Ogawa, F., Malavasi, E. L. V., Crummie, D. K., Eykelenboom, J. E., Soares, D. C., Mackie, S., Porteous, D. J., & Millar, J. K. (2014). DISC1 complexes with TRAK1 and Miro1 to modulate anterograde axonal mitochondrial trafficking. *Human Molecular Genetics*, *23*(4), 906–919. https://doi.org/10.1093/HMG/DDT485

249) Ota, K. T., Liu, R. J., Voleti, B., Maldonado-Aviles, J. G., Duric, V., Iwata, M., Dutheil, S., Duman, C., Boikess, S., Lewis, D. A., Stockmeier, C. A., DiLeone, R. J., Rex, C., Aghajanian, G. K., & Duman, R. S. (2014). REDD1 is essential for stress-induced synaptic loss and depressive behavior. *Nature Medicine*, *20*(5), 531–535. https://doi.org/10.1038/NM.3513

250) Ottis, P., Bader, V., Trossbach, S. V., Kretzschmar, H., Michel, M., Leliveld, S. R., & Korth, C. (2011). Convergence of two independent mental disease genes on the protein level: recruitment of dysbindin to cell-invasive disrupted-in-schizophrenia 1 aggresomes. *Biological Psychiatry*, *70*(7), 604–610. https://doi.org/10.1016/J.BIOPSYCH.2011.03.027

251) Ozeki, Y., Tomoda, T., Kleiderlein, J., Kamiya, A., Bord, L., Fujii, K., Okawa, M., Yamada, N., Hatten, M. E., Snyder, S. H., Ross, C. A., & Sawa, A. (2003). From the Cover: Disrupted-in-Schizophrenia-1 (DISC-1): Mutant truncation prevents binding to NudE-like (NUDEL) and inhibits neurite outgrowth. *Proceedings of the National Academy of Sciences of the United States of America*, *100*(1), 289. https://doi.org/10.1073/PNAS.0136913100

252) Pan, J. X., Xia, J. J., Deng, F. L., Liang, W. W., Wu, J., Yin, B. M., Dong, M. X., Chen, J. J., Ye, F., Wang, H. Y., Zheng, P., & Xie, P. (2018). Diagnosis of major depressive disorder based on changes in multiple plasma neurotransmitters: a targeted metabolomics study. *Translational Psychiatry 2018 8:1*, *8*(1), 1–10. https://doi.org/10.1038/s41398-018-0183-x

253) Pandey, H., Bourahmoune, K., Honda, T., Honjo, K., Kurita, K., Sato, T., Sawa, A., & Furukubo-Tokunaga, K. (2017). Genetic interaction of DISC1 and Neurexin in the development of fruit fly glutamatergic synapses. *Npj Schizophrenia 2017 3:1*, *3*(1), 1–11. https://doi.org/10.1038/s41537-017-0040-6

254) Pandey, J. P., & Smith, D. S. (2011). A Cdk5-Dependent Switch Regulates Lis1/Ndel1/Dynein-Driven Organelle Transport in Adult Axons. *The Journal of Neuroscience*, *31*(47), 17207. https://doi.org/10.1523/JNEUROSCI.4108-11.2011

255) Park, J. M., Wilbur, J. E., Park, L., & Goff, D. C. (2008). Chronic Mental Illness. *Massachusetts General Hospital Comprehensive Clinical Psychiatry*, 887–893. https://doi.org/10.1016/B978-0-323-04743-2.50066-4

256) Park, S. J., Jeong, J., Park, Y. U., Park, K. S., Lee, H., Lee, N., Kim, S. M., Kuroda, K., Nguyen, M. D., Kaibuchi, K., & Park, S. K. (2015). Disrupted-in-schizophrenia-1 (DISC1) Regulates Endoplasmic Reticulum Calcium Dynamics. *Scientific Reports 2015 5:1*, *5*(1), 1–11. https://doi.org/10.1038/srep08694

257) Park, S. J., Lee, S. B., Suh, Y., Kim, S. J., Lee, N., Hong, J. H., Park, C., Woo, Y., Ishizuka, K., Kim, J. H., Berggren, P. O., Sawa, A., & Park, S. K. (2017). DISC1 Modulates Neuronal Stress Responses by Gate-Keeping ER-Mitochondria Ca2+ Transfer through the MAM. *Cell Reports*, *21*(10), 2748–2759. https://doi.org/10.1016/J.CELREP.2017.11.043/ATTACHMENT/ADE7867B-F2A5-4097-85AB-1BECE8A612A1/MMC2.PDF

258) Patricia Jacobs, B. A., Brunton, M., Frackiewicz, A., Newton, M., L Cook, P. J., & Robson, E. B. (1970). Studies on a family with three cytogenetic markers. *Annals of Human Genetics*, *33*, 325–336.

259) Paylor, R., Hirotsune, S., Gambello, M. J., Yuva-Paylor, L., Crawley, J. N., & Wynshaw-Boris, A. (1999). Impaired Learning and Motor Behavior in Heterozygous Pafah1b1 (Lis1) Mutant Mice. *Learning & Memory*, *6*(5), 521. https://doi.org/10.1101/LM.6.5.521

260) Pfeiffenberger, C., Lear, B. C., Keegan, K. P., & Allada, R. (2010). Locomotor activity level monitoring using the Drosophila Activity Monitoring (DAM) System. *Cold Spring Harbor Protocols*, *2010*(11). https://doi.org/10.1101/PDB.PROT5518

261) Pickard, B. S., Thomson, P. A., Christoforou, A., Evans, K. L., Morris, S. W., Porteous, D. J., Blackwood, D. H. R., & Muir, W. J. (2007). The PDE4B gene confers sex-specific protection against schizophrenia. *Psychiatric Genetics*, *17*(3), 129–133. https://doi.org/10.1097/YPG.0B013E328014492B

262) Pils, M., Rutsch, J., Eren, F., Engberg, G., Piehl, F., Cervenka, S., Sellgren, C., Troßbach, S., Willbold, D., Erhardt, S., Bannach, O., & Korth, C. (2023). Disrupted-in-schizophrenia 1 protein aggregates in cerebrospinal fluid are elevated in patients with first-episode psychosis. *Psychiatry and Clinical Neurosciences*, *77*(12), 665–671. https://doi.org/10.1111/pcn.13594

263) Pitale, P. M., Gorbatyuk, O., & Gorbatyuk, M. (2017). Neurodegeneration: Keeping ATF4 on a Tight Leash. *Frontiers in Cellular Neuroscience*, *11*, 410. https://doi.org/10.3389/FNCEL.2017.00410

264) Pletnikov, M. V., Ayhan, Y., Nikolskaia, O., Xu, Y., Ovanesov, M. V., Huang, H., Mori, S., Moran, T. H., & Ross, C. A. (2008). Inducible expression of mutant human DISC1 in mice is associated with brain and behavioral abnormalities reminiscent of schizophrenia. *Molecular Psychiatry*, *13*(2), 173–186. https://doi.org/10.1038/SJ.MP.4002079

265) Pletnikov, M. V., Xu, Y., Ovanesov, M. V., Kamiya, A., Sawa, A., & Ross, C. A. (2007). PC12 cell model of inducible expression of mutant DISC1: new evidence for a dominant-negative mechanism of abnormal neuronal differentiation. *Neuroscience Research*, *58*(3), 234–244. https://doi.org/10.1016/J.NEURES.2007.03.003

266) Pohl, C., & Dikic, I. (2019). Cellular quality control by the ubiquitin-proteasome system and autophagy. *Science (New York, N.Y.)*, *366*(6467), 818–822. https://doi.org/10.1126/SCIENCE.AAX3769

267) Prabakaran, R., Rawat, P., Thangakani, A. M., Kumar, S., & Gromiha, M. M. (2021). Protein aggregation: in silico algorithms and applications. *Biophysical Reviews*, *13*(1), 71. https://doi.org/10.1007/S12551-021-00778-W

268) Ptashne, M. (1992). *A Genetic Switch: Phage λ and Higher Organisms* (2nd ed.). Cambridge, Mass. : Cell Press : Blackwell Scientific Publications.

269) Qiu, S., Xiao, C., & Meldrum Robertson, R. (2017). Different age-dependent performance in Drosophila wild-type Canton-S and the white mutant w1118 flies. *Comparative Biochemistry and Physiology. Part A, Molecular & Integrative Physiology*, *206*, 17–23. https://doi.org/10.1016/J.CBPA.2017.01.003

270) Qiu, Y., Chen, C. N., Malone, T., Richter, L., Beckendorf, S. K., & Davis, R. L. (1991). Characterization of the memory gene dunce of Drosophila melanogaster. *Journal of Molecular Biology*, *222*(3), 553–565. https://doi.org/10.1016/0022-2836(91)90496-S

271) Qu, M., Tang, F., Wang, L., Yan, H., Han, Y., Yan, J., Yue, W., & Zhang, D. (2008). Associations of ATF4 gene polymorphisms with schizophrenia in male patients. *American Journal of Medical Genetics Part B: Neuropsychiatric Genetics*, *147B*(6), 732–736. https://doi.org/10.1002/AJMG.B.30675

272) Ramos, A., Rodríguez-Seoane, C., Rosa, I., Trossbach, S. V., Ortega-Alonso, A., Tomppo, L., Ekelund, J., Veijola, J., Järvelin, M. R., Alonso, J., Veiga, S., Sawa, A., Hennah, W., García, Á., Korth, C., & Requena, J. R. (2014). Neuropeptide precursor VGF is genetically associated with social anhedonia and underrepresented in the brain of major mental illness: its downregulation by DISC1. *Human Molecular Genetics*, *23*(22), 5859. https://doi.org/10.1093/HMG/DDU303

273) Rampino, A., Walker, R. M., Torrance, H. S., Anderson, S. M., Fazio, L., Di Giorgio, A., Taurisano, P., Gelao, B., Romano, R., Masellis, R., Ursini, G., Caforio, G., Blasi, G., Millar, J. K., Porteous, D. J., Thomson, P. A., Bertolino, A., & Evans, K. L. (2014). Expression of DISC1-Interactome Members Correlates with Cognitive Phenotypes Related to Schizophrenia. *PLOS ONE*, *9*(6), e99892. https://doi.org/10.1371/JOURNAL.PONE.0099892

274) Raznahan, A., Lee, Y., Long, R., Greenstein, D., Clasen, L., Addington, A., Rapoport, J. L., & Giedd, J. N. (2011). Common functional polymorphisms of DISC1 and cortical

maturation in typically developing children and adolescents. *Molecular Psychiatry*, *16*(9), 917. https://doi.org/10.1038/MP.2010.72

275) Reichert, H. (2002). Conserved genetic mechanisms for embryonic brain patterning. *The International Journal of Developmental Biology*, *46*(1), 81–87. https://doi.org/10.1387/IJDB.11902691

276) Reiner, O., Albrecht, U., Gordon, M., Chianese, K. A., Wong, C., Gal-Gerber, O., Sapir, T., Siracusa, L. D., Buchberg, A. M., Caskey, C. T., & Eichele, G. (1995). Lissencephaly gene (LIS1) expression in the CNS suggests a role in neuronal migration. *The Journal of Neuroscience*, *15*(5), 3730. https://doi.org/10.1523/JNEUROSCI.15-05-03730.1995

277) Reiner, O., Carrozzo, R., Shen, Y., Wehnert, M., Faustinella, F., Dobyns, W. B., Caskey, C. T., & Ledbetter, D. H. (1993). Isolation of a Miller-Dicker lissencephaly gene containing G protein β-subunit-like repeats. *Nature*, *364*(6439), 717–721. https://doi.org/10.1038/364717a0

278) Rigo, F., Filošević, A., Petrović, M., Jović, K., & Andretić Waldowski, R. (2021). Locomotor sensitization modulates voluntary self-administration of methamphetamine in Drosophila melanogaster. *Addiction Biology*, *26*(3). https://doi.org/10.1111/ADB.12963

279) Ripke, S., Neale, B. M., Corvin, A., Walters, J. T. R., Farh, K. H., Holmans, P. A., Lee, P., Bulik-Sullivan, B., Collier, D. A., Huang, H., Pers, T. H., Agartz, I., Agerbo, E., Albus, M., Alexander, M., Amin, F., Bacanu, S. A., Begemann, M., Belliveau, R. A., … O'Donovan, M. C. (2014). Biological Insights From 108 Schizophrenia-Associated Genetic Loci. *Nature*, *511*(7510), 421. https://doi.org/10.1038/NATURE13595

280) Ripke, S., Sanders, A. R., Kendler, K. S., Levinson, D. F., Sklar, P., Holmans, P. A., Lin, D. Y., Duan, J., Ophoff, R. A., Andreassen, O. A., Scolnick, E., Cichon, S., St. Clair, D., Corvin, A., Gurling, H., Werge, T., Rujescu, D., Blackwood, D. H. R., Pato, C. N., … Gejman, P. V. (2011). Genome-wide association study identifies five new schizophrenia loci. *Nature Genetics*, *43*(10), 969–978. https://doi.org/10.1038/NG.940

281) Roche, J., & Potoyan, D. A. (2019). Disorder Mediated Oligomerization of DISC1 Proteins Revealed by Coarse-Grained Molecular Dynamics Simulations. *Journal of Physical Chemistry B*, *123*(45), 9567–9575. https://doi.org/10.1021/acs.jpcb.9b07467

282) Rodriguez, V., Alameda, L., Quattrone, D., Tripoli, G., Gayer-Anderson, C., Spinazzola, E., Trotta, G., Jongsma, H. E., Stilo, S., La Cascia, C., Ferraro, L., La Barbera, D., Lasalvia, A., Tosato, S., Tarricone, I., Bonora, E., Jamain, S., Selten, J. P., Velthorst, E., … Vassos, E. (2023). Use of multiple polygenic risk scores for distinguishing schizophrenia-spectrum disorder and affective psychosis categories in a first-episode sample; the EU-GEI study. *Psychological Medicine*, *53*(8), 3396. https://doi.org/10.1017/S0033291721005456

283) Rodríguez-Seoane, C., Ramos, A., Korth, C., & Requena, J. R. (2015). DISC1 regulates expression of the neurotrophin VGF through the PI3K/AKT/CREB pathway. *Journal of Neurochemistry*, *135*(3), 598–605. https://doi.org/10.1111/JNC.13258

284) Rousseau, F., Schymkowitz, J., & Serrano, L. (2006). Protein aggregation and amyloidosis: confusion of the kinds? *Current Opinion in Structural Biology*, *16*(1), 118–126. https://doi.org/10.1016/J.SBI.2006.01.011

285) Sachs, N. A., Sawa, A., Holmes, S. E., Ross, C. A., DeLisi, L. E., & Margolis, R. L. (2005). A frameshift mutation in Disrupted in Schizophrenia 1 in an American family

with schizophrenia and schizoaffective disorder. *Molecular Psychiatry*, *10*(8), 758–764. https://doi.org/10.1038/SJ.MP.4001667

286) Sada-Fuente, E., Aranda, S., Papiol, S., Heilbronner, U., Moltó, M. D., Aguilar, E. J., González-Peñas, J., Andreu-Bernabeu, Á., Arango, C., Crespo-Facorro, B., González-Pinto, A., Fañanás, L., Arias, B., Bobes, J., Costas, J., Martorell, L., Schulze, T. G., Kalman, J. L., Vilella, E., & Muntané, G. (2023). Common genetic variants contribute to heritability of age at onset of schizophrenia. *Translational Psychiatry 2023 13:1*, *13*(1), 1–9. https://doi.org/10.1038/s41398-023-02508-0

287) Samardžija, B., Juković, M., Zaharija, B., Renner, É., Palkovits, M., & Bradshaw, N. J. (2023). Co-Aggregation and Parallel Aggregation of Specific Proteins in Major Mental Illness. *Cells*, *12*(14). https://doi.org/10.3390/cells12141848

288) Samardžija, B., Petrović, M., Zaharija, B., Medija, M., Meštrović, A., Bradshaw, N. J., Filošević Vujnović, A., & Andretić Waldowski, R. (2024). Transgenic Drosophila melanogaster Carrying a Human Full-Length DISC1 Construct (UAS-hflDISC1) Showing Effects on Social Interaction Networks. *Current Issues in Molecular Biology*, *46*(8), 8526–8549. https://doi.org/10.3390/cimb46080502

289) Sanchez-Pulido, L., & Ponting, C. P. (2011). Structure and evolutionary history of DISC1. *Human Molecular Genetics*, *20*(R2), 175–181. https://doi.org/10.1093/hmg/ddr374

290) Sasaki, S., Mori, D., Toyo-oka, K., Chen, A., Garrett-Beal, L., Muramatsu, M., Miyagawa, S., Hiraiwa, N., Yoshiki, A., Wynshaw-Boris, A., & Hirotsune, S. (2005). Complete Loss of Ndel1 Results in Neuronal Migration Defects and Early Embryonic Lethality. *Molecular and Cellular Biology*, *25*(17), 7812. https://doi.org/10.1128/MCB.25.17.7812-7827.2005

291) Sasaki, S., Shionoya, A., Ishida, M., Gambello, M. J., Yingling, J., Wynshaw-Boris, A., & Hirotsune, S. (2000). A LIS1/NUDEL/cytoplasmic dynein heavy chain complex in the developing and adult nervous system. *Neuron*, *28*(3), 681–696. https://doi.org/10.1016/S0896-6273(00)00146-X

292) Sawamura, N., Ando, T., Maruyama, Y., Fujimuro, M., Mochizuki, H., Honjo, K., Shimoda, M., Toda, H., Sawamura-Yamamoto, T., Makuch, L. A., Hayashi, A., Ishizuka, K., Cascella, N. G., Kamiya, A., Ishida, N., Tomoda, T., Hai, T., Furukubo-Tokunaga, K., & Sawa, A. (2008). Nuclear DISC1 regulates CRE-mediated gene transcription and sleep homeostasis in the fruit fly. *Molecular Psychiatry*, *13*(12), 1138–1148. https://doi.org/10.1038/mp.2008.101

293) Sawamura, N., Sawamura-Yamamoto, T., Ozeki, Y., Ross, C. A., & Sawa, A. (2005). A form of DISC1 enriched in nucleus: altered subcellular distribution in orbitofrontal cortex in psychosis and substance/alcohol abuse. *Proceedings of the National Academy of Sciences of the United States of America*, *102*(4), 1187–1192. https://doi.org/10.1073/PNAS.0406543102

294) Scarr, E., Sundram, S., Keriakous, D., & Dean, B. (2007). Altered Hippocampal Muscarinic M4, but Not M1, Receptor Expression from Subjects with Schizophrenia. *Biological Psychiatry*, *61*(10), 1161–1170. https://doi.org/10.1016/j.biopsych.2006.08.050

295) Schäppi, L., Stegmayer, K., Viher, P. V., & Walther, S. (2018). Distinct Associations of Motor Domains in Relatives of Schizophrenia Patients—Different Pathways to Motor Abnormalities in Schizophrenia? *Frontiers in Psychiatry*, *9*(APR), 23. https://doi.org/10.3389/FPSYT.2018.00129

296) Schindelin, J., Arganda-Carreras, I., Frise, E., Kaynig, V., Longair, M., Pietzsch, T., Preibisch, S., Rueden, C., Saalfeld, S., Schmid, B., Tinevez, J. Y., White, D. J., Hartenstein, V., Eliceiri, K., Tomancak, P., & Cardona, A. (2012). Fiji: an open-source platform for biological-image analysis. *Nature Methods*, *9*(7), 676–682. https://doi.org/10.1038/NMETH.2019

297) Schurov, I. L., Handford, E. J., Brandon, N. J., & Whiting, P. J. (2004). Expression of disrupted in schizophrenia 1 (DISC1) protein in the adult and developing mouse brain indicates its role in neurodevelopment. *Molecular Psychiatry*, *9*(12), 1100–1110. https://doi.org/10.1038/SJ.MP.4001574

298) Scialo, F., Sriram, A., Stefanatos, R., & Sanz, A. (2016). Practical Recommendations for the Use of the GeneSwitch Gal4 System to Knock-Down Genes in Drosophila melanogaster. *PloS One*, *11*(8). https://doi.org/10.1371/JOURNAL.PONE.0161817

299) Scott, M. R., & Meador-Woodruff, J. H. (2019). Intracellular compartment-specific proteasome dysfunction in postmortem cortex in schizophrenia subjects. *Molecular Psychiatry 2019 25:4*, *25*(4), 776–790. https://doi.org/10.1038/s41380-019-0359-7

300) Scott, M. R., Rubio, M. D., Haroutunian, V., & Meador-Woodruff, J. H. (2016). Protein Expression of Proteasome Subunits in Elderly Patients with Schizophrenia. *Neuropsychopharmacology : Official Publication of the American College of Neuropsychopharmacology*, *41*(3), 896–905. https://doi.org/10.1038/NPP.2015.219

301) Sehgal, A., Joiner, W., Crocker, A., Koh, K., Sathyanarayanan, S., Fang, Y., Wu, M., Williams, J. A., & Zheng, X. (2007). Molecular analysis of sleep: wake cycles in Drosophila. *Cold Spring Harbor Symposia on Quantitative Biology*, *72*, 557–564. https://doi.org/10.1101/SQB.2007.72.018

302) Seidisarouei, M., Schäble, S., van Wingerden, M., Trossbach, S. V., Korth, C., & Kalenscher, T. (2022). Social anhedonia as a Disrupted-in-Schizophrenia 1-dependent phenotype. *Scientific Reports*, *12*(1). https://doi.org/10.1038/s41598-022-14102-3

303) Shao, L., Lu, B., Wen, Z., Teng, S., Wang, L., Zhao, Y., Wang, L., Ishizuka, K., Xu, X., Sawa, A., Song, H., Ming, G., & Zhong, Y. (2017). Disrupted-in-Schizophrenia-1 (DISC1) protein disturbs neural function in multiple disease-risk pathways. *Human Molecular Genetics*, *26*(14), 2634–2648. https://doi.org/10.1093/hmg/ddx147

304) Shaw, P., Cirelli, C., Greenspan, R., & Tononi, G. (2000). Correlates of sleep and waking in Drosophila melanogaster. *Science (New York, N.Y.)*, *287*(5459), 1834–1837. https://doi.org/10.1126/SCIENCE.287.5459.1834

305) Shen, C. L., Tsai, S. J., Lin, C. P., & Yang, A. C. (2023). Progressive brain abnormalities in schizophrenia across different illness periods: a structural and functional MRI study. *Schizophrenia 2023 9:1*, *9*(1), 1–9. https://doi.org/10.1038/s41537-022-00328-7

306) Shinoda, T., Taya, S., Tsuboi, D., Hikita, T., Matsuzawa, R., Kuroda, S., Iwamatsu, A., & Kaibuchi, K. (2007). DISC1 regulates neurotrophin-induced axon elongation via interaction with Grb2. *The Journal of Neuroscience : The Official Journal of the Society for Neuroscience*, *27*(1), 4–14. https://doi.org/10.1523/JNEUROSCI.3825-06.2007

307) Sialana, F. J., Wang, A. L., Fazari, B., Kristofova, M., Smidak, R., Trossbach, S. V., Korth, C., Huston, J. P., de Souza Silva, M. A., & Lubec, G. (2018). Quantitative Proteomics of Synaptosomal Fractions in a Rat Overexpressing Human DISC1 Gene Indicates Profound Synaptic Dysregulation in the Dorsal Striatum. *Frontiers in Molecular Neuroscience*, *11*. https://doi.org/10.3389/FNMOL.2018.00026

308) Singh, K. K., De Rienzo, G., Drane, L., Mao, Y., Flood, Z., Madison, J., Ferreira, M., Bergen, S., King, C., Sklar, P., Sive, H., & Tsai, L. H. (2011). Common DISC1 polymorphisms disrupt Wnt/GSK3β-signaling and brain development. *Neuron*, *72*(4), 545. https://doi.org/10.1016/J.NEURON.2011.09.030

309) Siuciak, J. A., Chapin, D. S., McCarthy, S. A., & Martin, A. N. (2007). Antipsychotic profile of rolipram: efficacy in rats and reduced sensitivity in mice deficient in the phosphodiesterase-4B (PDE4B) enzyme. *Psychopharmacology*, *192*(3), 415–424. https://doi.org/10.1007/S00213-007-0727-X

310) Smith, D. S., Niethammer, M., Ayala, R., Zhou, Y., Gambello, M. J., Wynshaw-Boris, A., & Tsai, L. H. (2000). Regulation of cytoplasmic dynein behaviour and microtubule organization by mammalian Lis1. *Nature Cell Biology*, *2*(11), 767–775. https://doi.org/10.1038/35041000

311) Smoller, J. W., Kendler, K. K., Craddock, N., Lee, P. H., Neale, B. M., Nurnberger, J. N., Ripke, S., Santangelo, S., Sullivan, P. S., Neale, B. N., Purcell, S., Anney, R., Buitelaar, J., Fanous, A., Faraone, S. F., Hoogendijk, W., Lesch, K. P., Levinson, D. L., Perlis, R. P., … O'Donovan, M. (2013). Identification of risk loci with shared effects on five major psychiatric disorders: a genome-wide analysis. *Lancet (London, England)*, *381*(9875), 1371–1379. https://doi.org/10.1016/S0140-6736(12)62129-1

312) Soares, D. C., Bradshaw, N. J., Zou, J., Kennaway, C. K., Hamilton, R. S., Chen, Z. A., Wear, M. A., Blackburn, E. A., Bramham, J., Böttcher, B., Millar, J. K., Barlow, P. N., Walkinshaw, M. D., Rappsilber, J., & Porteous, D. J. (2012). The mitosis and neurodevelopment proteins NDE1 and NDEl1 form dimers, tetramers, and polymers with a folded back structure in solution. *Journal of Biological Chemistry*, *287*(39), 32381–32393. https://doi.org/10.1074/jbc.M112.393439

313) Soares, D. C., Carlyle, B. C., Bradshaw, N. J., & Porteous, D. J. (2011). DISC1: Structure, Function, and Therapeutic Potential for Major Mental Illness. *ACS Chemical Neuroscience*, *2*(11), 609–632. https://doi.org/10.1021/CN200062K

314) Soda, T., Frank, C., Ishizuka, K., Baccarella, A., Park, Y. U., Flood, Z., Park, S. K., Sawa, A., & Tsai, L. H. (2013). DISC1–ATF4 transcriptional repression complex: dual regulation of the cAMP-PDE4 cascade by DISC1. *Molecular Psychiatry 2013 18:8*, *18*(8), 898–908. https://doi.org/10.1038/mp.2013.38

315) Sohi, M., Alexandrovich, A., Moolenaar, G., Visse, R., Goosen, N., Vernede, X., Fontecilla-Camps, J. C., Champness, J., & Sanderson, M. R. (2000). Crystal structure of Escherichia coli UvrB C-terminal domain, and a model for UvrB-UvrC interaction. *FEBS Letters*, *465*(2–3), 161–164. https://doi.org/10.1016/S0014-5793(99)01690-7

316) Sommer, I. E., Tiihonen, J., van Mourik, A., Tanskanen, A., & Taipale, H. (2020). The clinical course of schizophrenia in women and men—a nation-wide cohort study. *Npj Schizophrenia 2020 6:1*, *6*(1), 1–7. https://doi.org/10.1038/s41537-020-0102-z

317) Song, C., Wang, X.-N., Yan, L., Wang, H.-Y., & Wang, C.-H. (2023). The interaction between autophagy and inflammation in Schizophrenia: insight into mTOR-PI3K/Akt pathways and glial phenotype expression. *Journal of Affective Disorders Reports*, *12*, 100567. https://doi.org/10.1016/J.JADR.2023.100567

318) St Clair, D., Blackwood, D., Muir, W., Carothers, A., Walker, M., Spowart, G., Gosden, C., & Evans, H. J. (1990). Association within a family of a balanced autosomal translocation with major mental illness. *The Lancet*, *336*, 13–16.

319) Steinecke, A., Gampe, C., Nitzsche, F., & Bolz, J. (2014). DISC1 knockdown impairs the tangential migration of cortical interneurons by affecting the actin cytoskeleton. *Frontiers in Cellular Neuroscience*, *8*(JULY). https://doi.org/10.3389/FNCEL.2014.00190/ABSTRACT

320) Sullivan, P. F., Kendler, K. S., & Neale, M. C. (2003). Schizophrenia as a Complex Trait: Evidence From a Meta-analysis of Twin Studies. *Archives of General Psychiatry*, *60*(12), 1187–1192. https://doi.org/10.1001/ARCHPSYC.60.12.1187

321) Swan, A., Nguyen, T., & Suter, B. (1999). Drosophila Lissencephaly-1 functions with Bic-D and dynein in oocyte determination and nuclear positioning. *Nature Cell Biology 1999 1:7*, *1*(7), 444–449. https://doi.org/10.1038/15680

322) Szeszko, P. R., Hodgkinson, C. A., Robinson, D. G., DeRosse, P., Bilder, R. M., Lencz, T., Burdick, K. E., Napolitano, B., Betensky, J. D., Kane, J. M., Goldman, D., & Malhotra, A. K. (2008). DISC1 is Associated with Prefrontal Cortical Gray Matter and Positive Symptoms in Schizophrenia. *Biological Psychology*, *79*(1), 103. https://doi.org/10.1016/J.BIOPSYCHO.2007.10.011

323) Tai, C. Y., Dujardin, D. L., Faulkner, N. E., & Vallee, R. B. (2002). Role of dynein, dynactin, and CLIP-170 interactions in LIS1 kinetochore function. *The Journal of Cell Biology*, *156*(6), 959. https://doi.org/10.1083/JCB.200109046

324) Tan, Y., Zhu, J., & Hashimoto, K. (2024). Autophagy-related gene model as a novel risk factor for schizophrenia. *Translational Psychiatry 2024 14:1*, *14*(1), 1–10. https://doi.org/10.1038/s41398-024-02767-5

325) Tanaka, M., Ishizuka, K., Nekooki-Machida, Y., Endo, R., Takashima, N., Sasaki, H., Komi, Y., Gathercole, A., Huston, E., Ishii, K., Hui, K. K. W., Kurosawa, M., Kim, S. H., Nukina, N., Takimoto, E., Houslay, M. D., & Sawa, A. (2017). Aggregation of scaffolding protein DiSC1 dysregulates phosphodiesterase 4 in Huntington's disease. *Journal of Clinical Investigation*, *127*(4), 1438–1450. https://doi.org/10.1172/JCI85594

326) Tarendeau, F., Boudet, J., Guilligay, D., Mas, P. J., Bougault, C. M., Boulo, S., Baudin, F., Ruigrok, R. W. H., Daigle, N., Ellenberg, J., Cusack, S., Simorre, J. P., & Hart, D. J. (2007). Structure and nuclear import function of the C-terminal domain of influenza virus polymerase PB2 subunit. *Nature Structural & Molecular Biology*, *14*(3), 229–233. https://doi.org/10.1038/NSMB1212

327) Taylor, M. S., Devon, R. S., Millar, J. K., & Porteous, D. J. (2003). Evolutionary constraints on the Disrupted in Schizophrenia locus. *Genomics*, *81*(1), 67–77. https://doi.org/10.1016/S0888-7543(02)00026-5

328) Teng, S., Thomson, P. A., Mccarthy, S., Kramer, M., Muller, S., Lihm, J., Morris, S., Soares, D. C., Hennah, W., Harris, S., Camargo, L. M., Malkov, V., Mcintosh, A. M., Millar, J. K., Blackwood, D. H., Evans, K. L., Deary, I. J., Porteous, D. J., & Mccombie,

W. R. (2018). Rare disruptive variants in the DISC1 Interactome and Regulome: association with cognitive ability and schizophrenia. *Molecular Psychiatry*, *23*, 1270–1277. https://doi.org/10.1038/mp.2017.115

329) The Human Protein Atlas. (2024). *Tissue expression of DISC1*. https://www.proteinatlas.org/ENSG00000162946-DISC1/tissue

330) Therianos, S., Leuzinger, S., Hirth, F., Goodman, C. S., & Reichert, H. (1995). Embryonic development of the Drosophila brain: formation of commissural and descending pathways. *Development (Cambridge, England)*, *121*(11), 3849–3860. https://doi.org/10.1242/DEV.121.11.3849

331) Thomson, P. A., Duff, B., Blackwood, D. H. R., Romaniuk, L., Watson, A., Whalley, H. C., Li, X., Dauvermann, M. R., Moorhead, T. W. J., Bois, C., Ryan, N. M., Redpath, H., Hall, L., Morris, S. W., Van Beek, E. J. R., Roberts, N., Porteous, D. J., St Clair, D., Whitcher, B., … Lawrie, S. M. (2016). Balanced translocation linked to psychiatric disorder, glutamate, and cortical structure/function. *Npj Schizophrenia*, *2*. https://doi.org/10.1038/npjschz.2016.24

332) Thomson, P. A., Malavasi, E. L. V., Grünewald, E., Soares, D. C., Borkowska, M., & Millar, J. K. (2013). DISC1 genetics, biology and psychiatric illness. *Frontiers in Biology*, *8*(1), 1. https://doi.org/10.1007/S11515-012-1254-7

333) Tomppo, L., Hennah, W., Lahermo, P., Loukola, A., Tuulio-Henriksson, A., Suvisaari, J., Partonen, T., Ekelund, J., Lönnqvist, J., & Peltonen, L. (2009). Association between genes of Disrupted in schizophrenia 1 (DISC1) interactors and schizophrenia supports the role of the DISC1 pathway in the etiology of major mental illnesses. *Biological Psychiatry*, *65*(12), 1055–1062. https://doi.org/10.1016/J.BIOPSYCH.2009.01.014

334) Torres, U. S., Duran, F. L. S., Schaufelberger, M. S., Crippa, J. A. S., Louzã, M. R., Sallet, P. C., Kanegusuku, C. Y. O., Elkis, H., Gattaz, W. F., Bassitt, D. P., Zuardi, A. W., Hallak, J. E. C., Leite, C. C., Castro, C. C., Santos, A. C., Murray, R. M., & Busatto, G. F. (2016). Patterns of regional gray matter loss at different stages of schizophrenia: A multisite, cross-sectional VBM study in first-episode and chronic illness. *NeuroImage. Clinical*, *12*, 1–15. https://doi.org/10.1016/J.NICL.2016.06.002

335) Trossbach, S. V., Bader, V., Hecher, L., Pum, M. E., Masoud, S. T., Prikulis, I., Schäble, S., De Souza Silva, M. A., Su, P., Boulat, B., Chwiesko, C., Poschmann, G., Stühler, K., Lohr, K. M., Stout, K. A., Oskamp, A., Godsave, S. F., Müller-Schiffmann, A., Bilzer, T., … Korth, C. (2016). Misassembly of full-length Disrupted-in-Schizophrenia 1 protein is linked to altered dopamine homeostasis and behavioral deficits. *Molecular Psychiatry*, *21*(11), 1561–1572. https://doi.org/10.1038/mp.2015.194

336) Trossbach, S. V., Hecher, L., Schafflick, D., Deenen, R., Popa, O., Lautwein, T., Tschirner, S., Köhrer, K., Fehsel, K., Papazova, I., Malchow, B., Hasan, A., Winterer, G., Schmitt, A., Meyer zu Hörste, G., Falkai, P., & Korth, C. (2019). Dysregulation of a specific immune-related network of genes biologically defines a subset of schizophrenia. *Translational Psychiatry*, *9*(1). https://doi.org/10.1038/s41398-019-0486-6

337) Trubetskoy, V., Pardiñas, A. F., Qi, T., Panagiotaropoulou, G., Awasthi, S., Bigdeli, T. B., Bryois, J., Chen, C. Y., Dennison, C. A., Hall, L. S., Lam, M., Watanabe, K., Frei, O., Ge, T., Harwood, J. C., Koopmans, F., Magnusson, S., Richards, A. L., Sidorenko, J., … van Os, J. (2022). Mapping genomic loci implicates genes and synaptic biology in schizophrenia. *Nature*, *604*(7906), 502. https://doi.org/10.1038/S41586-022-04434-5

338) Tsai, J. W., Chen, Y., Kriegstein, A. R., & Vallee, R. B. (2005). LIS1 RNA interference blocks neural stem cell division, morphogenesis, and motility at multiple stages. *The Journal of Cell Biology*, *170*(6), 935–945. https://doi.org/10.1083/JCB.200505166

339) UCSC Genome Browser v466. (2024). *Human hg38 chr1:231,094,436-231,508,918 UCSC Genome Browser v466*. https://genome.ucsc.edu/cgi-bin/hgTracks?db=hg38&lastVirtModeType=default&lastVirtModeExtraState=&virtModeType=default&virtMode=0&nonVirtPosition=&position=chr1%3A231094436%2D231508918&hgsid=2303225376_Ou9GrEAC0IMHHlfYz1UbgmEb7Jna

340) Vallee, R. B., Seale, G. E., & Tsai, J. W. (2009). Emerging roles for myosin II and cytoplasmic dynein in migrating neurons and growth cones. *Trends in Cell Biology*, *19*(7), 347. https://doi.org/10.1016/J.TCB.2009.03.009

341) Van Erp, T. G. M., Hibar, D. P., Rasmussen, J. M., Glahn, D. C., Pearlson, G. D., Andreassen, O. A., Agartz, I., Westlye, L. T., Haukvik, U. K., Dale, A. M., Melle, I., Hartberg, C. B., Gruber, O., Kraemer, B., Zilles, D., Donohoe, G., Kelly, S., McDonald, C., Morris, D. W., … Turner, J. A. (2016). Subcortical brain volume abnormalities in 2028 individuals with schizophrenia and 2540 healthy controls via the ENIGMA consortium. *Molecular Psychiatry*, *21*(4), 547. https://doi.org/10.1038/MP.2015.63

342) van Haren, N. E. M., Pol, H. E. H., Schnack, H. G., Cahn, W., Brans, R., Carati, I., Rais, M., & Kahn, R. S. (2008). Progressive brain volume loss in schizophrenia over the course of the illness: evidence of maturational abnormalities in early adulthood. *Biological Psychiatry*, *63*(1), 106–113. https://doi.org/10.1016/J.BIOPSYCH.2007.01.004

343) Van Os, J., Kenis, G., & Rutten, B. P. F. (2010). The environment and schizophrenia. *Nature*, *468*(7321), 203–212. https://doi.org/10.1038/NATURE09563

344) Varese, F., Smeets, F., Drukker, M., Lieverse, R., Lataster, T., Viechtbauer, W., Read, J., Van Os, J., & Bentall, R. P. (2012). Childhood adversities increase the risk of psychosis: a meta-analysis of patient-control, prospective- and cross-sectional cohort studies. *Schizophrenia Bulletin*, *38*(4), 661–671. https://doi.org/10.1093/SCHBUL/SBS050

345) Vasistha, N. A., Johnstone, M., Barton, S. K., Mayerl, S. E., Thangaraj Selvaraj, B., Thomson, P. A., Dando, O., Grünewald, E., Alloza, C., Bastin, M. E., Livesey, M. R., Economides, K., Magnani, D., Makedonopolou, P., Burr, K., Story, D. J., Blackwood, D. H. R., Wyllie, D. J. A., McIntosh, A. M., … Chandran, S. (2019). Familial t(1;11) translocation is associated with disruption of white matter structural integrity and oligodendrocyte–myelin dysfunction. *Molecular Psychiatry*, *24*(11), 1641–1654. https://doi.org/10.1038/s41380-019-0505-2

346) Vecsey, C. G., Baillie, G. S., Jaganath, D., Havekes, R., Daniels, A., Wimmer, M., Huang, T., Brown, K. M., Li, X. Y., Descalzi, G., Kim, S. S., Chen, T., Shang, Y. Z., Zhuo, M., Houslay, M. D., & Abel, T. (2009). Sleep deprivation impairs cAMP signaling in the hippocampus. *Nature*, *461*(7267), 1122. https://doi.org/10.1038/NATURE08488

347) Vergnolle, M. A. S., & Taylor, S. S. (2007). Cenp-F Links Kinetochores to Ndel1/Nde1/Lis1/Dynein Microtubule Motor Complexes. *Current Biology*, *17*(13), 1173–1179. https://doi.org/10.1016/j.cub.2007.05.077

348) Vernon, E., Meyer, G., Pickard, L., Dev, K., Molnar, E., Collingridge, G. L., & Henley, J. M. (2001). GABA(B) receptors couple directly to the transcription factor ATF4.

Molecular and Cellular Neurosciences, *17*(4), 637–645.
https://doi.org/10.1006/MCNE.2000.0960

349) Vincent, A. C., & Struhl, K. (1992). ACR1, a yeast ATF/CREB repressor. *Molecular and Cellular Biology*, *12*(12), 5394. https://doi.org/10.1128/MCB.12.12.5394

350) Vlasova, R. M., Iosif, A. M., Ryan, A. M., Funk, L. H., Murai, T., Chen, S., Lesh, T. A., Rowland, D. J., Bennett, J., Hogrefe, C. E., Maddock, R. J., Gandal, M. J., Geschwind, D. H., Schumann, C. M., Van de Water, J., Kimberley McAllister, A., Carter, C. S., Styner, M. A., Amaral, D. G., & Bauman, M. D. (2021). Maternal Immune Activation during Pregnancy Alters Postnatal Brain Growth and Cognitive Development in Nonhuman Primate Offspring. *The Journal of Neuroscience : The Official Journal of the Society for Neuroscience*, *41*(48), 9971–9987.
https://doi.org/10.1523/JNEUROSCI.0378-21.2021

351) Voce, A., McKetin, R., Burns, R., Castle, D., & Calabria, B. (2018). The relationship between illicit amphetamine use and psychiatric symptom profiles in schizophrenia and affective psychoses. *Psychiatry Research*, *265*, 19–24.
https://doi.org/10.1016/J.PSYCHRES.2018.04.015

352) Wang, A. L., Chao, O. Y., Nikolaus, S., Lamounier-Zepter, V., Hollenberg, C. P., Lubec, G., Trossbach, S. V., Korth, C., & Huston, J. P. (2022). Disrupted-in-schizophrenia 1 Protein Misassembly Impairs Cognitive Flexibility and Social Behaviors in a Transgenic Rat Model. *Neuroscience*, *493*, 41–51.
https://doi.org/10.1016/j.neuroscience.2022.04.013

353) Wang, Q., Charych, E. I., Pulito, V. L., Lee, J. B., Graziane, N. M., Crozier, R. A., Revilla-Sanchez, R., Kelly, M. P., Dunlop, A. J., Murdoch, H., Taylor, N., Xie, Y., Pausch, M., Hayashi-Takagi, A., Ishizuka, K., Seshadri, S., Bates, B., Kariya, K., Sawa, A., … Brandon, N. J. (2011). The psychiatric disease risk factors DISC1 and TNIK interact to regulate synapse composition and function. *Molecular Psychiatry*, *16*(10), 1006–1023. https://doi.org/10.1038/MP.2010.87

354) Wang, S., Liang, Q., Qiao, H., Li, H., Shen, T., Ji, F., & Jiao, J. (2016). DISC1 regulates astrogenesis in the embryonic brain via modulation of RAS/MEK/ERK signaling through RASSF7. *Development (Cambridge)*, *143*(15), 2732–2740.
https://doi.org/10.1242/DEV.133066/264061/AM/DISC1-REGULATES-ASTROGENESIS-IN-THE-EMBRYONIC

355) Wang, X., Ye, F., Wen, Z., Guo, Z., Yu, C., Huang, W. K., Rojas Ringeling, F., Su, Y., Zheng, W., Zhou, G., Christian, K. M., Song, H., Zhang, M., & Ming, G. li. (2019). Structural interaction between DISC1 and ATF4 underlying transcriptional and synaptic dysregulation in an iPSC model of mental disorders. *Molecular Psychiatry 2019 26:4*, *26*(4), 1346–1360. https://doi.org/10.1038/s41380-019-0485-2

356) Wang, X., Ye, F., Wen, Z., Guo, Z., Yu, C., Huang, W. K., Rojas Ringeling, F., Su, Y., Zheng, W., Zhou, G., Christian, K. M., Song, H., Zhang, M., & Ming, G. li. (2021). Structural interaction between DISC1 and ATF4 underlying transcriptional and synaptic dysregulation in an iPSC model of mental disorders. *Molecular Psychiatry*, *26*(4), 1346.
https://doi.org/10.1038/S41380-019-0485-2

357) Wang, Y., Zhang, H., Zhong, H., & Xue, Z. (2021). Protein domain identification methods and online resources. *Computational and Structural Biotechnology Journal*, *19*, 1145. https://doi.org/10.1016/J.CSBJ.2021.01.041

358) Wang, Z. T., Lu, M. H., Zhang, Y., Ji, W. L., Lei, L., Wang, W., Fang, L. P., Wang, L. W., Yu, F., Wang, J., Li, Z. Y., Wang, J. R., Wang, T. H., Dou, F., Wang, Q. W., Wang, X. L., Li, S., Ma, Q. H., & Xu, R. X. (2018). Disrupted-in-schizophrenia-1 protects synaptic plasticity in a transgenic mouse model of Alzheimer's disease as a mitophagy receptor. *Aging Cell*, *18*(1), e12860. https://doi.org/10.1111/ACEL.12860

359) Watanabe, M., Khu, T. M., Warren, G., Shin, J., Stewart, C. E., & Roche, J. (2023). Evidence of DISC1 as an arsenic binding protein and implications regarding its role as a translational activator. *Frontiers in Molecular Biosciences*, *10*, 1308693. https://doi.org/10.3389/FMOLB.2023.1308693/BIBTEX

360) Waters, F., & S. Manoach, D. (2012). Sleep dysfunctions in schizophrenia: A practical review. *Open Journal of Psychiatry*, *2*(04), 384–392. https://doi.org/10.4236/OJPSYCH.2012.224054

361) Weamer, E. A., Emanuel, J. E., Varon, D., Miyahara, S., Wilkosz, P. A., Lopez, O. L., DeKosky, S. T., & Sweet, R. A. (2009). The relationship of excess cognitive impairment in MCI and early Alzheimer's disease to the subsequent emergence of psychosis. *International Psychogeriatrics*, *21*(1), 78–85. https://doi.org/10.1017/S1041610208007734

362) Wei, J., Graziane, N. M., Gu, Z., & Yan, Z. (2015). DISC1 Protein Regulates γ-Aminobutyric Acid, Type A (GABAA) Receptor Trafficking and Inhibitory Synaptic Transmission in Cortical Neurons. *The Journal of Biological Chemistry*, *290*(46), 27680. https://doi.org/10.1074/JBC.M115.656173

363) White, J. H., McIllhinney, R. A. J., Wise, A., Ciruela, F., Chan, W. Y., Emson, P. C., Billinton, A., & Marshall, F. H. (2000). The GABAB receptor interacts directly with the related transcription factors CREB2 and ATFx. *Proceedings of the National Academy of Sciences of the United States of America*, *97*(25), 13967–13972. https://doi.org/10.1073/PNAS.240452197

364) Wong, T. Y., Radua, J., Pomarol-Clotet, E., Salvador, R., Albajes-Eizagirre, A., Solanes, A., Canales-Rodriguez, E. J., Guerrero-Pedraza, A., Sarro, S., Kircher, T., Nenadic, I., Krug, A., Grotegerd, D., Dannlowski, U., Borgwardt, S., Riecher-Rössler, A., Schmidt, A., Andreou, C., Huber, C. G., … Nickl-Jockschat, T. (2020). An overlapping pattern of cerebral cortical thinning is associated with both positive symptoms and aggression in schizophrenia via the ENIGMA consortium. *Psychological Medicine*, *50*(12), 2034–2045. https://doi.org/10.1017/S0033291719002149

365) World Health Organisation. (2022). *International Classification of Diseases for Mortality and Morbidity Statistics* (11th ed.). https://icd.who.int/browse11/l-

366) World Health Organization. (2024). *Clinical descriptions and diagnostic requirements for ICD-11 mental, behavioural and neurodevelopmental disorders*. World Health Organization. https://iris.who.int/bitstream/handle/10665/375767/9789240077263-eng.pdf?sequence=1&isAllowed=y

367) Wulff, K., Dijk, D. J., Middleton, B., Foster, R. G., & Joyce, E. M. (2012). Sleep and circadian rhythm disruption in schizophrenia. *The British Journal of Psychiatry : The Journal of Mental Science*, *200*(4), 308–316. https://doi.org/10.1192/BJP.BP.111.096321

368) Wynshaw-Boris, A. (2007). Lissencephaly and LIS1: insights into the molecular mechanisms of neuronal migration and development. *Clinical Genetics*, *72*(4), 296–304. https://doi.org/10.1111/J.1399-0004.2007.00888.X

369) Xiang, X., Osmani, A. H., Osmani, S. A., Xin, M., & Morris, N. R. (1995). NudF, a nuclear migration gene in Aspergillus nidulans, is similar to the human LIS-1 gene required for neuronal migration. *Molecular Biology of the Cell*, *6*(3), 297. https://doi.org/10.1091/MBC.6.3.297

370) Xiao, Y., Lui, S., Deng, W., Yao, L., Zhang, W., Li, S., Wu, M., Xie, T., He, Y., Huang, X., Hu, J., Bi, F., Li, T., & Gong, Q. (2015). Altered cortical thickness related to clinical severity but not the untreated disease duration in schizophrenia. *Schizophrenia Bulletin*, *41*(1), 201–210. https://doi.org/10.1093/SCHBUL/SBT177

371) Yang, K., Longo, L., Narita, Z., Cascella, N., Nucifora, F. C., Coughlin, J. M., Nestadt, G., Sedlak, T. W., Mihaljevic, M., Wang, M., Kenkare, A., Nagpal, A., Sethi, M., Kelly, A., Di Carlo, P., Kamath, V., Faria, A., Barker, P., & Sawa, A. (2022). A multimodal study of a first episode psychosis cohort: potential markers of antipsychotic treatment resistance. *Molecular Psychiatry*, *27*(2), 1184. https://doi.org/10.1038/S41380-021-01331-7

372) Yang, Y., Liu, S., Jiang, X., Yu, H., Ding, S., Lu, Y., Li, W., Zhang, H., Liu, B., Cui, Y., Fan, L., Jiang, T., & Lv, L. (2019). Common and specific functional activity features in schizophrenia, major depressive disorder, and bipolar disorder. *Frontiers in Psychiatry*, *10*(FEB), 52. https://doi.org/10.3389/FPSYT.2019.00052/FULL

373) Ye, F., Kang, E., Yu, C., Qian, X., Jacob, F., Yu, C., Mao, M., Poon, R. Y. C., Kim, J., Song, H., Ming, G. li, & Zhang, M. (2017). DISC1 Regulates Neurogenesis via Modulating Kinetochore Attachment of Ndel1/Nde1 during Mitosis. *Neuron*, *96*(5), 1041-1054.e5. https://doi.org/10.1016/j.neuron.2017.10.010

374) Yerabham, A. S. K., Mas, P. J., Decker, C., Soares, D. C., Weiergräber, O. H., Nagel-Steger, L., Willbold, D., Hart, D. J., Bradshaw, N. J., & Korth, C. (2017). A structural organization for the Disrupted in Schizophrenia 1 protein, identified by high-throughput screening, reveals distinctly folded regions, which are bisected by mental illness-related mutations. *Journal of Biological Chemistry*, *292*(16), 6468–6477. https://doi.org/10.1074/jbc.M116.773903

375) Yerabham, A. S. K., Müller-Schiffmann, A., Ziehm, T., Stadler, A., Köber, S., Indurkhya, X., Marreiros, R., Trossbach, S. V., Bradshaw, N. J., Prikulis, I., Willbold, D., Weiergräber, O. H., & Korth, C. (2018). Biophysical insights from a single chain camelid antibody directed against the Disrupted-in-Schizophrenia 1 protein. *PLoS ONE*, *13*(1). https://doi.org/10.1371/journal.pone.0191162

376) Yerabham, A. S. K., Weiergräber, O. H., Bradshaw, N. J., & Korth, C. (2013). Revisiting Disrupted-in-Schizophrenia 1 as a scaffold protein. In *Biological Chemistry* (Vol. 394, Issue 11, pp. 1425–1437). https://doi.org/10.1515/hsz-2013-0178

377) Young-Pearse, T. L., Suth, S., Luth, E. S., Sawa, A., & Selkoe, D. J. (2010). Biochemical and Functional Interaction of Disrupted-in-Schizophrenia 1 and Amyloid Precursor Protein Regulates Neuronal Migration during Mammalian Cortical Development. *The Journal of Neuroscience*, *30*(31), 10431. https://doi.org/10.1523/JNEUROSCI.1445-10.2010

378) Yu, M., Linn, K. A., Shinohara, R. T., Oathes, D. J., Cook, P. A., Duprat, R., Moore, T. M., Oquendo, M. A., Phillips, M. L., McInnis, M., Fava, M., Trivedi, M. H., McGrath, P., Parsey, R., Weissman, M. M., & Sheline, Y. I. (2019). Childhood trauma history is linked to abnormal brain connectivity in major depression. *Proceedings of the National Academy of Sciences of the United States of America*, *116*(17), 8582–8590. https://doi.org/10.1073/PNAS.1900801116/SUPPL_FILE/PNAS.1900801116.SAPP02.PDF

379) Yumerefendi, H., Tarendeau, F., Mas, P. J., & Hart, D. J. (2010). ESPRIT: an automated, library-based method for mapping and soluble expression of protein domains from challenging targets. *Journal of Structural Biology*, *172*(1), 66–74. https://doi.org/10.1016/J.JSB.2010.02.021

380) Zaharija, B., & Bradshaw, N. J. (2024). Aggregation of Disrupted in Schizophrenia 1 arises from a central region of the protein. *Progress in Neuro-Psychopharmacology and Biological Psychiatry*, *130*. https://doi.org/10.1016/j.pnpbp.2023.110923

381) Zaharija, B., Odorčić, M., Hart, A., Samardžija, B., Marreiros, R., Prikulis, I., Juković, M., Hyde, T. M., Kleinman, J. E., Korth, C., & Bradshaw, N. J. (2022). TRIOBP-1 Protein Aggregation Exists in Both Major Depressive Disorder and Schizophrenia, and Can Occur through Two Distinct Regions of the Protein. *International Journal of Molecular Sciences*, *23*(19). https://doi.org/10.3390/IJMS231911048

382) Zaharija, B., Samardžija, B., & Bradshaw, N. J. (2020). The TRIOBP Isoforms and Their Distinct Roles in Actin Stabilization, Deafness, Mental Illness, and Cancer. *Molecules (Basel, Switzerland)*, *25*(21), 1–18. https://doi.org/10.3390/molecules25214967

383) Zhang, M., Zhao, S., Chen, Y., Zhang, X., Li, Y., Xu, P., Huang, Y., & Sun, X. (2022). Chronic Stress in Bipolar Disorders Across the Different Clinical States: Roles of HPA Axis and Personality. *Neuropsychiatric Disease and Treatment*, *18*, 1715. https://doi.org/10.2147/NDT.S372358

384) Zhao, L., Zhao, J., Zhong, K., Tong, A., & Jia, D. (2022). Targeted protein degradation: mechanisms, strategies and application. *Signal Transduction and Targeted Therapy 2022 7:1*, *7*(1), 1–13. https://doi.org/10.1038/s41392-022-00966-4

385) Zhu, S., Abounit, S., Korth, C., & Zurzolo, C. (2017). Transfer of disrupted-in-schizophrenia 1 aggregates between neuronal-like cells occurs in tunnelling nanotubes and is promoted by dopamine. *Open Biology*, *7*(3). https://doi.org/10.1098/rsob.160328

8. List of figures

9. List of tables

10. Appendix

A)


B)

C)

D)

E)

Appendix I. Increased 24-hour locomotor activity in pan-neuronal DISC1 expression line and UAS-*DISC1-2ⁿᵈ* control line. The average locomotor activity per minute was measured in 3-5 days old first generation male transgenic flies (UAS-*DISC1-2ⁿᵈ*, *elav-Gal4* × UAS-*DISC1*/*SM6a* progenies (UAS>*Gal4*)) and controls (*wt*, *elav-Gal4*) over the course of five consecutive days, in L/D (light/dark) conditions. Statistical analysis was performed on n=48 flies per line, using one-way ANOVA with Tukey post-hoc test. $p < 0.05$ = statistically significant (*); $p > 0.05$ = not significant (ns). **A)** Average 24-h locomotor activity of transgenic UAS-*DISC1-2ⁿᵈ* and UAS>*Gal4* versus *wt* control. **B)** Average 24-h activity of all lines, divided into 12-h L/D periods (white/black boxes). **C)** Comparison of *wt* and *elav-Gal4* controls over the 5-day period. **D)** Comparison of UAS-*DISC1-2ⁿᵈ* and *wt* over the 5-day period. **E)** Comparison of the UAS>*Gal4* progeny line and *wt*, over the 5-day period. *wt* – wild type line (*Canton S*); *elav-Gal4* – pan-neuronal driver line.
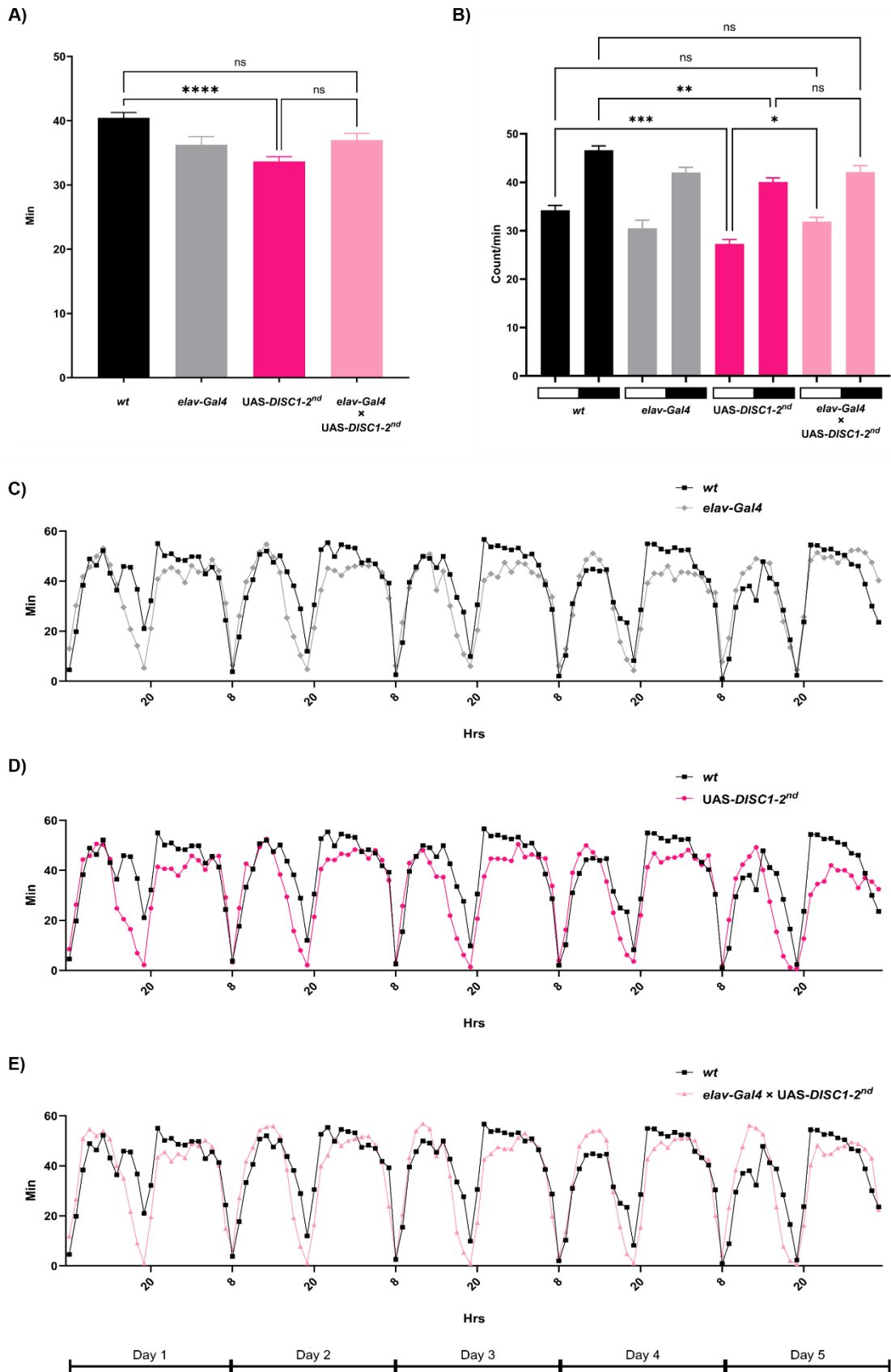
Appendix II. UAS-*DISC1-2nd* line, but not UAS>*Gal4* progenies, exhibit decrease in total sleep amount. The average duration of sleep, shown in minutes, was measured in 3-5 days old first generation male transgenic flies with gene insertion on the third chromosome (UAS-*DISC1-2nd* and *elav-Gal4* × UAS-*DISC1-2nd* progenies (UAS>*Gal4*)), and corresponding controls (*wt*, *elav-Gal4*) during the 5-day period, in L/D (light/dark) conditions. Sleep was defined as no beam interruption for five or more minutes. Results are depicted as an average of a 24-hour period. Statistical analysis was performed on n=48 flies per line, using one-way ANOVA with Tukey post-hoc test. $p < 0.05$ = statistically significant (*); $p > 0.05$ = not significant (ns). **A)** Average overall sleep amount of UAS-*DISC1-2nd* and UAS>*Gal4* progeny lines versus *wt*. **B)** Average sleep amount of all lines, divided into 12-h L/D periods (white/black boxes). **C)** Comparison of *wt* and *elav-Gal4* controls over the 5-day period. **D)** Comparison of UAS-*DISC1-2nd* and *wt* over the 5-day period. **E)** Comparison of the UAS>*Gal4* progeny line and *wt*, over the 5-day period. *wt* – wild type line (*Canton S*); *elav-Gal4* – pan-neuronal driver line.

11. Biography
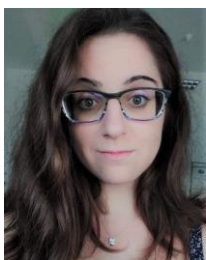
Beti Zaharija

Address: Dolnja cesta 19, 51219, Čavle, Croatia

Email address: beti.zaharija@gmail.com

Phone number: (+385) 91 567 9862

Website: bradshawlab.uniri.hr

Date of birth: 07/12/1994

Nationality: Croatian

EDUCATION

[2019 – Present] **PhD program "Medicinal Chemistry"**

Faculty of Biotechnology and Drug Development, University of Rijeka, Croatia

○ Thesis topic "Investigating the aggregation of DISC1 and TRIOBP-1 in neuropsychiatric disorders". Mentor: Nicholas J. Bradshaw, PhD.

[2016 – 2018] **Master of Science**

Faculty of Biotechnology and Drug Development, University of Rijeka, Croatia

○ Graduate program "Medicinal Chemistry".
○ Master's thesis project "*In vitro* SUMOylation of proteins involved in mental illness"; Centre for High-throughput Technologies, University of Rijeka.

[2013 – 2016] **Bachelor of Science**

Faculty of Biotechnology and Drug Development, University of Rijeka, Croatia

○ Undergraduate program "Biotechnology and Drug Research".
○ Bachelor's thesis: "Neurobiological Mechanisms of Obsessive-Compulsive Disorder".

RESEARCH EXPERIENCE

[2019 – Present] **PhD student/Assistant**

Faculty of Biotechnology and Drug Development, University of Rijeka, Croatia

Main activities and responsibilities:
○ Assistant on a project "Characterization of aggregated protein in neuropsychiatric disorders including *Drosophila* models". Mentor: Nicholas J. Bradshaw, PhD.
○ Funded by a Croatian Science Foundation project grant: "Istraživanje shizofrenije kroz ekspresiju netopivih proteina" (#9424).

[09/2022 – 02/2023] **Doctoral internship**

Forschungszentrum Jülich, Institute of Biological Information Processing, Germany

Main activities and responsibilities:
○ Characterizing the relevance of different regions of the DISC1 protein using biophysical approaches. Mentor: PD Dr. Oliver H. Weiergräber.
○ Funded by Alexander von Humboldt Foundation.

[04/2022 – 05/2022] **Doctoral internship**

The University of Cambridge, Department of Genetics, United Kingdom

Main activities and responsibilities:
○ Learning the techniques used in *Drosophila* research, in the context of neurodegenerative diseases. Mentor: Prof. Cahir O'Kane.

233

[01/2019 – 10/2019] **Postgraduate Research**

The University of Edinburgh, MRC Institute of Genetics & Molecular Medicine, United Kingdom

Main activities and responsibilities:
- Study of a copy number variant associated with schizophrenia and autism. Mentor: Dr. Kirsty Millar.

[03/2018 – 11/2018] **Graduate Research**

Faculty of Biotechnology and Drug Development, University of Rijeka, Croatia

Main activities and responsibilities:
- Master's thesis title: "*In vitro* SUMOylation of proteins involved in mental illness". Mentor: Nicholas J. Bradshaw, PhD.
- Project funded by a University of Rijeka project grant for young researchers: "SUMOilacija proteina uključenih u kronične mentalne bolesti" (#969).

PUBLICATIONS

- Samardžija B, Petrović M, **Zaharija B**, Medija M, Meštrović A, Bradshaw NJ, Filošević Vujnović A, Andretić Waldowski R. Transgenic *Drosophila melanogaster* Carrying a Human Full-Length DISC1 Construct (UAS-*hflDISC1*) Showing Effects on Social Interaction Networks. Curr. Issues Mol Biol. 2024 Aug 3;46(8):8526-8549. doi: 10.3390/cimb46080502. PMID: 39194719; PMCID: PMC11352338.

- **Zaharija B**, Bradshaw NJ. Aggregation of Disrupted in Schizophrenia 1 arises from a central region of the protein. Prog Neuropsychopharmacol Biol Psychiatry. 2024 Mar 2; 130:110923. doi: 10.1016/j.pnpbp.2023.110923. Epub 2023 Dec 21. PMID: 38135095.

- Samardžija B, Juković M, **Zaharija B**, Renner É, Palkovits M, Bradshaw NJ. Co-Aggregation and Parallel Aggregation of Specific Proteins in Major Mental Illness. Cells. 2023 Jul 13;12(14):1848. doi: 10.3390/cells12141848. PMID: 37508512; PMCID: PMC10378145.

- **Zaharija B**, Bradshaw NJ. Mapping the Domain Structure and Aggregation Propensity of Proteins Using a Gateway Plasmid Vector System. Methods Mol Biol.2023;2551:649-677. doi: 10.1007/978-1-0716-2597-2_39. PMID: 36310230.

- **Zaharija B**, Odorčić M, Hart A, Samardžija B, Marreiros R, Prikulis I, Juković M, Hyde TM, Kleinman JE, Korth C, Bradshaw NJ. TRIOBP-1 Protein Aggregation Exists in Both Major Depressive Disorder and Schizophrenia, and Can Occur through Two Distinct Regions of the Protein. Int J Mol Sci. 2022 Sep 21;23(19):11048. doi: 10.3390/ijms231911048. PMID: 36232351; PMCID: PMC9569677.

- Samardžija B, Pavešić Radonja A, **Zaharija B**, Bergman M, Renner É, Palkovits M, Rubeša G, Bradshaw NJ. Protein Aggregation of NPAS3, Implicated in Mental Illness, Is Not Limited to the V304I Mutation. J Pers Med. 2021 Oct 23;11(11):1070. doi: 10.3390/jpm11111070. PMID: 34834422; PMCID: PMC8623263.

- **Zaharija B**, Samardžija B, Bradshaw NJ. The TRIOBP Isoforms and Their Distinct Roles in Actin Stabilization, Deafness, Mental Illness, and Cancer. Molecules. 2020 Oct 27;25(21):4967. doi: 10.3390/molecules25214967. PMID: 33121024; PMCID: PMC766329

AWARDS

Grants and scholarships

- Erasmus+ Internship grant for higher education training (2022/2023)
- Alexander von Humboldt Foundation scholarship (2022)
- IUBMB YSF grant (2022)
- Erasmus+ Internship grant, University of Rijeka (2018/2019)
- University of Rijeka's Scholarship for excellence (2017/2018)
- Čavle municipality Scholarship for excellence (2008 - 2017)

IUBMB-FEBS-PABMB Congress (2022). Poster presentation: "Determination of the domain structure of DISC1 in mammalian cells identifies a region crucial for its aggregation in schizophrenia"

YOUNG SCIENTISTS' FORUM (2022). Poster presentation: "Determination of the domain structure of DISC1 in mammalian cells identifies a region crucial for its aggregation in schizophrenia"

FENS Regional Meeting (2021). Poster presentation: Insight into the structure of Disrupted in Schizophrenia 1 throughintegration of bioinformatics and empirical data"

MIND & BRAIN - 60th International Neuropsychiatric Congress (2021). Oral presentation: "Assessing the aggregation propensity of DISC1 in chronic mentalillnesses"

26th International Student Congress Of (bio)Medical Sciences (2020). Oral presentation: "Protein aggregation of DISC1 caused by its disruption in mental illness"

3rd Interdisciplinary Symposium "InHealth", Rijeka (2018). Oral presentation: "The effects of DISC1 Ser704Cys polymorphism on patients with schizophrenia"